



**Screw thread motility of polarly flagellated bacteria
enhances movement through structured environments**

Dissertation

zur Erlangung des akademischen Grades
Doktor der Naturwissenschaften (Dr. rer. nat.)

dem Fachbereich Biologie und Chemie der
Justus-Liebig-Universität Gießen

am 21.05.2019

vorgelegt von

Marco Julian Kühn

geboren in Freiburg im Breisgau

angefertigt am Institut für Mikrobiologie und Molekularbiologie
unter der Leitung von Prof. Dr. Kai Thormann

Gießen, Mai 2019

Die Untersuchungen zur vorliegenden Arbeit wurden von Oktober 2014 bis Februar 2019 unter der Leitung von Prof. Dr. Kai Thormann am Institut für Mikrobiologie und Molekularbiologie an der Justus-Liebig-Universität Gießen durchgeführt.

1. Gutachter

Prof. Dr. Kai Thormann

Institut für Mikrobiologie und Molekularbiologie
Justus-Liebig-Universität Gießen
Heinrich-Buff-Ring 26-32, 35392 Gießen

2. Gutachter

Apl. Prof. Dr. Peter Friedhoff

Institut für Biochemie
Justus-Liebig-Universität Gießen
Heinrich-Buff-Ring 17, 35392 Gießen

Die während der Promotion erzielten Ergebnisse sind zum Teil in folgenden Originalpublikationen veröffentlicht:

Kühn, M. J., F. K. Schmidt, B. Eckhardt, and K. M. Thormann (2017). Bacteria exploit a polymorphic instability of the flagellar filament to escape from traps. *Proceedings of the National Academy of Sciences* 114, pp. 6340–6345.

Kühn, M. J., F. K. Schmidt, N. E. Farthing, F. M. Rossmann, B. Helm, L. G. Wilson, B. Eckhardt, and K. M. Thormann (2018). Spatial arrangement of several flagellins within bacterial flagella improves motility in different environments. *Nature Communications* 9.5369.

Erklärung

Ich habe die vorgelegte Dissertation selbständig und ohne unerlaubte fremde Hilfe und nur mit den Hilfen angefertigt, die ich in der Dissertation angegeben habe. Alle Textstellen, die wörtlich oder sinngemäß aus veröffentlichten Schriften entnommen sind, und alle Angaben, die auf mündlichen Auskünften beruhen, sind als solche kenntlich gemacht. Bei den von mir durchgeführten und in der Dissertation erwähnten Untersuchungen habe ich die Grundsätze guter wissenschaftlicher Praxis, wie sie in der „Satzung der Justus-Liebig-Universität Gießen zur Sicherung guter wissenschaftlicher Praxis“ niedergelegt sind, eingehalten.

Gießen, 21.05.2019

Marco Julian Kühn

Alle Beobachter, die eingehender über die Bewegung der Thiospirilien berichten, werden nicht müde, den fesselnden Anblick, den ein von zahlreichen Exemplaren erfülltes Präparat dem Mikroskopiker bietet, in lebhaften Farben zu schildern. In der Tat ist es ein außerordentlich anziehendes Schauspiel, Hunderte der winzigen Schlangen sich nach allen Richtungen durch das Gesichtsfeld schrauben zu sehen: hier in stetigen, geraden Bahnen, dort in unregelmäßig gekrümmten Linien. Bald hält ein Exemplar mitten im Laufe inne, um nach kurzer Ruhe wieder davon zu eilen, bald zuckt hier und dort eines auf ein kurzes Stück zurück und nimmt gleich wieder die ursprüngliche Bewegungsrichtung auf. Andere wieder ändern endgültig, aber in aller Ruhe und ohne jede Hast die eingehaltene Richtung, indem sie in der gleichen Bahnlinie, die sie bisher verfolgten, rückwärts schwimmen, so daß also der ursprünglich vorn befindliche Pol nunmehr das Hinterende bildet.

- Johannes Buder, 1915

Contents

Abstract	1
Zusammenfassung	3
I. Introduction	5
1. Variety of microbial motion	5
1.1. Prokaryotic active motion	5
1.2. Prokaryotic passive motion	6
2. The bacterial flagellum	6
2.1. Basal body	7
2.2. Hook	7
2.3. Filament	9
2.3.1. Structure of the flagellar filament	9
2.3.2. Filament polymorphism	11
2.3.3. Filament modification and composition	12
2.4. Assembly of flagellar structures	14
2.4.1. Assembly sequence	14
2.4.2. Hierarchical regulation of flagellar assembly	15
3. Flagella-mediated motility	16
3.1. Swimming in liquid	16
3.1.1. Basic conditions	16
3.1.2. High efficiency motor rotation	17
3.1.3. High efficiency navigation	17
3.1.4. High efficiency propulsion	17
3.2. Moving in structured environments	18
3.2.1. Basic conditions	18
3.2.2. Making use of multiple flagella	18
3.2.3. Swarming over surfaces	19
3.2.4. Spreading in soil	19
3.2.5. High torque motors for high viscosity	21
3.2.6. Propulsion by cell body rotation and deformation	21
4. Swimming and turning mechanisms	22
4.1. General mechanism of thrust generation by a rotating flagellum	22
4.1.1. Low Reynolds number regime	22
4.1.2. Generating thrust	23
4.2. Flagellation patterns and consequences for swimming	25
4.2.1. Navigation with peritrichous flagella	26

4.2.2. Navigation with a single polar flagellum	28
4.2.3. Navigation with other types of flagellation patterns	29
4.3. Chemotactic control of swimming and turning	30
4.3.1. Chemoreceptors	31
4.3.2. Basic signalling scheme	31
5. Model organism and aim of this thesis	32
5.1. <i>Shewanella putrefaciens</i> CN-32	32
5.2. Research objectives	33
 II. Publications contributing to this thesis	 34
1. Bacteria exploit an instability of the flagellar filament to escape from traps	34
1.1. Summary	34
1.2. Contribution	35
2. Spatial arrangement of several flagellins improves motility in different environments	54
2.1. Summary	54
2.2. Contribution	55
 III. Discussion	 95
1. Observing <i>screw thread</i> formation	95
1.1. Visualising flagella and filament behaviour	95
1.2. Experimental conditions and natural habitat of <i>Shewanella putrefaciens</i>	96
2. Formation of the <i>screw thread</i>	97
2.1. Characteristics of the conditions that trigger <i>screw thread</i> formation	97
2.1.1. Agarose-glass interface	97
2.1.2. Bulk liquid supplemented with Ficoll	97
2.2. Mechanism of <i>screw thread</i> formation	98
2.2.1. Fundamental principle	98
2.2.2. Additional factors that facilitate <i>screw thread</i> formation	98
2.3. Characteristics of the <i>screw thread</i> motility at sub-microscopic scales	100
2.3.1. Relative movement of filament and cell body	100
2.3.2. Universal joint function of the hook	100
2.3.3. <i>Screw-like</i> movement during free swimming	101
2.3.4. <i>Screw-like</i> movement in confined spaces	101
3. Examples of filament wrapping in other species	102
3.1. Similar behaviours observed before	102
3.2. <i>Screw thread</i> formation in other bacteria	102
3.3. General distribution of filament wrapping	105

4. Benefit of <i>screw thread</i> formation	105
4.1. Navigating structured environments	105
4.2. General benefits for swimming motion	107
5. The two flagellins of <i>Shewanella putrefaciens</i>	107
5.1. Similarities and differences of FlaA and FlaB filaments	107
5.1.1. Helical shape	107
5.1.2. Posttranslational modification	108
5.2. How can the different stability to <i>screw thread</i> formation be explained?	109
6. Segmentation of the flagellar filament	110
6.1. Why is one flagellin not sufficient?	110
6.2. How is the segmentation of the filament achieved?	112
6.3. Why make the filament's base more stable?	113
6.4. Can <i>screw thread</i> formation explain the maintenance of multiple flagellins in other species?	114
7. Outlook	115
 References	 119
 Acknowledgements	 140
 Curriculum vitae	 141

Abstract

Many bacteria from diverse habitats are motile by means of flagella, long protein filaments that adopt a helical shape and are rotated at their base by a complex motor embedded in the cell envelope. Although flagella are often associated with swimming in aquatic environments, they can in fact be used in many different ways allowing movement also in viscous media or structured environments like soil, mucus or tissue. Generally, bacteria with multiple flagella are considered to be better equipped for movement in structured environments because they can generate more torque. On the other hand, bacteria that possess a single filament, usually at the cell pole, are generally considered to be adapted for fast swimming in bulk liquids. This might be valid as a basic scheme, but many bacteria are subject to different or changing environments that pose distinct demands on the motility apparatus. Hence, motile bacteria need strategies to manage various, distinct environmental conditions. This could be the use of multiple motility apparatuses, like flagella and pili, or the use of two sets of flagella, one for potent swimming in bulk liquid and one for efficient movement over surfaces or through structured media.

The findings presented in this thesis show that even a single polar flagellum can be adapted for both robust free swimming in bulk liquid as well as efficient movement through structured environments. This is achieved by balancing the properties of the flagellar filament to allow a certain degree of instability when the load on the filament increases due to increasing viscous drag, while still providing enough stability for regular swimming under free-swimming conditions. Many marine bacteria, such as our model organism *Shewanella putrefaciens*, can swim forwards or backwards depending on the direction of motor rotation and turn by a *run-reverse-flick* mechanism. High-speed microscopy of swimming cells with fluorescently labelled flagellar filaments in a structured environment revealed that this regular swimming behaviour is often not sufficient to back out from dead ends or to squeeze through narrow passages. Instead, *S. putrefaciens* was found to wrap its flagellar filament around its cell body, resembling a *screw thread*, and move between agarose patch and glass surface in a *screw*-like fashion without slip of the flagellar helix. This means that with each full rotation of the flagellum the cell moves by the height of one helix coil. This behaviour is triggered by an instability at the base of the filament when the motor rotates in backward direction and the viscous drag-induced torsional forces exceed the stability of the filament, which is therefore trying to invert the handedness of the helix.

The filament of *S. putrefaciens* is composed of two different flagellin subunits: FlaA, which forms a short segment at the base of the filament, and FlaB, which forms the remaining, major segment of the filament. This segmentation is most likely achieved by a temporal control of flagellin transcription with *flaA* being transcribed before *flaB*. Thus, FlaA is produced and exported first and forms the basal segment. Genetically modified strains that produce full-length filaments only consisting of either FlaA or FlaB showed impaired movement performance in either structured environments or under free-swimming conditions, respectively. Particularly, FlaB-only mutants showed strongly increased frequency of *screw thread* formation while FlaA-only mutants showed no *screw thread* formation at all. Thus, introducing the FlaA segment with its distinct properties stabilises the flagellar filament and balances *screw thread* formation. Holographic microscopy, population-wide motility assays and numerical simulations of wild-type and mutant cells suggested that the wild-type filament is a trade-off between swimming efficiency and the ability to switch to the *screw thread* motility mode. Hence, wild-type cells are well-equipped for motility in a wide range of conditions, both for swimming in bulk liquid as well as for *screw*-like movement in structured environments. Furthermore, the wild type forms a heterogeneous

population of cells that differ in the length of the FlaA segment. Therefore, subpopulations of cells are more likely to switch to *screw thread* mode than others, but a fraction of the population will always be well-equipped for movement in a specific environment.

The mechanisms of *screw thread* formation is fundamental and potentially applies to many polarly flagellated bacteria. This is supported by recent findings of the *screw thread* motility mode in more species, all of them being polarly flagellated but having varying numbers of flagellar filaments. Building the filament from more than one flagellin modifies its properties and can affect all aspects of flagella-mediated motility, which might explain why about half of all flagellated bacteria possess more than one flagellin gene. The ability to wrap the filament around the cell body under high-load conditions provides a motility mode for more efficient movement in structured environments. This potentially facilitates navigation in various habitats like marine sediment, soil or other porous media, polysaccharides and mucus, as well as viscous or constricted passages in animal hosts. Possibly, movement through a biofilm matrix might also be facilitated.

Zusammenfassung

Viele Bakterien aus unterschiedlichsten Habitaten bewegen sich mit Hilfe von Flagellen fort. Flagellen sind lange Proteinfilamente, die eine helikale Form annehmen und an ihrer Basis über einen komplexen, in der Zellohülle eingebetteten Motor rotieren. Auch wenn Flagellen meist mit Schwimmen in aquatischen Umgebungen in Verbindung gebracht werden, finden sie auf viele unterschiedliche Arten Verwendung. So erlauben sie auch die Fortbewegung in viskosen oder strukturierten Umgebungen wie Böden, Schleimen oder Geweben und spielen bei der Anheftung an Oberflächen eine Rolle. Grundsätzlich wird angenommen, dass Bakterien mit mehreren Flagellen besser für die Fortbewegung in strukturierten Umgebungen ausgestattet sind. Demgegenüber wird angenommen, dass Bakterien mit einem einzelnen Filament, üblicherweise am Zellpol, für schnelles Schwimmen in wässrigem Milieu angepasst sind. Das mag als Grundkonzept zutreffen, allerdings sind viele Bakterien unterschiedlichen oder sich verändernden Bedingungen ausgesetzt, die individuelle Anforderungen an den Motilitätsapparat stellen. Daher benötigen motile Bakterien Strategien, um mit unterschiedlichsten Umweltbedingungen zurechtzukommen. Dies kann die Verwendung von mehreren Fortbewegungsapparaten sein, wie Flagellen und Pili, oder die Verwendung von zwei Flagellensystemen, eines für leistungsfähiges Schwimmen in Flüssigkeiten und eines für effiziente Fortbewegung durch strukturierte Medien.

Die in dieser Arbeit dargestellten Erkenntnisse zeigen, dass sogar ein einzelnes polares Flagellum sowohl an robustes freies Schwimmen in wässrigen Flüssigkeiten als auch an effiziente Fortbewegung durch strukturierte Umgebungen angepasst werden kann. Das wird durch Austarieren der Eigenschaften des Flagellenfilaments erreicht, sodass bei zunehmender Last auf das Filament durch steigende Reibungskräfte eine gewisse Instabilität möglich ist, aber gleichzeitig ausreichend Stabilität bei regulärem, freiem Schwimmen gewährleistet wird. Viele marine Bakterien, wie unser Modellorganismus *Shewanella putrefaciens*, können abhängig von der Drehrichtung des Motors vorwärts oder rückwärts schwimmen und sich durch einen „vorwärts-rückwärts-abknicken“ (*run-reverse-flick*) Drehmechanismus neu ausrichten. Mittels Hochgeschwindigkeitsmikroskopie von schwimmenden Zellen mit fluoreszenzmarkierten Flagellenfilamenten in einer strukturierten Umgebung konnte gezeigt werden, dass dieses reguläre Schwimmverhalten oft nicht ausreicht, um aus einer Sackgasse zu entkommen oder sich durch enge Durchgänge zu bewegen. Stattdessen wickelt *S. putrefaciens* sein Flagellenfilament um den eigenen Zellkörper und bewegt sich schraubenartig zwischen Agarose- und Glasoberfläche fort. Dies geschieht ohne Durchdrehen der flagellaren Helix, das heißt, mit jeder vollen Rotation des Flagellums bewegt sich die Zelle um die Höhe einer Helixwendel fort. Dieses Verhalten wird durch eine Instabilität an der Basis des Filaments beim Drehen des Motors in Rückwärtsrichtung ausgelöst, wenn die durch den Reibungswiderstand verursachten Torsionskräfte die Stabilität des Filaments übersteigen und versuchen die Händigkeit der Helix zu invertieren.

Das Filament von *S. putrefaciens* besteht aus zwei unterschiedlichen Flagellinuntereinheiten: FlaA, welches ein kurzes Segment an der Basis des Filaments bildet, und FlaB, welches das Hauptsegment ausmacht. Diese Segmentierung wird höchstwahrscheinlich durch eine zeitliche Kontrolle der Flagellintranskription erreicht, wobei *flaA* vor *flaB* transkribiert wird. Daher wird FlaA zuerst produziert und exportiert und bildet das basale Fragment. Genetisch modifizierte Stämme, die Filamente mit Wildtyplänge produzieren, aber entweder nur aus FlaA oder nur aus FlaB bestehen, zeigten eine Beeinträchtigung der Fortbewegung in strukturierten Umgebungen bzw. bei freiem Schwimmen. Im Speziellen wurde für eine reine FlaB Mutante (*FlaB-only*) eine stark erhöhte

Schraubenbildungsfrequenz, dagegen für eine reine FlaA Mutante (*FlaA-only*) überhaupt keine Schraubenbildung beobachtet. Das Einbringen des FlaA-Segments mit seinen individuellen Eigenschaften stabilisiert also das Flagellenfilament und sorgt für ein Gleichgewicht der Schraubenbildung. Holografische Mikroskopie, populationsweite Motilitätsversuche sowie numerische Simulationen des Wildtyps und der Filamentmutanten haben gezeigt, dass das Wildtypfilament ein Kompromiss zwischen Schwimmeffizienz und Schraubenbildung ist. Daher ist das Wildtypfilament für die Fortbewegung unter verschiedensten Bedingungen gut geeignet, sowohl zum Schwimmen in Flüssigkeiten als auch zur schraubenartigen Fortbewegung in strukturierten Umgebungen. Außerdem bildet der Wildtyp eine heterogene Population aus Zellen, die sich in der Länge des FlaA-Segments unterscheiden. Daher gibt es Subpopulationen aus Zellen, die häufiger zum Schraubenmodus wechseln als andere, wobei ein Teil der Population immer gut für die Fortbewegung in einer bestimmten Umgebung geeignet ist.

Der Mechanismus der Schraubenbildung ist fundamental und könnte potenziell für viele polar flagellierte Bakterien zutreffen. Das wird bestärkt durch die neuesten Entdeckungen der Schraubenbildung in weiteren Spezies, die alle polar flagelliert sind, aber eine unterschiedliche Anzahl an Flagellen besitzen. Das Filament aus mehr als einem Flagellin aufzubauen, verändert seine Eigenschaften und kann alle Bereiche der flagellenvermittelten Motilität beeinflussen. Das könnte erklären, warum ungefähr die Hälfte aller flagellierten Bakterien mehr als ein Gen für Flagelline besitzen. Die Fähigkeit, das Filament unter hoher Last um den Zellkörper zu wickeln, stellt eine Motilitätsform für eine effizientere Fortbewegung durch strukturierten Umgebungen dar. Das erleichtert vermutlich das Navigieren durch diverse Habitate wie marine Sedimente, Böden oder andere poröse Materialien, Polysaccharide und Schleime, sowie viskose oder enge Bereiche in tierischen Wirten. Möglicherweise könnte dadurch auch die Fortbewegung durch eine Biofilmmatrix erleichtert werden.

Part I.

Introduction

1. Variety of microbial motion

Movement is a fundamental component of life. Not only the macroscopic movement that we know from our walk, drive or sometimes run to work every morning, but also the microscopic and sub-microscopic movement. Microbial single cells and multicellular structures move to find certain conditions, for example nutrient- or oxygen-rich environments, and they move to get away from bad conditions or toxins. The underlying factors are often difficult to investigate as the motion driving machineries and mechanisms involve proteins, molecules and atomic particles, which, obviously, are very small. Despite the challenges that come with the size of all these players in microbial motion, astonishing mechanisms have been described and elucidated.

Bacteria, archaea and eukaryotic single cells as well as multicellular colonies or structures employ an impressive set of movement machineries and strategies to propel themselves in a wide range of conditions using all kinds of physical properties and cellular mechanisms. Microbial motility has developed in exceptional, diverse ways and forms, some leading to very fast swimming through liquids, others to slower movement over solid surfaces or even just to passive translocation depending on external forces. The examples given here are only a glimpse of what microorganisms are capable of, and likely many more stunning phenomena and mechanisms remain unexplored.

1.1. Prokaryotic active motion

At least three higher mechanistic principles of prokaryotic active movement have been described so far, which can often be adapted for propulsion in different environments. One of the most diverse and efficient mechanism used by bacteria and archaea alike is the rotation of helical cell appendages called flagella (covered in section 2) or archaella, respectively, which mediate propulsion in liquid media (3.1) but also in more complex environments and over surfaces (3.2).

Another common way to propel cells on surfaces is the extension and retraction of proteinaceous filaments, known as pili (Bradley 1980; Sun et al. 2000; Merz et al. 2000). Cells essentially reach out with their pili, hold on to something and pull the cell body in that direction. In *Pseudomonas aeruginosa* several modes of this twitching motility are known, characterised by different speeds and probably serving different purposes (Jin et al. 2011; Gibiansky et al. 2010). Pili-mediated motility is known to be an important factor for biofilm formation and host invasion of pathogenic bacteria, but also for predatory bacteria, like *Bdellovibrio bacteriovorus*, to enter the periplasmic space of the prey cell (O'Toole et al. 1998; Farinha et al. 1994; Evans et al. 2007).

The third principle is the use of motor proteins that either set small cell appendages in motion or directly move the whole cell body. For example, rapid movement of adhesins along a helical track is thought to drive the surface gliding motility of *Flavobacterium johnsoniae* (Nelson et al. 2008; Shrivastava et al. 2012; Nakane et al. 2013). In *Myxococcus xanthus*, the gliding motility is mediated by inner-membrane motor complexes

that move along a helical path from the leading to the lagging cell pole, driven by a proton-motive force. These focal adhesion complexes become immobilised upon substrate surface interaction via periplasmic and outer membrane subcomplexes and their right-handed helical movement is converted to a left-handed helical movement of the cell body (Mignot et al. 2007; Sun et al. 2011; Faure et al. 2016). This mechanism is mostly known as gliding motility over a surface, but the same principle might be used by *Synechococcus* to deform the cell wall and its coating S-layer, which creates waves moving along the cell body and fluid flows to propel the cell in a liquid environment (Ehlers et al. 2012). *Mycoplasma* species also have developed ways to glide over surfaces using motor proteins: In *M. mobile*, large cell surface proteins function as tiny legs that directly push against the substratum and *M. pneumoniae* possesses a dedicated region of the cell body which expands and contracts and thus drives the cell forward in an inchworm-like motion (Henderson et al. 2006; Miyata 2008).

1.2. Prokaryotic passive motion

When it comes to motility one usually thinks of sophisticated active motion, but cells have also developed strategies to exploit simple physical properties. Gas vesicles are used for buoyancy control (Walsby 1975), cells are sliding simply by expansive forces resulting from colony growth (i.e. being pushed by other cells; Martínez et al. 1999) and intracellular parasites such as *Listeria monocytogenes* and *Shigella flexneri* migrate passively by exploiting polymerisation of host cell actin (Stevens et al. 2006). A rather peculiar form of motility was observed in *Bacillus subtilis*: Taking advantage of slightly inclined surfaces, whole colonies can slide downwards by reducing the surface tension through secretion of surfactants (Hennes et al. 2017). All these mechanisms are very different from the active motion described above, but ultimately they result in the translocation of cells, and microorganisms have developed dedicated cellular systems to influence the physical properties of themselves or their surroundings to their advantage.

2. The bacterial flagellum

Section 1 briefly touched some of the many ways that microorganisms and prokaryotes in particular have developed to move in diverse environments with distinct properties and individual demands on the motility apparatus. One of them, the bacterial flagellum, takes a special role as it is an (almost) all-purpose means for fast and efficient movement in a broad variety of distinct environments and one of the best studied forms of bacterial motility.

The bacterial flagellum is a helical cell appendage that rotates to generate thrust (covered in detail in section 4.1.2). This should not be confused with the eukaryotic flagellum, which has a completely different structure and thrust is not generated by a rotating, but rather a beating filament (Ballowitz 1888; Gray 1955; Diniz et al. 2012). The bacterial flagellum is also fundamentally different from the archaeal flagellum, or archaellum (there is some controversy about the naming; Jarrell et al. 2012; Wirth 2012; Eichler 2012), which shows homology to type IV pili but not to the bacterial flagellum (Faguy et al. 1994; Faguy et al. 1999; Jarrell et al. 2012). The propulsion mechanisms, however, are very similar: A rotary motor embedded in the cell envelope drives a helical filament that generates thrust either forwards or backwards, depending on the direction of rotation and the rigidity of the filament.

Swimming microorganisms have been observed since the first microscopic devices were engineered (Van Leeuwenhoek 1683) and at the end of the 19th century scientists described the swimming behaviour and even the behaviour of the flagellar filament(s) with surprising detail (Bütschli 1884; Buder 1915). However, they apparently had no clue that the helical flagella of bacteria are rotating, driven by a motor embedded in the cell wall. Instead, they believed the flagella rotate by the contraction of individual filaments that constitute the flagellar bundle (Bütschli 1884; Buder 1915). Since then, advances in microscopic techniques but also in molecular and structural biology enabled scientists to reveal the astonishing nature of this molecular nanomachine and many building blocks as well as regulatory circuits and physical principles have been found and deciphered, yet much still remains to be elucidated.

The bacterial flagellum comprises three major parts: The basal body, which is the engine embedded in the cell envelope, the flagellar filament, which is the extracellular helical propeller and the hook, which acts as universal joint between the basal body and the filament (Fig. 1).

2.1. Basal body

The basal body is the most complex part of the flagellum, both in terms of structural complexity as well as interactions with other proteins and systems of the cell. Most importantly, the basal body anchors the flagellum at a specific location in the cell envelope and generates the torque that is driving the rotation of the flagellar filament. The central part is an axial rod that spans the cytoplasmic membrane, the periplasm and the outer membrane in Gram-negative, and the cytoplasmic membrane and the cell wall in Gram-positive bacteria (DePamphilis et al. 1971). In Gram-negative bacteria, the rod is connected to the periplasmic peptidoglycan layer and the outer membrane via ring-like structures, the P- and L-rings (Suzuki et al. 2004). Gram-positive bacteria, like *Bacillus subtilis*, lack those rings (Kubori et al. 1997). The MS-ring, consisting of ~ 26 copies of FliF, is inserted into the cytoplasmic membrane and connects to the cytoplasmic C-ring, which is composed of FliG, FliM and FliN (Ueno et al. 1992; Suzuki et al. 2004; Francis et al. 1994). The C-ring participates in torque generation and interacts with the chemotaxis system via phosphorylated CheY, resulting in switching the direction of motor rotation (Yamaguchi et al. 1986; Sockett et al. 1992; Welch et al. 1993; Irikura et al. 1993; Toker et al. 1997). The motor is powered by the chemical energy of an ion gradient (H^+ or Na^+) which is converted to rotational energy by the stator units that are anchored to the peptidoglycan layer surrounding the MS-ring. The stators can associate and dissociate dynamically, even switching between different types of stators while the whole structure is in motion (Blair et al. 1990; Kojima et al. 1999; Reid et al. 2006; Leake et al. 2006; Paulick et al. 2015). The inward ion flux through the stator complexes results in a conformational change of the stator units which are interacting with FliG and thus generate the torque that is further transmitted via the rod and the hook to the filament (Lloyd et al. 1996; Kojima et al. 2001; Zhou et al. 2002). Located in the cup-like structure of the C-ring and inserted into the central pore of the MS-ring, the flagellar type III secretion system (fTTSS) exports distal flagellar components like rod, hook and filament parts selectively, depending on the stage of the assembly (Minamino et al. 2004, 2008; Ferris et al. 2006).

2.2. Hook

The second part, the hook, doesn't seem to be that major at first, as it is only a short, highly curved filament that connects the basal body and the flagellar filament. However, it is essential to convert the angular rotation of the rod in the basal body to the angular rotation of the flagellar filament. Its function is therefore similar to

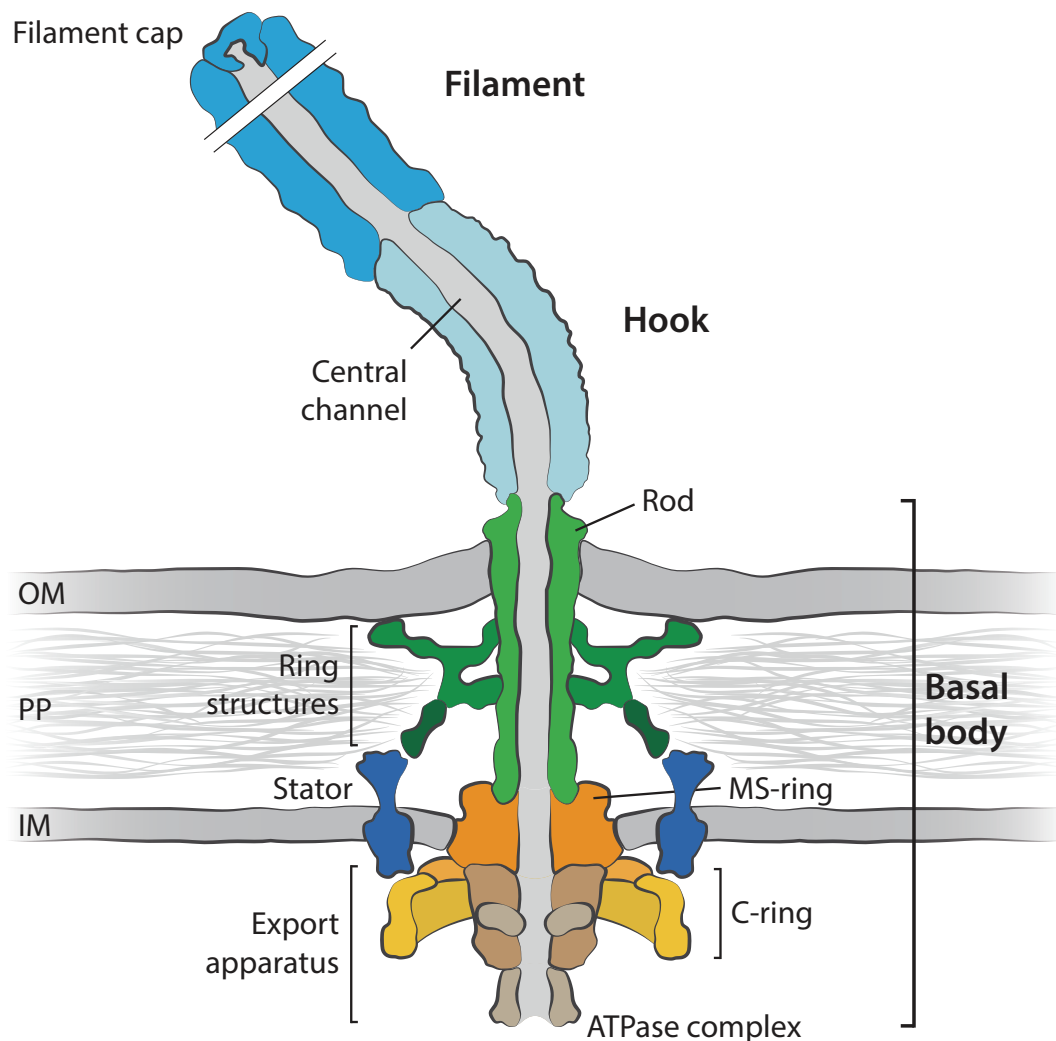


FIGURE 1. Schematic representation of the bacterial flagellum of Gram-negative bacteria. It comprises three major parts: The **Basal body**, which anchors the flagellum in the cell envelope and houses all the required parts for torque generation and rotation (C-ring + Stators) as well as the switch complex (C-ring) and the Export apparatus. The **Hook** is the universal joint between the basal body and the filament and is essential for efficient swimming and turning. The **Filament** is the propeller that generates thrust by rotation in the liquid surrounding the cell body (it was cut to fit on the page, but it actually accounts for about 99 % of the flagellum's complete length). OM: Outer membrane, PP: Periplasm, IM: Inner membrane. Based on cryoelectron tomography of the basal body of *Vibrio alginolyticus* (Zhu et al. 2017).

a universal joint and as such it allows flagella from all over the cell body to align and form a bundle to push the cell forward, for example in peritrichous bacteria like *Escherichia coli* or *Salmonella enterica* (Berg et al. 1972, 1973). In other species with only one flagellum at the cell pole, changes of the flexibility of the hook are important for the ability to actively and efficiently turn (Xie et al. 2011; Son et al. 2013). Without the hook, these cells could only reorient the cell body passively by Brownian motion (Ping 2012).

The hook is a tubular, helical filament made from ~ 120 FlgE proteins, very similar in structure to the flagellar filament, but very different on the amino acid level (Homma et al. 1990). Rather than simply being a bent rod, the hook is a short segment of a superhelical fibre that is made from eleven longitudinal protofilaments similar to the flagellar filament and it even shows polymorphic transformations as well (cf. section 2.3; Wagenknecht

et al. 1982; Morgan et al. 1993b; Kagawa et al. 1979; Kato et al. 1984). During rotation of the hook, the protofilaments constantly change between states of extension and compression, which correspond to positions at the long and short sides of the hook, respectively (Samatey et al. 2004).

2.3. Filament

The last major part, and the most prominent one, is the flagellar filament, a long helical cell appendage that is rotated at its base and thereby pushes against the surrounding liquid to generate thrust and fluid flows (see section 4). This is the main structure that drives swimming of the cells, but it is also used for attachment to biotic and abiotic surfaces (Haiko et al. 2013; Rossez et al. 2015), and it is an important proinflammatory factor for the immune system of higher eukaryotes (Hajam et al. 2017).

2.3.1. Structure of the flagellar filament

The flagellar filament has a very conserved core structure among all bacterial species with several thousand copies of flagellin proteins forming a hollow tube that extends from the cell body several micrometer into the surrounding medium. The flagellins subunits are stacked in a regular pattern which can be seen as individual protofilaments along the axis of the filament (Fig. 2 B-D). The protofilaments are arranged as longitudinal helical arrays forming the central channel (Fig. 2 E-G) through which new flagellin subunits are diffusing to the growing end of the filament (O'Brien et al. 1972). In this pattern, each flagellin subunit closely interacts with six adjacent subunits (Yonekura et al. 2003). Different numbers of protofilament strands have been reported for different bacteria, with *Salmonella enterica*, as the paradigm for filament structure, having eleven protofilaments and *Campylobacter jejuni* having only seven (O'Brien et al. 1972; Galkin et al. 2008). The distribution of protofilament numbers among bacterial species and the implications for filament properties and swimming behaviour are not well studied. However, it is believed that most filaments follow the *Salmonella* paradigm, because the sequence in the coiled-coil regions of flagellin responsible for polymerisation (D0, D1 domains) is highly conserved and most of the (few) analysed filaments do actually have eleven protofilaments (Beatson et al. 2006; Maki-Yonekura et al. 2010; Wang et al. 2017). Still, different numbers of protofilaments could explain the observed differences in macroscopic filament geometries in species like *Idiomarina loihiensis* (Shibata et al. 2005; Galkin et al. 2008; Fujii et al. 2008). In fact, Fujii et al. allocated many different flagella into three families depending on distinct filament morphologies, distinguishing between peritrichous, polar and lateral flagella.

The protofilaments are all made from the same protein and it is not trivial how a helical filament can be constructed by bonding identical subunits together in a regular manner (Namba et al. 1989). The helical shape is only possible because the flagellin subunits and thus the protofilaments can adopt two distinct configurations, an L- and a slightly shorter R-type. This was first suggested by Sho Asakura and later clearly resolved by electron cryomicroscopy of *Salmonella* filaments (Asakura 1970; Yonekura et al. 2003; Maki-Yonekura et al. 2010; Wang et al. 2017). In all bacterial species, the flagellin proteins show high sequence similarity in the conserved D0 and D1 domains, which are mostly responsible for filament formation and constitute the innermost domain of the tube (Figure 2 B-G; Namba et al. 1989). Both the D0 domain as well as the D1 domain include N- and C-terminal secondary structures (Fig. 2 A), which are arranged adjacently in the final flagellin fold (indicated by blue and green shading in Figure 2, respectively). The central sequence between the two D1 fragments (variable domain) is highly diverse in terms of length and amino acid composition, with some species possessing almost no such domain (Figure 2 B, E) to some with a large variable domain even further

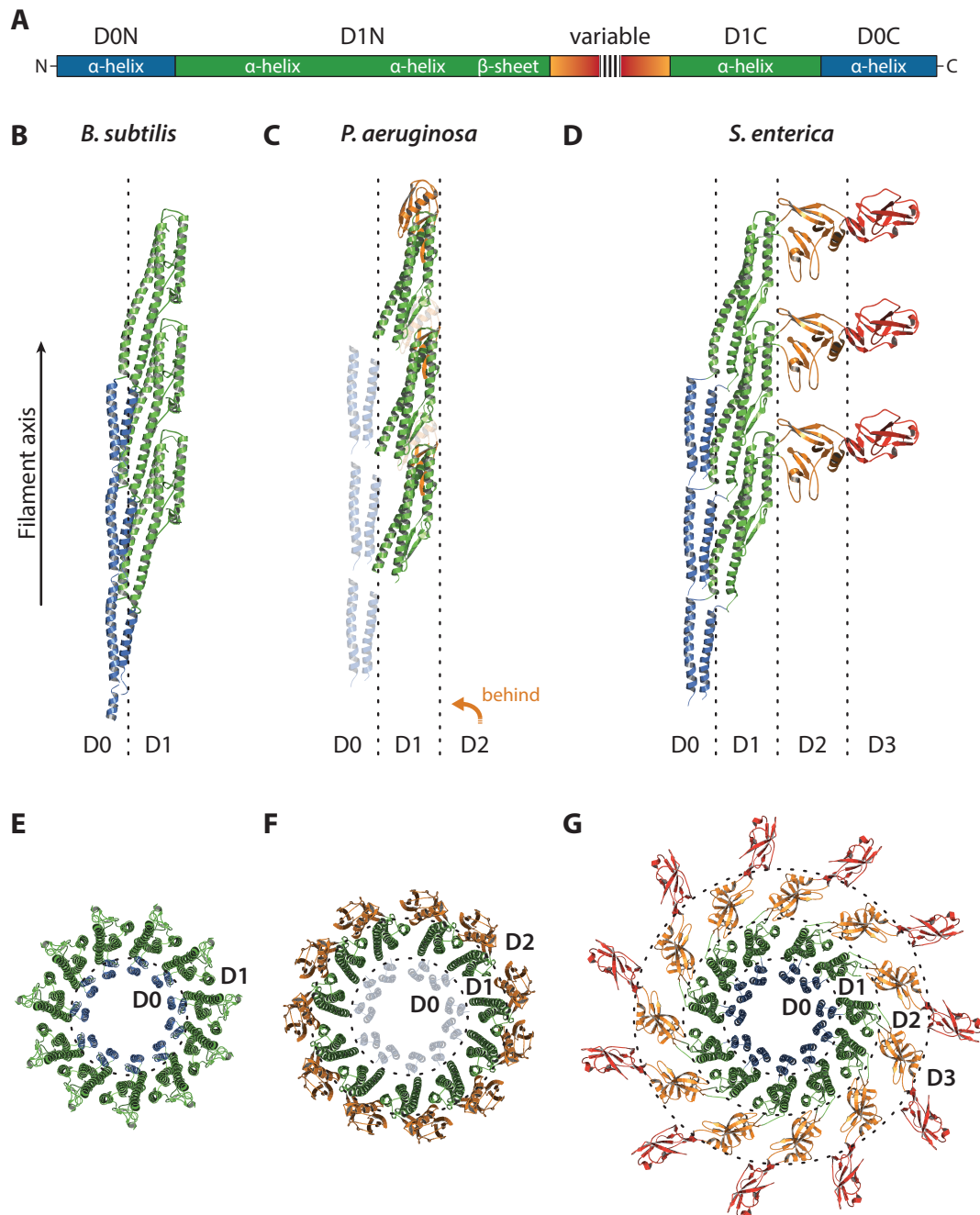


FIGURE 2. Architecture of the flagellar filament. **A** Domain organisation of the flagellin protein. The central, variable domain varies substantially in length and sequence among bacteria, while the D0 and D1 domains, which constitute the core of the filament, are highly conserved. **B - D** Longitudinal section of the filament of three different species with distinct flagellins. The flagellin subunits are stacked by interactions of the D0 and D1 domains, forming eleven longitudinal protofilaments. The core structure of the filament is very conserved, but the surface-forming domains (on the right) are highly diverse. The perspective is the same in all three panels, therefore the D2 domain in panel C is covered by the D1 domain. As the crystal structure of the *P. aeruginosa* flagellin lacks the D0 domain, it was replaced with the D0 domain of *Salmonella* for this illustration. **E - F** Cross section of the filament of the same species as in B-D showing the lateral arrangement of flagellin subunits. The structure of the core and central channel is conserved but the outer layer(s) and thus diameter of the filament varies substantially. Based on Yonekura et al. 2003; Maki-Yonekura et al. 2010; Wang et al. 2017; Imada 2018 using the protein data bank structures 5WJT (Wang et al. 2017), 4NX9 (Song et al. 2014), 1UCU (Yonekura et al. 2003).

divided into subdomains (Figure 2 D, G; Fedorov et al. 1988; Beatson et al. 2006). This greatly influences the overall thickness of the flagellar filament, and as these domains constitute the filament surface they are also responsible for the antigenic properties and diversity of the flagellar filament (Iino 1977; Joys 1985; Wei et al. 1985; Fedorov et al. 1988; Newton et al. 1991; Reid et al. 1999) and might influence swimming behaviour and the interaction with neighbouring flagella (Horstmann et al. 2017; Yoshioka et al. 1995). The conserved amino- and carboxy-terminal domains, on the other hand, are required for the flagellin-dependant proinflammatory responses mediated by Toll-like receptor 5 (Hayashi et al. 2001; Eaves-Pyles et al. 2001; Murthy et al. 2004). The vast sequence variations in the surface-exposed domains could also explain the differences in the adhesive properties of the flagellar filament (Haiko et al. 2013).

2.3.2. Filament polymorphism

Flagellar filaments with only one type of protofilament configuration are straight, either containing only L- or only R-type flagellin subunits (Yamashita et al. 1998). Different helix morphologies, also called polymorphs, are achieved by switching single or multiple protofilament strands to the opposite configuration. Theoretically, this results in 12 stable helix shapes which differ in diameter and pitch, but also in handedness (Fig. 3; Calladine 1975, 1976, 1978; Hasegawa et al. 1998). *In vitro* as well as *in vivo*, many of these have actually been observed, at least for *Salmonella* (Asakura 1970; Kamiya et al. 1976a,b; Hotani 1982; Darnton et al. 2007b; Turner et al. 2000). Each of these polymorphic states corresponds to a local energetic minimum and one polymorph can be converted reversibly into another one by changing the pH, salinity, temperature or the mechanical forces acting on the filament, for example by changing the motor rotation rate (Kamiya et al. 1976a,b; Hasegawa et al. 1982; Macnab et al. 1977; Hotani 1982; Darnton et al. 2007b). Polymorphic transitions were also observed when adding alcohol or sugar (Hotani 1980; Seville et al. 1993), but the most important ones relating the mechanics of the helix and correlated swimming behaviours are certainly the torsional forces. Another important factor that modifies the basic polymorphic forms are mutations in the flagellin gene (Kanto et al. 1991).

The differences in the tertiary structures of the L- and R-type configuration are very subtle and occur mostly in the outer-tube-forming D1 domain, while the D0 domain and thus the central tube of the filament remains rather stable (Maki-Yonekura et al. 2010; Wang et al. 2017). The conformational adjustments change the intermolecular connection to neighbouring flagellins and the protofilaments slide along each other along the filament axis.

Polymorphic transitions during swimming

Flagella of *S. enterica* or *E. coli* adopt the left-handed *normal* form when swimming forwards (cf. Fig 3) with the motor rotating counterclockwise, but they switch to other polymorphic configurations with different geometries and inverted handedness when switching to clockwise rotation (Shimada et al. 1975; Macnab et al. 1977; Turner et al. 2000). In these right-handed polymorphs (usually *semicoiled* or *curly*) the ratio of L- and R-type protofilaments is changed because of mechanical perturbation of the helix, which is caused by the viscous drag of the surrounding medium. Interestingly, the filament doesn't adopt the neighbouring *coiled* configuration first but skips polymorphic states (from L:R ratio 9:2 to 7:4 or 6:5, rather than to 8:3 first). The most simple explanation would be that the intermediate waveforms are much shorter and thus energetically unfavourable (Calladine 1978; Turner et al. 2000; Darnton et al. 2007b).

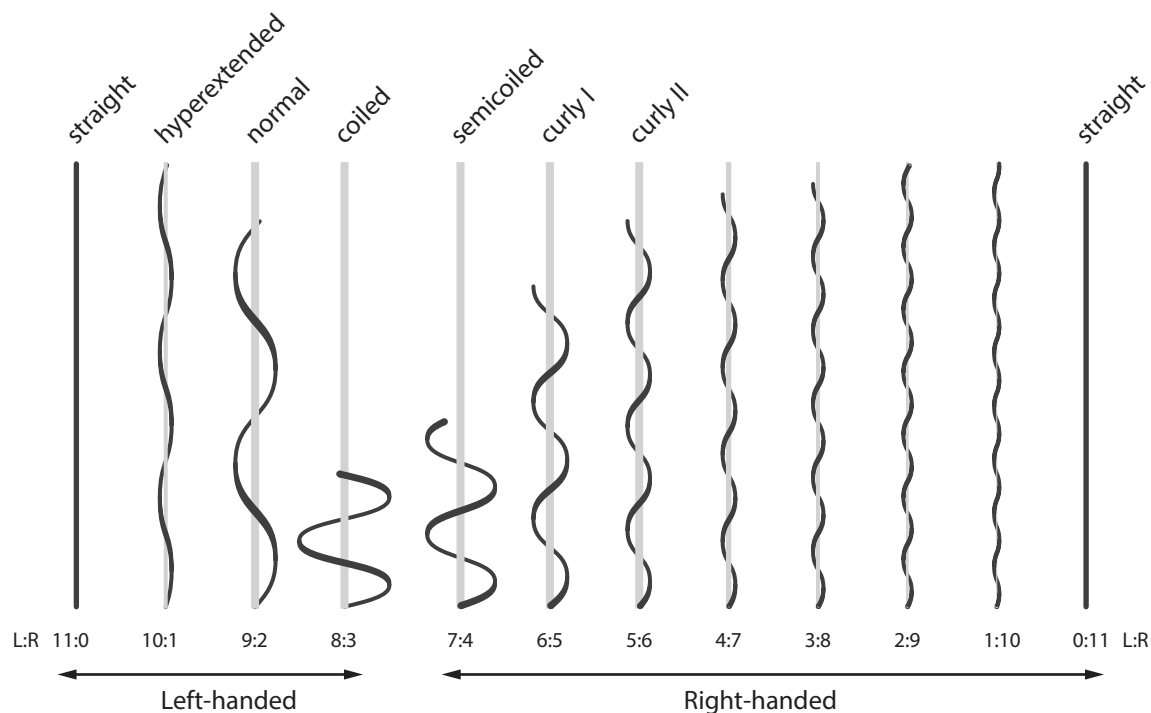


FIGURE 3. **Theoretical polymorphic forms of the flagellar filament.** Different ratios of L- and slightly shorter R-type protofilaments (L:R) result in 12 distinct helix morphologies. Four of these are left-handed, eight are right-handed. The named polymorphs were observed *in vitro* or *in vivo*. Transitions between polymorphic forms can be caused by torsional stress, changes in pH or ionic strength and several other conditions. Based on Calladine 1978; Darnton et al. 2007b.

Polymorphic transitions of complex flagella

This paradigm of switching polymorphic forms is not entirely transferable to every species. In the α -proteobacteria *Bradyrhizobium lupini* and *Sinorhizobium meliloti* the flagellar filaments are more stable to polymorphic transformations because of interflagellin bonds that lock the helix in a rigid, right-handed conformation, which promotes motility in viscous environments (Götz et al. 1982; Trachtenberg et al. 1986; Scharf et al. 2001). Accordingly, no switch in handedness was ever observed, however, these flagella also rotate clockwise all the time and thus no opposite-handed torsional forces occur (Götz et al. 1987; Scharf 2002). Polymorphic transitions to different, right-handed helix shapes can still be triggered by changing the pH or increasing the viscous drag on the filament, so the basic principle of polymorphism seems to apply, but the stability to mechanical stress is different (Scharf 2002).

2.3.3. Filament modification and composition

Sheath

Although the core of the flagellar filament is highly conserved, there are many different modifications to the surface of the filament and not all of them are encoded in the flagellin sequence. Some bacteria, such as *Vibrio cholerae*, *Vibrio parahaemolyticus* or *Helicobacter pylori*, possess a membrane-like sheath around their filament, probably being an extension of the outer membrane (Follet et al. 1963; Fuerst et al. 1988; McCarter et al. 1990; Luke et al. 1995; Allen et al. 1971; Zhu et al. 2017). How exactly the filament rotates with the sheath is not fully understood, just as the exact function of the sheath. Some reports exist that indicate a decreased

recognition of sheathed *V. cholerae* flagella by the innate immune system, probably by stabilising the filament and reducing the release of flagellin (Sang et al. 2008). In *Aliivibrio fischeri*, the release of outer membrane vesicles was found to be increased by the rotation of the sheathed flagellum. Together with the vesicles, peptidoglycan, lipopolysaccharide and the outer membrane protein OmpU are released, which promotes squid host colonisation (Brennan et al. 2014; Aschtgen et al. 2016).

Posttranslational modification of flagellin

Other, common differences in filament surface structures are posttranslational modifications of flagellin proteins, like glycosylation or methylation, which are highly diverse and widely spread, both in Gram-negative and Gram-positive bacteria in general as well as in many plant and human pathogens (Logan 2006; Nothaft et al. 2010; Hayakawa et al. 2012; Ichinose et al. 2013; Merino et al. 2014; De Maayer et al. 2016). Glycan modifications occur mostly in the surface-exposed domains of flagellin and were found to be involved in virulence and attachment but also in filament assembly and filament stability and thus motility (Guerry et al. 1996; Szymanski et al. 2002; Logan et al. 2002; Goon et al. 2003; Arora et al. 2005; Guerry et al. 2006; Taguchi et al. 2006, 2008, 2009; Bubendorfer et al. 2013; Faulds-Pain et al. 2014). Methylation of *Salmonella* flagellins, on the other hand, does not have an obvious effect on flagellar functions (Tronick et al. 1971). So far, almost all of the glycan modifications were reported to occur at serine or threonine residues via O-linked glycosylation, but N-linked glycosylation also exists (Logan 2006; Hayakawa et al. 2012). Although only a few glycosylation pathways have been elucidated (Fox 2002; Miller et al. 2008; Schoenhofen et al. 2009; Yamamoto et al. 2011; Bubendorfer et al. 2013), it was suggested that glycosyltransfer occurs in the cytoplasm in close proximity to the basal body before the flagellin monomers get exported. In *Campylobacter jejuni*, some parts of the glycosylation machinery were actually found to colocalise with flagellar components at the cell pole (Ewing et al. 2009).

Multiple flagellins

Structural differences of flagellar filaments can, of course, originate from different amino acid sequences of the flagellin subunits. This is the most obvious cause for distinct filament properties among bacteria, but the use of multiple, genetically distinct flagellins can also influence the filament composition within just one species. In fact, about half of all known flagellated bacteria possess more than a single flagellin gene, most likely acquired by gene duplication (Logan et al. 1989; Alm et al. 1993; Faulds-Pain et al. 2011). The degree of variation between the flagellins as well as their individual regulation and function differ vastly between species. *S. enterica*, for example, possesses two flagellin genes, *fliC* and *fliB*, but uses only one at a time to build up the flagellar filaments (Andrewes 1922; Lederberg et al. 1956). This phase variation is regulated by a posttranscriptional mechanism relying on the invertible genetic switch element *hin* as well as the *fliC* repressor FljA (Pearce et al. 1967; Fujita et al. 1973; Suzuki et al. 1973; Silverman et al. 1979; Kutsukake et al. 1980; Bonifield et al. 2003). Several functions were suggested for the remodelling of the filament, including temporary evasion of the host's immune system, evasion of predators by altered motility or antigenic properties and adaption to changing environmental conditions (Ikeda et al. 2001; Wildschutte et al. 2004; Matz et al. 2005; McQuiston et al. 2008). The amino acid sequences are highly similar with the most differences located in the central, surface-exposed domains, indicating that mostly the surface interaction of the filament is influenced by the use of the alternative flagellin protein (Wilson et al. 1993).

Many other bacteria with more than one flagellin gene do actually assemble mixed filaments with some or all of the different types of flagellin incorporated. Numbers range from only two in species like *Campylobacter jejuni*, *Campylobacter coli*, *Helicobacter pylori*, *Bacillus thuringiensis* (Nuijten et al. 1990; Guerry et al. 1991; Kostrzynska et al. 1991; Lovgren et al. 2009) to several (here: three to six) like in *Bdellovibrio bacteriovorus*, *Bradyrhizobium lupini*, *Sinorhizobium meliloti*, *Aliivibrio fischeri*, *Vibrio vulnificus*, *Agrobacterium tumefaciens*, *Caulobacter crescentus* (Lambert et al. 2006; Scharf et al. 2001; Millikan et al. 2004; Kim et al. 2014; Mohari et al. 2018; Driks et al. 1989; Ely et al. 2000; Faulds-Pain et al. 2011) and even up to fifteen distinct flagellins reported for *Magnetococcus marinus* MC-1 (Kanehisa et al. 2008; Faulds-Pain et al. 2011). The exact function of each flagellin type is mostly unclear, sometimes one of them is the most dominant one, making a fully functional filament alone, sometimes several but not all flagellins are required and generally a lot of functional redundancy exists. Some filaments show a distinct spatial distribution of segments made from only one type of flagellin, which is rather complex in *C. crescentus* having six flagellins of which at least three form a discrete segment (Driks et al. 1989) or *B. bacteriovorus* also having six flagellins of which only one is absolutely required for a full-length filament and the others show high redundancy (Lambert et al. 2006). In other bacteria, more simple spatial organisation of flagellin segments was found, like in *H. pylori* forming only two distinct segments (Kostrzynska et al. 1991). The filaments of *B. lupini* and *S. meliloti*, described as complex flagella, are thought to be assembled from heterodimers of the essential flagellin FlaA and one of the two or three other flagellins, respectively (Trachtenberg et al. 1986; Scharf et al. 2001). All in all, there seems to be a huge variation between the numbers as well as the regulation and function of different flagellin types and very little is known about the exact advantage of having more than just one flagellin gene.

2.4. Assembly of flagellar structures

2.4.1. Assembly sequence

Flagellar assembly starts with the determination of the assembly site, which can happen either randomly by diffusion or via landmark proteins (Schuhmacher et al. 2015). In the peritrichous bacteria *Escherichia coli* and *Salmonella enterica* no clear determination factor for flagellar placement have been identified so far, however, in *Bacillus subtilis*, also peritrichous, the flagella are distributed symmetrically around the cell body, but missing at the cell poles (Guttenplan et al. 2013). Here, the SRP-like GTPase FlhF and MinD-like ATPase FlhG are involved in determining the assembly sites as well as the number of flagella resulting in the defined flagellation pattern of *B. subtilis*. FlhG and FlhF are also participating in the correct placement of flagella in bacteria with other flagellation patterns, like polar or bipolar localisation, as well as regulating the number of flagella (Campos-García et al. 2000; Dasgupta et al. 2000; Van Amsterdam et al. 2004; Kusumoto et al. 2006; Balaban et al. 2011). FlhF and FlhG are known to collaborate in several species and in *Vibrio cholerae* it was shown that FlhF recruits one of the earliest components of the flagellum, FliF, to the cell pole (Bange et al. 2007; Kusumoto et al. 2008; Schniederberend et al. 2013; Green et al. 2009).

FliF forms the MS-ring within the cytoplasmic membrane and acts as scaffold for the next element, the C-ring, consisting of FliG, FliM and FliN. At the same time, the cytoplasmic type III secretion system (TTSS) is also assembled. One component of the export apparatus, FlhA, probably localises at the assembly site even before FliF (Li et al. 2011). The first components outside of the cytoplasmic membrane are the rod proteins and, as such, they are using the flagellar TTSS, except for the P- and L-ring proteins, which are secreted through the Sec pathway (Chevance et al. 2008). Together, the cytoplasmic membrane-associated parts and the rod

form a pore that reaches through the whole cell envelope and allows secretion and assembly of the hook components, mainly the hook filament protein FlgE (Cohen et al. 2014). The rather precise length of the hook (~ 55 nm), which is required for correct function, is achieved by measuring the length with a “molecular ruler” (FliK), that is frequently inserted into the growing hook and secreted thereby. During this process, the N-terminus of FliK interacts with the hook cap structure, which slows down the secretion process. Hence, as soon as the hook has the correct length, the C-terminal domain of FliK is positioned in close proximity to the substrate-specificity-determining component of the fTTSS, FlhB, and the interaction induces the switch of the secretion specificity (Hirano et al. 1994; Minamino et al. 2006; Ferris et al. 2006; Erhardt et al. 2011). The completion of the hook-basal body complex is also an important intermediate checkpoint for all flagellated bacteria, which is followed by the very high production of the filament building blocks, the flagellins (Hughes et al. 1993). To prevent premature aggregation of flagellin monomers in the cytoplasm, the flagellin-specific chaperone FliS binds to the C-terminal region of flagellin, which is important for polymerisation, and facilitates its export by the fTTSS (Yokoseki et al. 1995; Auvray et al. 2001; Ozin et al. 2003; Muskotál et al. 2006). Flagellin monomers are then diffusing through the narrow channel formed by the hook-basal body complex and the growing filament in an unfolded or semi-unfolded state and self-assemble at the tip with the help of the pentameric cap protein FliD (Iino 1969; Yonekura et al. 2000). The filament growth is controlled by an injection-diffusion mechanism and the length is determined by the rate at which the filament growth decreases (Iino 1974; Renault et al. 2017; Hughes 2017).

2.4.2. Hierarchical regulation of flagellar assembly

Three-tiered hierarchy

The assembly of the flagellum is organised in a transcriptional hierarchy that ensures that flagellar components are only produced once the preceding intermediate states are completed (McCarter 2006). The paradigm for enteric bacteria is the three-tiered assembly scheme of *S. enterica*, which is based on three distinct classes of promoters and regulators. The flagellar master regulators FlhD and FlhC are expressed in class I, likely depending on the housekeeping sigma factor σ^{70} (Yanagihara et al. 1999). Together with σ^{70} , FlhDC activate the transcription of the class II genes, including structural parts of the basal body as well as the two regulators for class III genes, σ^{28} (FliA) and its anti-sigma factor FlgM (Kutsukake et al. 1990; Ohnishi et al. 1990; Gillen et al. 1991). Transcription of class III genes strictly requires active FliA, which is sequestered by FlgM as long as FlgM is present in the cytoplasm (Chadsey et al. 1998). Once the hook-basal body intermediate is completed, FlgM gets exported by the fTTSS and the sigma factor FliA is no longer inhibited (Hughes et al. 1993). The final class of flagellar genes comprises the structural components of the filament, mainly the flagellins, as well as the stator complexes and chemotaxis-related regulatory factors (Fitzgerald et al. 2014).

Four-tiered hierarchy

Many other bacteria, including *Pseudomonas* or *Vibrio* species, have a four-tiered transcriptional hierarchy with an additional checkpoint after the rod assembly is initiated (Dasgupta et al. 2003; McCarter 2001, 2006). Another difference is the requirement of the alternative sigma factor σ^{54} and the corresponding enhancer binding protein (ebp) FleQ in *P. aeruginosa* and FlrA in *V. cholerae*, which act as flagellar master regulators in these organisms (Prouty et al. 2001; Hickman et al. 2008). These ebps form hexameric ring structures and bind between 100 and 200 bp upstream of the σ^{54} -dependant promoter, which induces transcription in

an ATP-dependant manner (Morett et al. 1993; Wigneshweraraj et al. 2008; Bush et al. 2012). These class I regulators activate transcription of structural components of the basal body in class II and the regulators for class III, FlrB and FlrC, which in turn activate transcription of more basal body parts for completion of the hook-basal body complex (Dasgupta et al. 2003; Wilhelms et al. 2011). The sigma factor σ^{28} for class IV promoters (FliA) is also expressed in class II and its activation mechanism via the secretion of its anti-sigma factor FlgM is similar to that of enteric bacteria. Likewise, the final class of genes in this four-tiered regulation hierarchy comprises filament building blocks, stator complexes and chemotaxis components (McCarter 2001, 2006; Wilhelms et al. 2011).

3. Flagella-mediated motility

3.1. Swimming in liquid

3.1.1. Basic conditions

Swimming in liquid is the paradigm for flagella-mediated movement. This type of motion (both by eukaryotes and prokaryotes) was the first to be observed, as soon as the early microscopes were available (Van Leeuwenhoek 1683), and considerable research began in the 19th century. Swimming in liquid, like water, buffer or nutrient broth, allows cells to move freely in all directions, and scientists can observe them easily with standard microscope equipment. Most of what is known about bacterial swimming was acquired by studying the cells under such conditions, typically by monitoring the swimmers in two dimensions or, much more advanced and more accurate, in three dimensions using tracking microscopes (Berg 1971) or physical principles and digital techniques (Garcia-Sucerquia et al. 2006; Wilson et al. 2011; Molaei et al. 2014; Taute et al. 2015). For many bacteria this experimental setup is likely accurate and resembles their natural habitat reasonably well, especially for aquatic bacteria (Leifson et al. 1964). However, many bacteria use their flagella to swim or move in different, more complex environments and studying their particular navigation mechanisms requires more accurate experimental adaptations to the cells' natural habitats (Raatz et al. 2015). Yet, those investigations in unrestricted liquid environments uncovered many aspects and mechanisms of how flagella work.

A volume of liquid allows cells to move more or less unrestricted in all direction and at the small size of (most) bacteria they only need to overcome the viscous drag of the surrounding medium, while inertia of their own mass plays almost no role (Purcell 1977, 1997). Without solid boundaries blocking the way frequently, cells can take advantage of higher swimming speeds on their quest for nutrients. On the other hand, nutrients are scarce and a significant amount of the available energy is spent for movement (Mitchell 1991, 2002). Small nutrient patches also dissipate quickly, so aquatic bacteria need an efficient chemotaxis system and a way to not "overshoot" (Stocker et al. 2008). Finally, solid objects and surfaces play an important role as well, as many nutrient sources are linked to larger organisms, like algae and higher eukaryotic organisms (Kogure et al. 1981; Rohwer et al. 2002; Ramanan et al. 2016). Thus, swimming mechanisms to find nutrients efficiently and fast, as well as strategies to stay near the nutrients, either by efficient chemotaxis or by attachment and colony formation, are required.

3.1.2. High efficiency motor rotation

One example for very efficient swimmers in freshwater environments are the swarmer cells of *Caulobacter crescentus*. They convert the proton-motive force that drives the rotation of the flagellar motor much more efficiently into torque than for example *Escherichia coli* or *Vibrio alginolyticus* (Li et al. 2006). The secret is to rotate the motor below a certain rate that still provides nearly 100 % efficiency. Above this rate the torque gain decreases while the increase of energy consumption remains constant. Thus, rotation rates above this “knee rate” are less efficient in terms of the torque-energy consumption ratio (Chen et al. 2000; Li et al. 2006). As *Caulobacter* swarmer cells produce only one flagellum and hence, the critical energy consumption is the movement and not the assembly (Mitchell 1991, 2002), this tradeoff between swimming efficiency and speed is an optimal adaption to its nutrient-poor habitat.

3.1.3. High efficiency navigation

Other bacteria from marine habitats were shown to benefit from their particular *run-reverse-flick* turning mechanism (cf. section 4.2.2) that comes with having just one polar flagellum (monotrichous) and not being able to tumble like bacteria that have multiple flagella all over the cell body (peritrichous). Because of the *flick* mechanism the effective diffusivity of *V. alginolyticus* is less than half of that of *E. coli*, meaning that its exploration capabilities are less effective than those of *E. coli* (Stocker 2011). This seems counterintuitive at first, but both *V. alginolyticus* as well as *Pseudoalteromonas haloplanktis*, another marine monotrichous bacterium, can outperform *E. coli* in terms of chemotaxis towards nutrient patches (Stocker et al. 2008; Xie et al. 2011). Xie et al. were able to show that *V. alginolyticus* can rapidly modulate the forward and backward run times, allowing the cells to correct mistakes, i.e. a *flick* that directs the cell down a nutrient gradient. In a later, theoretical work they further elaborated that forward and backward intervals during the three-step *run-reverse-flick* navigation cycle are beneficial in environments with scarce and erratically distributed nutrient patches (Xie et al. 2014). Other marine bacteria were even shown to be able to track a swimming algae due to their rapid chemosensory response (Barbara et al. 2003; Locsei et al. 2009). Using this dual strategy, the *run-reverse-flick* navigation coupled with the fast responding chemotaxis system, marine bacteria similar to *V. alginolyticus* or *P. haloplanktis* are ideally adapted for the hunt for nutrients in an environment that allows unrestricted swimming in all directions but also poses the challenge of widely distributed nutrient patches.

3.1.4. High efficiency propulsion

A common strategy in terms of efficient swimming of marine and freshwater bacteria is the use of a single polar flagellum in general. As already mentioned, in nutrient-scarce environments the critical energy consuming factor is the maintenance of flagellar rotation, rather than its biosynthesis (Mitchell 1991, 2002). Whereas bacteria were found to use multiple, usually proton-driven peritrichous flagella to move through viscous environments or over surfaces (McCarter et al. 1988, 1990; Atsumi et al. 1996; Darnton et al. 2007a), especially marine bacteria rather use a single sodium-driven flagellum at the cell pole for much faster motor rotation and swimming in liquids (Magariyama et al. 1994; Ping 2012). Using several flagella is not only more costly to assemble but also to rotate and for bacteria living in aqueous oligotrophic environments, like oceans or bodies of freshwater, they do not even provide a reasonable benefit. First of all, although multiple flagella do generate more torque than just one flagellum, the torque generated by the individual flagella does not add up. In a bundle of flagella, like in *E. coli*, each flagellum only produces roughly one third of the torque compared to a single flagellum (Darnton

et al. 2007a). In other words, powering multiple flagella as a bundle is less energy-efficient. The placement of the flagellum right at the cell pole is also an important speed determining factor as a single flagellum at a subpolar or lateral position dissipates energy into off-axis cell body rotation, i.e. wobbling (Darnton et al. 2007a). Furthermore, multiple flagella might be necessary to generate enough torque to drill through very viscous or structured environments (Atsumi et al. 1996; Darnton et al. 2007a), but during free swimming in liquid media shear and Brownian motion are the prevalent forces that restrain and redirect the cellular movement (Stocker 2011; Ping 2012). Therefore, the most efficient way to move in a volume of liquid seems to be the use of just one polar flagellum, with a motor adapted to high rotation rates and speed (Magariyama et al. 1994; Atsumi et al. 1996), coupled with a fast responding navigation system that relies on both the particular *run-reverse* or *run-reverse-flick* turning (Stocker 2011) as well as on the fast speed of the swimmer (Son et al. 2016). By this strategy cells can minimize the cost of flagellar biosynthesis and actuation, while providing a highly efficient propulsion mechanism well-adapted for liquid environments.

3.2. Moving in structured environments

3.2.1. Basic conditions

Moving in structured environments, like soil, viscous or mucosal media in animal hosts or surfaces in general, poses some fundamental differences compared to swimming in a body of liquid. First of all, such structured environments very often do not allow unrestricted movement in all directions, sometimes requiring more force to get through constricted spaces, but also navigation capabilities that allow going around obstacles or reversing from dead ends. On the other hand, those environments are usually nutrient-rich, allowing cells to produce and maintain multiple flagella (Wilson et al. 1993).

3.2.2. Making use of multiple flagella

Many bacteria associated with structured environments are known to produce several flagella, all over the cell body (peritrichous), like in the genera *Escherichia*, *Salmonella* and *Bacillus*, or located at one pole (lophotrichous), like in *Helicobacter pylori* and *Pseudomonas putida*, to give just a few examples (Leifson 1960; Adler 1965; Warren et al. 1983; Harwood et al. 1989). Of course, there are also exceptions, such as the soil bacterium *Pseudomonas fluorescens*, which usually grows one polar flagellum, but can have two as well (Ping et al. 2013). *Bradyrhizobium lupini* and *Sinorhizobium meliloti* possess multiple lophotrichous flagella as well, but these show a more complex structure than the flagella of *E. coli* and *Salmonella* and are thought to be more rigid and thus provide an even better propulsion in viscous environments (Götz et al. 1982). Typically, although not generally true, bacteria with multiple flagella outperform bacteria with a single flagellum in media with increased viscosity (Leifson 1960; Schneider et al. 1974). Even though the generated torque of many flagella does not perfectly add up it is still beneficial in high viscosity and as long as enough nutrients are available energy inefficiency isn't too much of a problem (Darnton et al. 2007a; Son et al. 2013).

Dual flagellation

The predominant flagellation pattern of marine and limnic bacteria is monopolar, however, some of them possess two sets of flagella. The polar one is used for swimming in unrestricted liquids and the alternative one, producing lateral (or peritrichous) flagella, for swimming in viscous media or swarming over surfaces, like in *Vibrio parahaemolyticus*, *Vibrio alginolyticus* or different *Aeromonas* species (McCarter et al. 1988, 1990;

Atsumi et al. 1996; Kirov et al. 2002; McCarter 2004). Many other bacteria also possess secondary flagellar systems which are expressed under diverse conditions, such as anaerobic growth, low temperature or high nutrient availability and were likely acquired by gene duplication or horizontal gene transfer (Poggio et al. 2007; Wang et al. 2008; Bubendorfer et al. 2012; Liu et al. 2007). For *Shewanella putrefaciens* it was shown that the lateral flagella modulate the turning angle and thus alter the navigation pattern, which improves spreading in structured environments (Bubendorfer et al. 2012, 2014).

3.2.3. Swarming over surfaces

A very clear morphological adaption due to changes in the environmental conditions and hence, the demands on the motility apparatus can be seen in bacteria that are able to swarm across wet surfaces. Swarming motility is a multicellular, flagella-driven movement that is characterised by a fast spreading of the colony at a macroscopic scale (Henrichsen 1972). It involves a clear cell differentiation from a bulk liquid swimmer cell to a surface swarmer cell that comes with the production of additional flagella and usually a surfactant that lowers the surface tension, sometimes also with the elongation of the cell body (Kearns 2010). Peritrichously flagellated bacteria, like *Proteus mirabilis*, *Escherichia coli*, *Salmonella enterica* or *Bacillus subtilis* produce more of their regular flagella (Hoeninger 1965; Harshey et al. 1994; Kearns et al. 2003). Monotrichously flagellated bacteria rather express an alternative set of genetically distinct flagella (see above; McCarter 2004). However, not all polarly flagellated bacteria with a second set of lateral flagella can swarm (Bubendorfer et al. 2012). The lack of surfactant production, for example due to a mutation in the corresponding gene(s), can already abolish swarming completely (Kearns 2010). Furthermore, the monopolarly flagellated bacterium *Pseudomonas aeruginosa* is capable of swarming motility without a second set of lateral flagella. Instead, it produces additional polar flagella and adjusts its motor by using a second set of stators, which generate higher torque (Toutain et al. 2005). Flagella-mediated swarming provides much faster translocation over surfaces than for example pili-mediated movement, but it also comes with increased costs for flagellar assembly and rotation. Interestingly, many of the known swarming-capable bacteria are associated with aqueous habitats, which indicates that these bacteria face changing environments from bulk fluids to interfaces between surfaces and liquids (Copeland et al. 2009).

Under laboratory conditions on hard-agar plates, different organisms can form very distinctive swarming patterns, like *bullseye*, *vortex* or *dendrites*, depending on environmental condition and cellular behaviour (Kearns 2010). Some strains even form clear lines between two approaching swarming colonies, known as the *Dienes phenomenon* (Senior 1977; Budding et al. 2009). At the microscopic scale, the cells move as multicellular rafts, more or less as a single layer of cells, through the secreted surfactin. They are propelled by flagella, which, although rotating in the wet surface film, do interact with the substrate surface and in some cases also with the flagella of adjacent cells forming intercellular filament bundles (Jones et al. 2004). Under these circumstances, even *E. coli* was found to back up from dead ends, which usually is not seen in peritrichous bacteria (cf. section 4.2.1; Turner et al. 2010).

3.2.4. Spreading in soil

Soil is one of the most complex and diverse environments that is found on earth, with large spatial and temporal variations in water, oxygen and nutrient availability, but also temperature as well as physical and chemical composition (Torsvik et al. 2002; Young et al. 2004; Or et al. 2007). Soil comprises a solid phase, consisting of

minerals and organic matter particles, and an aqueous phase with dissolved minerals, gasses and nutrients (Downie et al. 2012). Motility is heavily restrained by the solid phase, and temporary liquid films and pockets are essential for flagella-mediated motility (Griffin et al. 1968; Soby et al. 1983; Or et al. 2007; Wang et al. 2010). Maintaining flagella still makes sense even with decreasing water content, as they promote surface attachment and microcolony formation, which is believed to be the prevalent lifestyle in unsaturated soils (Chang et al. 2003; Young et al. 2004). With decreasing water saturation the actual swimming becomes more and more limited and other forms of motility become more important, including surface swarming in thin liquid films, but also non-flagella-mediated movement, like twitching, gliding and sliding/surfing (Harshey 2003; Hennes et al. 2017).

Major limiting factor of motility

Despite the relatively harsh and ever-changing conditions in soil, it probably supports the highest density as well as diversity of prokaryotes of all biosphere compartments, and motility, including flagellar propulsion, is an important factor for survival (Whitman et al. 1998; Or et al. 2007; Barahona et al. 2010). Active movement, although restricted, plays a crucial role for colonisation of plant roots by bacteria living in the rhizosphere (Czaban et al. 2007). This was shown for bacteria with just one polar flagellum (Weger et al. 1987; Turnbull et al. 2001; Ping et al. 2013) as well as for bacteria with multiple flagella (Scher et al. 1985; Catlow et al. 1990). This is interesting because single polar flagella are rather considered to be an adaption to aquatic environments (Xie et al. 2011; Ping 2012; Son et al. 2013), whereas multiple flagella are supposed to be beneficial in viscous and structured environments (Darnton et al. 2007a). In soil, however, motility decreases rapidly with decreasing water content because viscous and capillary pinning forces become stronger than the flagellar propulsion (Dechesne et al. 2010; Tecon et al. 2016). Furthermore, the minimal water potential that is required for flagella-mediated movement is very similar for bacteria with different number and arrangement of flagella (Dechesne et al. 2010; Tecon et al. 2016). This means that the global framework for motility is rather set by the physical properties of the soil than by individual flagellation of different bacteria. Those differences still play a role, but the exact benefits and mechanisms are not yet well understood.

Fungal highways

Pinning forces due to low water potential are not the only inhibiting factors for motility. The lack of connectedness of water reservoirs can also limit exploration range and dispersal of bacteria in soil (Wang et al. 2012). It was thus hypothesised that cellular movement in soil is restricted to hydrated microenvironments, with only rare flooding events expanding bacterial dispersal (Or et al. 2007; Dechesne et al. 2010; Tecon et al. 2016). However, bacteria have found other ways to overcome physical barriers such as air-filled pores. Several soil bacteria were reported to disperse along fungal hyphae (Kohlmeier et al. 2005; Wick et al. 2007; Furuno et al. 2010; Warmink et al. 2011) and the flagella were indeed accounted for increased dispersal in the unsaturated hyphae network (Pion et al. 2013). Although the maintenance of flagella might be energy-intensive and individual cellular motility is very restricted in unsaturated soil, rare water saturation events as well as the use of “fungal highways” compensate for the energy costs and increase the fitness of flagellated soil-inhabiting bacteria (Dechesne et al. 2010; Pion et al. 2013). Additionally, roles of flagella other than providing motility, such as biofilm formation, cell-surface and cell-cell interaction, likely play a role as well (Pion et al. 2013).

3.2.5. High torque motors for high viscosity

A whole class of motile bacteria, the ϵ -proteobacteria, are adapted to swimming at high speed in very viscous media that immobilise many other motile bacterial species. Members of the ϵ -proteobacteria are found in the digestive tracks of animals, where they need to move through mucous or tissue (Kiehlbauch et al. 1991; On 2001; Baar et al. 2003; Lertsethtakarn et al. 2011; Sterzenbach et al. 2008), but they also inhabit marine hydrothermal vents, sediments and other structured environments (McClung et al. 1983; Fera et al. 2004; Kodama et al. 2004; Takai et al. 2006; Sikorski et al. 2010). Although ϵ -proteobacteria generally have fewer flagella, typically one or a few at polar positions, they outperform peritrichous bacteria with multiple lateral flagella, even at very high viscosities (Hazell et al. 1986; Ferrero et al. 1988; Fenchel 1994). In viscous media that completely immobilise *E. coli*, *Campylobacter jejuni* and *Helicobacter pylori* swim at a speed higher than *E. coli*'s fastest general swimming speed (Hazell et al. 1986; Ferrero et al. 1988). *Helicobacter felis* is even capable of propelling itself between tissues (Lee et al. 1988). It is believed that a much higher torque generation enables ϵ -proteobacteria to move under such restricting conditions. The flagellar swimming torque of *H. pylori* is approximately three times higher than the torque of *E. coli* (Reid et al. 2006; Celli et al. 2009). Furthermore, the polar positioning of the flagella is important for full motility, but surprisingly, the spiral cell body shape was found to contribute only marginally to swimming in viscous media (Sycuro et al. 2010; Constantino et al. 2016). The higher torque generation probably originates from a more complex and significantly wider flagellar motor that can hold much more stator units at a considerably wider diameter than motors of enteric bacteria, like *E. coli* or *S. enterica* (Schuster et al. 1992; Hizukuri et al. 2010; Chen et al. 2011; Reboul et al. 2011; Beeby et al. 2016; Chaban et al. 2018).

3.2.6. Propulsion by cell body rotation and deformation

In all the examples mentioned so far, the flagellar filaments were always the primary propeller that rotate in the liquid surroundings of the cell body to generate thrust. But this is not the only way that flagella can contribute to motility. Spirochetes are long, thin bacteria that have a spiral or wave-like shape and they do move by the rotation of flagella, however, the filaments are located between the periplasmic cylinder and the outer membrane sheath and propel the cell by counterrotating or undulating the cell body (Li et al. 2000a; Wolgemuth 2015). Apart from the function as organelles of locomotion, the periplasmic flagella of spirochetes are also important as structural elements: Either the whole cell body shape is determined by the shape of the flagella, as in *Treponema denticola* (irregular spiral; Ruby et al. 1997) and *Borrelia burgdorferi* (flat wave; Goldstein et al. 1994), or only the polar ends, as in *Leptospira interrogans* (hook- or spiral-shaped polar ends; Bromley et al. 1979; Picardeau et al. 2001). The exact mechanism of how internal flagella propel the cell differs from species to species and is still not fully understood (Li et al. 2000a; Wolgemuth 2015). The most simple case is probably *T. denticola*, which has approximately two left-handed flagella attached at each cell pole that rotate counterclockwise (viewed from behind the moving cell; Charon et al. 1992). This results in backward propagating helical or irregularly shaped waves as well as counterrotation of the cell body, which translates *T. denticola* quite efficiently in gel-like medium (Ruby et al. 1998; Li et al. 2000a). The shape of *B. burgdorferi* is a flat-wave rather than a spiral, however, the propulsion mechanism is quite similar: Several flagella at each cell pole rotate counterclockwise around the cell axis and the cell body counterrotates but also deforms which generates backward moving flat waves (Goldstein et al. 1994, 1996; Vig et al. 2012). Other spirochetes have more complex movement patterns, like *L. interrogans*, which moves by gyrating differently-shaped opposite cell poles. The leading cell pole is shaped like a spiral, because very short periplasmic flagella are rotating

counterclockwise (viewed along the flagella towards the motor) and the lagging cell pole is shaped like a hook, because the flagella rotate clockwise (Noguchi 1918; Goldstein et al. 1990). The cells can switch swimming direction by inverting the sense of flagellar rotation and thus the cell pole shape and they become non-motile when the flagella from opposite cell poles rotate in the same direction (Berg et al. 1978; Goldstein et al. 1990). Therefore, the differently shaped cell poles and the counterrotation of the cell body are important for directed motion of *L. interrogans* and similar spirochetes.

Although these movement strategies only allow for slow swimming in water-like liquid ($\sim 2 - 15 \mu\text{m/s}$), spirochetes are able to move very efficiently through skin, break through epithelial barriers and into and out of blood vessels and can even cross the blood-brain barrier (Wolgemuth 2015). The robust propulsion capability of *B. burgdorferi* through dense materials even allows translation through a gelatin matrix with pore sizes below 70 nm, which is much smaller than its cell body diameter of about 300 nm. This makes pathogenic spirochetes like *B. burgdorferi* and *T. denticola* some of the most invasive mammalian pathogens (Botkin et al. 2006; Lin et al. 2014).

4. Swimming and turning mechanisms

Flagella-mediated swimming is driven by the rotation of a helical filament which is powered by a proton- or sodium-motive force (Manson et al. 1977; Hirota et al. 1983; Kojima et al. 1999). The motor rotation rates can differ quite considerably in different bacteria, with *Salmonella enterica* and *Escherichia coli* rotating each filament with $\sim 200 - 300 \text{ Hz}$ and *Vibrio alginolyticus* with $\sim 1700 \text{ Hz}$ (Lowe et al. 1987; Kudo et al. 1990; Magariyama et al. 1994). Cells can reach very fast swimming speeds ranging from about 25 to 75 $\mu\text{m/s}$ in commonly examined bacteria, such as *Escherichia coli*, *Pseudomonas aeruginosa* or *Vibrio cholerae*, up to 700 $\mu\text{m/s}$ in the peculiar bacterium *Ovobacter propellens* (population average speeds; Darnton et al. 2007a; Shigematsu et al. 1995; Fenchel et al. 2004). But swimming forward, no matter how fast, is just a fraction of what bacteria need to achieve to reach their destination. Just as important is how they change direction, which is heavily influenced by the number and location of flagella, but also how swimming and turning cycles are controlled by the chemotactic system.

4.1. General mechanism of thrust generation by a rotating flagellum

4.1.1. Low Reynolds number regime

Bacteria and other microorganisms generate thrust in liquid in a very different way than we and other large animals do. They have to, because the physical constraints are very different at the scale of a microorganism. This can be described by the Reynolds number, which is the ratio of the inertial forces to the viscous forces. The inertial forces are proportional to the dimension as well as to the speed of the swimmer, so for a microscopic organism moving at low speed the inertial forces are very small. Typical Reynolds numbers for bacterial propulsion are $\sim 10^{-4}$ to 10^{-5} , while for us the Reynolds number would be $\sim 10^4$ (Purcell 1977). In other words: While we rely on inertial forces to propel ourselves in fluids, inertia is almost negligible for bacteria and other microorganisms. We generate thrust by accelerating fluid, thereby coasting for a while after we stop moving. Microorganisms generate thrust by viscous shear and come to a stop almost immediately after they stop moving ($\sim 0.1 \mu\text{s}$; Purcell 1977). For us, this would be somewhat comparable to swimming

in a pool of molasses moving no part of our body faster than 1 cm/min. Also, in the low Reynolds regime it doesn't matter how fast one moves, if one redoes the past movements, one will always return to the same initial position. Purcell illustrated this with his famous scallop theorem: Imagine a macroscopic scallop with a hinge at one edge of the shell. If it opens the shell slowly and then closes it rapidly it would first move just a short distance mouth-first and then coast a large distance hinge-first (because of its inertia). A microscopic scallop, on the other hand, would simply retrace its steps, because the viscous forces dominate and it would not be able to coast (Purcell 1977). A real scallop actually moves by a different mechanisms, but the image exemplifies the discrepancy between propulsion in low and high Reynolds number regimes quite well.

These physical constraints at microscopic scales ultimately have a number of implications for swimming microorganisms: First, they can not use reciprocal motion, like the scallop, but rather have to use non-reversible, asymmetric motion, like the rotation of a helix (as long as you keep rotating) or the breast-stroke motion of the unicellular algae *Chlamydomonas reinhardtii*. It moves its flagella far away from the cell body during a power stroke but close to the cell body during a recovery stroke, which is a cyclic but asymmetric motion (Ringo 1967; Berg 2004). The second important implication is that inertia is negligible, so every motion is determined by the forces exerted at the moment and all the forces have to be balanced, because otherwise the microorganism would accelerate, which it does not (Purcell 1977). Finally, although this is more important for chemotaxis than for propulsion, movement of the liquid surrounding the cell body is strongly decreased due to interference with the cell surface (Shapiro 1961; Purcell 1977). So if a microswimmer moves, it takes its nearby liquid environment along and it only gradually falls behind. This means that the transport of molecules to and from the cell body is entirely controlled by diffusion (Purcell 1977).

4.1.2. Generating thrust

The fundamental mechanism to generate forward thrust is identical in all flagellated bacteria, no matter if they possess only a single flagellum or several flagella that form a bundle and thus almost behave like a single filament. We now know, of course, that the filament or filament bundle is rotating, thus propagating helical waves along the filament axis (Fig. 4). However, that was not obvious for a surprisingly long time. Up to the 1970s, many scientists were more convinced that the helical filament is waving or wobbling, similar to the waving or beating of eukaryotic flagella and cilia. This probably has to do with the fact that when scientists had begun to seriously investigate the motion of the propulsive organelles of microorganisms, they only observed the filaments extending from the cell surface, both from eukaryotes and prokaryotes alike, and they couldn't know that they are of fundamentally different structure. The first theory about how motion could be achieved was developed for flagellated eukaryotes and later adapted to flagellated prokaryotes (Bütschli 1884; Buder 1915). This theory stated that there must be contracting filaments that go around the helix in a circular fashion, thus deforming the helix periodically so that it propagates waves along its axis. Nobody could imagine a rotating joint that connects the filament and the cell body, especially for peritrichous bacteria with filaments coming out of the cell body in all directions. The key experiments that proved that prokaryotic flagella are indeed rotating were done by cross-linking filaments with antibodies as well as linking two cell bodies together via the hook and anti-hook antibodies (Greenbury et al. 1966; DiPierro et al. 1968; Silverman et al. 1972; Berg et al. 1973). Later, a similar approach was used to tether cells to glass, which finally demonstrated the correlation between counterclockwise (CCW) rotation and runs and between clockwise (CW) rotation and tumbles in *E. coli* (Silverman et al. 1974; Larsen et al. 1974).

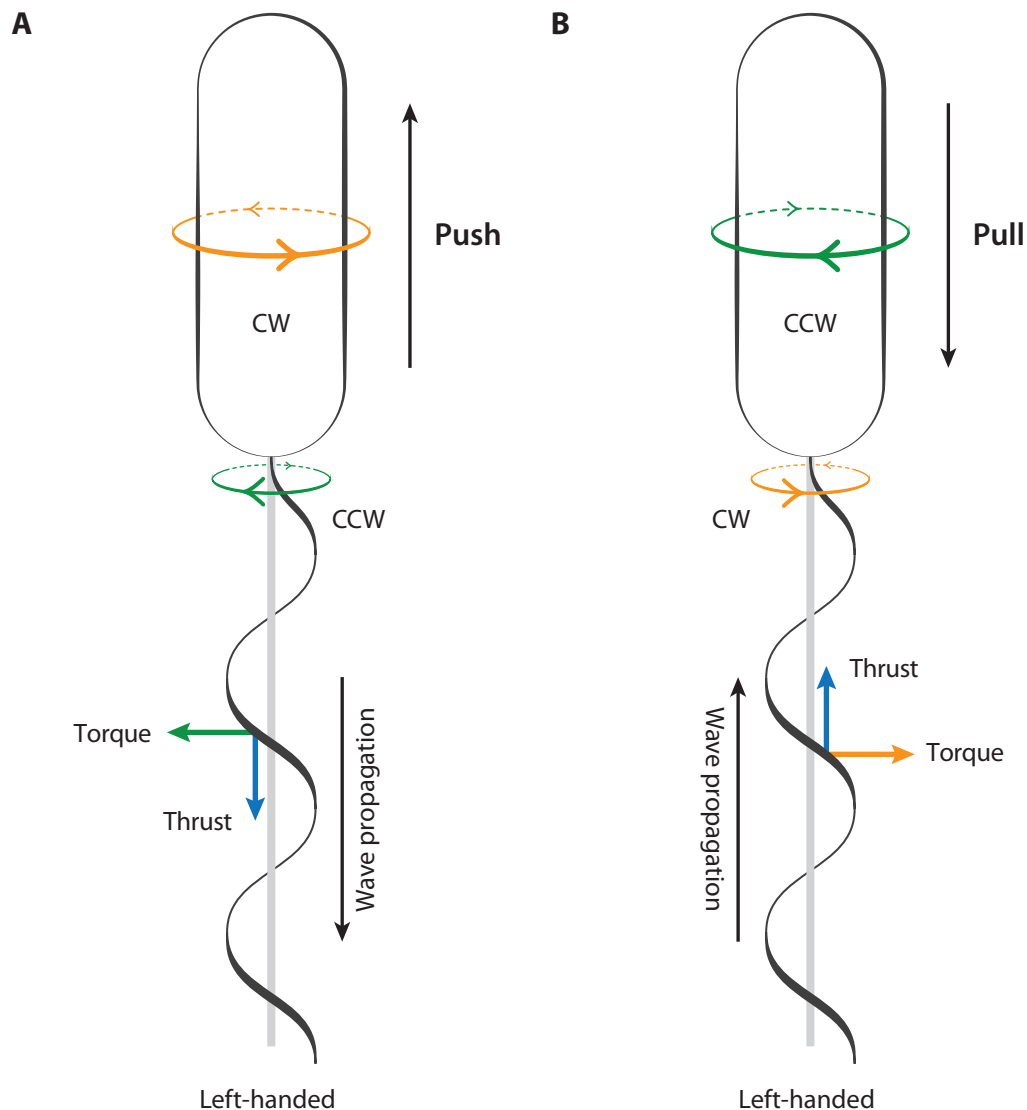


FIGURE 4. General mechanism of thrust generation with a rotating helical filament. A A left-handed helix is rotated at its base at the cell pole in a counterclockwise direction (CCW; viewed from behind the cell body) which generates waves propagating away from the cell body. The helical segments exert force on the liquid, which has components perpendicular and parallel to the helical axis (grey line). The perpendicular components generate torque and the parallel components generate thrust that pushes the cell forward. The rotation of the flagellar filament is balanced by the clockwise (CW) counterrotation of the cell body. **B** If the helix is rotated in the CW direction and the handedness remains left-handed, the waves propagate towards the cell body and the forces are inverted, now pulling the cell body backwards. The counterrotation of the cell body is also inverted (CCW). Based on Buder 1915.

Forward swimming

The mechanism to generate forward thrust is exemplified in Fig. 4 A for a left-handed helix, but it works analogously for right-handed helices rotating in the opposite direction. The left-handed helix is rotated at its base in a counterclockwise direction, viewed from behind the cell body. This causes helical waves to propagate away from the cell body towards the tip of the helix. If one considers only a tiny segment of the filament, it behaves like a straight rod moving to the left and further around the helical axis (green arrow). This segment exerts a force on the liquid which has components parallel (blue arrow) as well as perpendicular (green arrow) to the helical axis. While rotating, the forces generated in the parallel direction add up, providing thrust that

pushes the cell body forward. The forces generated in the perpendicular (or rather circumferential) direction also add up, averaging to zero in one helical turn and generating torque. When the cell is swimming at constant speed, all the forces acting on it must balance, otherwise it would accelerate. Therefore, the thrust generated by the filament must be balanced by the viscous drag due to the translation of the cell body and the torque must be balanced by the viscous drag due to the counterrotation of the cell body. As the cell body is very large compared to the flagellum, it rotates more slowly in the opposite direction (CW in this case). For example, an *E. coli* cell rotating its flagellar bundle CCW at ~ 100 Hz would rotate CW around its cellular length axis at ~ 10 Hz (Berg 2004).

Backward swimming

As a basic principle, all the forces can be inverted by inverting the direction of helix rotation (here: from CCW to CW; Fig. 4 B). The waves are then propagating towards the cell body and thrust is generated by the sum of the axial components again, now in the opposite direction pulling the cell body backwards. Torque is also generated in the opposite direction, so the cell body counterrotates in the opposite direction as well (CCW in this case). However, this is only true as long the handedness and the overall geometry of the helix remain the same, which in fact is the case for quite a lot of species. If the handedness of the helix is inverted with a motor reversal (due to the opposite-handed torsional forces of the viscous drag), the waves propagate away from the cell body again and the generated thrust pushes the cell body forward. Rigid flagellar helices that can pull a cell body have already been observed a hundred years ago and by now the basic mechanism of a helix that retains its handedness during reverse rotation is generally accepted (Buder 1915; Goto et al. 2005). Taken together, the handedness of the helix determines if CCW or CW rotation generates forward thrust and the rigidity of the helix determines if motor reversals generate thrust in the opposite direction (for a stable helix) or if the handedness inverts, adopting a different polymorphic form (cf. Fig. 3) and continues to push in the same direction (for more unstable helices). Essentially, all of these options are possible and many can be seen in different species (see section 4.2 below).

4.2. Flagellation patterns and consequences for swimming

The mechanism described above enables bacteria to propel themselves forwards and potentially backwards, however, for full navigation capabilities cells also need to be able to change their swimming direction and to regulate when or rather how often they change it. The frequency of directional changes is controlled by the chemotaxis machinery (see 4.3), but the turning mechanism itself is inherent to the flagellum with distinct demands on basal body, hook and filament. By alternating smooth forward swimming and directional changes the cells execute a random walk and by modifying the run length they apply a bias to it, which ultimately takes them where they want to go (Berg et al. 1972). Chemotaxis, the response to chemical stimuli, was first studied extensively in *Escherichia coli* and *Salmonella enterica*, which change direction by a behaviour first named “twiddling” and later “tumbling” (Berg et al. 1972). Because most of the early work has been done with these peritrichously flagellated bacteria, tumbling is often used as a synonym for any turning mechanism. This is unfortunate because turning mechanisms are diverse and heavily depend on the flagellation pattern and on the properties of the hook and the filament. Figure 5 summarises some of the known swimming and turning behaviours that come with distinct flagellation patterns. Some of the underlying mechanisms are well understood, like for the peritrichously or polarly flagellated bacteria, others still pose a lot of questions. Ultimately, it is necessary to study the behaviour of the flagellar filament(s) during swimming and turning, which

requires high-speed microscopy and a way to actually see the filaments properly, for example by fluorescent labelling (Turner et al. 2000, 2016). Although this technique is available since almost 20 years, it still proves to be challenging and technical artefacts need to be ruled out vigorously.

4.2.1. Navigation with peritrichous flagella

The classical turning mechanism and the paradigm for swimming, navigation and chemotaxis is the *run-tumble* motion of peritrichous bacteria, mostly studied in *Escherichia coli* and *Salmonella enterica* (Fig. 5; Macnab et al. 1977; Turner et al. 2000). Peritrichously flagellated bacteria possess several flagella, in the given examples about four to six, scattered randomly all over the cell body (Adler 1965; Berg 1991). Forward swimming, termed *run*, is achieved by simultaneous counterclockwise rotation of all flagella as described above, with the filaments forming a bundle behind the cell body (Silverman et al. 1974; Larsen et al. 1974; Macnab 1977; Turner et al. 2000). The filaments aggregate because of hydrodynamic forces but also because of geometrical constraints (Machin 1963; Macnab 1977; Lim et al. 2012; Maniyeri et al. 2014). The bundle behaves almost like a single filament, although it performs not as efficiently probably because of lateral interaction of the filaments (Darnton et al. 2007a). The flagellar motors are distributed randomly over the cell surface so the rotational axes are all pointing straight out of the cell body. Hence, a flexible, rotational joint, the hook (cf. section 2.2), is essential to convert the angular rotation of the motors to the angular rotation of the filament bundle (Berg et al. 1973; Brown et al. 2012).

Tumbles

The forward runs last for about 1 sec for *E. coli* and are intermitted by short tumbling events, typically lasting 0.1 sec (Berg 2004). The tumbling results from at least one flagellum rotating in the opposite, clockwise, direction, thereby breaking out of the bundle and pointing in a random direction. When this left-handed helix is rotated CW, the right-handed torsional stress exerted on the filament by the viscous drag triggers the transformation to a right-handed configuration, usually in a sequence from semicoiled to curly, that doesn't necessarily need to be completed along the whole filament (cf. Fig 3; Macnab et al. 1977; Turner et al. 2000). Hence, the helical waves keep progressing away from the cell body and this flagellum keeps pushing the cell, however, in a different direction which turns the cell body by a random degree. This can be achieved by only one flagellum rotating CW, but also by several, which is affecting the turning angle (Turner et al. 2000; Berg 2004) and which is possibly another strategy to navigate up a gradient (Vladimirov et al. 2010). When all flagella return to CCW rotation the bundle rejoins and another run sequence starts. The cells don't have a preferred forward direction, so after a tumble either end goes first (Berg et al. 1995).

If all flagella rotate CW, which doesn't naturally happen, all helices convert to a right handed form, still pushing the cell body (Khan et al. 1978; Togashi et al. 1997). This means that bacteria with peritrichous flagellation, or rather generally with filaments that convert to the opposite handedness due to the viscous drag, are not able to reverse under normal conditions. Under conditions of spatial restriction however, both *B. subtilis* and *E. coli* can reverse by flipping the whole filament bundle over (Cisneros et al. 2006; Turner et al. 2010). They are not really swimming backwards, but rather backing up by switching their forward direction.

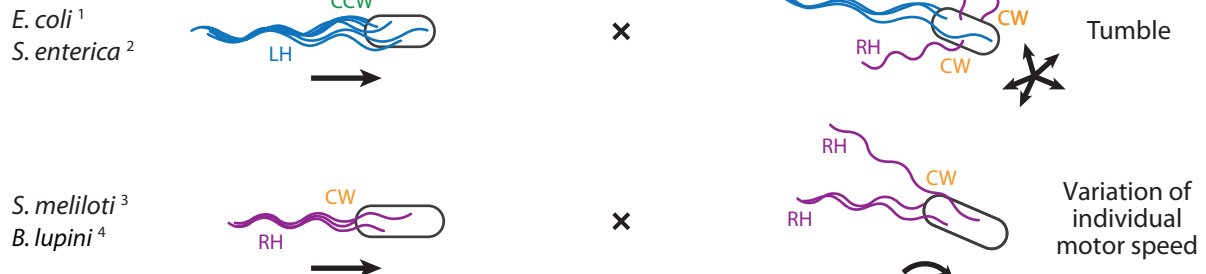
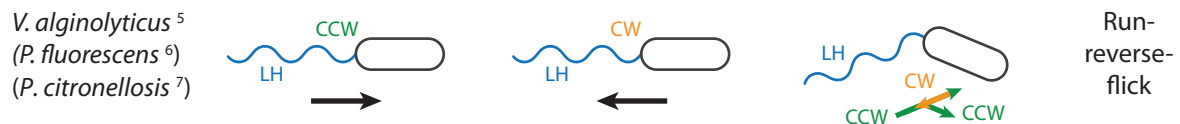
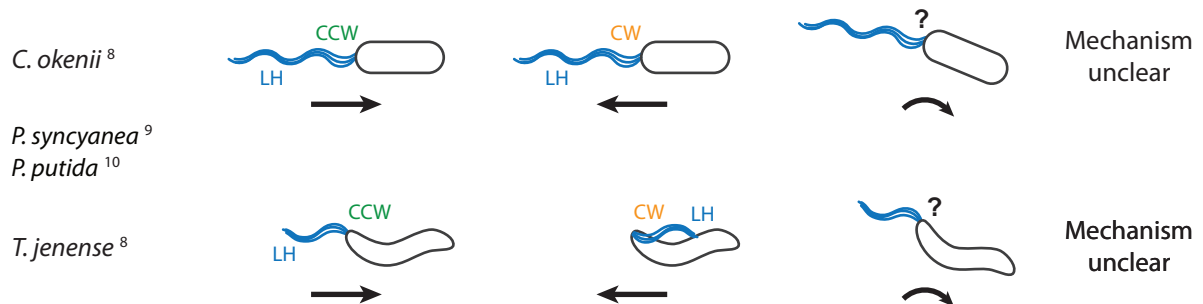
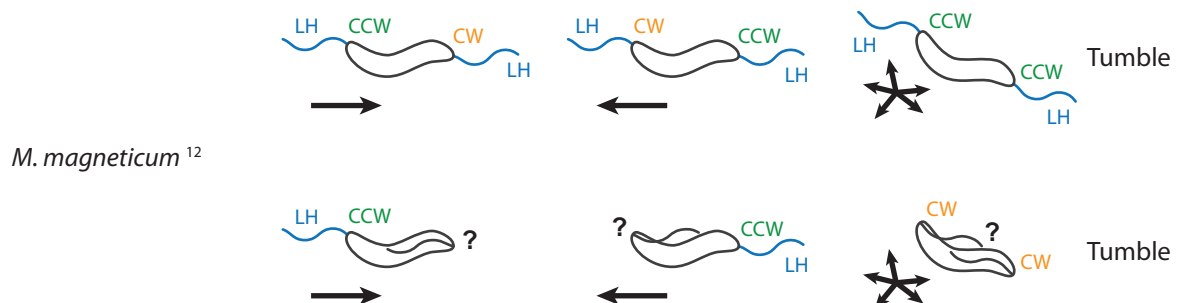
Flagellation**Peritrichous****Polar****Lophotrichous****Medial****Bipolar**

FIGURE 5. Swimming and turning with different types of flagellation. Only swimming and turning mechanisms (and the corresponding publications) are depicted that were studied with respect to cellular and flagellar filament behaviour. Depending on the configuration as well as the properties of the hook and filament different swimming and turning mechanisms are possible. Some bacteria can reverse by reversing the direction of motor rotation. For a detailed description see section 4.2. LH/RH: Left-/right-handed flagellum, CCW/CW: counterclockwise/clockwise motor rotation. The arrows indicate the swimming direction. Based on 1: Turner et al. 2000; 2: Macnab et al. 1977; 3: Götz et al. 1987; Armitage et al. 1997; 4: Scharf 2002; 5: Xie et al. 2011; Son et al. 2013; 6: Ping et al. 2013; 7: Taylor et al. 1974; 8: Buder 1915; 9: Reichert 1909; 10: Hintsche et al. 2017; 11: Armitage et al. 1997, 1999; 12: Murat et al. 2015.

Turning by motor speed variation

A special type of swimming and turning was described for *Sinorhizobium meliloti* and *Bradyrhizobium lupini*, which have two to ten complex flagella inserted peritrichously (Götz et al. 1982; Scharf 2002). These flagella are more rigid and locked in a right-handed configuration, but forward thrust is generated analogously to *E. coli* and *Salmonella*, just in a CW sense (Götz et al. 1987; Scharf 2002). CCW rotation, on the other hand, was never observed. Accordingly, a change of swimming direction is not achieved by motor reversals and tumbling, but rather by modifying the rotation speed of individual motors (Sourjik et al. 1996; Platzer et al. 1997; Armitage et al. 1997; Scharf 2002). This drives the bundle apart and the filaments point in different directions, thus turning the cell body (Scharf 2002). The bundle rejoins when all filaments resume coordinated maximum speed.

4.2.2. Navigation with a single polar flagellum

Bacteria with a single polar flagellum, termed monotrichous, are very common in unrestricted liquid environments, like limnic waters and oceans. In fact, about 90 % of the motile marine bacteria show such a flagellation pattern (Leifson et al. 1964). The flagellum is ideally inserted at the tip of one pole so that its rotational axis aligns with the cellular length axis. In reality, subpolar localisation occurs as well which results in wobbling of the cell body and thus dissipation of energy. Cells with a left-handed helix swim forwards by CCW rotation, as described above (Fig. 4 A actually resembles this type of swimming most closely). Monotrichous bacteria can also have right-handed helices and thus swim forwards by CW rotation, as observed for *Caulobacter crescentus* (Koyasu et al. 1984).

Run-reverse-flick

In contrast to peritrichous bacteria, monotrichous bacteria can reverse, or back up, by reversing the direction of motor rotation, as long as the helix geometry remains the same (Fig. 4 B). This behaviour was in fact described for polarly flagellated bacteria already in the early days of modern flagellar research (Taylor et al. 1974). Directional changes were believed to occur due to Brownian motion, which in fact turns a cell body at all times rendering it impossible to swim in a straight line for a long period of time (Taylor et al. 1974; Berg 2004; Ping 2012). *Pseudomonas citronellolis* and *Pseudomonas fluorescens* are considered to navigate by such a *run-reverse* mechanism, but the actual turning occurs because of Brownian motion (Taylor et al. 1974; Ping et al. 2013). In 2011, Xie et al. were able to image the behaviour of the flagellar filament of *Vibrio alginolyticus* during turning events using fluorescent labelling and high-speed microscopy. This revealed a three-step turning mechanism, termed *run-reverse-flick* (Xie et al. 2011). After a reversal with the filament pulling, when the cell switches back to forward swimming with the filament pushing, the flagellum bends, or flicks, so that the rotational axis is at an angle with the cellular axis (cf. Fig 5). This pushes the flagellated pole in a different direction and thereby turns the cell body. The mechanism was elucidated by Son et al. by demonstrating that the filament flicks when the hook gets compressed and thereby buckles upon switching to forward swimming (Son et al. 2013). This mechanism also requires the rigidity of the hook to change dynamically depending on the swimming mode: When the filament is rotating CW, thereby pulling, the hook becomes more flexible and during CCW rotation and thus pushing, the hook becomes more rigid, so that the axes of the flagellar helix and the cell body can realign after a flick.

Furthermore, the *flicking* was found to be speed dependant in *V. alginolyticus*: Slower cells mostly swim in a *run-reverse* pattern, while cells swimming faster than $\sim 20 - 30 \mu\text{m/s}$ mostly move in a *run-reverse-flick* pattern (Son et al. 2013, 2016). Faster cells turning by a *flick* are also more efficiently accumulating near the peak of a nutrient gradient, and *V. alginolyticus* can actively increase the frequency of beneficial *flicking* reorientations by increasing the swimming speed (Son et al. 2016). The modulation of the swimming speed in response to the concentration of a chemoattractant, known as chemokinesis, has already been observed for several marine bacteria (Barbara et al. 2003; Garren et al. 2014). The combination of chemokinesis and *flicking* strongly enhances both the speed of climbing a nutrient gradient as well as the efficiency of accumulation near the peak of the nutrient gradient.

The full spectrum of this swimming and turning mode was analysed only for *Vibrio alginolyticus*, however, similar swimming behaviours of many other monotrichous bacteria indicate that this mechanism is universal and widespread among bacteria with a single polar flagellum (Son et al. 2013, 2015). An early study of *P. citronellolis* describes its *run* and *reverse* swimming behaviour without imaging the flagella, however, the authors observed directional changes after returning to forward swimming, indicating the same *run-reverse-flick* turning mechanism (Taylor et al. 1974). Another study about the swimming behaviour of *P. fluorescens* claims sophisticated swimming behaviours including turning during forward runs, flipping and hovering, however, the behaviour of the filament was not considered, so it is very well possible that the same turning mechanism applies (Ping et al. 2013). The *reverse* and *flick* mechanisms are so fundamental that they are assumed to apply for many, if not all, monotrichous bacteria, including the freshwater bacterium *C. crescentus* with its right-handed flagellum (Liu et al. 2014). However, reverse swimming by a pulling flagellum requires the rigidity of the filament to withstand the opposite-handed torsional stress exerted during reverse rotation and the *flick* requires a well-balanced and dynamically adapting flexibility of the hook.

4.2.3. Navigation with other types of flagellation patterns

Essentially, all kinds of flagellation patterns are possible, however, the navigation mechanism for some of the more peculiar patterns, like in *Magnetococcus marinus* MC-1 or *Ovobacter propellens*, are not well understood (Frankel et al. 1997; Fenchel et al. 2004). Here, only the at least somewhat elucidated swimming mechanism of lophotrichously, medial and bipolarly flagellated bacteria will be further introduced (cf. Fig 5).

Lophotrichous

Quite similar to the polar flagellation is the lophotrichous pattern, which is characterised by a number of flagella greater than one, inserted at one pole. These flagella form a bundle and behave like a single filament while rotating in the forward direction, CCW for left-handed helices, similar to peritrichous flagella. The direction of swimming can potentially be inverted by switching to CW rotation with the filament bundle pulling. This, however, requires the filaments to remain as a stable bundle pointing away from the cell body and keeping their handedness. According to early observations, this is in fact the case for *Chromatium okenii* (Buder 1915). In contrast, the short filament bundle of *Thiospirillum jenense* was found to collapse upon CW rotation and flip over, now pointing in the opposite direction and rotating around the cell body in an “umbrella” („Regenschirm“) shape (Buder 1915). Interestingly, similar observations, both with the flagellar bundle in the stable puller as well as in the flipped-over pusher configuration, were made for *Pseudomonas syncyanea* during backward swimming (Reichert 1909). Although these early observations were technically limited and detailed explanations of the

swimming behaviours were lacking, a recent publication confirmed these two pulling modes by fluorescent labelling, high-speed microscopy and tracking algorithms for *Pseudomonas putida* (Hintsche et al. 2017). The detailed analysis of the filament bundle behaviour also shed more light on a possible turning mechanism, which was unclear before, and directional changes were only attributed to Brownian motion. The new insights will be discussed later, as they are heavily intertwined with the results of this thesis (see discussion section 3.2).

Medial

Rhodobacter sphaeroides possesses a single flagellum which is inserted at a medial (mid-cell) position (Armitage et al. 1987). In a way, it resembles polarly flagellated bacteria, but the swimming is more similar to *S. meliloti* or *B. lupini* with exclusive CW rotation to push the cell forward and no CCW rotation and reversing (Armitage et al. 1987). Directional changes are achieved in a different way, however: The motor rotation simply stops, causing the filament to coil and the cell to reorient due to Brownian motion, but also due to continued slow rotation of the coiled filament (Armitage et al. 1997, 1999). The stop of the motor is triggered by the chemotaxis machinery, like usually reversals are, but here a molecular brake stops the motor completely (Pilizota et al. 2009).

Bipolar

Bipolarly (or amphitrichously) flagellated bacteria have single (or multiple) flagella inserted at both poles of the cell body, so that one flagellum is always pushing the cell while the other one is potentially pulling the cell analogously to polar or lophotrichous reversals. Early work on *Spirillum volutans* indicated that the leading flagella are rather flipped over all the time (Metzner 1920), but a recent publication shows that *Magnetospirillum magneticum* can indeed swim with one left-handed flagellum pushing (rotating CCW) and the opposite, also left-handed flagellum pulling (rotating CW; cf. Fig 5; Murat et al. 2015). This mechanism works in both directions, so that *run* and *reverse* swimming is not distinguishable. Leading filaments flipped over and rotating around the cell body, like in *S. volutans* or *T. jenense*, were also observed frequently and termed “parachute”. However, detailed examinations of the filament behaviour were hampered by technical challenges in imaging at sufficient spatial and temporal resolution. Directional changes were found to occur when both filaments rotate in the same direction, either both pointing away from the cell body (presumably rotating CCW) or both rotating around the cell body (presumably rotating CW). These turning events were termed *tumbles*, but the mechanism is completely different from that of peritrichous *tumbles*.

4.3. Chemotactic control of swimming and turning

Chemotaxis is the ability of microorganisms to actively direct their movement towards favourable conditions or away from unfavourable conditions. The first tactic behaviour of bacteria was described by Theodor Engelmann, who noticed that certain bacterial species accumulate at a spot of light or swim towards specific concentrations of oxygen (Engelmann 1881a,b). The modern work on chemotaxis began when Julius Adler demonstrated that *E. coli* has a “sense of taste”, being the first to analyse its chemotactic behaviour towards different nutrients like serine and aspartate quantitatively (Adler 1965, 1966). Furthermore, he found that *E. coli* cells still respond to chemicals even in mutants defective for the uptake and metabolism of these chemicals, demonstrating that bacteria can recognise the molecules per se (Adler 1987).

Ultimately, the chemotactic behaviour is a random walk: Cells move in a certain direction and frequently change this direction by diverse mechanisms, usually involving a motor reversal (cf. section 4.2). By regulating the frequency of directional changes, increasing run times or modulating the swimming speed, a bias is applied to the random walk which results in an overall movement of the cell up a chemical gradient, although only at a fraction of the run speed ($\sim 10\%$ for *E. coli*; Berg 2004).

4.3.1. Chemoreceptors

Chemoeffectors, the chemotactically active molecules, are sensed by the so called methyl-accepting chemotaxis proteins (mcp), which can bind a limited number of different ligands (Berg 2004). The number of different mcps varies from only one to several dozens among bacteria (Wadhams et al. 2004). Mcps are usually trans-membrane proteins with a conserved, cytoplasmic signalling domain and a periplasmic sensory domain that binds the chemoeffectors (Krikos et al. 1983; Russo et al. 1983; Morgan et al. 1993a; Falke et al. 2001; Milburn et al. 1991). Together with the histidine kinase CheA and the coupling factor CheW, they form complexes of mcp dimers that further aggregate to trimers and eventually to huge clusters, which, in some bacteria such as *E. coli*, localise at one cell pole (Alley et al. 1992; Maddock et al. 1993; Gestwicki et al. 2000). The receptors further interact with the methyltransferase CheR and the two response regulators CheB (an aspartate kinase/methylesterase) and CheY (an aspartate kinase).

The basic mechanism is a two component signalling pathway, in which a phosphate group is transferred from a histidine kinase (CheA) to a response regulator (CheY and CheB) which is coupled to an effector (FliM of the flagellar basal body and the methylesterase domain of CheB, respectively). The active form of the first regulator, CheY-P, diffuses to the cytoplasmic C-ring of the flagellar motor and induces a conformational change in the switch complex, comprising subunits of FliM and FliN tetramers, which changes the sense of motor rotation (Toker et al. 1996; Bren et al. 1998; Duke et al. 2001; Sagi et al. 2003; Paul et al. 2006). CheY-P can also act as a motor brake as in *Rhodobacter sphaeroides* or slow down the rotation rate as in *Sinorhizobium meliloti* (Armitage et al. 1997; Scharf 2002). CheY-P is continuously dephosphorylated by the phosphatase CheZ and therefore the activity of CheA balances the level of CheY-P and thus the frequency of the chemotactic response (Hess et al. 1988; Wylie et al. 1988). The other active effector, CheB-P, activates its own methylesterase domain which demethylates the mcp, thereby increasing its sensitivity (Kehry et al. 1985; Anand et al. 2002). On the other hand, the receptors are methylated by the methyltransferase CheR, which decreases the sensitivity (Springer et al. 1977). Hence, the level of methylation and thus the sensitivity of the receptors is balanced by the activity of CheA, but also by the activity of CheR (Sourjik 2004; Wadhams et al. 2004).

4.3.2. Basic signalling scheme

Taken together, in an equilibrium state, with no change in chemoeffector concentration, a certain level of CheY-P frequently induces a chemotactic response (for simplification only turns are considered). This equilibrium state is balanced by the activity of CheA and CheZ. If an attractant binds, a conformational change in the receptor reduces the activity of CheA and thus the concentration of CheY-P falls. This decreases the probability of motor reversals and hence, the run length is increased. In other words, if a cell is swimming in the right direction, it keeps going in that direction. At the same time, the concentration of CheB-P falls as well, reducing its methylesterase activity and additionally the structural change of the receptor increases the activity of the methyltransferase CheR. Together, this increases the level of receptor methylation, which in turn increases

the CheA activity. So the binding of an attractant both decreases and increases the activity of CheA, however, the methylation is a slow process. Hence, the receptor complex makes a temporal comparison between the present and past chemoeffector concentration. If a cell swims up a favourable gradient, the methylation lags behind the receptor occupancy and the system goes out of balance with the kinase getting inactivated. This extends the runs in the favourable direction. Slowly, the methylation process catches up, thus providing a way to adapt to changing chemoeffector concentrations: If the concentration remains at a certain (higher or lower) level, the receptor activity is adjusted by the methylation level and the system returns to its equilibrium state (Berg 2004).

5. Model organism and aim of this thesis

The research described in this thesis focused on the flagella-mediated motion of the γ -proteobacterium *Shewanella putrefaciens* CN-32, but the new insights into swimming and filament behaviour are fundamental and potentially apply to many polarly flagellated bacteria, both monotrichous and lophotrichous, as already confirmed by several later studies.

5.1. *Shewanella putrefaciens* CN-32

Members of the genus *Shewanella* are characterised by a wide respiratory diversity with the ability to use a vast array of organic and inorganic terminal electron acceptors (Hau et al. 2007). These include chlorinated compounds, radionuclides and other environmental pollutants, but also soluble and insoluble forms of iron, manganese and many other metal compounds, even plutonium and uranium (Myers et al. 1988, 1990; Boukhalfa et al. 2007; Icopini et al. 2009; Lovley et al. 1991; Caccavo et al. 1992). Because of these traits, *Shewanella* typically was considered a model organism for bioremediation, metal reduction and energy-generating biocatalysis (Hau et al. 2007). In the recent years however, *Shewanella oneidensis* and *Shewanella putrefaciens*, the model organism of this thesis, were employed to study dual stator dynamics and dual flagellar behaviours, respectively. These aquatic bacteria are robust swimmers and proved to be an excellent platform for research on motility that doesn't follow the enteric paradigm (Paulick et al. 2009, 2015; Bubendorfer et al. 2012, 2013, 2014).

S. putrefaciens is rod shaped, about 2-3 μm long, and possesses a polar flagellum for regular swimming and navigation (Bubendorfer et al. 2012). The flagellum is unsheathed and driven by a sodium-motive force, as in other *Shewanella* species (Paulick et al. 2009). Forward and backward swimming works as described above for other polarly flagellated bacteria and the *run-reverse-flick* turning was regularly observed during the work of this thesis. Under specific conditions, *S. putrefaciens* can produce a second set of peritrichous or lateral flagella, like *Vibrio alginolyticus* or *Vibrio parahaemolyticus*, but they are not sufficient to provide swarming motility and rather modify the turning angle, which improves spreading in soft agar (Bubendorfer et al. 2014). The lateral flagellar motors are driven by a proton-motive force and do not interact with the chemotactic machinery via CheY-P and thus these flagella always rotate counterclockwise, thereby pushing the cell. This thesis focuses on the behaviour of the polar filament, so most experiments were done with deletions of the lateral flagellins resulting in a loss of the lateral filaments, but the overall regulation and function of the polar system is not affected.

5.2. Research objectives

The project of this thesis started with an observation that I made during imaging the interplay of polar and lateral flagella of *S. putrefaciens* using the fluorescent labelling technique of Turner et al. 2000. As mentioned above, the lateral flagella improve spreading in soft agar, and we were interested in visualising this at the single cell level including the behaviour of the two sets of flagellar filaments. It soon proved to be rather challenging to actually visualise both filaments at the same time on a single cell, but along the way I observed a cell that was stuck and used its polar flagellum in a very odd way. It had pushed itself forwards into a dead end, with the filament pointing away from the cell body, but suddenly the filament flipped over and wrapped around the cell body. By this action, it reversed the swimming direction and ultimately got free, returning back to regular forward swimming. We were quite puzzled by this behaviour which we had not seen ever before (including during regular backward swimming) and we wanted to know what was happening in detail. So, the first part of this thesis aimed at characterising and understanding this filament wrapping behaviour. In contrast to the other examples of a filament flipping over given in section 4.2, these new image sequences were much more detailed in terms of spatial and temporal resolution as well as in the particular conditions that led to the filament wrapping around the cell body. Thus, we were able to elucidate the underlying mechanism and suggest a possible use of this behaviour that we termed *screw thread* motility, or *screw thread* formation (formerly just *screw* formation), due to the resemblance of the filament to a screw thread, rather than a corkscrew (see part II section 1). This project heavily benefited from the collaboration with the physicist Prof. Bruno Eckhardt and his doctoral student Felix Schmidt at Philipps-Universität Marburg, who contributed with a simulation of the filament behaviour and a lot of detailed questions from the physical perspective. We mostly couldn't answer those questions, but they still helped us a lot in understanding what was going on with the flagellar filament of *Shewanella putrefaciens*.

The second project of this thesis focused on the composition of the flagellar filament and how it affects the frequency of *screw thread* formation and the swimming behaviour in general. The polar flagellum of *S. putrefaciens* is made from two different flagellin subunits, FlaA and FlaB, which are arranged as distinct segments in the assembled flagellar filament. In a mutant lacking the *flaA* gene, the FlaB protein can form a full-length filament on its own. Such a pure FlaB filament showed greatly increased frequency of *screw thread* formation compared to the wild-type filament with a FlaA segment at the base of the filament. The second project thus aimed at understanding the effects of the two distinct filament segments on *screw thread* formation and swimming behaviour as well as the mechanism responsible for the distinct spatial segmentation of the flagellar filament. We were finally able to verify the physiological relevance of the *screw thread* motility as well as to clearly show the advantage of the maintenance and utilisation of more than one type of flagellin (see part II section 2). Again, this project took a huge advantage from the collaboration with the group of Prof. Eckhardt and additionally with Dr. Laurence Wilson and his PhD student Nicola Farthing at University of York, who tracked *Shewanella* cells in three dimensions and thus took the single-cell analysis of swimming parameters to the next level.

Part II.

Publications contributing to this thesis

1. Bacteria exploit a polymorphic instability of the flagellar filament to escape from traps

1.1. Summary

Monotrichously flagellated bacteria can use their polar flagella to swim either forwards with the flagellum pushing or backwards with the flagellum pulling. The direction of swimming is determined by the direction of motor rotation, counterclockwise (CCW) for forward and clockwise (CW) for backward swimming for a left-handed helix. The handedness of the flagellar helix remains the same because the filament is stable enough to withstand the right-handed torsional forces that act upon the helix during backward swimming. Monopolarly flagellated bacteria are typical inhabitants of aquatic ecosystems, marine and limnic waters alike, and a single polar flagellum is well-suited for navigating bulk liquids. However, they also face complex porous environments, like sediments or organic particles, but also viscous environments associated with animal hosts. Constricted spaces and dead ends can trap cells and substantially restrict motility and spreading. These environments require more force to pass or strategies to back out of traps. Polarly flagellated bacteria can do so by reversing, however, regular backward swimming might not be sufficient.

We studied the cellular motion together with the flagellar filament behaviour of the marine and sediment bacterium *Shewanella putrefaciens* CN-32 at an agarose-glass interface that mimics the intersection between bulk liquid and structured environment (Kühn et al. 2017, Fig. S1 A). Flagellar filaments were made visible by selectively binding a maleimide-ligated fluorescent dye to cysteine residues that were genetically introduced into the flagellin genes, replacing surface-exposed serine or threonine residues. This enabled high-speed microscopy of swimming cells and filaments at the same time.

At the intersection of free-swimming areas and areas with constricted space between agarose and glass we frequently observed cells getting stuck and trying to get out of the trap by switching between CCW and CW rotation. Sometimes cells succeeded to free themselves by regular reversals, but more frequently the forces exerted by the CW-rotating, pulling flagellum were insufficient. Under these circumstances, we frequently observed the flagellar filament wrapping quickly around the cell body, adopting a different polymorphic shape with a wider diameter and reduced pitch, somewhat resembling the shape of a screw thread (in contrast to the flagellum pointing away from the cell body resembling a corkscrew; Kühn et al. 2017, Fig. 1, Movie S1). The transition itself was too fast to visualise in detail but it clearly happened shortly after switching to CW rotation. By wrapping the filament, the cell was able to get free and move in this *screw thread* configuration without slip of the flagellar helix (i.e. the overall shape of the helical waveform did not change relative to the medium, cf. Kühn et al. 2017, Fig. 2 A, Movie S2). After several seconds, the cell switched back to regular forward swimming which unwound the filament, now returning to its normal configuration pointing away from the cell body.

This flagellar behaviour was reliably reproducible with this experimental setup. Furthermore, we found that increasing the viscosity of the medium with Ficoll, a highly branched polymer, triggers the formation of the *screw thread* also in bulk liquid (Kühn et al. 2017, Fig. 3 A). However, cells in *screw thread* mode moved at a much lower speed than cells swimming forward or backward regularly (Fig. 3 B). The filament waves moved along the cell body with a lot of slip, therefore not translating the cell efficiently (Kühn et al. 2017, Fig. 2 B, Movie S4). This indicated that the movement in *screw thread* mode is only beneficial in structured environments where the filament can interact with asperities on the surface and efficiently translate the cell body backwards without slip of the flagellar helix.

Because increasing the viscosity slows down flagellar rotation we used a similar experimental setup as described above (cells trapped between agarose patch and glass) but supplemented the culture medium with Ficoll. This allowed us to obtain a better temporal resolution to monitor the formation and release of the *screw thread* in more detail. This revealed an unwinding of the flagellar helix prior to *screw thread* formation when the motor switched to CW rotation (Kühn et al. 2017, Fig. 4, Movie S5). The same filament behaviour was observed in physical simulations conducted by our cooperation partners from Marburg: Above a certain CW motor torque and hence, above a certain force acting on the flagellar helix, the first loop of the helix unwound and bent towards a right-handed helix (Kühn et al. 2017, Fig. 4, Movie S6). However, the conversion of the helix was not completed as the filament was moving towards the cell body, wrapping around it and adopting a stable, left-handed polymorphic configuration, both in experiment as well as in the simulation. In this flipped-over state the forces no longer push the flagellum towards a right-handed helix, so it is a way to bypass the torsional stress exerted on the regular filament during reverse rotation.

As this mechanism is fundamentally applicable for flagellar helices that are rigid enough to withstand the torsional stress during regular backward swimming but become unstable if the forces exceed a certain magnitude, we suggested that this flagellar behaviour is a common mode of escape from traps or movement through structured environments in a wide range of polarly flagellated bacteria. Indeed, similar behaviours have since been reported for a growing number of polarly flagellated bacteria from very diverse habitats, including marine, soil and human host environments (Hintsche et al. 2017; Kinosita et al. 2017; Constantino et al. 2018).

1.2. Contribution

All the biological experiments were performed by me (strain constructions, microscopy, Western blots, motility assays, data analysis). The physical simulation was done by Felix Schmidt and Bruno Eckhardt. All authors designed the research, analysed the data and wrote the manuscript.

Bacteria exploit a polymorphic instability of the flagellar filament to escape from traps

Marco J. Kühn^a, Felix K. Schmidt^{b,c}, Bruno Eckhardt^{b,c}, and Kai M. Thormann^{a,1}

^aInstitut für Mikrobiologie und Molekularbiologie, Justus-Liebig-Universität Giessen, 35392 Giessen, Germany; ^bFachbereich Physik, Philipps-Universität Marburg, 35032 Marburg, Germany; and ^cLOEWE Zentrum für Synthetische Mikrobiologie, Philipps-Universität Marburg, 35032 Marburg, Germany

Edited by Howard C. Berg, Harvard University, Cambridge, MA, and approved May 10, 2017 (received for review January 30, 2017)

Many bacterial species swim by rotating single polar helical flagella. Depending on the direction of rotation, they can swim forward or backward and change directions to move along chemical gradients but also to navigate their obstructed natural environment in soils, sediments, or mucus. When they get stuck, they naturally try to back out, but they can also resort to a radically different flagellar mode, which we discovered here. Using high-speed microscopy, we monitored the swimming behavior of the monopolarly flagellated species *Shewanella putrefaciens* with fluorescently labeled flagellar filaments at an agarose–glass interface. We show that, when a cell gets stuck, the polar flagellar filament executes a polymorphic change into a spiral-like form that wraps around the cell body in a spiral-like fashion and enables the cell to escape by a screw-like backward motion. Microscopy and modeling suggest that this propagation mode is triggered by an instability of the flagellum under reversal of the rotation and the applied torque. The switch is reversible and bacteria that have escaped the trap can return to their normal swimming mode by another reversal of motor direction. The screw-type flagellar arrangement enables a unique mode of propagation and, given the large number of polarly flagellated bacteria, we expect it to be a common and widespread escape or motility mode in complex and structured environments.

Shewanella | flagella | motility | structured environment

Motility is an important element of bacterial life in a range of different environments (1–5) and a driving factor in processes as diverse as the spreading of diseases and degradation of biomaterial (6, 7). For active movement, many bacteria rely on flagella, long helical proteinaceous filaments extending from the cell's surface, which they rotate at the filament's base by a membrane-embedded motor and which allow effective swimming through liquid environments or swarming across surfaces (8). The prominent helical flagellar filament is composed of 11 protofilaments consisting of the filament's building block, the protein flagellin. Any number of these 11 protofilaments may adopt a certain conformation (“L” or “R”) that produces bending and a helical twist, resulting in an overall helical configuration of the filament (9, 10). Different ratios of L to R protofilaments enable the formation of 12 different polymorphic states of the filament, 2 of which are straight (L or R only), 3 of which are left-handed, and 7 of which are right-handed (11–13). External perturbations, such as increasing force or torque, may lead to switches between the filament's polymorphic forms (14–17). This important property of the flagellum is exploited by bacteria to adjust their swimming behavior.

Most flagellar motors are bidirectional and allow counter-clockwise (CCW) and clockwise (CW) rotation (as seen from the tip of the flagellum looking toward the motor) (18, 19). The paradigmatic example *Escherichia coli* has five or six flagellar filaments arranged in a peritrichous pattern around the cell body. CCW rotation leads to association of the flagella into a left-handed bundle driving smooth swimming of the cell (“run”). Upon switching one or several motors to CW rotation, the corresponding flagella will transform into a right-handed helix, which leaves the flagellar bundle and leads to cellular realignments

(“tumble”). Upon resuming CCW rotation, the bundle is reestablished, and the cell runs smoothly into a new direction (20, 21). By adjusting the run lengths between tumbles, the cells can move along signal gradients in a biased random walk toward preferred environmental niches (22). In contrast to the run-and-tumble movement of bacteria with peritrichous flagellation, cells of many bacterial genera with polar flagella (such as *Vibrio*, *Pseudomonas*, *Aeromonas*, and *Shewanella*, to name just a few) navigate by “run–reverse–flick” patterns. Although CCW rotation of a left-handed helix drives the cells forward, motor reversal to CW rotation does not transform flagellar helicity into a right-handed shape as in *E. coli*. Instead, the flagellum remains left-handed, and the cells are pulled backward (23). Upon resuming CCW rotation, the filament is compressed and the cell is reoriented as a consequence of buckling of the flagellum in the hook region, the flexible structure joining flagellar filament and motor (24, 25). However, other bacteria, such as *Rhodobacter sphaeroides*, navigate by “run–stop–run” cycles. In this species, a single right-handed flagellum is rotated in a CW fashion to drive the cells forward. During periodic stops of the motor, cellular reorientation occurs through conversion of the flagellar filament from a helical to a relaxed coiled form (26). These examples illustrate how bacteria take advantage of the flagellar polymorphism and rigidity to effectively modulate their swimming behavior.

Studies on movement of single bacteria and the behavior and position of the flagellar filaments are almost entirely restricted to free-swimming cells. However, many motile bacterial species reside in soil, sediments, and other porous environments with pore sizes of only a few micrometers or less (27), and other bacteria, including many pathogens, have to move through diverse structured environments such as mucus layers, tissues, or biofilm matrices. It has been shown that *E. coli* or *Bacillus subtilis* strains can efficiently move through pores with diameters that exceed the diameter of the cells only slightly (28). When entering

Significance

It has long been established that flagella provide an efficient means of movement for bacteria in planktonic environments (free swimming) or across surfaces (swarming). However, rather little is known about bacterial motility in structured environments. In this study, we demonstrate that polarly flagellated bacteria can exploit a polymorphic instability of the flagellar filament for a third type of flagella-mediated movement in which the flagellum wraps around the cell body and the cells back out from narrow passages in a screw-like motion.

Author contributions: M.J.K., F.K.S., B.E., and K.M.T. designed research; M.J.K. and F.K.S. performed research; M.J.K., F.K.S., B.E., and K.M.T. analyzed data; and M.J.K., F.K.S., B.E., and K.M.T. wrote the paper.

The authors declare no conflict of interest.

This article is a PNAS Direct Submission.

¹To whom correspondence should be addressed. Email: kai.thormann@mikro.bio.uni-giessen.de.

This article contains supporting information online at www.pnas.org/lookup/suppl/doi:10.1073/pnas.1701644114/-DCSupplemental.

wedge-shaped narrow passages, bacteria have been observed to back up, either by reversing their motor or by a flip of their flagellar bundle (29). In these cases, the flagellum or the flagellar bundle points away from the cell body. In this study, we performed single-cell tracking of the sediment isolate *Shewanella putrefaciens* CN-32 to explore flagella-mediated movement of a polarly flagellated species within structured environments.

Results and Discussion

Trapped Cells Show an Unusual Behavior of the Flagellar Filament.

S. putrefaciens CN-32 is a bacterium with a primary single polar flagellum and additional lateral flagella that are implicated in realignment of the cells during swimming (30, 31). To concentrate on the role of the main polar flagellum, we used an *S. putrefaciens* CN-32 strain, which we genetically engineered to not produce the lateral flagellum by deleting the corresponding flagellin-encoding genes. To visualize flagellar filaments by fluorescence microscopy, we genetically introduced threonine-to-cysteine substitutions into the environment-exposed surface of the two flagellins, the building blocks of the filament, which were then used for the ligation of maleimide-ligated fluorescent dyes. Details of the strain constructions are given in *SI Materials and Methods*. To create a suitable structured environment that enables microscopic recordings of swimming cells, we used an agarose surface that was overlaid with a sample of medium containing an appropriate dilution of cells with fluorescently labeled flagella. A coverslip was added on top so that the liquid-covered uneven surface of the agarose provided a structured environment with varying distances between agarose and the glass surface (Fig. S1).

Fluorescence imaging revealed that the polar flagellum of *S. putrefaciens* CN-32 is on average ~ 6.5 μm in length and exhibits a left-handed helical structure (diameter, 0.6 μm ; pitch, 1.9 μm), which mediates forward and backward swimming upon CCW and CW rotation, respectively. Free-swimming cells displayed

the expected “run–reverse–flick” motility patterns (30), whereas cells that got stuck between the glass coverslip and the agarose surface showed flagellar rotation without spatial propagation. In an effort to escape the trap, cells alternated between CCW and CW rotation of the motors. In cases where these changes in flagellar rotation did not suffice to free the cell, we frequently noticed that the flagellar filament eventually wrapped around the cell body, forming a spiral- or screw-like large helix (Fig. 1, *Movie S1*, and *Dataset S1*). This behavior was often accompanied by a backward translation of the cell body in a screw-like motion for up to several seconds. Notably, during this backward maneuver, the general orientation of the flagellar helix relative to the substratum did not change while the cell moved through the spiral formed by the flagellum (Fig. 24 and *Movie S2*). Once the cells had escaped the narrow passage, the motor reversed direction and the filament unwound the spiral to resume its normal helicity and position behind the cell, which then continued moving by normal forward swimming. Some cells could not escape by this mechanism and alternated between the two positions of the filament without moving the cell (*Movie S3*).

Efficient Backward Screwing Requires Surface Contact. Because immobilizing the cell body increases the forces acting on the flagellar filament (32), we explored the possibility to trigger the transition also during free swimming by increasing the viscosity and hence the drag on the cell. To this end, we monitored cellular movement and position of the flagellar filament of free-swimming cells in media supplemented with increasing amounts of Ficoll to enhance the viscosity (33). In Ficoll-free media, we observed almost no cells with filaments wrapped around the cell body (Fig. 3). However, with increasing Ficoll concentrations, the number of cells displaying screw formation increased significantly to more than 74% of the population for Ficoll concentrations up to 25% (Fig. 3). The flagellum wrapped around the cell body rotated in CW direction. This suggests that the forces on the cell and the

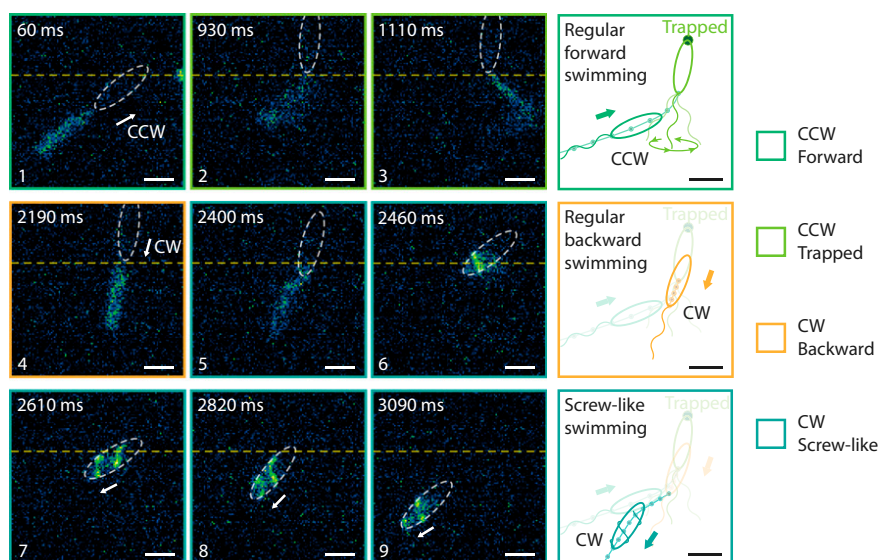


Fig. 1. Approach, trapping, and escape of a bacterium between agarose and cover slide. (From Left to Right and Top to Bottom) The bright structures in the microscope image result from the fluorescently labeled flagellum. The cell body is indicated by a dotted ellipsoid. The yellow dashed line marks the position of the flagellated cell pole when the cell got stuck and maintained in subsequent frames to display the backward motion of the cell. The cartoon on the right summarizes the sequence of events and highlights the switch from counterclockwise (CCW) rotation of the motor (green frames) to clockwise (CW) rotation (orange frames; viewed from behind the cell). The cell approaches from the Lower Left (frame 1), moves upward, and then gets stuck (frames 2 and 3). While still pushing forward, the flagellum wiggles circularly in an instability known to occur for stronger applied torque. It then switches direction of rotation to CW (frame 4), and the flagellum wraps around the cell (frames 5 and 6). The strong forces during screw formation caused the cell to move, as indicated by the reorientation of the cell body between frames 5 and 6. The cell continues to the Lower Left, as indicated in frames 7–9. Exposure time was 30 ms; the number in the upper left corner of each micrograph displays the time each still image was taken from the movie (*Movie S1* and *Dataset S2*). (Scale bars: 2 μm). The freely rotating flagellum (frames 1–5) appears blurry because the rotation of the helical filament in normal medium is faster than the exposure time.

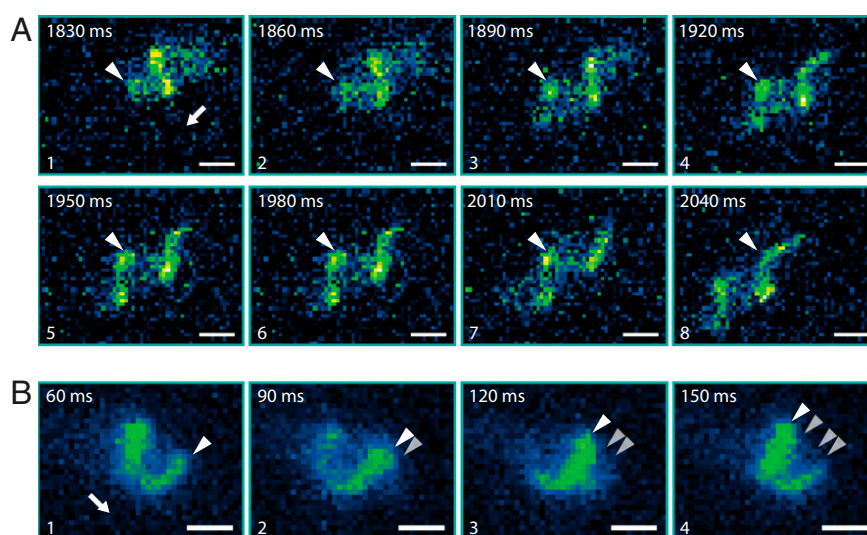


Fig. 2. Screw-like propagation relies on interaction between the flagellar filament and asperities on the surface. The white arrow indicates the orientation of the cell body (flagellated pole). The white triangles indicate one peak of the flagellar waveform. (A) Still images taken from [Movie S2](#) showing screw-like propagation of a cell that is stuck between agarose medium and the coverslip surface while the waveform of the flagellar helix does not move relative to the surrounding medium. (B) Still images taken from [Movie S4](#) showing screw-like propagation of a free swimming cell (at least 50 μm away from the coverslip). Here, the flagellar helix waveform is moving relative to the surrounding medium, as indicated. (Image exposure time, 30 ms; scale bars, 1 μm.)

flagellar filament induce the formation of the spiral around the cell. At 10% Ficoll, the cells with the filament wrapped around the cell body moved slowly at about 5 μm/s, which is barely above the general background diffusion of immobile cells caused by Brownian motion and general drift (~3 μm/s), but significantly slower than cells that were still pushed or pulled by the flagellar filament (both at ~16 μm/s). Moreover, the flagellum moved around the cell body without efficient translation (Fig. 2B and [Movie S4](#)). In contrast, for cells near surfaces, the flagellar helix

maintained a fixed location relative to the surroundings and the cell (Fig. 2A and [Movie S2](#)). We therefore propose that the propagation relies on an interaction between the flagellum and asperities on a surface, while continuous rotation of the flagellum around its molecular axis by the motor prevents strong binding. Thus, the screw-like state allows a backward movement of cells across surfaces or through appropriately structured environments but is not effective under free-swimming conditions with increased viscosity.

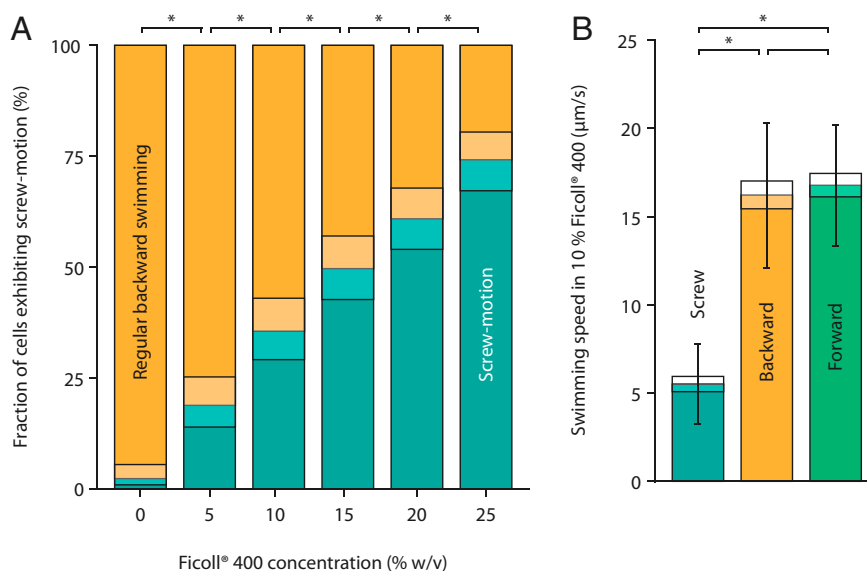


Fig. 3. Inducing the transition to screw mode in media with higher viscosity (Left) and differences in swimming speed (Right). (A) Adding Ficoll 400 increases the viscosity and causes a larger torque when the cells switch from CCW to CW rotation. The fraction of cells in the “screw” state increases with Ficoll concentration (determined far away from surfaces). The viscosities are ~2, 5, 10, 18, and 33 cP for 5%, 10%, 15%, 20%, and 25% Ficoll 400, respectively. Bars with an asterisk indicate that the differences are significant (Fisher’s exact test of independence; $P \leq 0.05$, Bonferroni corrected). The exact P values from 0 to 25% Ficoll are 1.36×10^{-12} , 2.90×10^{-6} , 3.96×10^{-4} , 4.27×10^{-3} , and 3.67×10^{-4} , respectively. The number of counted backward swimming events are 309, 316, 313, 317, 324, and 313, respectively. Shaded boxes display 95% confidence intervals. (B) Measurements of the swimming speed show that, although forward and backward swimming have very similar speeds, the motion in the screw state is reduced. Bars with an asterisk indicate that the differences are significant (two-sample t test; $P \leq 0.01$, Bonferroni corrected). The exact P values are $<2.20 \times 10^{-16}$ for screw vs. backward and screw vs. forward and 0.3 for backward vs. forward. For each swimming mode, 105 cell tracks were analyzed. Error bars represent SD; shaded boxes display 95% confidence intervals.

Screw Formation Is Triggered by a Polymorphic Filament Instability at CW Rotation. The effects of Ficoll are to slow down the motion of the flagellum and to increase the drag forces (32, 34). We therefore used Ficoll-supplemented medium on agarose surfaces to reduce the speed of the rotating flagellar filament, allowing us to obtain sufficient temporal resolution to monitor its motion and morphology during formation and release of the large helix around the cell body (Fig. 4, Fig. S2, Movie S5, and Dataset S2). Flagella of stuck cells rotating in CCW direction generally maintained the left-handed helical shape; however, diameter and pitch varied dynamically, indicative of flagellar filament polymorphism. When the rotational direction switched to CW, the flagellar helix quickly became unstable.

To gain more insight into the origin and the dynamics of the transition, we implemented an established model for the flagellum as an elastic rod coupled to the fluid through resistive force theory (35, 36). The elastic forces acting on the filament come from changes in the shape of the filament, from the interaction between segments of the filament and between filament and cell body. They are represented by free energies and local interaction potentials. Different polymorphisms of the flagellum can be implemented by switches in the equilibrium parameters and the requirement that the local minimum of the free energy is chosen, as shown for *E. coli* in refs. 37 and 38. The crystal structure of the *S. putrefaciens* CN-32 flagellar filament will be different from that of well-studied organisms like *E. coli*. However, we anticipate that its general mechanical properties and the different polymorphisms will not differ significantly, as the *S. putrefaciens* sequence and deduced structure is very similar to that of *Salmonella* in all five α -helices that constitute the polymorphic structural part of the filament (Fig. S34). From our observations, we can deduce at least two equilibria, one for a stretched-helix

flagellum typical during normal swimming, and one for the coiled state when the flagellum is wrapped around the cell body. For the frictional forces, we use resistive force theory, which characterizes the forces on the segments by three local friction coefficients, one each for motion perpendicular to the flagellum's centerline, for motion along the centerline, and for rotations around the centerline. No measurements of the various parameters have been reported thus far, so we adopted values obtained for *E. coli*. Although some uncertainty about the precise values for the elastic constants and the presence of other morphologies during the transition remain, numerical simulations for several different parameter choices show that the qualitative features of the flagellar dynamics are insensitive to the details of the parameter choice. The full set of equations and the complete list of parameters values are given in *SI Materials and Methods*.

Close to the cell body we have to take the driving and the increased flexibility of the filament in the hook region into account. Because the hook region itself is not resolved in the numerical simulations, we model its properties by the boundary conditions. The flagellum's rotation is driven by a constant motor torque. The angle under which the filament leaves the cell surface is not prescribed, accounting for the fact that the bacterial hook is much more flexible than the flagellum (24). The torque applied by the motor is split into a component parallel to the axis of the motor, and one parallel to the filament, with a parameter that controls the relative contributions. Formation of the screw was reliably observed when 10–50% of the torque acted along the centerline of the filament.

The motion of the flagellum with two different morphologies is shown in Movies S5 and S6, and the snapshots in Fig. 4. Both model and observations show that, when initiated with a left-handed spiral rotating CCW, the flagellum pushes the bacterium

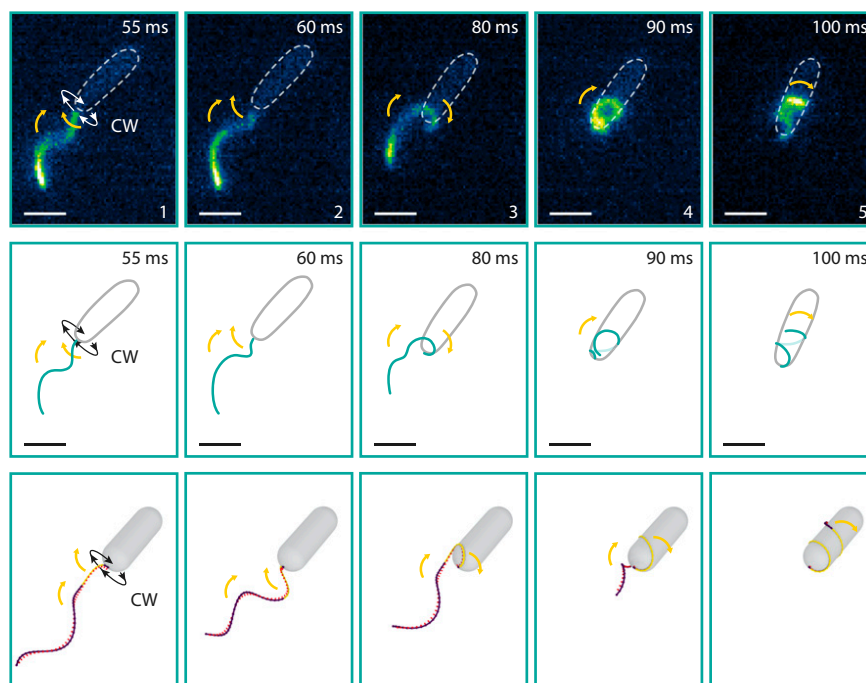


Fig. 4. Comparison between observed and simulated flagellar states during screw formation. The upper panel shows flagellar states taken from Movie S5. These images are inverted horizontally to match the correct handedness of the flagellar helix (*SI Materials and Methods*). The flagellar filament was fluorescently labeled, and the medium was supplemented with 20% Ficoll 400 to slow down flagellar rotation (exposure, 5 ms; scale bars, 2 μ m). The cell body is indicated by a dotted ellipsoid. Yellow arrows indicate the movement of the flagellar filament. The same states are depicted as cartoons in the middle panel. The lower panel displays the corresponding images from the simulation of screw formation (Movie S6). The stretched helix configuration is color-coded in purple, whereas the coiled state is marked in yellow. Details of the numerical simulation are described in *SI Materials and Methods*. Both imaging and simulations show that CW rotation results in an instability at the base of the flagellar filament, leading to a pull of the filament toward the cell body and, eventually, wrapping of the flagellum around the cell.

along. When increasing the torque on the cell, the flagellum begins to move sideways, as also observed in [Movie S1](#) and in Fig. 1 (frames 2 and 3). Upon switching to CW rotation, the flagellum begins to pull on the bacterium. As the forces on the filament increase, the first loop of the helix above the motor is stretched and bends around toward a right-handed helix. In elastic filaments, such transitions in helicity under stress are known as “perversions” (39). Here, however, the formation of the perversion is not completed. Instead, the flagellum switches to another equilibrium shape reminiscent to the left-handed coiled forms observed for the *E. coli* flagellum (11, 13). The orientation of the filament, deduced from the direction of the tangent along filament, which initially points away from the cell, locally changes direction and points toward the cell. This induces a force on the upper part of the flagellum that pulls it toward the cell and the flagellum begins to wrap around the cell body. Because the formation of the perversion and the transition to a right-handed helix is not completed, the filament remains a left-handed helix.

The instability discovered and described here is different from the buckling instability described by Son et al. (24) and Xie et al. (25). They showed that the hook region buckles when the bacterium switches from a backward pull to a forward push: During the pull, the flagellum is stretched, but during the push, it experiences a strong compression, which, combined with the high flexibility of the hook region, triggers the buckling instability and the directional change. The instability described here occurs during the pulling phase, where the flagellum is stretched, and the motor forces push toward a right-handed helix. During normal swimming, when the cell body is free to rotate, the instability is avoided because the applied torque is reduced by the counterrotation of the cell body (32). When the bacterium is stuck, or the friction on the cell body is enlarged by an increase in viscosity, the full torque of the motor acts on the flagellum and triggers the transition to the screw-like state. The transition might also be assisted by an increase in torque due to the acquisition of additional motor proteins, which has been shown to occur under conditions of high load on the flagellum (40, 41).

Conclusions

Flagella-mediated movement is a common means of locomotion for bacteria and has previously been demonstrated to mediate swimming through liquid environments or swarming across surfaces. We have shown here that, in polarly flagellated species, these organelles of locomotion can, in addition to regular planktonic swimming through liquids or swarming across surfaces, provide a third type of movement, a screwing motion through structured environments. We also show that screwing is an efficient means to release cells that have been trapped in narrow passages. This flagellar behavior is an example of “failure turned into function” (42) by a biological system, and, given the wide range of monopolarly flagellated bacterial species (43), we expect it to be a common mode of escape or movement among bacteria in structured environments.

Materials and Methods

Bacterial Strains. Bacterial strains and plasmids are summarized in [Tables S1](#) and [S2](#). Construction of plasmids and genetically modified strains of *S. putrefaciens* CN-32 was essentially carried out as previously described (44, 45). Detailed information on strain construction, growth conditions, and media is provided in [SI Materials and Methods](#).

Visualizing Flagellar Filaments. To visualize the flagellar filaments, maleimide-ligated dyes were coupled to surface-exposed cysteine residues, which were specifically introduced into the flagellins, FlaA and FlaB, of the *S. putrefaciens* CN-32 polar flagellum as previously described (46, 47). A number of motility controls ensured that the modification did not negatively affect cell motility ([SI Materials and Methods](#)). Cells of an exponentially growing LB culture (OD₆₀₀, 0.6) were harvested by centrifugation (1,200 × *g*, 5 min, room temperature) and resuspended in 50 μ L of PBS. For all cell-handling steps, the tip of the pipette tip was cut to prevent shearing off flagellar filaments. A volume of 0.5–1 μ L of Alexa Fluor 488 C5 maleimide fluorescent dye (Thermo Fisher Scientific) was added, and the cell suspension was incubated in the dark for 15 min. Cells were sedimented again and carefully washed once with 1 mL of PBS to remove residual unbound dye. After final resuspension in LM100 medium in an appropriate volume (usually to reach a final OD₆₀₀ of 0.2), the cells were kept shaking in the dark until microscopy, but never longer than 1 h. If necessary, LM100 medium was supplemented with Ficoll 400 for final resuspension. Ficoll 400 was always diluted to the appropriate concentration from a 50% (wt/vol) stock solution in LM. After coupling of the maleimide fluorescent dye, the cells were carefully washed before microscopic analysis.

For microscopy in bulk medium (always about 100 μ m away from the glass surface), a 250- μ L aliquot was loaded on a swim slide (coverslip fixed on a microscope slide by four silicone droplets (Baysilone; VWR International) to generate a space of about 1 mm). For microscopy in structured environments, a 1- to 3- μ L aliquot was spotted on an agarose slide and topped with a coverslip before the liquid was taken up by the agarose surface. Agarose slides were made by pipetting hot LM100 medium with 1% (wt/vol) agarose between a microscope slide and a coverslip, both separated by two microscope slides as spacers. After solidification, the coverslip and both microscope slide spacers were removed, leaving an uneven surface on the microscopic scale ([Fig. S1](#)). Movies were taken at room temperature at a custom microscope setup (Visitron Systems) with a Leica DMI 6000 B inverse microscope (Leica) equipped with a pco.edge sCMOS camera (PCO), a SPECTRA light engine (lumencor), and an HCPL APO 63 \times /1.4–0.6 objective (Leica) using a custom filter set (T495lpxr, ET525/50m; Chroma Technology). Usually, 200–500 frames were taken with an exposure time of 5 ms as a compromise between temporal resolution and optical contrast. Image processing and analysis were carried out using the ImageJ distribution Fiji (48). Cells were counted using the cell counter plugin, and swimming-speed measurement was done using the TrackMate (semiautomatic) or MTrackJ (manual) plugin. Details on the statistical analysis can be found in [SI Materials and Methods](#).

Numerical Model for the Flagellum. The equations, potentials, parameters, and method of integration for the numerical simulations are given in [SI Materials and Methods](#).

ACKNOWLEDGMENTS. We are grateful to Ulrike Ruppert for technical support. The study was supported by Grants TH 831/6-1 (to K.M.T.) and EC 102/14-1 (to B.E.) from the Deutsche Forschungsgemeinschaft within the Priority Program SPP1617 “Microswimmers.”

- Kelly FX, Dapsis KJ, Lauffenburger DA (1988) Effect of bacterial chemotaxis on dynamics of microbial competition. *Microb Ecol* 16:115–131.
- Lauffenburger DA (1991) Quantitative studies of bacterial chemotaxis and microbial population dynamics. *Microb Ecol* 22:175–185.
- Fenchel T (2002) Microbial behavior in a heterogeneous world. *Science* 296:1068–1071.
- Alexandre G, Greer-Phillips S, Zhulin IB (2004) Ecological role of energy taxis in microorganisms. *FEMS Microbiol Rev* 28:113–126.
- Reichenbach T, Mobilia M, Frey E (2007) Mobility promotes and jeopardizes biodiversity in rock-paper-scissors games. *Nature* 448:1046–1049.
- Josenshans C, Suerbaum S (2002) The role of motility as a virulence factor in bacteria. *Int J Med Microbiol* 291:605–614.
- Pandey G, Jain RK (2002) Bacterial chemotaxis toward environmental pollutants: Role in bioremediation. *Appl Environ Microbiol* 68:5789–5795.
- Kearns DB (2010) A field guide to bacterial swarming motility. *Nat Rev Microbiol* 8:634–644.
- Asakura S (1970) Polymerization of flagellin and polymorphism of flagella. *Adv Biophys* 1:99–155.
- Calladine CR (1975) Construction of bacterial flagella. *Nature* 255:121–124.
- Calladine CR (1978) Change of waveform in bacterial flagella: The role of mechanics at the molecular level. *J Mol Biol* 118:457–479.
- Calladine CR (1976) Design requirements for the construction of bacterial flagella. *J Theor Biol* 57:469–489.
- Hasegawa K, Yamashita I, Namba K (1998) Quasi- and nonequivalence in the structure of bacterial flagellar filament. *Biophys J* 74:569–575.
- Macnab RM, Ornston MK (1977) Normal-to-curly flagellar transitions and their role in bacterial tumbling. Stabilization of an alternative quaternary structure by mechanical force. *J Mol Biol* 112:1–30.

15. Hotani H (1982) Micro-video study of moving bacterial flagellar filaments. III. Cyclic transformation induced by mechanical force. *J Mol Biol* 156:791–806.
16. Darnton NC, Berg HC (2007) Force-extension measurements on bacterial flagella: Triggering polymorphic transformations. *Biophys J* 92:2230–2236.
17. Darnton NC, Turner L, Rojevsky S, Berg HC (2007) On torque and tumbling in swimming *Escherichia coli*. *J Bacteriol* 189:1756–1764.
18. Berg HC (2003) The rotary motor of bacterial flagella. *Annu Rev Biochem* 72:19–54.
19. Morimoto YV, Minamino T (2014) Structure and function of the bi-directional bacterial flagellar motor. *Biomolecules* 4:217–234.
20. Berg HC (2004) *E. coli in Motion* (Springer, New York).
21. Berg HC, Brown DA (1972) Chemotaxis in *Escherichia coli* analysed by three-dimensional tracking. *Nature* 239:500–504.
22. Sourjik V, Wingreen NS (2012) Responding to chemical gradients: Bacterial chemotaxis. *Curr Opin Cell Biol* 24:262–268.
23. Berg HC (1991) Bacterial motility: Handedness and symmetry. *Ciba Found Symp* 162: 58–69, discussion 69–72.
24. Son K, Guasto JS, Stocker R (2013) Bacteria can exploit a flagellar buckling instability to change direction. *Nat Phys* 9:494–498.
25. Xie L, Altindal T, Chattopadhyay S, Wu XL (2011) From the Cover: Bacterial flagellum as a propeller and as a rudder for efficient chemotaxis. *Proc Natl Acad Sci USA* 108: 2246–2251.
26. Armitage JP, Pitta TP, Vigeant MA, Packer HL, Ford RM (1999) Transformations in flagellar structure of *Rhodobacter sphaeroides* and possible relationship to changes in swimming speed. *J Bacteriol* 181:4825–4833.
27. Ranjard L, Richaume A (2001) Quantitative and qualitative microscale distribution of bacteria in soil. *Res Microbiol* 152:707–716.
28. Männik J, Driessen R, Galajda P, Keymer JE, Dekker C (2009) Bacterial growth and motility in sub-micron constrictions. *Proc Natl Acad Sci USA* 106:14861–14866.
29. Cisneros L, Dombrowski C, Goldstein RE, Kessler JO (2006) Reversal of bacterial locomotion at an obstacle. *Phys Rev E Stat Nonlin Soft Matter Phys* 73:030901.
30. Bubendorfer S, Koltai M, Rossmann F, Sourjik V, Thormann KM (2014) Secondary bacterial flagellar system improves bacterial spreading by increasing the directional persistence of swimming. *Proc Natl Acad Sci USA* 111:11485–11490.
31. Bubendorfer S, et al. (2012) Specificity of motor components in the dual flagellar system of *Shewanella putrefaciens* CN-32. *Mol Microbiol* 83:335–350.
32. Purcell EM (1997) The efficiency of propulsion by a rotating flagellum. *Proc Natl Acad Sci USA* 94:11307–11311.
33. Chen X, Berg HC (2000) Torque-speed relationship of the flagellar rotary motor of *Escherichia coli*. *Biophys J* 78:1036–1041.
34. Martinez VA, et al. (2014) Flagellated bacterial motility in polymer solutions. *Proc Natl Acad Sci USA* 111:17771–17776.
35. Vogel R, Stark H (2012) Motor-driven bacterial flagella and buckling instabilities. *Eur Phys J E Soft Matter* 35:15.
36. Lighthill J (1976) Flagellar hydrodynamics. *SIAM Rev* 18:161–230.
37. Vogel R, Stark H (2013) Rotation-induced polymorphic transitions in bacterial flagella. *Phys Rev Lett* 110:158104.
38. Vogel R, Stark H (2010) Force-extension curves of bacterial flagella. *Eur Phys J E Soft Matter* 33:259–271.
39. McMillen T, Goriely A (2002) Tendril perversion in intrinsically curved rods. *J Nonlinear Sci* 12:241–281.
40. Lele PP, Hosu BG, Berg HC (2013) Dynamics of mechanosensing in the bacterial flagellar motor. *Proc Natl Acad Sci USA* 110:11839–11844.
41. Tipping MJ, Delalez NJ, Lim R, Berry RM, Armitage JP (2013) Load-dependent assembly of the bacterial flagellar motor. *MBio* 4:e00551-13.
42. Berg HC (2013) Cell motility: Turning failure into function. *Nat Phys* 9:460–461.
43. Leibson E, Cosenza BJ, Murchelano R, Cleverdon RC (1964) Motile marine bacteria. I. Techniques, ecology, and general characteristics. *J Bacteriol* 87:652–666.
44. Lassak J, Henche AL, Binnenkade L, Thormann KM (2010) ArcS, the cognate sensor kinase in an atypical Arc system of *Shewanella oneidensis* MR-1. *Appl Environ Microbiol* 76:3263–3274.
45. Gibson DG, et al. (2009) Enzymatic assembly of DNA molecules up to several hundred kilobases. *Nat Methods* 6:343–345.
46. Guttenplan SB, Shaw S, Kearns DB (2013) The cell biology of peritrichous flagella in *Bacillus subtilis*. *Mol Microbiol* 87:211–229.
47. Rossmann F, et al. (2015) The role of FlhF and HubP as polar landmark proteins in *Shewanella putrefaciens* CN-32. *Mol Microbiol* 98:727–742.
48. Schindelin J, et al. (2012) Fiji: An open-source platform for biological-image analysis. *Nat Methods* 9:676–682.
49. Bubendorfer S, et al. (2013) Analyzing the modification of the *Shewanella oneidensis* MR-1 flagellar filament. *PLoS One* 8:e73444.
50. Laemmli UK (1970) Cleavage of structural proteins during the assembly of the head of bacteriophage T4. *Nature* 227:680–685.
51. Shimada K, Kamiya R, Asakura S (1975) Left-handed to right-handed helix conversion in *Salmonella* flagella. *Nature* 254:332–334.
52. Rashid R, Chee SM, Raghunath M, Wohland T (2015) Macromolecular crowding gives rise to microviscosity, anomalous diffusion and accelerated actin polymerization. *Phys Biol* 12:034001.
53. Chirico G, Langowski J (1996) Brownian dynamics simulations of supercoiled DNA with bent sequences. *Biophys J* 71:955–971.
54. Adhyapak TC, Stark H (2015) Zipping and entanglement in flagellar bundle of *E. coli*: Role of motile cell body. *Phys Rev E Stat Nonlin Soft Matter Phys* 92:052701.
55. Cash JR, Karp AH (1990) A variable order Runge-Kutta method for initial value problems with rapidly varying right-hand sides. *ACM Trans Math Softw* 16:201–222.
56. Miller VL, Mekalanos JJ (1988) A novel suicide vector and its use in construction of insertion mutations: Osmoregulation of outer membrane proteins and virulence determinants in *Vibrio cholerae* requires *toxR*. *J Bacteriol* 170:2575–2583.

Supporting Information

Kühn et al. 10.1073/pnas.1701644114

SI Materials and Methods

Bacterial Strains, Growth Conditions, and Media. All strains used in this study are listed in Table S1. *Escherichia coli* strains DH5 α - λ pir and WM3064 and *Shewanella putrefaciens* CN-32 were grown in LB medium at 37 and 30 °C, respectively. Cultures of the 2,6-diaminoheptanedioic acid (DAP)-auxotroph *E. coli* WM 3064 were supplemented with DAP at a final concentration of 300 μ M. To solidify media, LB agar was prepared using 1.5% (wt/vol) agar. For soft-agar plates, 0.2–0.3% (wt/vol) agar was used. Whenever necessary, media were supplemented with 50 mg/mL kanamycin, 50 μ M phenamil, and/or 10% (wt/vol) sucrose. Agarose pads for microscopy were prepared by solidifying LM100 medium [10 mM Hepes, pH 7.3; 100 mM NaCl; 100 mM KCl; 0.02% (wt/vol) yeast extract; 0.01% (wt/vol) peptone; 15 mM lactate] with 1% (wt/vol) agarose.

Strains and Vector Constructions. All genetic manipulations of *S. putrefaciens* CN-32 were introduced into the chromosome by sequential double homologous recombination using the suicide vector pNPTS138-R6K essentially as described previously (44). Plasmids and corresponding oligonucleotides are summarized in Tables S2 and S3, respectively. All kits for preparation and purification of nucleic acids (VWR International) and enzymes (Fermentas) were used according to the manufacturers' protocols. Plasmids were constructed using standard Gibson assembly protocols (45) and introduced into *Shewanella* cells by conjugative mating with *E. coli* WM3064 as donor. In-frame deletions were generated by combining ~500-bp fragments of the upstream and downstream regions of the gene to generate a deletion leaving only a few codons of the designated gene. Gene versions encoding flagellins bearing threonine-to-cysteine substitutions were reintegrated into those deletion strains in basically the same fashion. The design of these substitutions is described in detail below. As a background strain, we used *S. putrefaciens* CN-32 S2576 lacking the ability to produce lateral flagella due to deletion in the genes encoding the secondary flagellin subunits (31).

Visualizing Flagellar Filaments. To visualize the flagellar filaments, maleimide-ligated dyes were coupled to surface-exposed cysteine residues, which were specifically introduced into the flagellins, FlaA and FlaB, of the *S. putrefaciens* CN-32 polar flagellum. However, the flagellins of the close relative *S. oneidensis* MR-1 were shown to be modified by O-linked glycosylation via threonine or serine residues. Single substitutions of the corresponding residues resulted in a clearly visible shift in the protein's position when separated by polyacrylamide electrophoresis (PAGE) due to loss of the modification (49). We therefore performed a similar Western immunoblot analysis on the *S. putrefaciens* CN-32 flagellins bearing the serine- and threonine-to-cysteine substitutions to rule out that a functionally important modification was lost by the substitution. To determine potential differences in the molecular mass of flagellin protein, lysates from exponentially growing LB cultures were obtained for Western blot analyses by harvesting cells corresponding to an OD₆₀₀ of 10 by centrifugation, resuspending in sample buffer (50), and heating at 95 °C for 5 min. After separation by SDS/PAGE using 15% (wt/vol) polyacrylamide gels, the proteins were transferred to a nitrocellulose Roti-PVDF membrane (Roth) by semidry transfer. For detection of flagellins FlaA1 and FlaB1, polyclonal antibodies were used that were raised against the N-terminal conserved region of *Shewanella oneidensis* MR-1 FlaB (Eurogentec Deutschland) in the dilution of 1:500. Anti-rabbit IgG-horseradish peroxidase

antibody (Thermo Fisher Scientific) was used as secondary antibody at a dilution of 1:20,000. For signal detection, the membranes were incubated with SuperSignalH West Pico Chemiluminescent Substrate (Thermo Scientific) and documented using the CCD System LAS 4000 (Fujifilm). The *S. putrefaciens* CN-32 flagellins were detected at a position corresponding to a molecular mass of ~37 kDa (FlaA1) or ~35 kDa (FlaB1) and thus significantly higher than the estimated molecular mass (~28.5 kDa for both FlaA1 and FlaB1), strongly indicating that both FlaA1 and FlaB1 are decorated by modifications. No mass shifts were detected for the flagellins harboring the cysteine substitutions, demonstrating that no modified serine or threonine residues were lacking (Fig. S3).

Handedness of the Flagellar Helix and Orientation of the Microscope Images. Images of the flagellar helix, in regular or in screw mode, show a different pattern depending on the *z* position of the focal plane (51). An image taken of a left-handed helix appears to be left-handed when the focal plane is above the cell. However, when the focal plane is below the cell, the helix appears right-handed. This is due to the image of the cell body, which always seems to be below the focal plane, although it might be above the focal plane. To determine the handedness properly, the focal plane was slowly shifted through the cell body to reliably localize the cell body and to determine whether the flagellar helix continues upward or downward. In this study, this was done for 115 cells with normal flagellar filament and 108 cells with filaments in screwing mode using cell cultures with fluorescently labeled flagellar filaments (not or slowly rotating). The regular flagellar helix, aligned with the cell axis, was found to be left-handed. The flagellar helix wrapped around the cell body was also found to be left-handed. Because the appearance of the handedness of the flagellar helix depends on the *z* position of the focal plane and the image from the microscope is inverted technically, the microscopic images and movies were inverted appropriately, as stated in the legends, so that the visible handedness matches the true handedness of the flagellar helix.

Statistics. Calculations were carried out in R, version 3.3.2, unless stated otherwise. Two-sided testing was used for all tests. The swimming behavior of the double flagellin-labeled strain (S4401) in medium with increased viscosity was investigated by supplementing LM medium with Ficoll 400 and recording multiple videos in bulk medium for each Ficoll 400 concentration from 0 to 25%, corresponding to 2, 5, 10, 18, and 33 cP (52). The experiment was repeated three times with always about 100 counted cells per concentration, resulting in a total of at least 300 counts. Only backward swimming was considered, and we determined whether it was regular backward swimming (flagellar filament behind the cell body aligned with the cell axis) or screw mode (flagellar filament wrapped around the cell body). Significance was tested pairwise using the Fisher's exact test of independence ($P < 0.05$, Bonferroni corrected). The 95% confidence intervals were calculated with the exact binomial test.

These videos were also used to measure forward, backward, and screw swimming speed using the MTrackJ, version 1.5.1, plugin in the ImageJ distribution Fiji (48). For each swimming mode, 105 tracks were evaluated. Significance was tested using a two-sample *t* test ($P < 0.01$, Bonferroni corrected). Mean, SD, and 95% confidence intervals were calculated in Microsoft Excel 2013.

To determine swimming speeds and time between reversals, nine videos (three biological replicates with three technical replicates each) were recorded for each strain (S2576 and S4401)

as described above. Cell tracks were obtained to measure the speed of individual cells as well as the total swim time. For calculating the mean of the swimming speeds, the track data were randomized and excess data were deleted to match the sample size of the comparative strain (598 for each strain). A two-sample t test was used to test significance ($P < 0.05$). Although both datasets were not perfectly normally distributed but slightly skewed to the left, the test should be reliable as both datasets show very similar distribution. Mean, SD, and 95% confidence intervals were calculated in Microsoft Excel 2013.

Cell tracks were examined manually to count reversals. The average time between reversals was calculated for each biological replicate using the total swim time. Therefore, the sample size is only three, and normal distribution could not be tested. Significance, mean, SD, and 95% confidence intervals were calculated similarly to swim speed calculations.

Numerical Model for the Flagellum. The numerical simulations are based on equations for an elastic rod and resistive force theory (35, 36), extended to allow for multiple polymorphic equilibrium states (38). The position along the rod is measured by the arclength s and the torsional state of the rod at position s is described by the rotational strain vector $\Omega(s)$. The flagellum is assumed to have a circular cross-section and a helical rest state, characterized by a vector $\Omega_0 = (0, \kappa_0, \tau_0)$. The curvature κ_0 and torsion τ_0 are related to the helix radius R and pitch P by the following:

$$\begin{aligned}\tau_0 &= \frac{2\pi P}{4\pi^2 R^2 + P^2}, \\ \kappa_0 &= \frac{4\pi^2 R}{4\pi^2 R^2 + P^2}.\end{aligned}\quad [\text{S1}]$$

Deviations from this rest state give quadratic contributions to the free energy:

$$\mathcal{F}_K = \int_0^L \left(\frac{A}{2} \right) [(\Omega_1 - \Omega_{0,1})^2 + (\Omega_2 - \Omega_{0,2})^2] + \left(\frac{C}{2} \right) (\Omega_3 - \Omega_{0,3})^2 ds, \quad [\text{S2}]$$

where A is the bending and C is the torsional rigidity.

The polymorphic states of the flagellum can be characterized by their equilibrium helical parameters $\Omega_0 = (0, \kappa_0, \tau_0)$. Transitions between the states are obtained by local minimization of the free energies for the different polymorphic states (38). From the observations, we can unambiguously deduce only two states, one corresponding to the initial helix during swimming, and the other to the state with the flagellum wrapped around the cell. Further states could be added as well, but without independent evidence for their existence and parameters, their addition has an element of arbitrariness. We label the two conformational states S for the stretched rest state and C for the coiled state around the cell. For each state, the curvature $\kappa_0^{S,C}$ and torsion $\tau_0^{S,C}$ are related to the helix radius $R_{S,C}$ and pitch $P_{S,C}$ by Eq. S1. For the quadratic deviations, we take the same elastic coefficients A and C , because we do not have independent numbers for the different equilibrium states. The flagellum is assumed to relax locally to the configuration with minimal free energy:

$$\mathcal{F}_K = \int_0^L \min(f_K^S(\Omega(s)), f_K^C(\Omega(s)) + \delta_C) ds, \quad [\text{S3}]$$

with δ_C indicating the energy difference between coiled and stretched state.

To control the amount of stretching of the flagellum, a global harmonic spring potential is added:

$$\mathcal{F}_S = (K/2) \int_0^L (\partial \mathbf{r} / \partial s)^2 ds, \quad [\text{S4}]$$

with an elastic constant that keeps the variations in length within 0.1%.

The elastic forces follow from variational derivative $\delta \mathcal{F} / \delta \mathbf{r}$ of the combined functional $\mathcal{F}_K + \mathcal{F}_S$. In the numerical representation, the flagellum is divided into N discrete segments that are characterized by a position \mathbf{r}_i and a local tripod of unit vectors $[\mathbf{f}^{(i)}, \mathbf{v}^{(i)}, \mathbf{u}^{(i)}]$ to keep track of the torsional state of the flagellum. The points are distributed uniformly along the flagellum, so that each segment has a length $h = L_0/N$, where L_0 is the contour length of the flagellum. The unit vectors \mathbf{u} are related to the positions by $\mathbf{u}_i = (\mathbf{r}_{i+1} - \mathbf{r}_i) / |\mathbf{r}_{i+1} - \mathbf{r}_i|$. The vectors \mathbf{f}_i for the initial helix configuration are obtained from the relation $\mathbf{f}_i = (\mathbf{u}_{i-1} \times \mathbf{u}_i) / \sin(\theta_i)$, where θ_i is the angle between segment $i-1$ and i . For each time step of the simulation, \mathbf{f}_i is adjusted following the procedure proposed by Chirico and Langowski (53). The tripod is completed with the vector $\mathbf{v}_i = \mathbf{u}_i \times \mathbf{f}_i$.

The local strain Ω for each segment is calculated according to the following:

$$\begin{aligned}\Omega_1^i &= -\frac{\theta_i}{\sin \theta_i} \mathbf{v}_i \cdot \mathbf{u}_{i+1}, \\ \Omega_2^i &= \frac{\theta_i}{\sin \theta_i} \mathbf{f}_i \cdot \mathbf{u}_{i+1}, \\ \Omega_3^i &= \phi_i,\end{aligned}\quad [\text{S5}]$$

where ϕ_i is the local twist angle,

$$\sin \phi_i = \cos \theta_i (\mathbf{v}_i \cdot \mathbf{f}_{i+1}) - (\mathbf{v}_i \cdot \mathbf{u}_{i+1})(\mathbf{u}_i \cdot \mathbf{f}_{i+1}) + \frac{(\mathbf{f}_i \cdot \mathbf{u}_{i+1})(\mathbf{u}_i \cdot \mathbf{v}_{i+1})}{1 + \cos \theta_i}. \quad [\text{S6}]$$

The derivative of the free energy for the stretching force is obtained analytically, so that, for instance, the force acting on segment i is given by the following:

$$\mathbf{f}_s^i = -K[(L_i - L_0)\mathbf{u}_i - (L_{i+1} - L_0)\mathbf{u}_{i+1}], \quad [\text{S7}]$$

whereas the derivatives of the free energy corresponding to bending and twisting forces are calculated by finite differences.

The flagellum's rotation is driven by a constant motor torque M_0 , applied to the first segment. To account for the effects of the bacterial hook, which is much more flexible than the flagellum (24), this segment is allowed to rotate freely and thereby transmit the torque to the following segments. The dynamics of the motor segment are described by the following:

$$\begin{aligned}\omega_0 &= \mu_0 [\mathbf{M}_0^z + \mathbf{M}_0^u - A[(\Omega_1 - \Omega_{0,1})\mathbf{f}_0 + (\Omega_2 - \Omega_{0,2})\mathbf{v}_0] \\ &\quad - C(\Omega_3 - \Omega_{0,3})\mathbf{u}_0],\end{aligned}\quad [\text{S8}]$$

where the total torque is split between a component parallel the axis of the motor $\mathbf{M}_0^z = M_0(\sqrt{1 - \alpha^2 \sin^2 \phi_m} - \alpha \cos \phi_m)\mathbf{e}_z$, and one parallel to the first segment, $\mathbf{M}_0^u = \alpha M_0 \mathbf{u}_1$, with the parameter α controlling the relative contributions. ϕ_m is the angle between the tangential motor segment \mathbf{u}_0 and the first filament segment \mathbf{u}_1 . Finally, μ_0 is the motor segment's self-mobility, which depends of the rotational and the translational friction. The boundary

conditions on the final segment are that no external torque is applied so that it is torque free.

In addition to the elastic forces, we have to model the interactions with the cell body, and also between segments of the flagellum, because the deformations become very large and parts of the flagellum come into mechanical contact. The cell body is modeled as a cylindrical object of radius $R_{\text{cell}} = 0.45 \mu\text{m}$ that is sufficiently long that the flagellum does not pass underneath it. In the images, a length $H_{\text{cell}} = 3 \mu\text{m}$ is shown. The flagellum is assumed to be 20 nm thick, and distances between approaching segments are computed following a procedure proposed by Adhyapak and Stark (54). In both cases, the repulsion between the segments of the flagellum and other segments or the cell body was modeled with a Lennard-Jones-type potential, truncated at its minimum, so that the forces vary continuously,

$$\Phi_c = \begin{cases} \epsilon \left[(r_m/r)^{12} - 2(r_m/r)^6 \right], & \text{if } r \leq r_m \\ 0, & \text{otherwise} \end{cases} \quad [\text{S9}]$$

where r_m is either the cell radius or the radius of the filament and is the strength of the potential.

For the frictional forces, we use resistive force theory (36). The local motion of the flagellum's segments is characterized by three local friction coefficients (36) that depend on the geometry of the flagellum:

$$\gamma_{\perp} = \frac{4\pi\eta}{\ln(0.09l/r_f) + 1/2} \quad [\text{S10}]$$

is the friction coefficient for motion perpendicular to the flagellum's centerline, where η is the viscosity, r_f is the radius of the filament, and $l = \sqrt{4\pi^2 R^2 + P^2}$ is the contour length of one helical turn. The tangential friction coefficient is as follows:

$$\gamma_{\parallel} = \frac{2\pi\eta}{\ln(0.09l/r_f)}, \quad [\text{S11}]$$

and the friction encountered by the filament during rotation is characterized by the following:

$$\gamma_r = 4\pi\eta r_f^2. \quad [\text{S12}]$$

The friction coefficients and the mobilities μ_t and μ_r that enter in the equations of motion are related by the following:

$$\mu_t = \mathbf{u}_i \otimes \mathbf{u}_i / \gamma_p + (1 - \mathbf{u}_i \otimes \mathbf{u}_i) / \gamma_n, \quad [\text{S13}]$$

and $\mu_r = 1/\gamma_r$. The translational equation of motion for segment i is then obtained from the elastic forces \mathbf{F}_{el} (2, 3) the stretching

force \mathbf{F}_s (8) and the repulsive forces \mathbf{F}_c and \mathbf{F}_{fl} , resulting from filament–cell and filament–filament interactions (10):

$$\frac{d\mathbf{r}_i}{dt} = \mu_t (\mathbf{F}_{i,el} + \mathbf{F}_{i,s} + \mathbf{F}_{i,c} + \mathbf{F}_{i,fl}). \quad [\text{S14}]$$

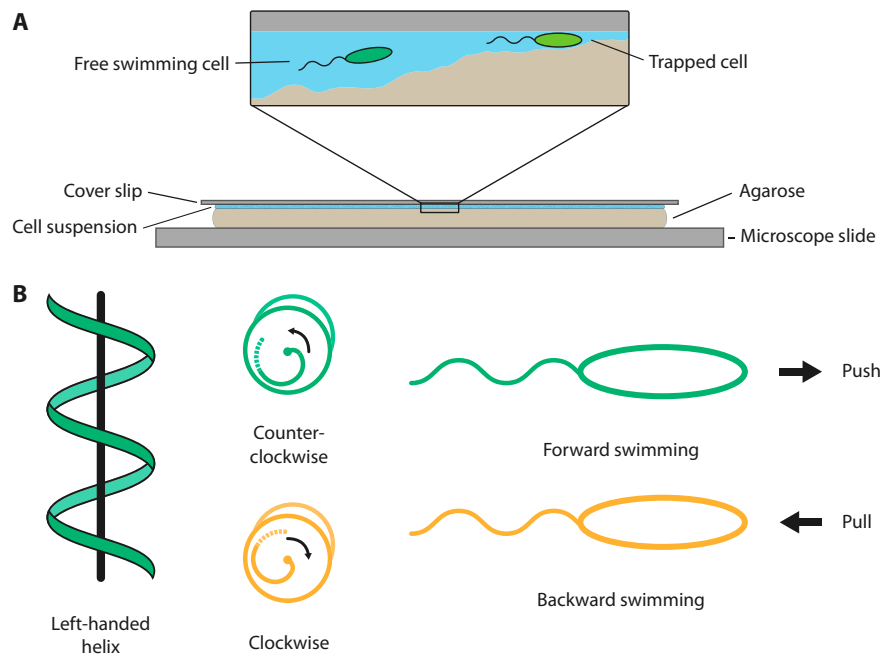
The change in the torsion angle ϕ_i of segment i depends on the elastic torque M_{el} only:

$$\frac{d\phi_i}{dt} = \mu_r M_{i,el}. \quad [\text{S15}]$$

To achieve high accuracy while keeping the computational costs down, the equations of motions were integrated using the Cash–Karp method (55), a high-order Runge–Kutta integrator with embedded error estimation and steps size control. During each partial integration step, the segment positions are updated according to $r_i(t + h_t) = r_i(t) + h_t v_i$, where h_t is the partial step size. Using the new positions and velocities $\mathbf{v}_i = d\mathbf{r}_i/dt$, the attached tripods are aligned in a second step, following the procedure proposed by Chirico and Langowski (53).

As initial conditions for the simulations, we took a left-handed helix with $P^S = 1.91 \mu\text{m}$ and $R^S = 0.315 \mu\text{m}$ in accordance with observations, resulting in $\tau^S = 1.59/\mu\text{m}$ and $\kappa^S = 1.64/\mu\text{m}$. We adapted the helix parameters of the second state to the parameters of the screw, namely, $R^C = 0.473 \mu\text{m}$ and $P^C = 1.44 \mu\text{m}$. The contour length of the flagellum was set to $L_c = 6 \mu\text{m}$, corresponding to two helical turns. The discretization length is $h = 0.15 \mu\text{m}$, comparable to the values taken by Vogel and Stark (35). For the elastic constants, no direct measurements of A and C have been reported so far. Although the flagellum's crystal structure differs from that of well-studied organisms like *E. coli*, we anticipate that its mechanical properties will not differ significantly from that of *E. coli*, and hence choose the values $A = C = 3.5 \text{ pN}\cdot\mu\text{m}^2$ in accordance to values obtained by Darnton and Berg (16). We also explored values between $A = C = 2.5 \text{ pN}\cdot\mu\text{m}^2$ and $A = C = 4 \text{ pN}\cdot\mu\text{m}^2$ to study the influence of the rigidity on the screw formation, without noting significant differences. The various parameters in the model for the flagellum and their values are summarized in Table S4.

To probe the effects of the polymorphic transitions, we also did simulations with a single equilibrium configuration. They also show the formation of the screw, but require stronger torque and need more time to wrap the flagellum around the cell. We anticipate that further polymorphic states will similarly assist the formation of the screw but will not bring about qualitative changes.



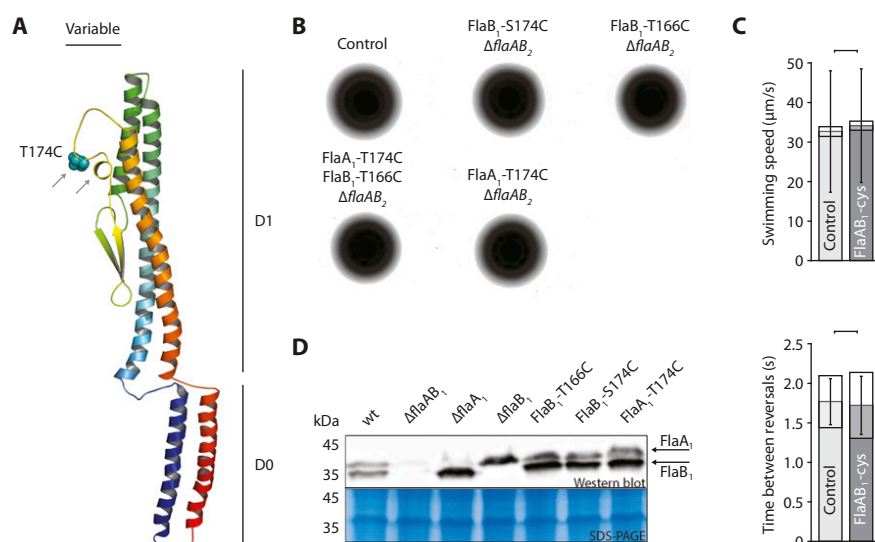


Fig. S3. Substitution of serine or threonine to cysteine in the variable domain of the polar flagellin monomers does not impair the swimming motility of *S. putrefaciens*. (A) Predicted structure of the polar flagellin FlaA1 of *Shewanella putrefaciens* CN-32 (calculated by PyMOL 1.3). The threonine 174-to-cysteine substitution site is indicated by a blue sphere. The approximate corresponding substitution sites (T166C and S174C) are indicated by gray arrows. Thus, all substitution sites in both flagellins are located in the variable domain (approximately amino acids 163–183), which is exposed to the surrounding medium in the assembled flagellar filament. (B) Radial extension of FlaAB₁-cys mutants and Δ flaAB₂ as background strain (control) in 0.25% soft agar. The strains are labeled accordingly. The substitutions do not reduce the extension radius. (C) Swim speed and time between reversals for FlaAB₁-cys are highly similar to its background strain Δ flaAB₂ (control). For each strain, 598 cell tracks were evaluated (TrackMate plugin for ImageJ). The differences are not significant (two-sample *t* test; *P* = 0.087 and 0.891, respectively). Time between reversals was measured over the whole population, so the sample size is only three. Error bars represent SD; shaded boxes represent 95% confidence intervals. (D) FlaA₁ and FlaB₁ immunostaining subsequent to separation of the protein crude extract by SDS/PAGE and Western transfer to a membrane. Substitution of serine or threonine to cysteine does not cause a mass shift of the flagellins. This would only occur if glycosylation sites were substituted to cysteine.

Table S1. Bacterial strains used in this study

Strain	Genotype	Purpose	Source
<i>Escherichia coli</i>			
DH5 α pir	ϕ 80dlacZ Δ M15 Δ (lacZYA-argF)U169 recA1 hsdR17 deoR thi-I supE44 gyrA96 relA1 λ pir	Cloning strain	Ref. 56
WM3064	thrB1004 pro thi rpsL hsdS lacZ Δ M15 RP4-1360 Δ (araBAD) 567 Δ dapA 1341::[erm pir(wt)]	Conjugation strain	W. Metcalf, University of Illinois at Urbana-Champaign, Champaign, IL
<i>Shewanella putrefaciens</i>			
S271	CN-32	Wild type	
S2576	Δ flaAB ₂ ; Δ Sputcn32 3455–56	Markerless deletion of both lateral flagellin genes	Ref. 31
S3807	Δ flaA1-ext; Δ Sputcn32 2586	Markerless deletion of polar minor flagellin gene	This study
S3810	Δ flaB1-ext; Δ Sputcn32 2585	Markerless deletion of polar major flagellin gene	This study
S4152	flaA1-T174C - Δ flaAB ₂	Markerless insertion of cysteine-labeled flaA1 gene into Δ flaA1-ext and deletion of lateral flagellin genes	This study
S4143	flaB1-T166C	Markerless insertion of cysteine labeled flaB1 gene into Δ flaB1-ext	This study
S4154	flaB1-T166C - Δ flaAB ₂	Markerless insertion of cysteine labeled flaB1 gene into Δ flaB1-ext and in-frame deletion of lateral flagellin genes	This study
S4156	flaB1-S174C - Δ flaAB ₂	Markerless insertion of cysteine labeled flaB1 gene into Δ flaB1-ext and deletion of lateral flagellin genes	This study
S4147	flaB1-S174C	Markerless insertion of cysteine labeled flaB1 gene into Δ flaB1-ext	This study
S4401	Δ flaAB ₂ flaA1T174C flaB1-T166C	Markerless insertion of cysteine labeled flaB1 gene into Δ flaB1-ext and cysteine labeled flaA1 gene into Δ flaA1-ext and deletion of lateral flagellin genes	This study

Table S2. Plasmids used in this study

Name	Insert	Purpose	Source
pNPTS138-R6KT	<i>mobRP4+</i> , <i>ori-R6K</i> , <i>sacB</i> , betagalactosidase fragment alpha, Km ^r	Suicide plasmid for in-frame deletions or integrations	Ref. 44
pNPTS138-R6KT-R6KT-flag-clusterII-KO	Δ <i>flaAB2</i> (Sputcn32_3455–56)	In-frame deletion fragment	Ref. 31
pNPTS138-R6KT- <i>flaA1</i> -KO-ext	Δ <i>flaB1</i> (Sputcn32_2586)	In-frame deletion fragment	This study
pNPTS138-R6KT- <i>flaB1</i> -KO-ext	Δ <i>flaB1</i> (Sputcn32_2585)	In-frame deletion fragment	This study
pNPTS138-R6KT- <i>flaA1</i> - T174C	<i>flaA1</i> -T174C (Sputcn32_2586)	In-frame insertion fragment; threonine 174 substituted with cysteine	This study
pNPTS138-R6KT- <i>flaB1</i> - T166C	<i>flaB1</i> -T166C (Sputcn32_2585)	In-frame insertion fragment; threonine 166 substituted with cysteine	This study
pNPTS138-R6KT- <i>flaB1</i> - S174C	<i>flaB1</i> -S174C (Sputcn32_2585)	In-frame insertion fragment; serine 174 substituted with cysteine	This study

Table S3. Oligonucleotides used in this study

ID	Name	Sequence	Purpose	Source
B 31	BamHI-flagL-fwd	AGG ATC CTG ACA CTG TAT TTA TGG CGC AGG	Construction of in-frame deletion vector pNPTS138R6KT-R6KT-flag-clusterII-KO	Ref. 31
B 32	OL-flagL-rev	CAG TAG ACC GTG AAC ACC TAA CAT ATT AAT TCT CCA G		
B 33	OL-flagL-fwd	GGT GTT CAC GGT CTA CTG CGT TAA TCT AGC TC		
B 34	PspOMI-flagL-rev	TGT CGG GCC CGT CGC CGT CGC ATT TTC GC		
B 35	Check-flagL-fwd	GTA TTA GCT TCG ATC GGG ATT GG	Check primer for <i>flaAB2</i>	Ref. 31
B 36	Check-flagL-rev	GTT ACC CTT TGG CGC ATC GG	Construction of in-frame deletion vector pNPTS138-R6KT- <i>flaA1</i> -KO-ext	This study
MJK 26	OL <i>flaA1</i> KO ext rv	GTG ACA GCG CAA TAG CCA TAG TAT TTT CCT CTT CTA AG		
MJK 27	OL <i>flaA1</i> KO ext fw	TAT GGC TAT TGC GCT GTC ACT ACT GGG ATA ATT TAC		
FR299	EcoRV <i>flaA1</i> KO fw	GAA TTC GTG GAT CCA GAT GAA GTT AAA GTG TCT GGG AAA CCC		
FR302	EcoRV <i>flaA1</i> KO rv	CAA GCT TCT CTG CAG GAT GCA TCG CAC CTT CAG AAA TTT GG	Construction of in-frame deletion vector pNPTS138-R6KT- <i>flaB1</i> -KO-ext	This study
MJK 28	OL <i>flaB1</i> KO ext rv	AGG CCA CTT GGG CCA TGA TCG TTT CCT CTG TA		
MJK 29	OL <i>flaB1</i> KO ext fw	GAT CAT GGC CCA AGT GGC CTT ATC ACT GCT GTA ATA G		
FR295	EcoRV <i>flaB1</i> _KO fw	GAA TTC GTG GAT CCA GAT ATA ACC AAC GTG CAG CGT TAG G		
FR298	EcoRV <i>flaB1</i> _KO rv	CAA GCT TCT CTG CAG GAT CAG CTA ATG CCA ACG CTT CTT C	Check primer for <i>flaAB1</i>	Ref. 31
B 49	Check-flagP-fwd	AAT TTT GAT GCG ACT ACC CCC G		
B 50	Check-flagP-rev	TAT CTA GAC CTG ACC CCA TGC C	Construction of in-frame insertion vector pNPTS138-R6KT- <i>flaA1</i> -T174C	This study
MJK 78	<i>FlaA1</i> -T174C-R	TCG TTA AAC AAC TAA CCA TTA AAC TCC CCG CAT TAT TGG		
MJK 79	<i>FlaA1</i> -T174C-F	TGG TTA GTT GTT TAA CGA TTG CAA CTT CAG GTG GTC G	Construction of in-frame insertion vector pNPTS138-R6KT- <i>flaB1</i> -T166C	This study
MJK 82	<i>FlaB1</i> -T166C-R	CTG ATG CAC AGG TTT TTG ACA CAG AAA TCG		
MJK 83	<i>FlaB1</i> -T166C-F	CAA AAA CCT GTG CAT CAG CAT TAA AAG TTG G	Construction of in-frame insertion vector pNPTS138-R6KT- <i>flaB1</i> -S174C	This study
MJK 86	<i>FlaB1</i> -S174C-R	ATA TCT AAA CAA CCA ACT TTT		
MJK 87	<i>FlaB1</i> -S174C-F	AAT GCT GAT GC AGT TGG TTG TTT AGA TAT TAA AGG CTC TGC		

Table S4. The various parameters in numerical model and their values

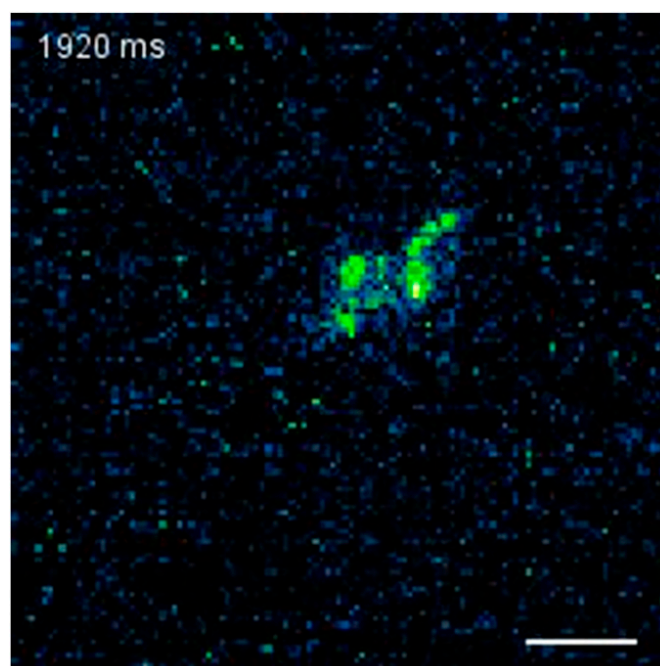
Parameter	Description	Values
R^S	Helical radius, stretched	0.315 μm
P^S	Helical pitch, stretched	1.91 μm
κ^S	Curvature, stretched	1.64/ μm
τ^S	Torsion, stretched	1.59/ μm
R^C	Helical radius, coiled	0.473 μm
P^C	Helical pitch, coiled	1.44 μm
κ^C	Curvature, coiled	1.71/ μm
τ^C	Torsion, coiled	0.829/ μm
L_c	Contour length	6.5 μm
A	Bending rigidity	3.5 $\text{pN}\cdot\mu\text{m}^2$
C	Twisting rigidity	3.5 $\text{pN}\cdot\mu\text{m}^2$
K	Stretching stiffness	10,000 $\text{pN}/\mu\text{m}$
R_{cell}	Cell radius	0.45 μm
H_{cell}	Cell height	3.0 μm
γ_{\perp}	Friction coefficient, normal to flagellum	2.85 η
γ_k	Friction coefficient, parallel to flagellum	1.61 η
γ_r	Rotational friction coefficient	0.0012 η
h_0	Segment length	0.125 μm
α	Relative motor contribution along first segment	0.25
M_0	Motor torque	7.6 $\text{pN}\cdot\mu\text{m}$
δc	Energy difference between states	0.1 pN

Dataset S1. Approach, trapping, and escape of a bacterium between agarose and coverslip (related to Movie S1)[Dataset S1](#)

Image sequence from high-speed fluorescence microscopy showing *Shewanella putrefaciens* CN-32 with fluorescently labeled polar flagellar filaments. The images are provided in two forms: as an .avi movie that runs continuously and as a flip-book (.pdf) that allows to move interactively from image to image. The cell approaches from the *Lower Left*, moves upward, and then gets stuck. While still pushing forward, the flagellum wiggles circularly in an instability known to occur for stronger applied torque. The flagellar motor then switches direction of rotation to CW and the flagellum wraps around the cell body. The cell backs out to the *Lower Left* and returns to regular forward swimming by switching motor rotation to CCW. Exposure time was 30 ms; playback speed is 10 fps. (Scale bar: 2 μm .) Still images of this movie were used in Fig. 1.

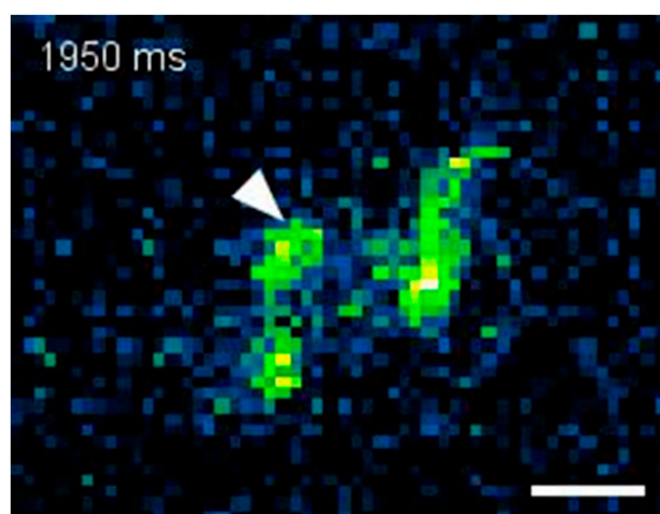
Dataset S2. Formation of the screw starts with an instability at the base of the flagellar filament (related to Movie S5)[Dataset S2](#)

Image sequence from high-speed fluorescence microscopy showing *Shewanella putrefaciens* CN-32 with fluorescently labeled polar flagellar filaments. The images are provided in two forms, as an .avi movie that runs continuously and as a flip-book (.pdf) that allows to move interactively from image to image. The cell is stuck between agarose and coverslip in medium supplemented with 20% Ficoll 400 to increase the viscosity and slow down the movement of the flagellar helix. These images show that CW rotation results in an instability at the base of the flagellar filament, leading to a pull of the filament toward the cell body and eventually wrapping of the flagellum around the cell body. Note that these images were inverted horizontally to match the correct handedness of the flagellar helix as detailed in *S1 Materials and Methods*. Exposure time was 5 ms; playback speed is 5 fps. (Scale bar: 2 μm .) Still images of this movie were used in Fig. 4 and Fig. S2.



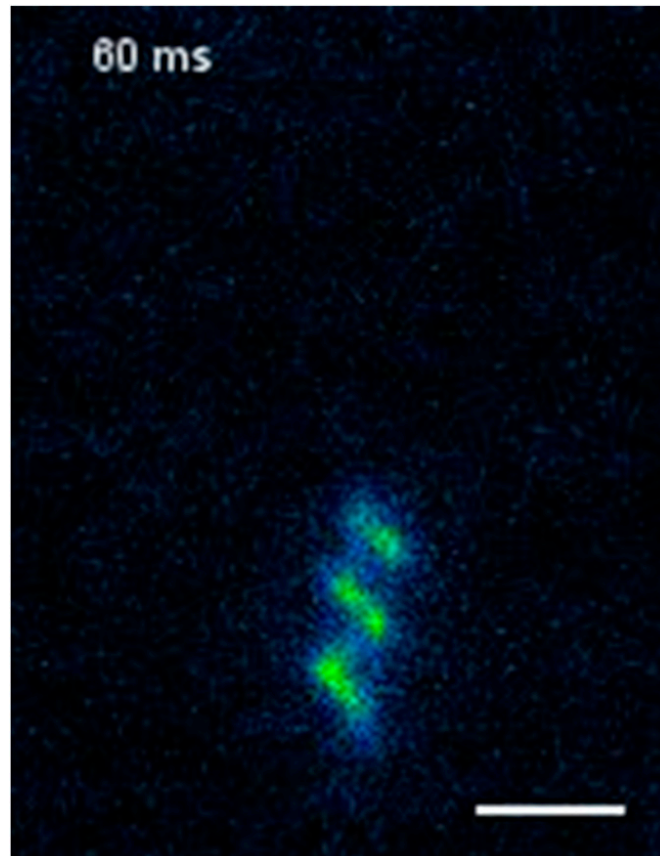
Movie S1. Approach, trapping, and escape of a bacterium between agarose and coverslip (related to Dataset S1). Image sequence from high-speed fluorescence microscopy showing *Shewanella putrefaciens* CN-32 with fluorescently labeled polar flagellar filaments. The images are provided in two forms: as an .avi movie that runs continuously and as a flip-book (.pdf) that allows to move interactively from image to image. The cell approaches from the *Lower Left*, moves upward, and then gets stuck. While still pushing forward, the flagellum wiggles circularly in an instability known to occur for stronger applied torque. The flagellar motor then switches direction of rotation to CW and the flagellum wraps around the cell body. The cell backs out to the *Lower Left* and returns to regular forward swimming by switching motor rotation to CCW. Exposure time was 30 ms; playback speed is 10 fps. (Scale bar: 2 μm .) Still images of this movie were used in Fig. 1.

[Movie S1](#)



Movie S2. Screw-like propagation relies on interaction between the flagellar filament and asperities on the surface. Image sequence selection from Movie S1 during propagation of the cell in screw mode. The white triangle indicates one peak of the flagellar waveform. While the cell moves to the *Lower Left*, the waveform of the flagellar helix does not move relative to the surrounding medium. Exposure time was 30 ms; playback speed is 1 fps. (Scale bar: 1 μm .) Still images of this movie were used in Fig. 2.

[Movie S2](#)

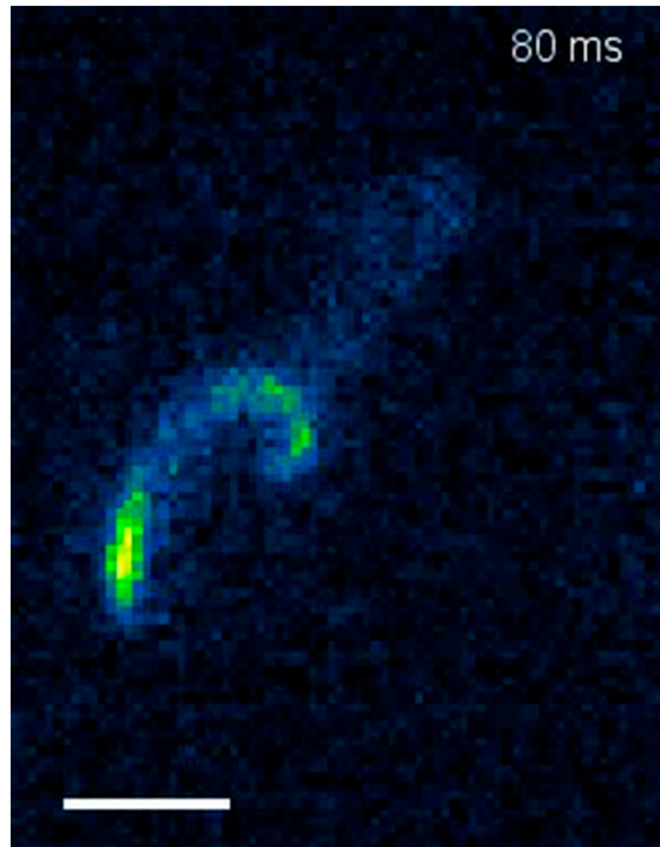


Movie S3. Repeated formation and unwinding of the flagellar screw. Image sequence from high-speed fluorescence microscopy showing *Shewanella putrefaciens* CN-32 with fluorescently labeled polar flagellar filaments. Although the cell body is stuck at the glass surface of the coverslip, the flagellar motor is still rotating, alternating between CW and CCW rotation. This leads to repeated formation and unwinding of the flagellar screw. Exposure time was 30 ms; playback speed is 10 fps. (Scale bar: 1 μm .) These images are inverted horizontally to match the correct handedness of the flagellar helix as detailed in *SI Materials and Methods*.

[Movie S3](#)

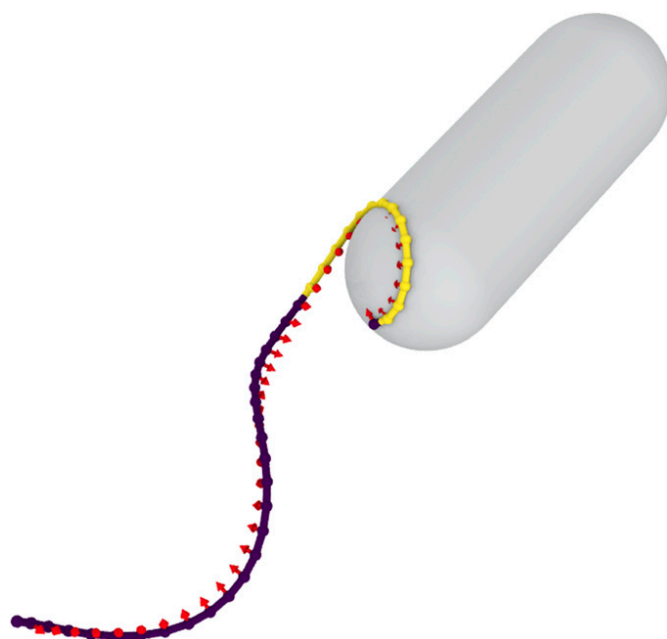


Movie S4



Movie S5. Formation of the screw starts with an instability at the base of the flagellar filament (related to Dataset S2). Image sequence from high-speed fluorescence microscopy showing *Shewanella putrefaciens* CN-32 with fluorescently labeled polar flagellar filaments. The images are provided in two forms, as an .avi movie that runs continuously and as a flip-book (.pdf) that allows to move interactively from image to image. The cell is stuck between agarose and coverslip in medium supplemented with 20% Ficoll 400 to increase the viscosity and slow down the movement of the flagellar helix. These images show that CW rotation results in an instability at the base of the flagellar filament, leading to a pull of the filament toward the cell body and eventually wrapping of the flagellum around the cell body. Note that these images were inverted horizontally to match the correct handedness of the flagellar helix as detailed in *SI Materials and Methods*. Exposure time was 5 ms; playback speed is 5 fps. (Scale bar: 2 μm .) Still images of this movie were used in Fig. 4 and Fig. S2.

[Movie S5](#)



Movie S6. Numerical simulation of the flagellum during screw formation. Simulation starts after switch from CCW to CW rotation. The red arrows indicate the rotational state of each segment, and the gray capsule-shaped object indicates the cell body. The stretched helix configuration is color-coded in purple, whereas the coiled state is marked in yellow. Details of the numerical simulations are described in *SI Materials and Methods*, and the parameters are given in Table S4. The rotation is driven by a motor torque of 6 pN· μ m, and the simulation time between each frame is 10 μ s, resulting in a total simulation time of 0.021 s. The simulation is visualized using OVITO.

[Movie S6](#)

2. Spatial arrangement of several flagellins within bacterial flagella improves motility in different environments

2.1. Summary

Shewanella putrefaciens CN-32 assembles its polar flagellar filament using two genetically distinct flagellins. They are arranged adjacently on the chromosome and by labelling them individually with a fluorescent dye we found that FlaA forms a short segment at the base of the flagellar filament while FlaB makes the major, distal part of the helix (Kühn et al. 2018, Fig. 1 a, Fig. S4). Although many flagellated bacteria maintain more than one flagellin gene, the role of multiple flagellins is largely unknown. Western blot analysis of deletion strains lacking major flagellar regulators showed that *flaA* and *flaB* are regulated differently: Both require the early flagellar regulators FlrA and RpoN (sigma factor 54), but only transcription of *flaB* requires FliA (sigma factor 28; Kühn et al. 2018, Fig. S2 b). The current model of flagellin expression implies that transcription of flagellins in general only starts once the hook-basal-body complex is completed and FliA becomes active. This usually ensures that the very high production of the flagellins only starts when the flagellum is ready to assemble the filament. Our findings suggest that in *S. putrefaciens* FlaA is already being produced before that and hence, a pool of FlaA most likely accumulates in the cytoplasm ready to be exported. As soon as the hook-basal-body complex is completed, the FlaA subunits get exported and begin to assemble the filament. Only then FliA is activated and FlaB production starts, probably at a much higher rate. Therefore, once FlaB subunits are ready, a short segment of the filament is already assembled. The higher numbers of FlaB likely outcompete FlaA, so that the major, distal segment of the filament is constructed mostly from FlaB (cf. Kühn et al. 2018, Fig. 2). In *S. putrefaciens*, the spatial arrangement of the two distinct flagellins is thus achieved by the use of two different promoters for *flaA* and *flaB*.

Consistent with our suggested model, deletion of *flaB* results in short filament stubs (because production of FlaA is not sufficient to make a full-length filament), while deletion of *flaA* results in a full-length filament exclusively made from FlaB. Furthermore, swapping the coding sequences of the flagellins also swaps the regulation and thus, FlaB now forms the short basal segment and FlaA makes up the major part of the filament. Accordingly, putting *flaA* under control of the *flaB* promoter and deleting *flaB* results in full-length filaments exclusively made from FlaA (cf. Kühn et al. 2018, Fig. 1). Fluorescence microscopy of mutant cells revealed that filaments predominantly consisting of FlaA adopt a different helix geometry than wild-type filaments. The FlaB-only filament, on the other hand, closely resembles the wild-type helix shape.

Different helix geometries could very well affect the swimming behaviour of the cells, so we determined three characteristic swimming parameters: Swimming speed, run length (i.e. the frequency of turns) and the turning angle. This was done by three dimensional tracking using holographic microscopy and algorithm-based data analysis. The different filament mutants, in fact, showed some variations in swimming behaviour, although all filament types still confer robust swimming motility. Clear differences were observed in swimming speed, but also in turning angle and one mutant was affected in turning frequency (Kühn et al. 2018, Fig. 3). This demonstrates that the composition and shape of the flagellar filament affect the free-swimming behaviour of the cells.

On the other hand, *S. putrefaciens* also uses its flagellum to navigate structured environments using the distinctive, *screw-like* motion that was described previously in the above publication (Kühn et al. 2017). Strikingly,

the composition and shape of the flagellar helix also significantly affects the *screw thread* formation. The wild type rarely switches to *screw thread* mode in regular medium, but shows increased *screw thread* formation in medium with increased viscosity. On the other hand, *screw thread* formation was considerably increased under both conditions in the FlaB-only mutant. In contrast, both mutants with filaments purely or mostly made from FlaA were never observed to switch to *screw thread* mode under the tested conditions (Kühn et al. 2018, Fig. 4 a).

We postulated that movement in *screw thread* mode only provides an advantage in structured environments but not under free-swimming conditions. With these filament mutants at hand we were able to verify the physiological benefit of the *screw thread* formation for navigating structured environments. To analyse the performance in structured environments we used soft-agar plates, in which cells swim through liquid-filled pockets formed by the loose agarose network and spread radially from the point of inoculation. While the *screw-thread*-forming strains (wild type and FlaB-only) spread considerably well, the mutants not able to switch to *screw thread* mode (FlaA-only and FlaBA) were severely impaired in spreading (Kühn et al. 2018, Fig. 1 i-l). Most importantly, the FlaA-only mutant, which showed robust free-swimming capabilities very similar to FlaB-only but faster (Kühn et al. 2018, Fig. 3 a-f), did not spread well in the structured soft-agar environment. This clearly demonstrates that the ability to wrap the filament around the cell body and move in the *screw thread* motility mode provides a huge advantage in structured environments.

Comparing the *screw thread* formation frequency of wild-type, FlaB-only and FlaA-only strains indicated that inserting a proximal FlaA segment makes the filament more stable to *screw thread* formation. This is in agreement with our previous observations that the formation of the *screw thread* starts with an instability in the first loop of the helix. Extended physical simulations with helix geometries resembling those of FlaA and FlaB filaments supported this hypothesis and indicated that the helix geometry alone could be responsible for the different stability to *screw thread* formation. Introducing the FlaA segment and increasing its length decreased the frequency of *screw thread* formation, both in the simulation as well as in experiment (Kühn et al. 2018, Fig. 4 a, b, Fig. S9 a, c).

The results described here demonstrate how bacteria can benefit from the maintenance of multiple flagellins and how they can construct a flagellar filament that is well-suited for swimming in bulk liquid but also for *screw thread* motility in structured environments. The distinct spatial segmentation of the flagellar helix balances the *screw thread* formation to only trigger when the load on the flagellum increases due to the cell body being stuck or constricted.

2.2. Contribution


Florian Rossmann and Bina Helm constructed some of the strains. All the other biological experiments were performed by me (main strain constructions, fluorescent microscopy, Western blots, motility assays, data analysis). Felix Schmidt and Bruno Eckhardt extended the numeric simulation which they had established in the previous publication (Kühn et al. 2017). Nicola Farthing and Laurence Wilson performed the holographic microscopy and determined the swimming parameters. Marco Kühn, Felix Schmidt, Laurence Wilson, Bruno Eckhardt and Kai Thormann designed the research and wrote the manuscript.

ARTICLE

<https://doi.org/10.1038/s41467-018-07802-w>

OPEN

Spatial arrangement of several flagellins within bacterial flagella improves motility in different environments

Marco J. Kühn¹, Felix K. Schmidt², Nicola E. Farthing^{3,4}, Florian M. Rossmann¹, Bina Helm¹, Laurence G. Wilson³ , Bruno Eckhardt² & Kai M. Thormann¹

Bacterial flagella are helical proteinaceous fibers, composed of the protein flagellin, that confer motility to many bacterial species. The genomes of about half of all flagellated species include more than one flagellin gene, for reasons mostly unknown. Here we show that two flagellins (FlaA and FlaB) are spatially arranged in the polar flagellum of *Shewanella putrefaciens*, with FlaA being more abundant close to the motor and FlaB in the remainder of the flagellar filament. Observations of swimming trajectories and numerical simulations demonstrate that this segmentation improves motility in a range of environmental conditions, compared to mutants with single-flagellin filaments. In particular, it facilitates screw-like motility, which enhances cellular spreading through obstructed environments. Similar mechanisms may apply to other bacterial species and may explain the maintenance of multiple flagellins to form the flagellar filament.

¹Institut für Mikrobiologie und Molekularbiologie, Justus-Liebig-Universität Gießen, 35392 Gießen, Germany. ²Fachbereich Physik und LOEWE Zentrum für Synthetische Mikrobiologie, Philipps-Universität Marburg, 35032 Marburg, Germany. ³Department of Physics, University of York, Heslington, York YO10 5DD, UK. ⁴Department of Mathematics, University of York, Heslington, York YO10 5DD, UK. These authors contributed equally: Marco J. Kühn, Felix K. Schmidt, Nicola E. Farthing. Correspondence and requests for materials should be addressed to L.G.W. (email: laurence.wilson@york.ac.uk) or to B.E. (email: bruno.eckhardt@physik.uni-marburg.de) or to K.M.T. (email: kai.thormann@mikro.bio.uni-giessen.de)

Active motility enables bacteria to establish themselves in their favorable environmental niche. For propulsion many bacterial species employ flagella, long helical proteinaceous filaments extending from the cell surface into the surrounding environment. They are rotated at the filaments' base by membrane-embedded motors, which commonly allow rotational switches to enable navigation¹. Each flagellar filament is composed of thousands of copies of flagellin subunits^{2,3} in a process that is tightly regulated at the expression level. Typically, expression of the flagellin genes requires alternative sigma factors, and production and export of the flagellins is initiated once assembly of the basal body and the hook joint structure is completed⁴. The flagellins are then transported through the filament and assembled at the tip of the growing flagellum^{5–7}.

Many bacterial species, such as *Escherichia coli*, harbor a single flagellin gene so that the resulting flagellar filament consists of only one type of subunit. However, about 45% of the flagellated bacterial species possess more than a single flagellin gene⁸, with numbers ranging up to fifteen copies as reported for *Magnetococcus* sp. MC-1⁹. *Salmonella* Typhimurium with two distinct flagellins undergoes phase variation and only utilizes one of the two flagellins at a time to build the filament¹⁰. In contrast, most other bacterial species with multiple flagellins, such as *Bacillus thuringiensis*, *Bdellovibrio bacteriovorus*, *Campylobacter jejuni*, *Caulobacter crescentus*, *Helicobacter pylori*, *Sinorhizobium meliloti*, and *Vibrio* spp., have been shown to assemble the flagellar filament from all or at least most flagellins encoded in their genome^{8,11–20}. For *B. bacteriovorus*, *C. crescentus*, and *H. pylori*, it was demonstrated that the different flagellins exhibit a spatial arrangement within the filament^{12,14,16}.

The role of different flagellins within the flagellar filament is still mostly unclear. While in some systems one flagellin exhibits the major structural or functional role, a large degree of functional redundancy occurs in other multi-flagellin systems. However, depending on the species, loss of certain flagellins in such systems may result in changes in the filament's morphology and function, e.g., with respect to swimming speed, adhesion, or cytotoxicity^{8,12,20,21}. It has thus been suggested that the composition of the filament may be influenced by the environmental conditions^{8,18}.

Species of the genus *Shewanella* possess a single polar flagellum in the form of a left-handed helix, which pushes the cell during counterclockwise (CCW) rotation and pulls the cell upon switching to clockwise (CW) rotation. With few exceptions, the gene cluster encoding the components of the *Shewanella* polar flagellar system harbors two distinct flagellins^{22–24}. In this study, we explored the role of the two flagellins, FlaA and FlaB, of the polar flagellar system in *S. putrefaciens* CN-32. We determined how FlaA and FlaB production may result in spatial arrangement within the flagellar filament, which enabled us to create mutants with defined filament compositions. Subsequent microscopy and three-dimensional tracking of swimming trajectories demonstrated that the composition of the filament significantly affects the flagellar morphology and the motion during free-swimming and spreading through soft agar. In agreement with corresponding simulations on flagellar stability under rotation, the results strongly implied that the basal flagellar part formed by the flagellin FlaA benefits swimming under a range of different conditions. With the switch to FlaB in the remainder of the flagellin, the cells maintain the ability to wrap the filament around the cell body and execute a screw-like movement²³, which is highly beneficial for spreading through complex environments.

Results

Characterization of *S. putrefaciens* FlaA and FlaB. *S. putrefaciens* possesses a monopolar and a lateral flagellar system. We previously showed that the polar system predominantly mediates propulsion, chemotactic behavior and backward screwing

motion^{22,23,25}. In the following, only this polar filament will be addressed, and all experiments described here were conducted using a strain unable to produce the lateral flagellar filaments due to the lack of the corresponding flagellin-encoding genes ($\Delta flaA_2B_2$). For simplification, this strain will henceforth be referred to as wild type (FlaAB).

The two genes encoding the polar flagellins, *flaA* (Sputcn32_2586) and *flaB* (Sputcn32_2585), are arranged next to each other²² and encode proteins of 273 (FlaA) and 271 (FlaB) amino acids with estimated molecular masses of 28.6 (FlaA) and 28.4 (FlaB) kDa. They exhibit a high degree of conservation (86% identity; 91% similarity); most differences occur within the flagellin variable region which presumably faces the environment (Supplementary Fig. 1)^{3,6}.

We previously showed that both FlaA and FlaB are produced at estimated molecular masses of ~37 and ~35 kDa, respectively. This is higher than the masses deduced from the amino acid sequence (~28.5 kDa)²³, indicating modification of both flagellins, e.g., by glycosylation. To determine if the flagellins of *S. putrefaciens* are glycosylated, we introduced in-frame deletions into the genes encoding PseG (Sputcn32_2626) and Maf-1 (Sputcn32_2630), as the deletion of the orthologs in *S. oneidensis* results in completely non-glycosylated flagellins^{26,27}. Immunoblotting analysis of PAGE-separated crude extracts (Supplementary Fig. 2a) revealed that in both $\Delta pseG$ and $\Delta maf-1$ mutants the flagellins occur as a single band at a position according to their estimated molecular mass. Thus, within the cell population, both FlaA and FlaB are produced and both are likely modified by glycosylation. The difference in the molecular mass, presumably caused by a more extensive modification of FlaA, enabled us to determine the presence of each flagellin by immunoblotting, which helped to unravel the regulation of flagellin production later in this study.

Spatial arrangement of FlaA and FlaB in the filament. To explore the distribution of FlaA and FlaB in filament assembly at the single cell level, we performed fluorescence microscopy on cells in which FlaA, FlaB, or both, can be selectively labeled by coupling with a maleimide-ligated fluorophore (FlaA-Cys and FlaB-Cys). The corresponding serine/threonine to cysteine substitutions in the flagellin proteins do not affect swimming motility or flagellin decoration by glycosylation (Supplementary Fig. 3 and ref. ²³). We found that FlaA and FlaB exhibit a spatial arrangement within the flagellar filament (Fig. 1a, e; Supplementary Fig. 4). FlaA almost exclusively forms the base of the filament close to the cell body, which accounts for about 8–28% (17% average) of the fully assembled flagellum. The residual filament is predominantly composed of FlaB with some interspersed FlaA. Mutants completely lacking FlaB ($\Delta flaB$, FlaA stub) produced very short filaments, which barely supported swimming (Supplementary Fig. 5a, e, i, m) while $\Delta flaA$ mutants (FlaB-only) formed flagellar filaments that were not noticeably different from the wild-type filament in morphology or length (Fig. 1b, f; Supplementary Fig. 6). This spatial flagellin arrangement strongly suggested sequential production and/or export of FlaA and FlaB.

Previous studies on the closely related species *S. oneidensis* indicated that *flaA* and *flaB* are not organized in an operon with a single promoter but are regulated individually^{24,28}. Accordingly, q-RT-PCR revealed that in *S. putrefaciens* the *flaB* transcript is about twice as abundant as that of *flaA* (Supplementary Fig. 7a), also indicating individual regulation. We therefore monitored the production of FlaA and FlaB in mutants deleted in genes *rpoN*, *flrA*, and *fliA*, encoding main regulators of flagellation. Generally, in the group of polarly flagellated gammaproteobacteria, RpoN (σ^{54}) acts as a major general regulator of flagellation, FlrA is required for production of numerous structural flagellar components, and the sigma factor FliA (σ^{28}) is required for the

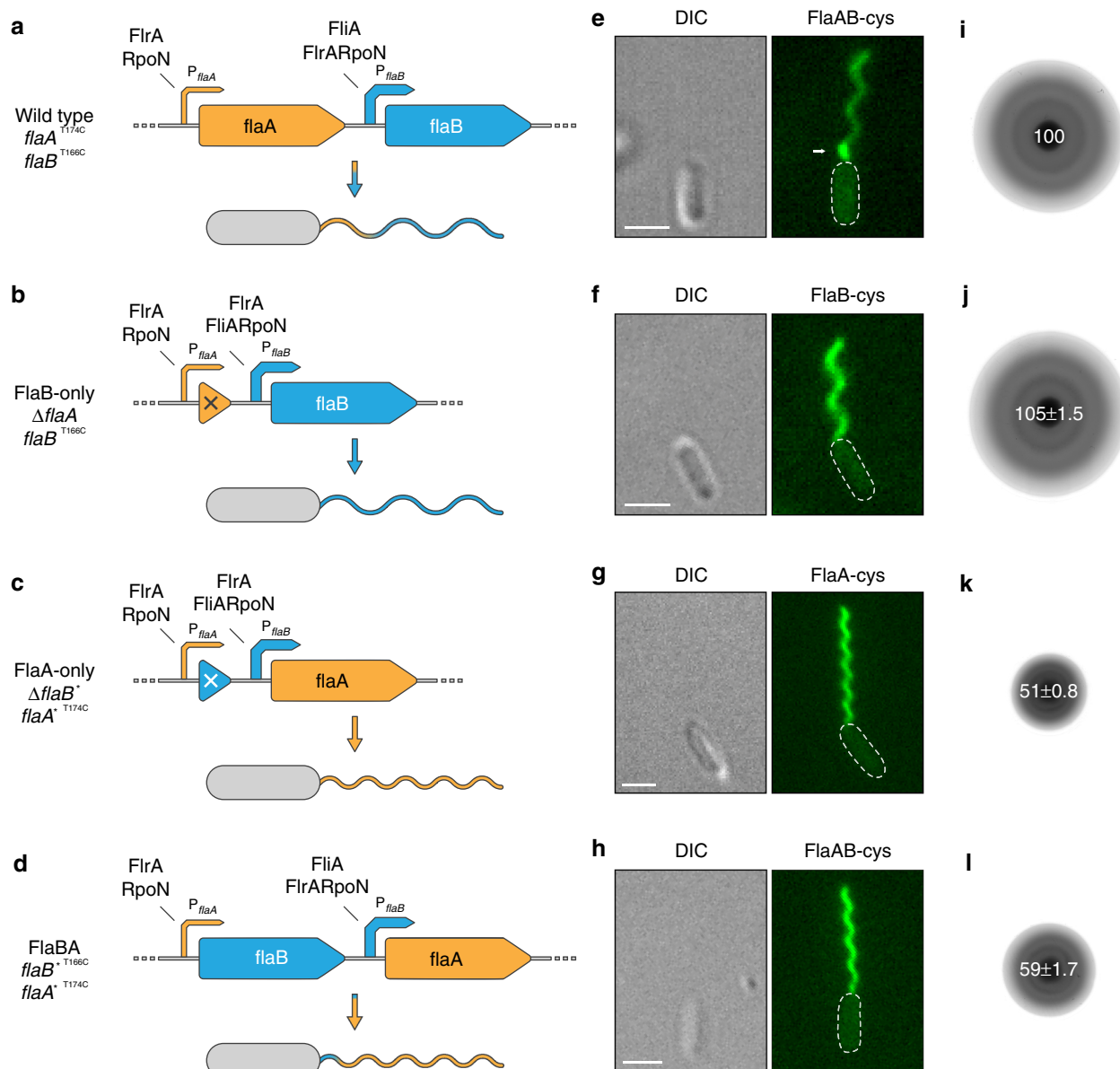


Fig. 1 Overview of the different types of polar flagellar filaments constructed in this study. In all strains the genes for the lateral flagellins were deleted. **a-d** Genetic organization of the polar flagellins and genetic modifications to obtain different filament types. In the wild-type context *flaA* lies upstream of *flaB* and transcription is controlled by a FliA-independent promoter (cp. Supplementary Fig. 2b). In contrast, transcription of *flaB* is controlled by a stronger, FliA-dependent promoter and mediates production of the major part of the flagellar filament. Expression of both genes relies on RpoN and FliA. A functional filament is only produced when at least one of the flagellar genes is expressed from the *flaB* promoter. If no flagellin is expressed from the *flaB* promoter only short filament stubs are formed (see Supplementary Fig. 5). Gene deletions are marked with a cross, swapping of the flagellin gene sequences is marked with an asterisk. P_{flaA/B} = *flaA/B* promoter. **e-h** Micrographs of cells with fluorescently labeled flagellar filaments displaying the outcome of the genetic editing of the flagellin genes. Panel **e** also shows the spatial distribution of the flagellins FlaA and FlaB in the wild-type filament (see also Supplementary Fig. 4). The FlaA portion is marked with an arrow. The increased fluorescence of FlaA compared to that of FlaB is likely due to a better accessibility of the cysteine residue during the fluorescent labeling process. Scale bars represent 2 μ m. **i-l** Radial expansion of cells with different types of flagellar filaments in 0.25% soft agar. Wild-type and FlaB-only cells spread well in this structured environment while the spreading ability of FlaA-only and FlaBA cells is strongly impaired. The numbers in the center of the colonies indicate the relative spreading compared to the wild type in percent (% \pm s.d.) of three individual experiments

production of late flagellar components such as flagellin. FliA is released from its inactivating anti-sigma factor FlgM upon completion of the basal body and the hook to avoid premature production of large amounts of flagellin⁴. Western immunoblotting revealed that, in *S. putrefaciens*, production of both FlaA and FlaB strictly requires RpoN and FliA. In contrast, in a Δ fliA mutant FlaA as well as the flagellin chaperone FliS, which is

required for export, were produced in normal amounts while FlaB was absent (Supplementary Fig. 2b, c). Hence, production of FlaA can already start before the hook-basal body complex is finished, but FlaB production requires hook completion and the subsequent export of the anti-sigma factor FlgM. This regulatory arrangement indicated that a pool of FlaA is already present and ready to be exported and assembled into the filament as soon as

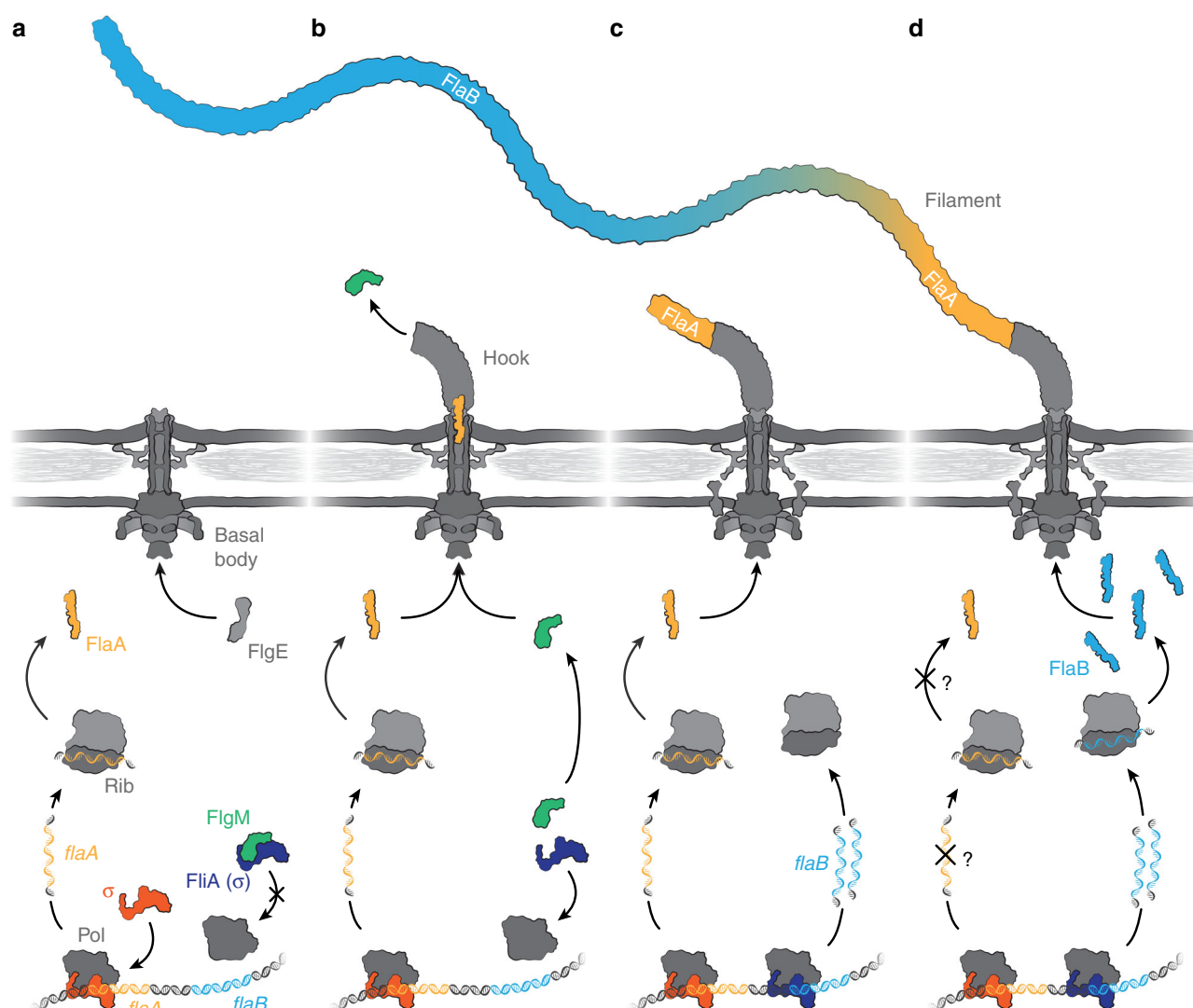


Fig. 2 Schematic model of the sequential production and export of FlaA and FlaB. The figure summarizes our current working model of how spatial arrangement of the two flagellins is achieved in *Shewanella putrefaciens*, depicted in four subsequent stages of the flagellar assembly. **a** The current model of flagellin expression suggests that transcription is inhibited as long as the alternative sigma factor 28 (FliA) is blocked by the anti-sigma factor FlgM. In *S. putrefaciens*, this only applies to FlaB while FlaA production does not depend on FliA (see Supplementary Fig. 2b). Therefore, a pool of FlaA is already present while the basal body is still being assembled. **b** Once the hook-basal-body complex is completed the export apparatus changes its specificity from hook proteins (FlgE) to the flagellins and other late assembly proteins. At this stage also the anti-sigma factor FlgM gets exported and FliA-dependent transcription of FlaB is initiated. **c** The already produced FlaA monomers get exported first and assemble at the base of the flagellar filament. **d** The increasing production of FlaB monomers passes that of FlaA and potentially FlaA transcription and/or translation may be reduced or even completely terminated (indicated by the question marks). Thus, FlaB constitutes the majority residual part of the flagellar filament. (Pol, RNA polymerase; Rib, ribosome; σ , sigma factor)

the hook is completed, while FliA-dependent production of FlaB is initiated (Fig. 2).

Accordingly, a strain with only *flaB* under control of the *flaA* promoter produced very short FlaB filaments (Supplementary Fig. 5b, f, m). In contrast, placing only *flaA* under control of the *flaB* promoter resulted in flagellar filaments exclusively consisting of FlaA (Fig. 1c, g), which were of almost normal length (~6.5 μ m) and also exhibited a left-handed helix. However, pitch, diameter and therefore number of turns of FlaA-only helical filaments differed significantly from FlaB-only or wild-type filaments (Supplementary Fig. 6). Finally, when placing *flaB* under the control of the *flaA* promoter and vice versa, a flagellar filament with FlaB forming a short basal segment was formed, while the residual filament consisted of FlaA (Fig. 1d, h;

Supplementary Fig. 4—FlaBA). Accordingly, the overall filament of these FlaBA mutants had a highly similar geometry as the FlaA-only filament (Supplementary Fig. 6).

Based on these results we propose that the sequential production pattern depends on two individual promoters driving the expression of *flaA* and *flaB*, respectively. The length of the proximal filament segments formed under control of the weaker FliA-independent *flaA* promoter showed a wide range, indicating flagellin production from this promoter varies substantially at the single cell level. Accordingly, overproduction of FlaA from a plasmid resulted in aberrantly long flagellar filaments (Supplementary Fig. 7b, c), indicating that the amount of available flagellin monomers is an important length determining factor. However, the data did not explain why flagellin production

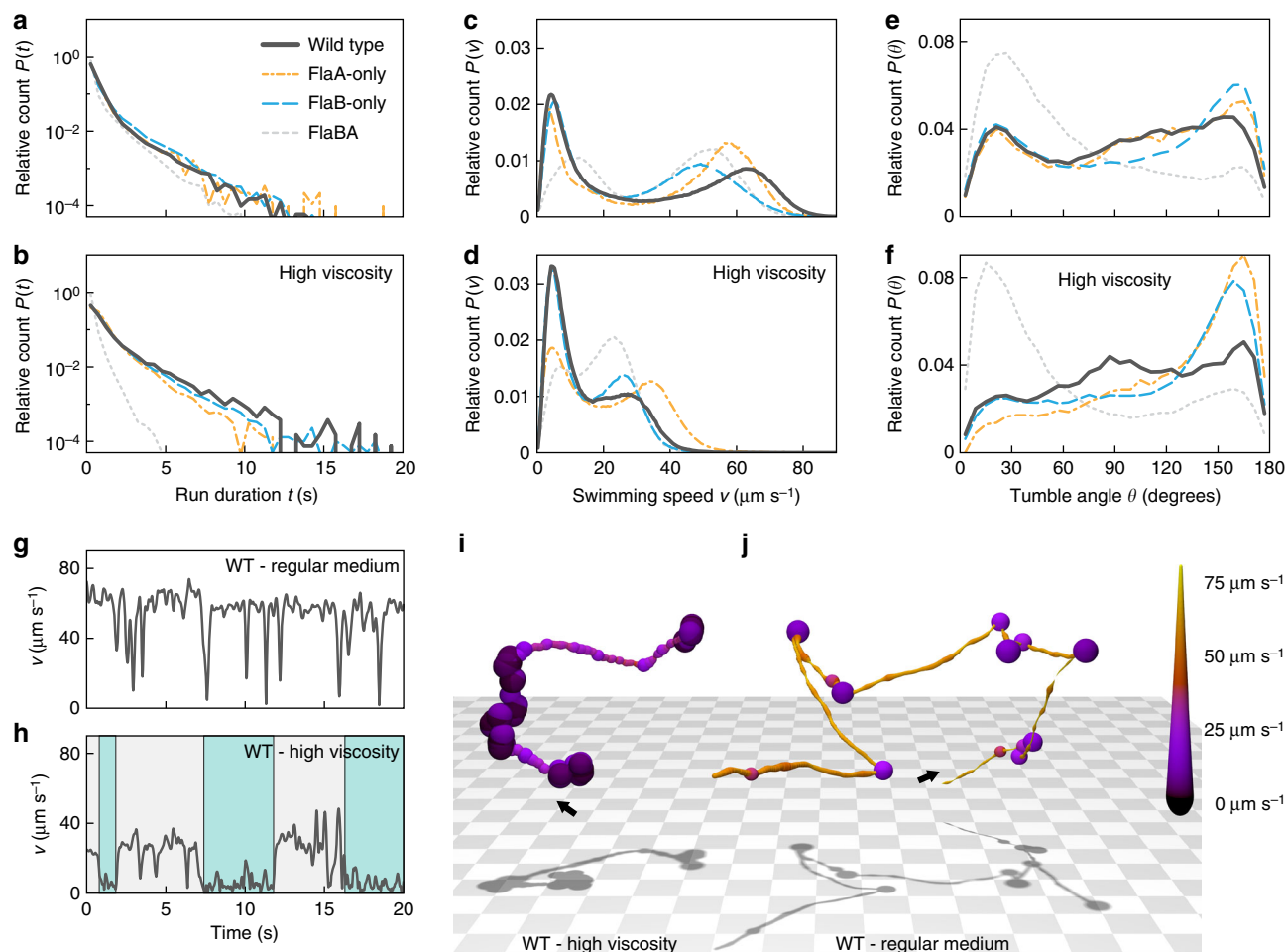


Fig. 3 Free-swimming behavior mediated by the four different flagellar filament types. Several thousand cell tracks were obtained for each strain by holographic microscopy. The diagrams show the relative counts to account for different sample sizes. **a, b** Run duration histograms for wild-type (FlaAB, dark grey solid lines), FlaA-only (orange mixed dashed lines), FlaB-only (blue long dashed lines) and FlaBA (light grey short dashed lines) cells in regular medium (upper panel) and medium with increased viscosity (lower panel). $P(t)$ indicates the probability of observing a run with a duration in the range t to $t+dt$. **c, d** Velocity distribution for the different filament types in regular medium and medium with increased viscosity, respectively. $P(v)$ indicates the probability of observing a cell swimming with a speed in the range v to $v+dv$. **e, f** Turning angle histograms for the different filament types in regular medium and medium with increased viscosity, respectively. Low and high turning angles correspond to weak deviations from straight swimming and near-reversals, respectively. $P(\theta)$ indicates the probability that a particular re-orientation event results in a change of direction in the range θ to $\theta+d\theta$. **g, h** Velocity series for a single wild-type cell in regular medium and a similar cell in high viscosity medium, respectively. Under conditions of increased viscosity the cell exhibits longer periods of swimming at a slower speed (the cyan-colored areas in panel **h**), indicative of screw formation. **i, j** Stereotypical cell tracks for wild-type cells in medium with increased viscosity (left) and regular medium (right). The tracks correspond to the velocity series in panels **g** and **h**. The starting points of the tracks are marked by arrows. The color coding and the line thickness represent the cells' swimming speed. The corresponding movie is provided as Supplementary Movie 1

from the *flaA* promoter only produces filament stubs, which indicates cessation of the expression from this promoter that may occur at the onset of *flaB* expression.

Filament composition affects flagella-mediated swimming. The different morphologies of the FlaA- and FlaB-only filaments suggested that the filament composition affects the swimming behavior of the cells^{8,29}. We therefore compared the spreading ability of the wild-type cells (FlaAB), FlaA-only (with *flaA* being expressed from the *flaB* promoter, resulting in filaments of normal length), FlaB-only and FlaBA mutants through soft agar. Here, the cells have to navigate through an intricate network of polysaccharide strands (Fig. 1i–l). Under these conditions, FlaB-only mutants spread as well as wild-type cells, while cells driven by FlaA-only or FlaBA filaments exhibited a pronounced decrease in spreading. As the inability of these filaments to

promote normal spreading in soft agar could be due to general differences in free swimming, we compared the free-swimming patterns of wild-type (FlaAB) cells to those driven by FlaA-only, FlaB-only and FlaBA filaments by three-dimensional holographic tracking (Fig. 3; example tracks given in panels i and j). This was carried out at normal and, to simulate flagellar performance at high load, at elevated viscosity (10% wt·vol⁻¹ Ficoll 400). From the trajectories obtained, three major swimming parameters were deduced: run duration, swimming velocity, and turning angle.

The run duration represents the time interval of swimming between directional changes. A shift toward shorter run durations may negatively affect effective spreading in soft agar while very long runs may hamper navigation. We found that under conditions of normal viscosity the distribution of run durations was very similar for all four strains with a descending slope

from short runs (1 s or less) toward longer runs up to about 20 s (Fig. 3a). Under conditions of elevated viscosity (Fig. 3b), the distributions of run durations remained similar except for the FlaBA mutant that exhibited a pronounced shift towards shorter runs, indicating a lower spreading ability of this strain.

The second major parameter, the swimming velocity, directly affects the speed of spreading. At normal viscosity, all four strains displayed a similar top speed and velocity distributions with two major subpopulations, a slow and a fast one (Fig. 3c). The slow population, which did not include completely non-motile cells, was comparable in size for the wild type and the FlaA-only and FlaB-only strains, but much broader for the FlaBA mutant. The mean speed increased from $5 \mu\text{m s}^{-1}$ for the first three strains to $15 \mu\text{m s}^{-1}$ for the FlaBA mutant. The velocity of the fast-moving subpopulation was different for all four strains: The wild-type cells had the highest speed ($\sim 63 \mu\text{m s}^{-1}$), followed by FlaA-only cells ($\sim 57 \mu\text{m s}^{-1}$), FlaBA cells ($\sim 53 \mu\text{m s}^{-1}$) and FlaB-only cells ($\sim 49 \mu\text{m s}^{-1}$). At elevated viscosity (Fig. 3d), the velocity distribution with a slow and a fast swimming major population persisted for all four strains, albeit at a lower overall speed. Under these conditions, FlaA-only cells were the fastest ($\sim 38 \mu\text{m s}^{-1}$), confirming earlier reports stating that a smaller helix diameter of a bacterial flagellum promotes swimming at elevated viscosity²⁹. The FlaA-only mutant was followed by wild-type and FlaB-only cells ($\sim 28\text{--}30 \mu\text{m s}^{-1}$) and FlaBA ($\sim 22 \mu\text{m s}^{-1}$). Notably, the size of the slow subpopulation of wild-type and FlaB-only cells increased compared to normal viscosity, but not the one of the other two strains.

The third major parameter, the turning angle, indicates how efficiently the cells can switch direction. Very high angles between 150° and 180° would indicate forward-backward (run-reverse) swimming without efficient directional changes and thus a decrease in spreading efficiency. All four strains showed a wide variation of turning angles from 0° to 180° . Under conditions of normal viscosity (Fig. 3e), the turning-angle profiles of wild-type, FlaA-only and FlaB-only cells were rather similar. However, at elevated viscosity (Fig. 3f), the wild-type cells maintained the wide distribution of turning angles, while for FlaA-only and FlaB-only mutants a large subpopulation exhibited directional changes at very high angles in a run-reverse mode, which would decrease efficient spreading. The FlaBA-mutant cells showed an aberrant behavior under both conditions, as a major subpopulation of the cells displayed rather low turning angles ($0\text{--}60^\circ$), resulting in a higher directional persistence.

The trajectory data on free-swimming cells demonstrated that the composition of the flagellar filament significantly affects the free-swimming behavior of the cells. However, the free-swimming capability of the different strains did not correlate well to the spreading capability in soft agar. This was particularly evident in the case of cells driven by FlaA-only filaments, which did not spread well in soft agar but outperformed FlaB-only mutants, the best spreaders in soft agar, in almost every aspect of free swimming. Discrepancies with the agar-based experiments are to be expected, as the tracking experiments measure the individual characteristics of cells in the absence of external perturbations, such as mechanical interactions with their environment. In contrast, the agar assays capture a holistic picture of motility, integrating speed, reversal rate, response to mechanical environment, etc. across a whole population³⁰, which cannot be adequately simulated by simply increasing the viscosity as in our free-swimming assays. We concluded that the poor spreading capability of the FlaA-only and FlaBA mutants in structured environments is not due to obvious deficits in free-swimming capabilities. The source of the differences must therefore be connected with other properties of the flagellum.

The FlaA segment stabilizes the flagellar filament. The analysis of swimming speed at high viscosity showed a pronounced increase in size of the slow subpopulation of wild-type and FlaB-only cells, but not of FlaBA and FlaA-only strains (Fig. 3c, d). Corresponding single-cell trajectories indicated that a drop in speed frequently followed a directional switch after which the cells continued at lower speed, but accelerated again after another switch of direction (Fig. 3h). We previously showed that under conditions of increased viscosity and while swimming backward with the filament pulling the cell, *S. putrefaciens* can exhibit a filament instability, which results in wrapping of the flagellar filament around the cell and a slow movement in a screw-like fashion²³. Therefore, we anticipated that the drop in swimming speed of wild-type and FlaB-only cells was due to screw formation. An analysis of the four strains' flagellar behavior at normal and high viscosity (Fig. 4a) confirmed that at normal viscosity only few cells of the wild-type population ($<5\%$) exhibited screw formation during backward swimming²³. Notably, under these conditions, already about half of the cells of FlaB-only mutants displayed screw formation, while this flagellar behavior was completely absent for FlaA-only or FlaBA cells. The screw-like swimming phenotype became significantly more pronounced at high viscosity, where about half of all backward-swimming wild-type and more than 85% of FlaB-only cells displayed the screwing behavior. Notably, also at increased viscosity, not a single FlaA-only or FlaBA mutant cell exhibited screwing motility, strongly indicating that a filament mainly or exclusively formed by FlaA is more stable when rotating CW and pulling the cells. This finding strongly suggested that the filaments' base formed by FlaA stabilizes the flagellum to prevent premature screw formation during free swimming. To further support this hypothesis, we introduced a second synthetic *flaA* gene into the chromosome directly downstream of the native *flaA* (FlaAAB; Supplementary Fig. 8a, c, e). As anticipated, the higher level of FlaA production increased the length of the basal FlaA segment on average from $\sim 17\%$ to $\sim 24\%$ of the overall filament. In this strain, the number of cells forming the screw at high viscosity dropped from about 50% to about 25%, and at normal viscosity almost no screws (2%) were observed (Supplementary Fig. 9a). Similarly, we constructed a FlaBBA mutant strain to probe if a longer FlaB segment at the filament's base affects the stability of the flagellum (Supplementary Fig. 8b, d, f). The length of the FlaB basal section increased from $\sim 6.8\%$ to $\sim 8.1\%$, but we did not observe any screw formation. Based on these findings, we conclude that the FlaA segment stabilizes the flagellar filament against screw formation to an extent which depends on the length of this segment.

The findings of the screw formation analysis correlate well with the observed differences in free-swimming speed distributions and spreading through obstructed environments such as soft agar. Wild-type and FlaB-only filaments readily form flagellar screws under conditions of high viscosity, which increases the population of slow free-swimming cells (cp. Fig. 3c, d) as free swimming in screwing mode does not allow effective propulsion²³. Accordingly, this increase in the slow population of free-swimming cells is absent in FlaBA and FlaA-only mutants, which lack the ability of screw formation. However, the latter two strains are hampered in spreading through structured and obstructed environments, the soft agar plates (Fig. 1k, l), strongly indicating that screw formation is significantly contributing to movement when the cells can make contact with a solid environment. In contrast, the differences in efficient turning angles observed under free-swimming conditions at high viscosity cannot be attributed to screw formation: compared to the wild-type FlaB-only cells, that are prone to screw formation, as well as FlaA-only cells, which are incapable of screw formation, tend to turn at high angles in less efficient forward-backward movement. Notably, in contrast to the mutants, the wild-type cells driven by the native FlaAB filament always performed very well under all conditions tested.

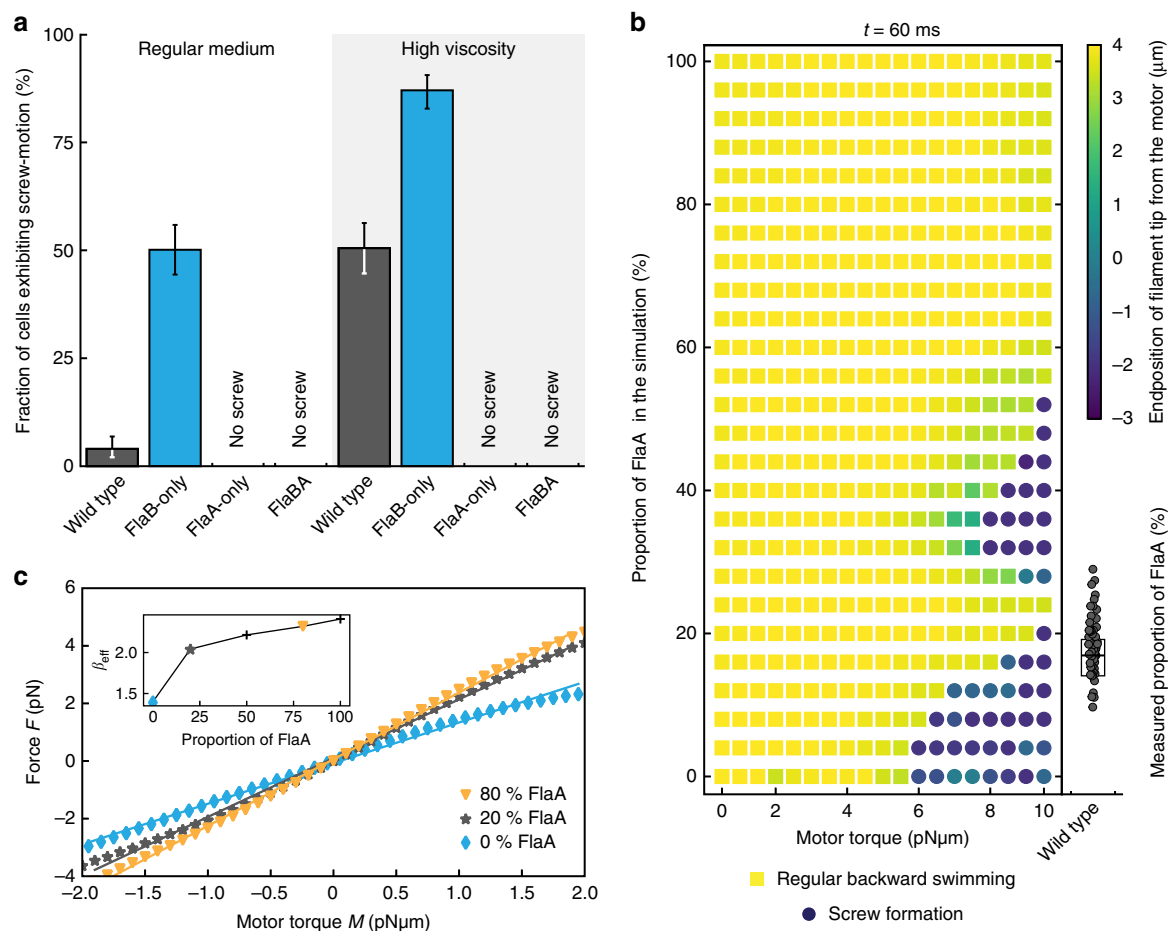


Fig. 4 Experimentally observed and simulated screw formation. **a** The probability of screw formation of wild-type (FlaAB) and FlaB-only cells increases in high viscosity, while for FlaA-only and FlaBA screw formation was never observed. Significance was tested for all filament combinations under both conditions and for each filament between the two conditions. If no screw was observed at all, significance was not tested. All tested combinations were significant ($P < 0.05$, Bonferroni corrected). Error bars indicate 95% confidence intervals. About 300 cells were counted for each strain. **b** Observation of screw formation for varying flagellin compositions at different motor torques after a simulation time of $t = 60$ ms. The simulation was carried out for flagella with an increasing number of FlaA segments, starting with a flagellum completely composed of FlaB (bottom of the diagram) and successively exchanging the segments to a FlaA configuration starting from the filament's base. Yellow squares indicate regular backward rotation, blue dots indicate screw formation. The color coding represents the z-position of the flagellum's free end, with negative values indicating a position below the motor segment (position 0). For comparison with the actual flagellin composition in the wild type experimentally measured FlaA proportions are given on the right. Data points are displayed as individual values (gray dots) measured for 50 filaments. The box spans the central half of the data, the black bar indicates the median. A movie of the simulation with FlaA-only and FlaB-only filaments is provided as Supplementary Movie 2. **c** Force-torque relation extracted from the numerical simulation. The mean force F on the flagellum varies linearly with motor torque M for both forward and backward swimming. Shown are the relations for a FlaB-only flagellum (blue diamonds), a 20% admixture of FlaA (gray stars) and an 80% admixture (orange triangles). The continuous lines are linear fits to the data. The slope β_{eff} in $F = \beta_{\text{eff}} M$ versus the FlaA content is shown in the inset: it increases rapidly up to about 20% FlaA and more slowly for larger fractions. A higher value of β_{eff} indicates a more efficient transfer of torque into driving force

Numerical simulations on behavior of the flagellar filament.

The mechanical properties of filaments and their effects on the dynamics can also be studied in numerical simulations. In an established model for filaments, the flagellum is replaced by a string of beads that are connected to each other by elastic bonds with preferred bonding angles, so that in equilibrium a helix with prescribed radius and pitch forms. The interaction with the surrounding fluid is given by resistive force theory (see ref. 23). Such a model reproduced the screw formation of the helix in dependence on the motor torque and thus the force acting on the flagellar helix. Here, we extend our previous model to the case of two flagellins by adjusting the parameters locally to those of the corresponding flagellins, while keeping all other parameters fixed. Specifically, FlaA forms narrow elongated helices (radius: $0.175 \mu\text{m}$; pitch $1.18 \mu\text{m}$) whereas FlaB forms wider and shorter helices (radius: $0.315 \mu\text{m}$; pitch $1.91 \mu\text{m}$; Supplementary Table 6).

In the simulations we can switch between the two flagellins at continuous positions along the flagellum. This allows us to study the properties of the flagellum as a function of the partitioning into FlaA and FlaB and of the motor torque. As the screw forms after about 60 ms ²³, the simulation was conducted for this period of time. For the wild-type flagellum composed of FlaA close to the cell and FlaB further away, we find that it is stable to screw formation for motor torques of less than about $5 \text{ pN}\mu\text{m}$. For larger torque, screws form, but the required torque varies with FlaA fraction: It reaches a local maximum in stability for a fraction of about 24%, where a torque of $8.5 \text{ pN}\mu\text{m}$ is needed to form the screw (Fig. 4b). This simulated region of enhanced stability corresponds well to our experimental findings that an increase to an average of 24% proximal FlaA, as observed in the FlaAB mutant, increases the filament's stability towards screw formation compared to that of the wild type (Supplementary Fig. 9c).

The model shows a second region with increased stability for FlaA fractions above about 40%, but that could not be reliably probed with our mutants. Turning the order of FlaA and FlaB around, no screws are formed until the FlaB part exceeds 40% (Supplementary Fig. 9d), and then the required torque falls with increasing fraction. This is in line with our experiments in which FlaB forms up to 10–12% of the flagellar filament's base and no screw formation occurs. Thus, the simulation not only reproduces our experimental findings but also suggests that introducing a proximal FlaA filament segment with a smaller diameter and pitch is already sufficient to result in the observed stabilization of the flagellar filament against screw formation, indicating the geometry of the helix as a key factor in the determination of the mechanical properties.

The simulations also allow to extract the propulsive force which the flagellum exerts on the cells. Up to the formation of the screw, the propulsive force F is proportional to the motor torque M , i.e., $F = \beta_{\text{eff}} \cdot M$. A larger value of the slope β_{eff} indicates a more efficient transfer of torque into driving force. The data in Fig. 4c show the linear relation between F and M for the cases of a pure FlaB flagellum and admixtures of 20 and 80% FlaA. The inset shows that the slope β_{eff} increases strongly with the FlaA content until about 20% and varies little thereafter. The data indicate a variation of the onset of screw formation depending on the FlaA fraction and show that in a range between 16 and 20% the cells achieve efficient forward propulsion and maintain the ability to form screws at high torque. This is well within the range of proximal segments we determined for wild-type cells (~8% to ~28%; Fig. 4b). With respect to this pronounced variability in length of the proximal FlaA segment within the flagellar filament, the experimental data in concert with the simulations strongly suggest that *S. putrefaciens* forms a highly heterogeneous cell population with respect to propulsion and the ability of screw formation. This may not be optimal at the single cell level but distributes the trade-off between torque generation and propulsive efficiency among the population, which allows efficient spreading of at least a fraction of the population under a wide range of conditions.

Discussion

About half of all flagellated bacteria possess more than a single flagellin-encoding gene, and it was demonstrated for several species that their flagellar filament is, in fact, assembled from more than one building block. However, it is still unclear why so many bacteria have maintained this arrangement. In this study, we showed that the *S. putrefaciens* flagellum is assembled from two different flagellins, FlaA and FlaB, in a spatially organized fashion and explored how this affects flagellar geometry and function. We provided evidence that the particular spatial assembly by two different flagellins benefits cellular motility when considering a wide range of environmental conditions, free swimming under normal and elevated viscosity and spreading through structured environments. We show that a proximal FlaA segment stabilizes the flagellar filaments to provide a compromise between propulsion and the ability to wrap the flagellum around the cell, which benefits motility in structured environments. In *S. putrefaciens*, the length of this proximal stabilizing segment shows a high variability, leading to a heterogeneous population well equipped for different environmental conditions. Taken together, our results provide quantitative support for the hypothesis that structural aspects of filament assembly drive the maintenance of multiple flagellin-encoding genes⁸.

How do the bacteria form a spatially organized filament? Our study strongly suggests that the arrangement is achieved by sequential production and export of different amounts of FlaA and FlaB, based on individually regulated promoters rather than differences in assembly efficiency as previously proposed for *S.*

*oneidensis*³¹. A very similar spatial pattern of FlaA/FlaB occurs in the flagellum of the latter species (Supplementary Fig. 10), strongly indicating a similar timing of flagellin production and export, which therefore appears to be conserved among *Shewanella* sp.^{24,28,31}. A similar sequential flagellin production may underlie the spatial flagellin distributions in other flagellar filaments composed of two flagellins, e.g. in *Campylobacter coli* or *Helicobacter pylori*, while the more complex flagellar filaments of *Caulobacter crescentus* or *Bdellovibrio bacteriovorus*, both produced from six individual flagellin subunits, likely require a more complex regulation^{8,12,14,16,32}. However, several important aspects of regulation remain to be elucidated in *S. putrefaciens*: Flagellin expression and production from the *flaA* promoter is not constitutive, and flagellar filaments produced from this promoter never reach normal length (Supplementary Fig. 5m). Furthermore, the length of the proximal flagellar segment also depends on whether *flaA* or *flaB* is expressed from the *flaA* promoter (Fig. 1; Supplementary Fig. 5 and 8). We therefore hypothesize that, in the wild type, at the onset of FlaB production *flaA* expression is restricted or even shut down by a yet unknown mechanism at the transcriptional and posttranscriptional level. Flagellin expression from differentially controlled promoters suggest that *Shewanella* sp. are capable of regulating the composition and properties of the flagellar filament by tuning the amount of incorporated FlaA in response to yet unknown environmental signals. In *S. oneidensis*, production of FlaA has been shown to be under control of the flagellar regulators FlrB and FlrC²⁸, which may therefore be involved in this regulation. It is also yet unclear which differences between the flagellins determine the different filament morphologies, as FlaA and FlaB are highly conserved. For *S. oneidensis* it has been proposed that the functional difference between FlaA and FlaB is due to four amino-acid residues within the flagellins³¹. Three of these residues are conserved in *S. putrefaciens* FlaA and FlaB, but did not affect swimming upon substitution (Supplementary Fig. 11). Thus, other residues or factors, such as the differences in flagellin glycosylation, account for the difference in filament morphology and function.

Our study shows that an assembly of the flagellar filament by one or two different flagellins affects its mechanistic properties, which has significant consequences for several aspects of flagellar function in different environments. Directional changes of many monopolarly flagellated bacteria are mediated by combined bending of flagellar filament and hook, the structure which joins filament and motor, during the typical run-reverse-flick movement^{25,33–35}. Thus, the proximal FlaA segment in *S. putrefaciens* likely has a positive effect on robust directional changes at high and fast swimming at normal viscosity. In contrast, a proximal FlaB segment as in the FlaBA mutant filament rather suppresses directional switches at high angles. The trajectories of this mutant with an enrichment in small turning angles also point towards rather short motor breaks or very short intervals of rotational switching. This may occur more frequently at elevated viscosity, as indicated by the shorter run periods under these conditions, which may be explained by differences in load associated with the composition of the flagellar filament^{36,37}. We have previously demonstrated that *S. putrefaciens* may wrap its polar flagellar filament around the cell body in a spiral-like fashion upon CW rotation, and this process starts with an instability of the proximal filament segment at high load²³. Our experimental and simulation data strongly suggest that the spatial localization of FlaA at the filament's base stabilizes the flagellum, which may be already conferred by the smaller diameter and pitch of the flagellar helix in this region. Spatial distributions with one flagellin primarily localized at the base of the flagellar filament were reported previously for *C. crescentus*¹⁴ and *H. pylori*¹⁶ and suggest that these segments fulfill a similar role in optimizing flagella-mediated swimming in these species.

Beyond monopolarly flagellated *S. putrefaciens*, the screwing mode of movement with the flagellar filament(s) wrapped around the cell body was shown for the lophotrichously flagellated species *Burkholderia* sp. RPE64, *Aliivibrio fischerii*, and *Pseudomonas putida*^{38,39} and bipolarly flagellated *Helicobacter suis*⁴⁰. In all cases, full flagellar screw formation significantly slowed down the speed of free-swimming cells. More efficient propulsion by screwing motility was observed when the cells had surface contact^{23,39}. In many of their natural environments flagellated bacteria have to move through structured environments, such as sediments, mucus layers or biofilm matrices, where the bacteria constantly are at risk of getting stuck in passages too narrow for cells to pass. In these environments, polarly flagellated bacteria may employ the flagella-mediated screwing motility to escape from traps or to enable the passage through mucus-filled ducts of higher organisms^{23,39}, however, clear evidence for such a role was missing so far. In this study, we provided a mutant (FlaA-only), which is completely incapable of screwing motility. This strain retains vigorous free swimming, but spreading through soft agar is drastically diminished, demonstrating that this mode of motility very likely gives a significant advantage for moving through structured environments. We expect screwing motility to be similarly important for numerous other polarly flagellated bacterial species in structured environments.

Methods

Bacterial strains, growth conditions, and media. *Shewanella* and *Escherichia coli* strains that were used in this study are listed in Supplementary Table 1. *Shewanella* strains were grown in LB medium at room temperature or 30 °C, *E. coli* in LB medium at 37 °C. Selective media were supplemented with 50 mg ml⁻¹ kanamycin and/or 10% (wt vol⁻¹) sucrose when appropriate. For the 2,6-diaminoheptanedioic acid (DAP)-auxotroph *E. coli* WM 3064 media were supplemented with DAP at a final concentration of 300 μM. To solidify media, LB agar was prepared using 1.5% (wt vol⁻¹) agar for regular plates and 0.15–0.25% (wt vol⁻¹) select agar (Invitrogen) for soft-agar plates.

Strains and vector constructions. Gene knock-out and substitution strains of *Shewanella* were constructed by sequential double homologous recombination. Briefly, in-frame deletions were generated by combining approximately 500-bp fragments of the up- and downstream regions of the designated gene. Only a few codons (typically around six) were left in the genome to prevent disruption of regulatory elements for other genes. In-frame insertions were constructed and re-integrated into those deletion strains in basically the same fashion. Substitution of single or multiple nucleotides was done by inserting a modified fragment into the corresponding deletion strain. Regular genetic manipulations of *S. putrefaciens* CN-32 and *S. oneidensis* MR-1 were introduced into the chromosome by double homologous recombination via the suicide plasmid pNPTS-R6K⁴¹. Plasmids were constructed using standard Gibson assembly protocols⁴² and introduced into *Shewanella* cells by conjugative mating with *E. coli* WM3064 as donor. Plasmids and corresponding oligonucleotides are listed in Supplementary Tables 2 and 3, respectively.

The *S. putrefaciens* strains featuring two flagellin genes under the control of the *flaA* promoter were constructed as described above using synthetic flagellin genes (Genescript) that were codon optimized for *E. coli* K-12 to prevent gene loss by homologous recombination with the native flagellin gene (sequences see Supplementary Table 5). The synthetic gene was introduced downstream of the native gene with a copy of the native Shine-Dalgarno sequence of *flaA* and a spacer of 12 random base pairs.

The FlaA-overproduction plasmid was constructed using standard Gibson assembly protocols⁴² and introduced into *Shewanella* cells by conjugative mating with *E. coli* WM3064 as donor. Both *flaA* and *flaB* were introduced into pBTOK downstream of the anhydrotetracycline-inducible promoter each with their own AGGAGG Shine-Dalgarno sequence and with a spacer of 12 random base pairs. Gene expression was induced after 1 h of growth in LB with 10 ng ml⁻¹ anhydrotetracycline.

Flagellar filament staining and microscopy. Flagellar filaments were visualized by exchanging surface-exposed threonine residues of the flagellin monomers to cysteine residues and selectively coupling maleimide-ligated fluorescent dyes to the SH-group of cysteine²³. To rule out that cysteine substitutions within the flagellin negatively affect the swimming behavior we performed Western Blot analysis, soft agar assays and single cell speed analysis.

For microscopy, cells of an exponentially growing LB culture (OD600 = 0.6) were harvested by centrifugation (1200 × g, 5 min, room temperature) and resuspended in 50 μl PBS. To prevent flagella being sheared off, the pipette tip was

always cut off when pipetting cells. 0.5–1 μl Alexa Fluor 488 C5 maleimide (Thermo Fisher Scientific) or CF[™] 488 maleimide (Sigma-Aldrich) was added and the cell suspension was incubated in the dark for 15 min. Cells were sedimented again and carefully washed with 1 ml of PBS to remove residual unbound dye. After final resuspension in LM100 medium (10 mM HEPES, pH 7.3; 100 mM NaCl; 100 mM KCl; 0.02% (wt vol⁻¹) yeast extract; 0.01% (wt vol⁻¹) peptone; 15 mM lactate) the cells were kept shaking in the dark until microscopy, but never longer than 30 min. Image sequences of typically 150–300 frames and 20–50 ms exposure time were taken at room temperature using a custom microscope setup (Visitron Systems) based on a Leica DMI 6000 B inverse microscope (Leica) equipped with a pco.edge sCMOS camera (PCO), a SPECTRA light engine (lumencor), and an HCPL APO ×63/1.4–0.6 objective (Leica) using a custom filter set (T495lpxr, ET525/50m; Chroma Technology).

Determining flagellar screw formation. To determine the screw formation frequency of the four types of flagellar filament mutants, an aliquot of stained cells was loaded on a swim slide and monitored about 100 μm away from the glass surfaces. For each filament type movies of three biological replicates were recorded on subsequent days in regular LM medium and LM supplemented with 15 % (wt vol⁻¹) Ficoll[®] 400 (diluted from a 50 % (wt vol⁻¹) stock solution). This small, highly branched polymer has been observed to act as a purely viscous contribution to the solvent rheology in experiments with *E. coli*⁴³. Several image sequences of 200 frames at 30 ms exposure time were taken for each condition. Screw formation was determined manually for backward swimming cells or cells switching to backward swimming. For each condition about 300 backward swimming events were counted.

Determining flagellar helix parameters. To measure the pitch, diameter and axis length of the flagellum the cells were prepared as described above and supplemented with 50 μM phenamil prior to loading on the swimslide. Phenamil stopped or at least slowed down the rotation of the Na⁺-driven motor so that images of the helical waveform of the flagella could be obtained. The proportion of the proximal flagellin fragment could only be measured for FlaA, as this flagellin shows brighter fluorescence and could be clearly distinguished from the cell body and the remaining part of the flagellum. Parameters were measured using the ImageJ distribution Fiji⁴⁴.

To determine the handedness of the different types of flagellar filaments z-stack image sequences of fluorescently labeled flagella were recorded as described above. Shifting the focal plane through the cell body shows characteristic patterns for left-handed and right-handed helices. The flagellar helices of all flagella types were found to be left-handed.

Protein separation and western immunoblotting. For western immunoblotting, cell lysates of exponentially growing LB cultures were obtained by centrifuging cells corresponding to an OD600 = 10 and resuspending the cell pellet in Laemmli buffer⁴⁵. Prior to protein separation by SDS/PAGE using 12% (wt · vol⁻¹) polyacrylamide gels the samples were heated to 95 °C for 5 min. Subsequently, the proteins were transferred to a nitrocellulose Roti-PVDF membrane (Roth) by semidry transfer. The polar flagellins FlaA and FlaB (of *S. putrefaciens* and *S. oneidensis* alike) were detected with polyclonal antibodies which were raised against the N-terminal conserved region of *S. MR-1* FlaB (Eurogentec Deutschland) in the dilution of 1:500. As secondary antibody anti-rabbit IgG-horseradish peroxidase (Thermo Fisher Scientific, prod. # 31460) was used at a dilution of 1:20,000. FLAG-tagged Flis was detected with a monoclonal, horseradish-peroxidase-conjugated antibody raised against the FLAG-tag (Sigma Aldrich, prod. # A8592) in the dilution of 1:1000. The horseradish peroxidase signal was detected with the CCD System LAS 4000 (Fujifilm) after incubating the membranes with SuperSignalH West Pico Chemiluminescent Substrate (Thermo Scientific) for one minute. If portions of gels or blots are shown the full gels or blots can be found in Supplementary Figure 12.

Soft-agar spreading assay. Spreading ability in complex environments was carried out in soft-agar medium. LB medium supplemented with 0.15–0.25% (wt vol⁻¹) select agar (Invitrogen) was heated carefully and cooled to 30–40 °C before pouring the plates. After solidification 2 μl of exponentially grown cultures were spotted on the plates and incubated in a moist environment over night at room temperature. Plates were scanned before the swim colonies merged using an Epson V700 Photo Scanner. Cells to be directly compared were always incubated on the same plate.

Statistics of filament parameters and screw formation. Significance of the relative transcription levels (qRT-PCR) and the filament parameter measurements were tested with a two-sided two-sample *t*-test or Welch's *t*-test (*P* < 0.05, Bonferroni corrected) in R version 3.3.2. Mean, Median and SD were calculated in Microsoft Excel 2013. For each flagellar filament type pitch, diameter, axis length and if possible the proportion of the proximal filament fragment of the flagellum of 50 cells were measured. The actual length of the filament (arc length) was calculated in Excel 2013. Significance of screw formation (only if screws were observed at all) was tested pairwise with two-sided Fisher's exact test (*P* < 0.05, Bonferroni

corrected) in R version 3.3.2. 95% confidence intervals were calculated with the exact binomial test. For each flagellar filament type and condition about 100 backward swimming events were counted on 3 subsequent days, resulting in a total of about 300 counts for each filament type and condition. All measurements and the corresponding statistics are summarized in Supplementary Table 4.

Isolation of total RNA and qRT-PCR. Total RNA of exponentially growing *S. putrefaciens* CN-32 cells (OD₆₀₀ = 0.5, three biological replicates) was extracted using the hot-phenol method⁴⁶. Briefly, the cells were incubated in SDS-acetate buffer (20 mM sodium acetate, 1 mM EDTA, 1% SDS, pH 5.5), with one and a half volumes of hot phenol (pH 4.3) at 65 °C for 10 min, inverting the tube every 2 min. After centrifugation, the aqueous phase was extracted twice using phenol-chloroform-isoamyl alcohol (25:24:1) and RNA was precipitated with 1/8 volume of 2 M sodium acetate solution (pH 5.2) and 2.5 volumes of ice cold ethanol (>96% v v⁻¹). After incubation at -20 °C overnight, the pellet was washed with ice cold ethanol (70% v v⁻¹), dried and resuspended in RNase-free water. The quality of the RNA was determined by agarose gel electrophoresis and concentration was measured at 260 nm. Residual DNA was removed with the Turbo DNA-free kit (Applied Biosystems) according to the manufacturer's instructions. The RNA extract was then applied for random-primed first-strand cDNA synthesis using BioScript reverse transcriptase (Bioline) according to the manufacturer's instructions. RNA and cDNA samples were stored at -80 °C. The cDNA samples were used as a template for qRT-PCR (C1000 Thermal Cycler with the CFX96 Real-Time System, Bio-Rad) using the SYBR green detection system, MicroAmp Optical 96-well reaction plates and Optica adhesive covers (Applied Biosystems). As *flaA* and *flaB* gene sequences are very similar the specificity of the used oligonucleotides (Supplementary Table 3) was verified by PCR using total DNA extracts (E.Z.N.A.® Bacterial DNA Kit, Omega) of Δ *flaA* and Δ *flaB* mutants. RNA samples treated without reverse transcriptase were used to test for DNA contaminations in the extracted RNA. PCR amplified DNA fragments of the flagellin locus (using oligonucleotides B 49 and B 50, Supplementary Table 3) were used as positive control and water as negative control. The cycle threshold (Ct) was determined automatically after 40 cycles (Real-Time CFX Manager 2.1, Bio-Rad). Ct values of the flagellin genes were normalized to the Ct values obtained for *gyrA* (Sputn32_2070). Primer efficiencies and relative transcript levels were determined according to Pfaffl⁴⁷ and used to estimate the differences in transcript amounts of the two flagellins.

Holographic cell tracking. Cells were grown according to the microscopy protocol above, but without the flagellar staining step. The cells were loaded into glass sample chambers measuring approximately 5 mm × 20 mm × 0.5 mm constructed from glass slides and UV-curing glue. The sample was illuminated using a fiber-coupled laser diode (wavelength λ = 642 nm) mounted in place of the condenser lens assembly on a Nikon Ti U inverted microscope. The sample was imaged using a standard bright field objective lens (×10, NA 0.3) onto a CMOS camera (Mikrotron MC-1362). Movies were acquired at 50 Hz for around 60 s, at a resolution of 1024 × 1024 pixels. This arrangement gave a sensitive volume of around 1.4 mm × 1.4 mm × 0.5 mm in which to track cells. This resulted in 4887 tracks for the wild type, 4611 tracks for FlaB-only, 1883 tracks for FlaA-only and 4850 tracks for FlaBA in regular medium and 1340 tracks for the wild type, 2558 tracks for FlaB-only, 3019 tracks for FlaA-only and 1623 tracks for FlaBA in high viscosity medium. Note that even the smallest data set adds up to over 5.5 h of recorded and analyzed swim time. The movies were analyzed offline to extract cell coordinates in each frame, and to assemble these coordinates into cell tracks using custom-written software routines^{48–51}. Cell tracks were smoothed with piecewise cubic splines to remove noise⁵² and analyzed to extract the instantaneous velocity, tumble angle and run time distribution.

The raw data was processed stepwise to obtain cell coordinates. We obtained a background image from each movie sequence by finding the median pixel value at each position in the image. We divided each image in a sequence by this static background, and applied the Rayleigh-Sommerfeld back-propagation approach⁴⁸, to produce a stack of numerically refocused images at various distances from the original optical plane. A spatial bandpass filter was applied during the reconstruction to reduce pixel noise; the filter preserved objects between 2 and 30 pixels in size. At our relatively low magnification (×10 total magnification), cells appear point-like in the resulting images. We applied a Sobel-type filter^{49,52} to obtain the position of each cell in three dimensions.

To reconstruct cell tracks an extract instantaneous velocities a custom software routine was written to connect the positions of cells between frames in order to assemble three-dimensional tracks. The position resolution carried an uncertainty of approximately ±0.5 μ m in the directions perpendicular to the optical axis, and ±1 μ m parallel to the optical axis in each frame, at this magnification. All cells were also subject to translational Brownian motion as they swam; the combination of high-frequency pixel noise and Brownian motion complicated efforts to calculate the time-derivatives of position, and therefore the swimming speed. To smooth short-time fluctuations associated with these noise sources, the cell tracks were fitted using piecewise cubic splines. This allowed us to reliably extract instantaneous cell velocities. This technique also allows us to reject the cells that are moving by Brownian alone. The spline-smoothed trajectory of a non-motile particle has a mean-squared displacement that scales with time, whereas a

swimming cell's mean squared displacement scales with time squared. By setting a threshold for the slope of the mean-squared displacement at short times, and a threshold for the total mean squared displacement after 2 s, we can effectively eliminate non-motile particles.

Extraction of tumble angle and run duration distribution was done by calculating the cell's instantaneous direction at each time point, along with the change in direction, $\theta(t)$, between subsequent time points. These data were scanned using a standard peak search algorithm to detect the position of maxima in $d\theta/dt$ above a threshold of 5°s⁻¹. These maxima were associated with reorientation events; residual effects of Brownian motion after the spline smoothing are sufficient to allow pauses followed by a resumption of swimming (equivalent to a reorientation angle near zero degrees) to be detected as reorientation events. Example data are shown in Supplementary Figure 13; 13a shows a single cell track (wild type, the same track shown in Fig. 3), and 13b displays a graph of $d\theta/dt$ against time in which the events noted as tumbles are highlighted with blue circles. The total change in swimming direction at each re-orientation event was calculated by comparing a cell's swimming direction 0.25 s before a maximum in $\theta(t)$ with the swimming direction 0.25 s after the maximum. The time between subsequent re-orientation events was used to build a distribution of run durations. Only tracks with two or more re-orientation events contributed to the run duration distributions.

Numerical model for the flagellar filament. The numerical model for the flagellar filament is based on that proposed by Vogel and Stark⁵³, and the same as the one used in Kühn et al.²³. It is based on a representation of the flagellum as a set of beads with mutual interactions such that they form a helix with prescribed radius R and pitch P at rest. The differences between FlaA and FlaB are reflected in the local radius R and pitch P of the helix: FlaA forms narrow helices with $R = 0.175 \mu$ m and $P = 1.18 \mu$ m, whereas FlaB forms wider helices with $R = 0.315 \mu$ m and $P = 1.91 \mu$ m. The torque-force relation is obtained by direct numerical integration of the equations of motion at fixed torque, and then by computing the mean force over 10 rotation periods to average out the oscillations that are connected with the positioning of the motor relative to the axis of the filament. As in the previous simulations²³, we observe that polymorphic transitions within the filament reduce the required torque, and thus have a quantitative but not a qualitative effect on the changes in mechanical properties^{53,54}.

With s the arclength along the rod, the torsional state of the rod is described by the rotational strain vector $\Omega(s)$. Deviations from the rest state give quadratic contributions to a free energy

$$\mathcal{F}_K = \int_0^L \left(\frac{A}{2} \right) \left[\left(\Omega_1 - \Omega_{0,1} \right)^2 + \left(\Omega_2 - \Omega_{0,2} \right)^2 \right] + \left(\frac{C}{2} \right) \left(\Omega_3 - \Omega_{0,3} \right)^2 ds, \quad (1)$$

where A is the bending and C the torsional rigidity.

Polymorphism is introduced by calculating the free energy relative to the different equilibrium states and taking the minimum: if the flagellum is stretched too far from one local minimum it can fall into the basin of attraction of another one and relax to a different configuration. For FlaB we find two relevant equilibrium configurations, but for FlaA there is no evidence for a second one. We take the same elastic coefficients A and C for all minima, since we do not have independent numbers for the different equilibrium states (neither for the polymorphic states nor for FlaA vs FlaB).

In addition to the torsional contribution the free energy also contains a global harmonic spring potential

$$\mathcal{F}_S = (K/2) \int_0^L (\partial \mathbf{r} / \partial s)^2 ds \quad (2)$$

with an elastic constant K that keeps the variations in length within 0.1%.

The interaction between flagellum and fluid is calculated within resistive force theory⁵⁵. There are three local friction coefficients that depend on the geometry of the flagellum:

$$\gamma_{\perp} = \frac{4\pi\eta}{\ln(0.09l/r_f) + 1/2} \quad (3)$$

is the friction coefficient for motion perpendicular to the centerline, with η the viscosity, r_f the radius of the filament and $l = \sqrt{4\pi^2 R^2 + P^2}$ the contour length of one helical turn. The tangential friction coefficient is

$$\gamma_{\parallel} = \frac{2\pi\eta}{\ln(0.09l/r_f)} \quad (4)$$

and the rotational coefficient is

$$\gamma_r = 4\pi\eta r_f^2 \quad (5)$$

As in Vogel and Stark and Kühn et al.^{23,53}, the equations of motion are integrated with an embedded Cash-Karp method⁵⁶, and determine the positions and velocities of the attached tripoid following the procedure proposed by Chirico

and Langowski⁵⁷. The runs are started with a left-handed helix with $P^S = 1.91 \mu\text{m}$ and $R^S = 0.315 \mu\text{m}$ for segments containing FlaB, and with $P^S = 1.18 \mu\text{m}$ and $R^S = 0.175 \mu\text{m}$ for segments containing FlaA. The contour length of the flagellum was set to $L_c = 6 \mu\text{m}$, corresponding to 2 to 4 helical turns, depending on the FlaA to FlaB ratio. The various parameters in the model for the flagellum and their values are summarized in Supplementary Table 6.

Code availability. The full code for the three-dimensional tracking has been published in the corresponding references^{49,52}. The full code for simulations of flagellar screw formation is available upon request from the corresponding authors.

Data availability

The tracking data are available at the York Research Database (<https://doi.org/10.15124/675b6083-2a6e-43d1-8511-b7c18bb1be9a>). Other data supporting the findings of the study are available in this article and its Supplementary Information files, or from the corresponding authors upon request. A reporting summary for this Article is available as a Supplementary Information file.

Received: 19 February 2018 Accepted: 22 November 2018

Published online: 18 December 2018

References

- Minamino, T. & Imada, K. The bacterial flagellar motor and its structural diversity. *Trends Microbiol.* **23**, 267–274 (2015).
- Wang, F. et al. A structural model of flagellar filament switching across multiple bacterial species. *Nat. Commun.* **8**, 960 (2017).
- Samatey, F. A. et al. Structure of the bacterial flagellar protofilament and implications for a switch for supercoiling. *Nature* **410**, 331–337 (2001).
- Chevalance, F. F. & Hughes, K. T. Coordinating assembly of a bacterial macromolecular machine. *Nat. Rev. Microbiol.* **6**, 455–465 (2008).
- Yonekura, K., Maki-Yonekura, S. & Namba, K. Structure analysis of the flagellar cap-filament complex by electron cryomicroscopy and single-particle image analysis. *J. Struct. Biol.* **133**, 246–253 (2001).
- Yonekura, K., Maki-Yonekura, S. & Namba, K. Complete atomic model of the bacterial flagellar filament by electron cryomicroscopy. *Nature* **424**, 643–650 (2003).
- Renault, T. T. et al. Bacterial flagella grow through an injection-diffusion mechanism. *eLife* **6**, 23136 (2017). eLife.
- Faulds-Pain, A. et al. Flagellin redundancy in *Caulobacter crescentus* and its implications for flagellar filament assembly. *J. Bacteriol.* **193**, 2695–2707 (2011).
- Kanehisa, M. et al. KEGG for linking genomes to life and the environment. *Nucleic Acids Res.* **36**, D480–D484 (2008).
- Lederberg, J. & Iino, T. Phase variation in *Salmonella*. *Genetics* **41**, 743–757 (1956).
- Lovgren, A., Zhang, M. Y., Engstrom, A. & Landen, R. Identification of two expressed flagellin genes in the insect pathogen *Bacillus thuringiensis* subsp. *alesti*. *J. Gen. Microbiol.* **139**, 21–30 (1993).
- Lambert, C. et al. Characterizing the flagellar filament and the role of motility in bacterial prey-penetration by *Bdellovibrio bacteriovorus*. *Mol. Microbiol.* **60**, 274–286 (2006).
- Nuijten, P. J., van Asten, F. J., Gaastra, W. & van der Zeijst, B. A. Structural and functional analysis of two *Campylobacter jejuni* flagellin genes. *J. Biol. Chem.* **265**, 17798–17804 (1990).
- Driks, A., Bryan, R., Shapiro, L. & DeRosier, D. J. The organization of the *Caulobacter crescentus* flagellar filament. *J. Mol. Biol.* **206**, 627–636 (1989).
- Ely, B., Ely, T. W., Crymes, W. B. Jr. & Minnich, S. A. A family of six flagellin genes contributes to the *Caulobacter crescentus* flagellar filament. *J. Bacteriol.* **182**, 5001–5004 (2000).
- Kostrzynska, M., Betts, J. D., Austin, J. W. & Trust, T. J. Identification, characterization, and spatial localization of two flagellin species in *Helicobacter pylori* flagella. *J. Bacteriol.* **173**, 937–946 (1991).
- Scharf, B., Schuster-Wolf-Buhring, H., Rachel, R. & Schmitt, R. Mutational analysis of the *Rhizobium lupini* H13-3 and *Sinorhizobium meliloti* flagellin genes: importance of flagellin A for flagellar filament structure and transcriptional regulation. *J. Bacteriol.* **183**, 5334–5342 (2001).
- McCarter, L. L. Polar flagellar motility of the Vibrionaceae. *Microbiol. Mol. Biol. Rev.* **65**, 445–462 (2001).
- Millikan, D. S. & Ruby, E. G. *Vibrio fischeri* flagellin A is essential for normal motility and for symbiotic competence during initial squid light organ colonization. *J. Bacteriol.* **186**, 4315–4325 (2004).
- Kim, S. Y. et al. Contribution of six flagellin genes to the flagellum biogenesis of *Vibrio vulnificus* and in vivo invasion. *Infect. Immun.* **82**, 29–42 (2014).
- Ikedo, J. S. et al. Flagellar phase variation of *Salmonella enterica* serovar Typhimurium contributes to virulence in the murine typhoid infection model but does not influence *Salmonella*-induced enteropathogenesis. *Infect. Immun.* **69**, 3021–3030 (2001).
- Bubendorfer, S. et al. Specificity of motor components in the dual flagellar system of *Shewanella putrefaciens* CN-32. *Mol. Microbiol.* **83**, 335–350 (2012).
- Kühn, M. J., Schmidt, F. K., Eckhardt, B. & Thormann, K. M. Bacteria exploit a polymorphic instability of the flagellar filament to escape from traps. *Proc. Natl Acad. Sci. USA* **114**, 6340–6345 (2017).
- Wu, L., Wang, J., Tang, P., Chen, H. & Gao, H. Genetic and molecular characterization of flagellar assembly in *Shewanella oneidensis*. *PLoS One* **6**, e21479 (2011).
- Bubendorfer, S., Koltai, M., Rossmann, F., Sourjik, V. & Thormann, K. M. Secondary bacterial flagellar system improves bacterial spreading by increasing the directional persistence of swimming. *Proc. Natl Acad. Sci. USA* **111**, 11485–11490 (2014).
- Sun, L. et al. Posttranslational modification of flagellin FlaB in *Shewanella oneidensis*. *J. Bacteriol.* **195**, 2550–2561 (2013).
- Bubendorfer, S. et al. Analyzing the modification of the *Shewanella oneidensis* MR-1 flagellar filament. *PLoS One* **8**, e73444 (2013).
- Shi, M., Gao, T., Ju, L., Yao, Y. & Gao, H. Effects of FlrBC on flagellar biosynthesis of *Shewanella oneidensis*. *Mol. Microbiol.* **93**, 1269–1283 (2014).
- Schneider, W. R. & Doetsch, R. N. Effect of viscosity on bacterial motility. *J. Bacteriol.* **117**, 696–701 (1974).
- Cates, M. E. Diffusive transport without detailed balance in motile bacteria: does microbiology need statistical physics? *Rep. Prog. Phys.* **75**, 042601 (2012).
- Sun, L. et al. Two residues predominantly dictate functional difference in motility between *Shewanella oneidensis* flagellins FlaA and FlaB. *J. Biol. Chem.* **289**, 14547–14559 (2014).
- Guerry, P., Alm, R. A., Power, M. E., Logan, S. M. & Trust, T. J. Role of two flagellin genes in *Campylobacter* motility. *J. Bacteriol.* **173**, 4757–4764 (1991).
- Xie, L., Altindal, T., Chattopadhyay, S. & Wu, X. L. Bacterial flagellum as a propeller and as a rudder for efficient chemotaxis. *Proc. Natl Acad. Sci. USA* **108**, 2246–2251 (2011).
- Son, K., Guasto, J. S. & Stocker, R. Bacteria can exploit a flagellar buckling instability to change direction. *Nat. Phys.* **9**, 494–498 (2013).
- Jabbarzadeh, M. & Fu, H. C. Dynamic instability in the hook-flagellum system that triggers bacterial flicks. *Phys. Rev. E* **97**, 012402 (2018).
- Yuan, J., Fahrner, K. A. & Berg, H. C. Switching of the bacterial flagellar motor near zero load. *J. Mol. Biol.* **390**, 394–400 (2009).
- Bai, F., Minamino, T., Wu, Z., Namba, K. & Xing, J. Coupling between switching regulation and torque generation in bacterial flagellar motor. *Phys. Rev. Lett.* **108**, 178105 (2012).
- Hintsche, M. et al. A polar bundle of flagella can drive bacterial swimming by pushing, pulling, or coiling around the cell body. *Sci. Rep.* **7**, 16771 (2017).
- Kinosita, Y., Kikuchi, Y., Mikami, N., Nakane, D. & Nishizaka, T. Unforeseen swimming and gliding mode of an insect gut symbiont, *Burkholderia* sp. RPE64, with wrapping of the flagella around its cell body. *ISME J.* **12**, 838–848 (2017).
- Constantino, M. A. et al. Bipolar lophotrichous *Helicobacter suis* combine extended and wrapped flagella bundles to exhibit multiple modes of motility. *Sci. Rep.* **8**, 14415 (2018).
- Lassak, J., Henche, A. L., Binnenkade, L. & Thormann, K. M. ArcS, the cognate sensor kinase in an atypical Arc system of *Shewanella oneidensis* MR-1. *Appl. Environ. Microbiol.* **76**, 3263–3274 (2010).
- Gibson, D. G. et al. Enzymatic assembly of DNA molecules up to several hundred kilobases. *Nat. Methods* **6**, 343–345 (2009).
- Martinez, V. A. et al. Flagellated bacterial motility in polymer solutions. *Proc. Natl Acad. Sci. USA* **111**, 17771–17776 (2014).
- Schindelin, J. et al. Fiji: an open-source platform for biological-image analysis. *Nat. Methods* **9**, 676–682 (2012).
- Laemmli, U. K. Cleavage of structural proteins during the assembly of the head of bacteriophage T4. *Nature* **227**, 680–685 (1970).
- Aiba, H., Adhya, S. & de Crombrughe, B. Evidence for two functional *gal* promoters in intact *Escherichia coli* cells. *J. Biol. Chem.* **256**, 11905–11910 (1981).
- Pfaffl, M. W. A new mathematical model for relative quantification in real-time RT-PCR. *Nucleic Acids Res.* **29**, e45 (2001).
- Lee, S. H. & Grier, D. G. Holographic microscopy of holographically trapped three-dimensional structures. *Opt. Express* **15**, 1505–1512 (2007).
- Wilson, L. & Zhang, R. 3D Localization of weak scatterers in digital holographic microscopy using Rayleigh-Sommerfeld back-propagation. *Opt. Express* **20**, 16735–16744 (2012).
- Jikeli, J. F. et al. Sperm navigation along helical paths in 3D chemoattractant landscapes. *Nat. Commun.* **6**, 7985 (2015).
- Wilson, L. G., Carter, L. M. & Reece, S. E. High-speed holographic microscopy of malaria parasites reveals ambidextrous flagellar waveforms. *Proc. Natl Acad. Sci. USA* **110**, 18769–18774 (2013).

52. Farthing, N. E. et al. Simultaneous two-color imaging in digital holographic microscopy. *Opt. Express* **25**, 28489–28500 (2017).
53. Vogel, R. & Stark, H. Motor-driven bacterial flagella and buckling instabilities. *Eur. Phys. J. E. Soft. Matter* **35**, 15 (2012).
54. Darnton, N. C., Turner, L., Rojevsky, S. & Berg, H. C. On torque and tumbling in swimming *Escherichia coli*. *J. Bacteriol.* **189**, 1756–1764 (2007).
55. Lighthill, J. Flagellar hydrodynamics. *SIAM Rev.* **18**, 161–230 (1976).
56. Cash, J. R. & Karp, A. H. A variable order Runge-Kutta method for initial value problems with rapidly varying right-hand sides. *ACM Trans. Math. Softw.* **16**, 201–222 (1990).
57. Chirico, G. & Langowski, J. Brownian dynamics simulations of supercoiled DNA with bent sequences. *Biophys. J.* **71**, 955–971 (1996).

Acknowledgements

M.J.K. and F.K.S. were supported by grants TH831/6-1 and BE102/14-1, respectively, from the Deutsche Forschungsgemeinschaft within the framework of the priority program 1726. N.E.F. and L.G.W. were supported by EPSRC grant no. EP/N014731/1. We are grateful to Ulrike Ruppert for technical support.

Author contributions

M.J.K., F.K.S., L.G.W., B.E., and K.M.T. conceived the project and designed experiments; M.J.K., F.M.R., and B.H. constructed strains, M.J.K. performed single-cell microscopic analysis and regulation studies, N.E.F. and L.G.W. performed holographic cell tracking, F.K.S. and B.E. provided numeric simulations. M.J.K., L.G.W., F.K.S., B.E., and K.M.T. wrote the paper. All authors discussed the results and commented on the manuscript.

Additional information

Supplementary Information accompanies this paper at <https://doi.org/10.1038/s41467-018-07802-w>.

Competing interests: The authors declare no competing interests.

Reprints and permission information is available online at <http://npg.nature.com/reprintsandpermissions/>

Publisher's note: Springer Nature remains neutral with regard to jurisdictional claims in published maps and institutional affiliations.



Open Access This article is licensed under a Creative Commons Attribution 4.0 International License, which permits use, sharing, adaptation, distribution and reproduction in any medium or format, as long as you give appropriate credit to the original author(s) and the source, provide a link to the Creative Commons license, and indicate if changes were made. The images or other third party material in this article are included in the article's Creative Commons license, unless indicated otherwise in a credit line to the material. If material is not included in the article's Creative Commons license and your intended use is not permitted by statutory regulation or exceeds the permitted use, you will need to obtain permission directly from the copyright holder. To view a copy of this license, visit <http://creativecommons.org/licenses/by/4.0/>.

© The Author(s) 2018

Spatial arrangement of several flagellins within bacterial flagella improves motility in different environments

Kühn et al

- Supplementary Information -

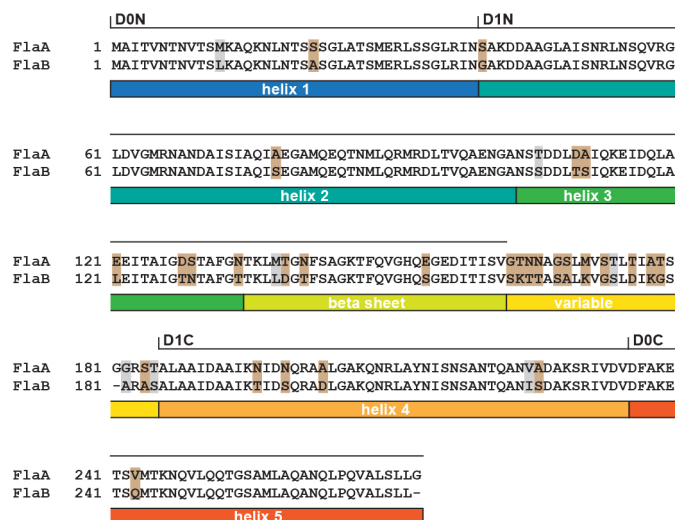
This document contains:

Supplementary Figures 1 - 13

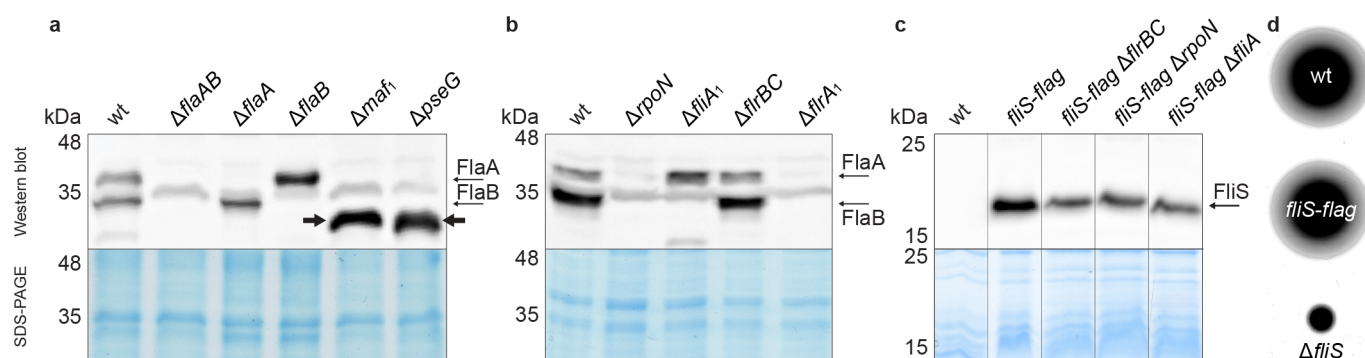
Supplementary Tables 1 - 6

Supplementary References

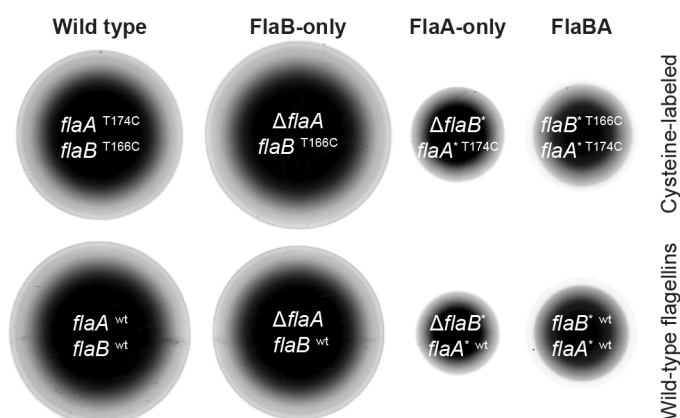
Supplementary Figures



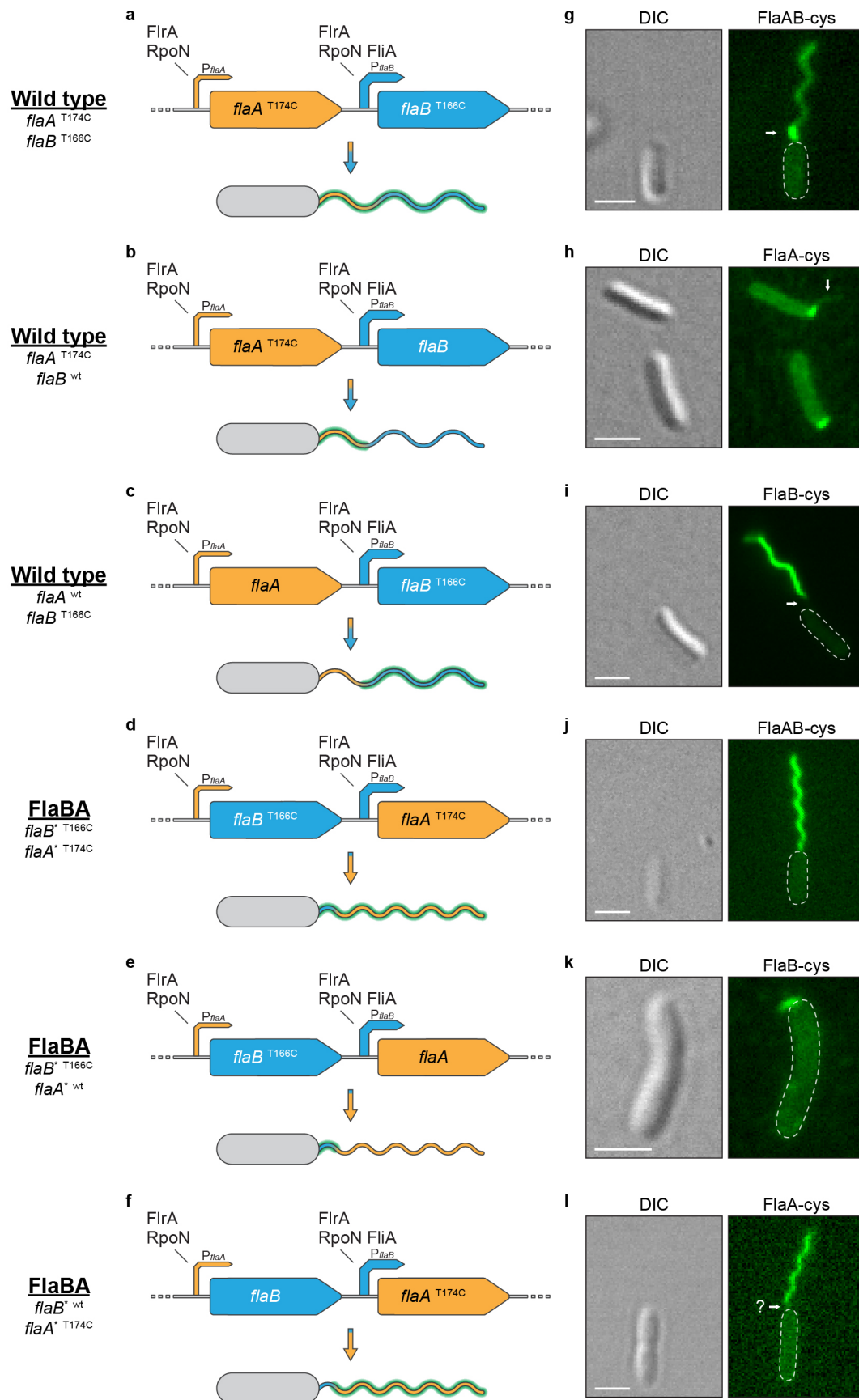
Supplementary Figure 1: Sequence alignment of the polar flagellins of *Shewanella putrefaciens* CN-32. Different residues are marked by brown boxes, different but similar residues are marked by grey boxes. The predicted flagellin domains are given below the sequence. Most differences are located in the variable region, which presumably is exposed to the surrounding medium. The cysteine substitution sites are also located within this region.



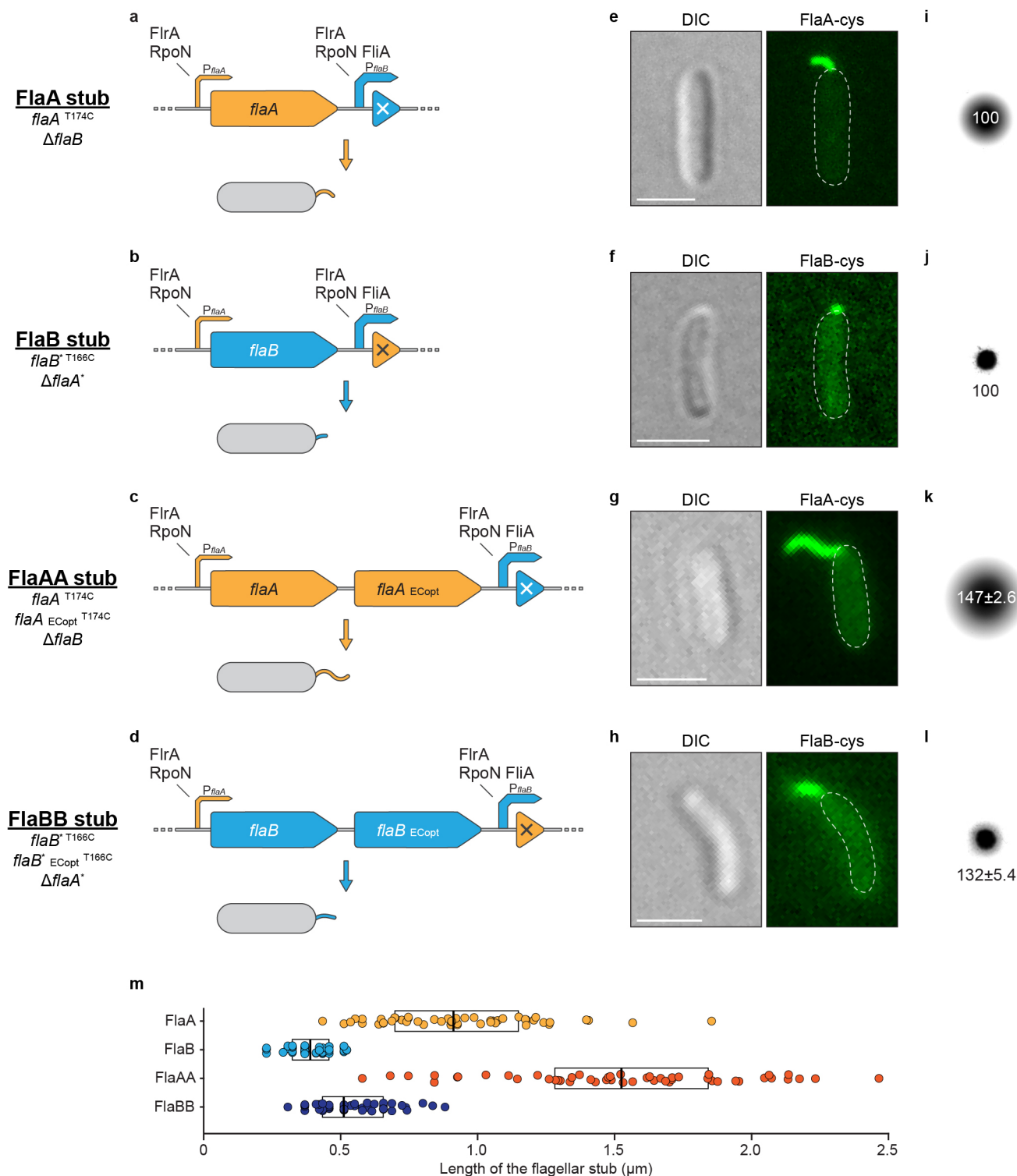
Supplementary Figure 2: Immunoblotting analysis of the polar flagellins and their chaperone FliS. Upper panels = immunoblots, lower panels = corresponding Coomassie-stained PAGE loading controls. **a** Detection of flagellins FlaA and FlaB in flagellin deletion strains and strains lacking two major glycosylation proteins, Maf1 and PseG. The thick arrows indicate the collapsed FlaA and FlaB bands. Likely due to different extents of glycosyl modifications, FlaA and FlaB can be discriminated by their molecular mass (thin arrows). **b** Detection of FlaA and FlaB in strains lacking the sigma factors 54 and 28 (RpoN and FliA, respectively) and other regulatory proteins for flagellar assembly (FliR and FliBC). **c** Detection of FLAG-tagged FliS in the same background strains as in **b**. Full blots are shown in Supplementary Fig. 13. **d** Radial expansion of cells producing FLAG-tagged FliS in 0.2% soft agar as control for functional integrity.



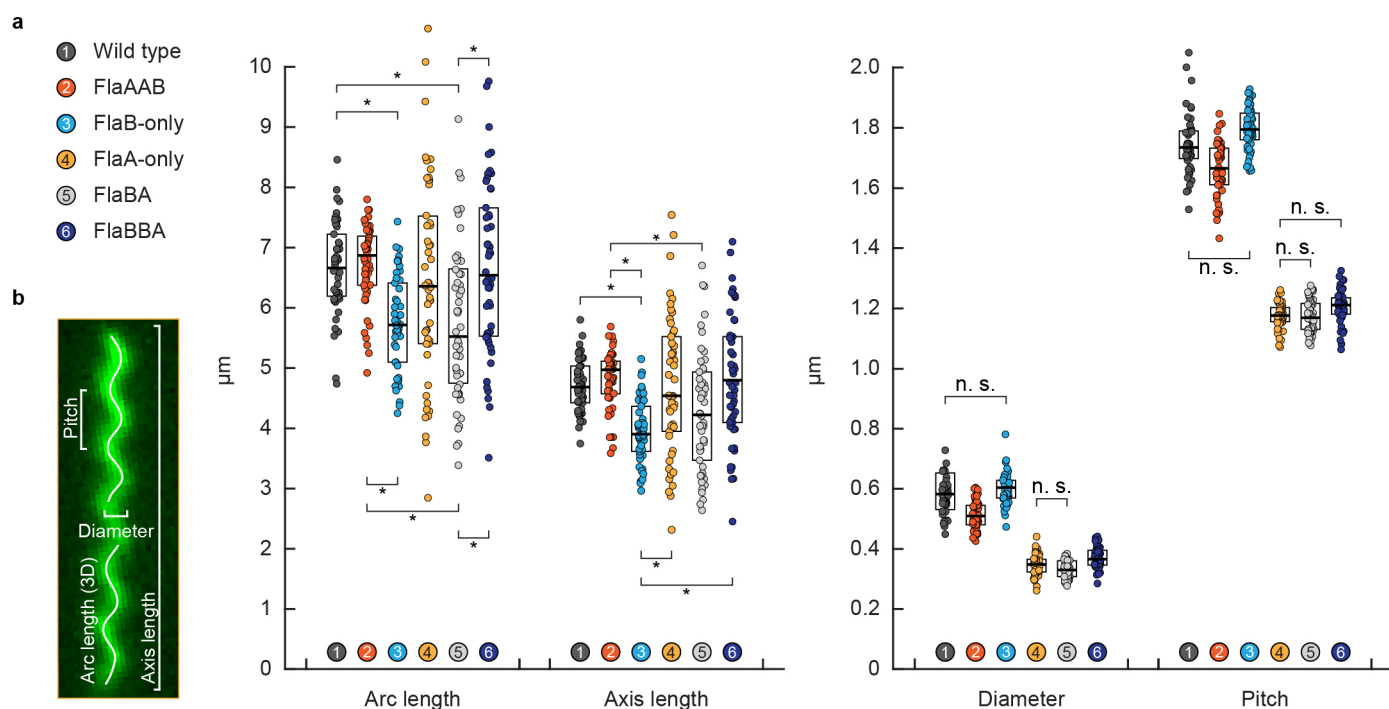
Supplementary Figure 3: Cysteine substitutions in the flagellins do not affect swimming motility. Radial expansion of the different filament type strains with cysteine-labeled and wild-type flagellins was tested in 0.2% soft agar. FlaBA was tested separately so it can only be compared internally. In all strains, including wild type, the lateral flagellins were deleted. The strains depicted in the upper row are also shown in Fig. 1 of the main manuscript, however, as a separate experiment. Asterisks indicate that these genes are expressed from the promoter of the other flagellin.



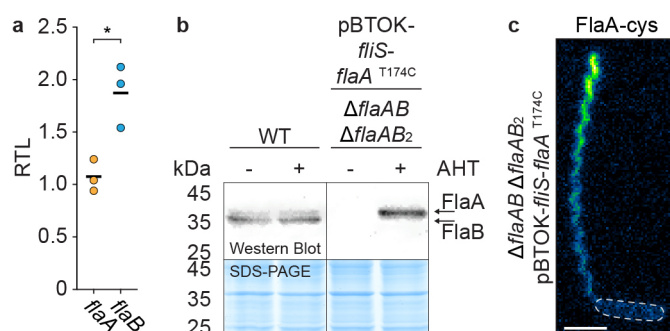
Supplementary Figure 4: Overview of the wild-type and FlaBA filaments essentially as in Fig. 1 of the main text. Additional strains are displayed that produce complete filaments but with only one of the cysteine-labeled flagellins. The glow effect around the filament segment(s) in panels **a - f** indicates which of the flagellin segments should be visible in the micrographs of the fluorescently labeled filaments in panels **g - l**. The arrows indicate the FlaA portion that is distinguishable from FlaB in the wild type (panel **g**), a faint FlaA signal in the FlaB segment (panel **h**), a gap (unlabeled FlaA) between cell body and the FlaB segment (panel **i**) and the segment where FlaB is expected but not visible in the FlaBA strain (panel **l**), respectively. Scale bars = 2 μ m.



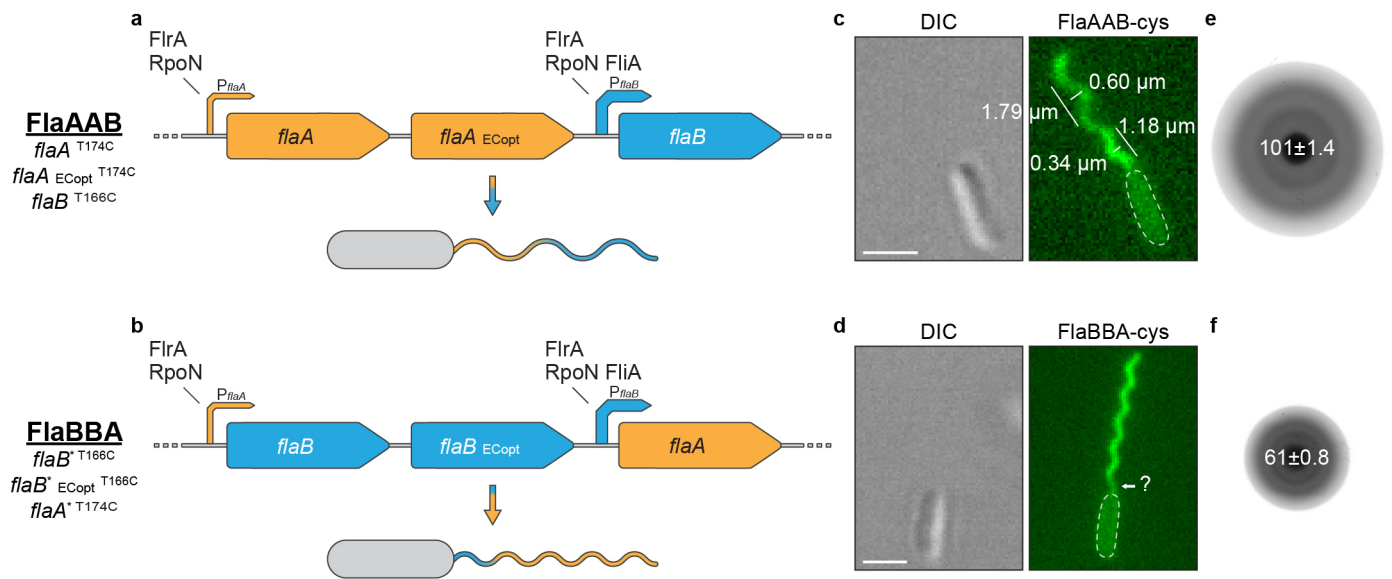
Supplementary Figure 5: Overview of the flagellar filaments that are formed by flagellins under the control of the *flaA* promoter. Lateral flagellin genes were always deleted. **a - d** Genetic organization of the flagellins and modifications to obtain different filaments. The DNA sequences of the duplicated flagellins were codon-optimized for *E. coli* (ECopt) to prevent recombination with the native flagellin genes. Gene deletions are marked with a cross, swapping of the gene sequences is marked with an asterisk. $P_{flaA/B}$ = *flaA/B* promoter. **e - h** Micrographs of cells with fluorescently labeled flagellar filaments displaying the outcome of the editing of the flagellin genes. All filaments produced only from the *flaA* promoter form very short stubs. Scale bars = 2 μm. **i - l** Radial expansion in 0.15% soft agar. Strains producing longer filament stubs can spread further. The numbers indicate the relative spreading compared to the corresponding single flagellin strain (% ± s.d.) of three individual experiments (two for FlaBB stub). **m** Length of the filament stubs measured from fluorescently labeled flagellar filaments. FlaB being produced from the *flaA* promoter forms shorter stubs than FlaA being produced from the same promoter. Duplication of a flagellin gene results in increased but not doubled length. Data points are displayed as individual values measured for 50 filaments for each strain. The boxes span the central half of the data points, the black bars indicate the median. Significance was tested for all combinations of all filament stub types. All tested combinations were significant ($P < 0.05$, Bonferroni corrected).



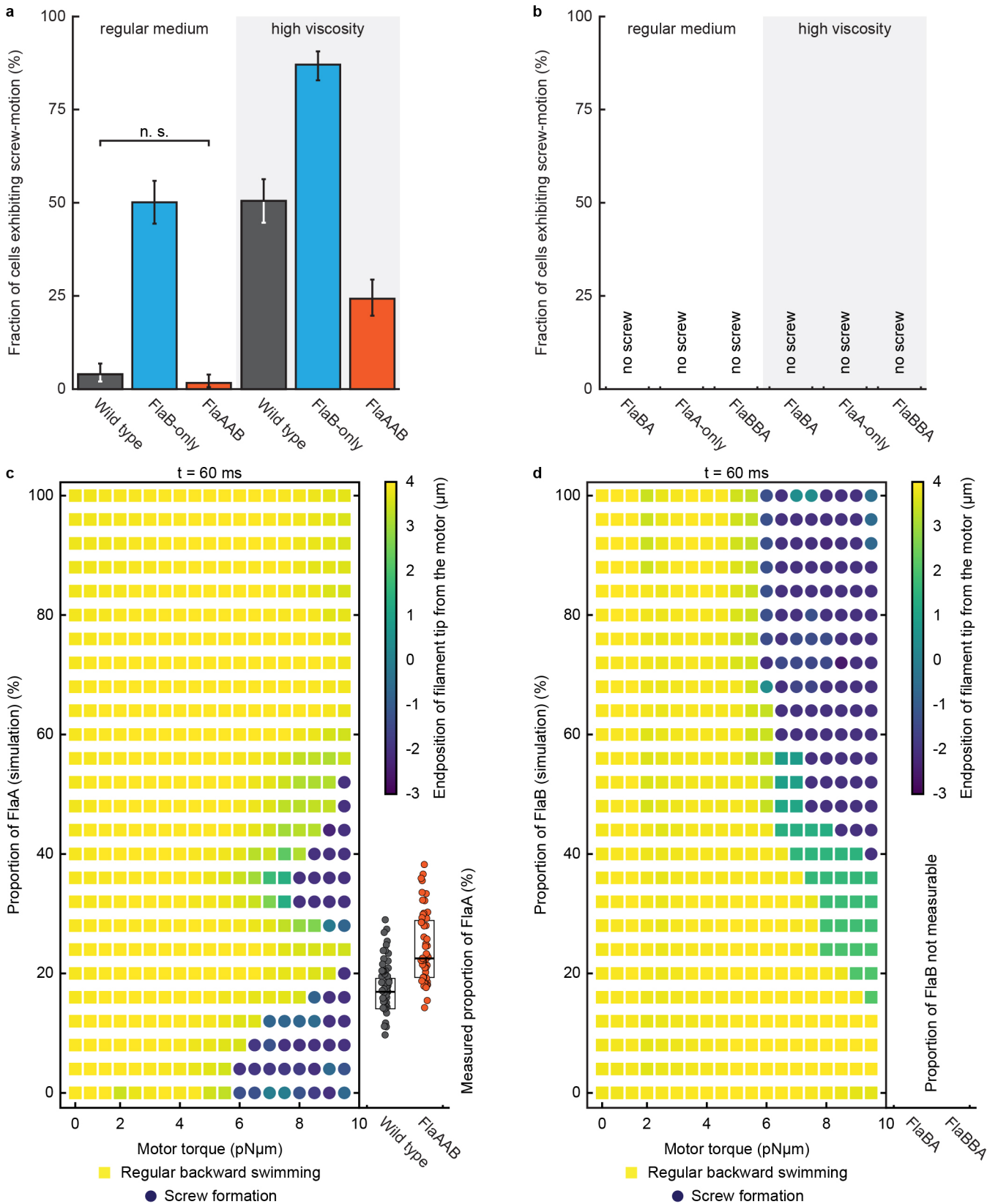
Supplementary Figure 6: Helix geometry of the different flagellar filament types as measured by fluorescent microscopy. **a** The geometric parameters of the flagellar helices are displayed as individual parameters measured for 50 flagellar filaments for each strain. The boxes span the central half of the data points, the black bars indicate the median. The numbered and colored dots indicate which strain is depicted in the diagram. Arc and Axis length show large cell to cell variations but are essentially very similar for all filament types. The three-dimensional arc length was calculated from the axis length, pitch and diameter. Pitch and diameter are very similar for the three filament types mainly or exclusively consisting of FlaB (wild type (FlaAB), FlaAAB and FlaB-only) as well as for the three filament types mainly or exclusively consisting of FlaA (FlaBA, FlaBBA and FlaA-only). Significance was tested for all combinations of filament types for each parameter individually. In the left diagram significant differences ($P < 0.05$, Bonferroni corrected) are indicated by an asterisk. In the right diagram only the non-significant differences are indicated (n.s.). **b** Illustration of which parameters were determined.



Supplementary Figure 7: Flagellin transcription levels and overexpression of *flaA*. **a** Relative transcript levels (RTL) quantified by qRT-PCR between the flagellin genes *flaA* and *flaB* of the *Shewanella putrefaciens* CN-32 wild-type strain. Transcription of *flaB* is about twice as high as of *flaA*. RTL for the three biological replicates are shown separately (colored dots) together with the mean value (black bar). The differences in RTL are significant ($P < 0.05$), indicated by an asterisk. **b** Immunoblotting analysis (with corresponding Coomassie stained PAGE loading control in the lower panels) of the overexpression of *flaA* (and its chaperone *fliS*) from a plasmid in a background strain lacking polar (*flaAB*) and lateral (*flaAB₂*) flagellin genes. The full blot is shown in Supplementary Fig. 13. The wild type without the plasmid (left) produces the native flagellins FlaA and FlaB which can be distinguished by their molecular weight (cp. Supplementary Fig. 2a). In the overexpression strain (right) FlaA is produced from the plasmid with the correct molecular weight, indicating that the post-transcriptional modification is not disturbed (cp. Supplementary Fig. 2a). Expression was induced with anhydrotetracycline (\pm AHT). This strain forms aberrantly long flagellar filaments only consisting of FlaA (micrograph shown in panel **c**) when induced with the same concentration of AHT as in **b**. The calculated arc length of the displayed flagellum is 18.7 μm . Scale bar = 2 μm .

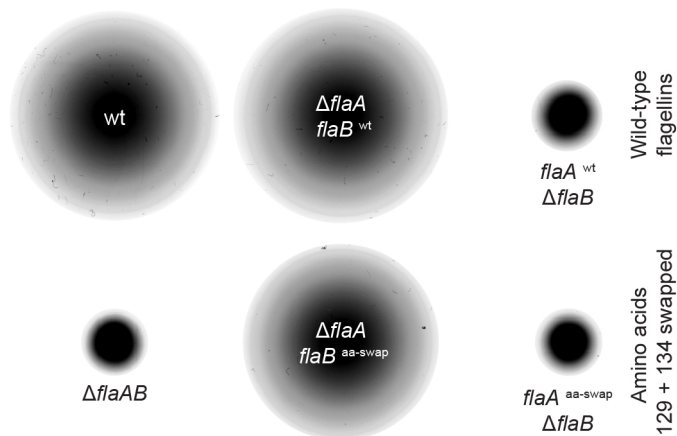
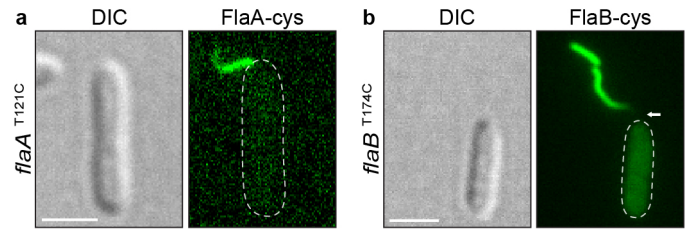


Supplementary Fig. 8: Overview of the flagellin duplication strains. In all strains the genes for the lateral flagellins were deleted. **a, b** Genetic organization of the flagellins and genetic modifications to obtain different filament types. The duplicated genes are both under the control of the *flxA* promoter producing two identical flagellin proteins. The DNA sequences of the synthetic flagellins were codon-optimized for *E. coli* (ECopt) to prevent recombination with the native flagellin genes. Swapping of the gene sequences is marked with an asterisk. *P_{flxA/B}* = *flxA/B* promoter. **c, d** Micrographs of cells with fluorescently labeled flagellar filaments displaying the outcome of the genetic editing of the flagellin genes. Duplication of the upstream flagellin gene increases the length of the proximal flagellin segment, although not doubling it (see also Supplementary Fig. 5). Here, the parameters of the proximal FlaA segment of the FlaAAB filament can be measured as it forms a complete helix turn (numbers in panel c). They fit well to the parameters of the FlaA-only filament, while the parameters of the remaining major segment fit well to the parameters of the FlaB-only filament (cp. Supplementary Fig. 6 and Supplementary Table 4). The proximal FlaB segment of the FlaBBA filament is still not clearly distinguishable from the cell body and the major part of the flagellum (panel d, question mark). Scale bars represent 2 μm. **e, f** Radial expansion of the flagellin duplication cells in 0.25% soft agar. The numbers indicate the relative spreading compared to the wild type (% ± s.d.) of three individual experiments (cp. Fig. 1i in the main manuscript). The FlaAAB strain performs comparatively well as the wild type and FlaB-only strains, while the FlaBBA strain spreads comparatively to the FlaBA and FlaA-only strains.

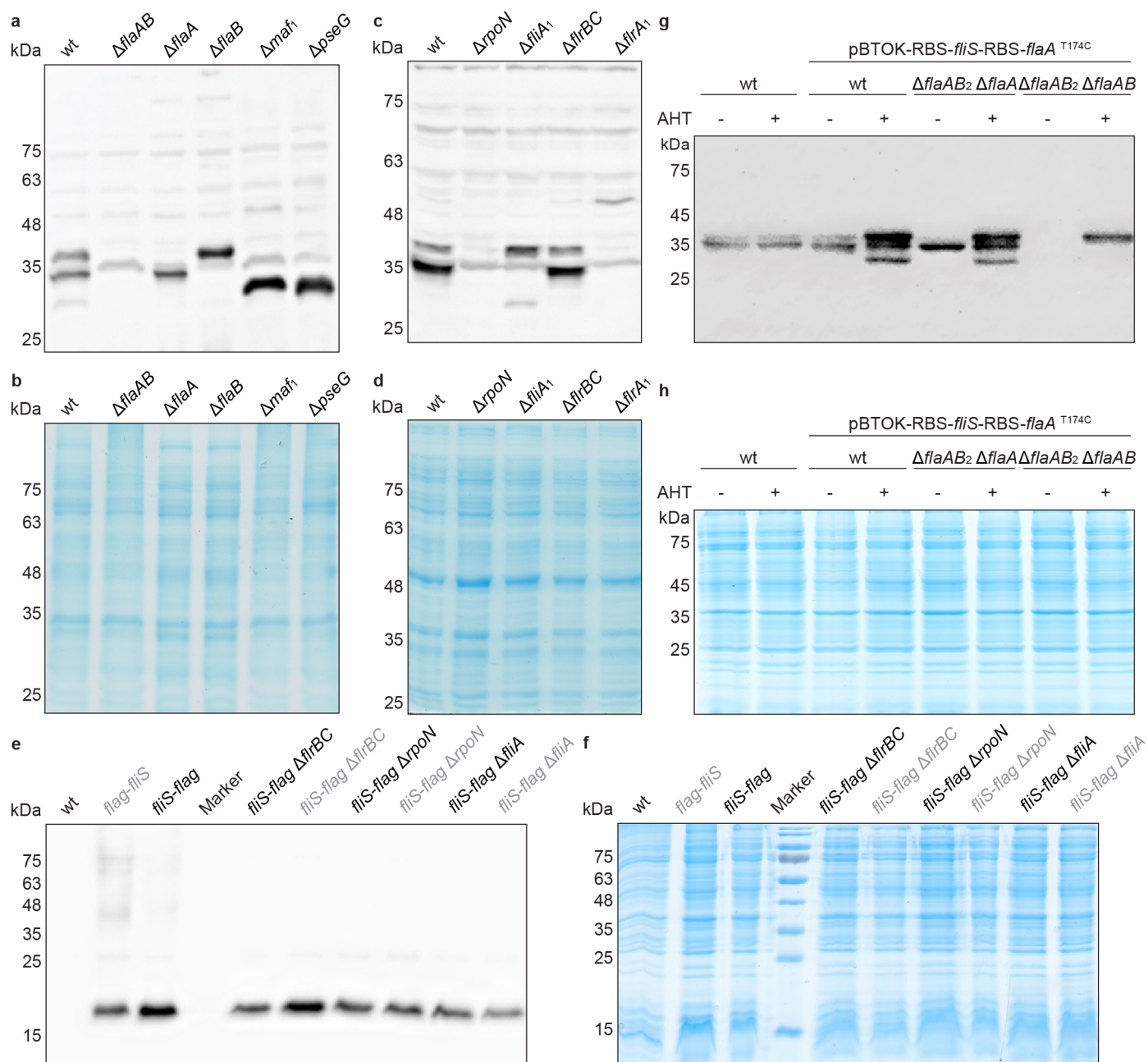


Supplementary Figure 9: Experimentally observed screw formation and simulation of screw formation. **a** and **c** are the same data as in Fig. 4 of the main text together with the flagellin duplication strains for comparison. **a, b** Screw formation observed for different filaments in regular and high viscosity. Significance was tested for all filament type combinations under both conditions and for each filament type between the two conditions. If no screw was observed at all, significance was not tested. Only the difference between wild type (FlaAB) and FlaAAB filament cells in regular medium is not significant (n.s.; $P < 0.05$, Bonferroni corrected). Error bars indicate 95% confidence intervals. About 300 cells were counted for each strain. **c, d** Observation of screw formation for varying flagellin compositions after a simulation time of $t = 60$ ms. The diagram in panel **c** is identical with the diagram in Fig. 4b. The simulation data displayed in panel **d** was obtained similarly but this time starting with a flagellum completely composed of FlaA (bottom of the diagram) and successively exchanging the segments to a FlaB configuration starting from the filament's base at the cell pole. The formation of a screw is indicated by blue circles. The color coding represents the z-position of the flagellum's free end, with negative values indicating a position below the motor segment (position 0). Blue-green squares therefore indicate filament instabilities that are, however, not comparable to proper screw formation.

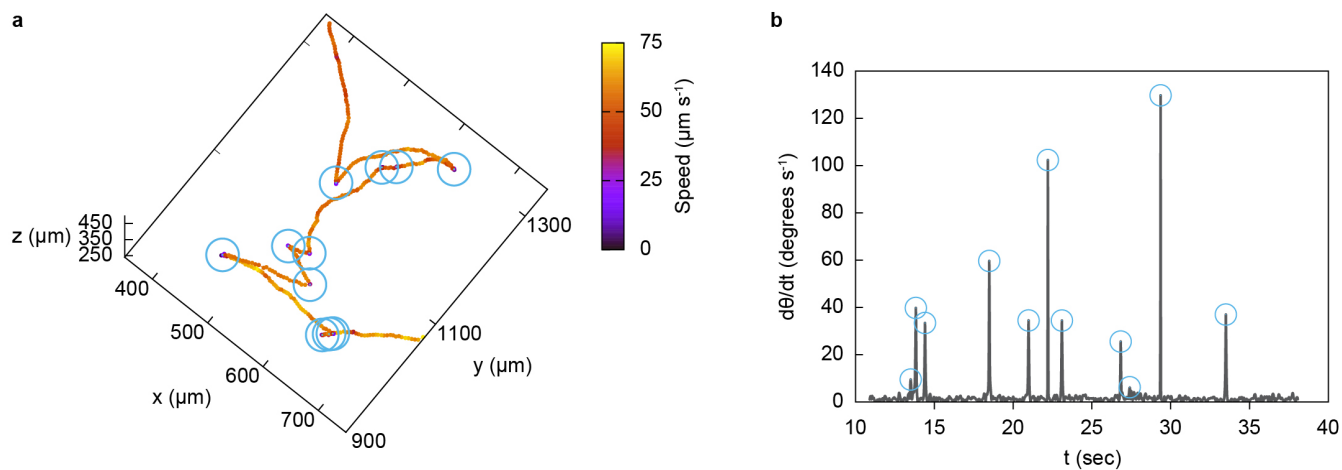
Supplementary Figure 10: The flagellins of *Shewanella oneidensis* MR-1 show a similar spatial distribution as the polar flagellins of *Shewanella putrefaciens* CN-32 in the assembled flagellum. **a** Micrograph of FlaA-cysteine-labeled cells. **b** Micrograph of FlaB-cysteine-labeled cells. The arrow indicates a gap (unlabeled FlaA) between cell body and the FlaB segment. Scale bars represent 2 μ m.



Supplementary Figure 11: Exchanging the amino acids of the flagellins FlaA and FlaB at the positions 129 and 134 does not affect the swimming ability of *Shewanella putrefaciens* CN-32 (here: radial expansion in 0.3% soft agar). It was proposed elsewhere that the corresponding homologous amino acids in *Shewanella oneidensis* MR-1 are responsible for the functional differences of the two flagellins ¹. The effect was analyzed in strains only expressing one of the two polar flagellins and both lateral flagellins.



Supplementary Figure 12: Full immunoblots and Coomassie-stained SDS-PAGE gels. **a** Blot and **b** gel of Supplementary Fig. 2a. **c** Blot and **d** gel of Supplementary Fig. 2b. **e** Blot and **f** gel of Supplementary Fig. 2c. Strains marked in grey were backup strains that were not used furthermore. Marker = MARKER VI Pre-colored, AppliChem. **g** Blot and **h** gel of Supplementary Fig. 7b. Expression was induced with anhydrotetracycline (\pm AHT).



Supplementary Figure 13: Example data of a cell track from the holographic cell tracking. **a** A nearly top-down view of the cell track shown in Fig. 3j of the main manuscript. Swimming speed is encoded by color according to the color bar on the right, and the re-orientation events are highlighted with blue circles. **b** A graph of the cell's change in swimming direction, $d\theta/dt$, as a function of time. Reorientation events are marked by blue circles, at points where $d\theta/dt$ rises above a threshold level of 5 degrees per second.

Supplementary Tables

Supplementary Table 1: Bacterial strains

Identifier	Relevant genotype	Purpose	Reference
<i>Escherichia coli</i>			
DH5α λ pir	ϕ 80d/lacZ Δ M15 Δ (lacZYA-argF)U169 recA ₁ hsdR17 deoR thi-l supE44 gyrA96 relA ₁ /λpir	cloning strain	2
WM3064	thrB1004 pro thi rpsL hsdS lacZ Δ M15 RP4- 1360 Δ (araBAD) 567ΔdapA 1341::[erm pir(wt)]	conjugation strain	3
<i>Shewanella putrefaciens</i>			
S271	CN-32	wild type	4
S2576	Δ flaAB ₂ (Sputcn32_3455-3456)	markerless deletion of both lateral flagellin genes	5
S2575	Δ flaAB ₁ (Sputcn32_2585-2586)	markerless deletion of both polar flagellin genes	5
S4433	Δ flaAB ₁ ; Δ flaAB ₂	markerless deletion of both polar and both lateral flagellin genes	this study
S3807	Δ flaA ₁ -ext (Sputcn32_2586)	markerless deletion of polar minor flagellin gene; extended knock-out	6
S3810	Δ flaB ₁ -ext (Sputcn32_2585)	markerless deletion of polar major flagellin gene; extended knock-out	6
S5179	Δ flaB ₁ ; Δ flaAB ₂	markerless deletion of polar major flagellin gene and both lateral flagellin genes	this study
S4387	Δ flaA ₁ ; Δ flaAB ₂	markerless deletion of polar minor flagellin gene and both lateral flagellin genes	this study
S5165	Δ flaB ₁ ; flaA ₁ (positions swapped); Δ flaAB ₂	markerless insertion of position swapped wild-type flaA ₁ gene and Δ flaB ₁ into Δ flaAB ₁ and deletion of lateral flagellin genes	this study
S4151	flaA ₁ -S169C	markerless insertion of cysteine-labeled flaA ₁ gene into Δ flaA ₁ -ext	this study
S4152	flaA ₁ -T174C; Δ flaAB ₂	markerless insertion of cysteine-labeled flaA ₁ gene into Δ flaA ₁ -ext and deletion of lateral flagellin genes	6
S4143	flaB ₁ -T166C	markerless insertion of cysteine-labeled flaB ₁ gene into Δ flaB ₁ -ext	6
S4154	flaB ₁ -T166C; Δ flaAB ₂	markerless insertion of cysteine-labeled flaB ₁ gene into Δ flaB ₁ -ext and deletion of lateral flagellin genes	6
S4352 FlaB-only	Δ flaA ₁ ; flaB ₁ -T166C; Δ flaAB ₂	markerless insertion of cysteine-labeled flaB ₁ gene into Δ flaB ₁ -ext and markerless deletion of flaA ₁ and Δ flaAB ₂	this study

S4401 Wild type	<i>flaA</i> ₁ -T174C; <i>flaB</i> ₁ -T166C; Δ <i>flaAB</i> ₂	markerless insertion of cysteine-labeled <i>flaB</i> ₁ gene into Δ <i>flaB</i> ₁ -ext and cysteine-labeled <i>flaA</i> ₁ gene into Δ <i>flaA</i> ₁ -ext and deletion of lateral flagellin genes	6
S4794 FlaA-only	Δ <i>flaB</i> ₁ ; <i>flaA</i> ₁ -T174C (positions swapped); Δ <i>flaAB</i> ₂	markerless insertion of position swapped, cysteine-labeled <i>flaA</i> ₁ gene and Δ <i>flaB</i> ₁ into Δ <i>flaAB</i> ₁ and deletion of lateral flagellin genes	this study
S4795 FlaB stub	<i>flaB</i> ₁ -T166C; Δ <i>flaA</i> ₁ (positions swapped); Δ <i>flaAB</i> ₂	markerless insertion of position swapped, cysteine-labeled <i>flaA</i> ₁ gene and Δ <i>flaB</i> ₁ into Δ <i>flaAB</i> ₁ and deletion of lateral flagellin genes	this study
S5219 FlaA stub	<i>flaA</i> ₁ -T174C; Δ <i>flaB</i> ₁ ; Δ <i>flaAB</i> ₂	markerless insertion of cysteine-labeled <i>flaA</i> ₁ gene into Δ <i>flaA</i> ₁ -ext and deletion of deletion of polar major flagellin gene and lateral flagellin genes	this study
S5538	<i>flaB</i> ₁ ; <i>flaA</i> ₁ -T174C (positions swapped); Δ <i>flaAB</i> ₂	markerless insertion of wild-type <i>flaB</i> ₁ gene downstream of the <i>flaA</i> ₁ promoter into S4794	this study
S5539 FlaBA	<i>flaB</i> ₁ -T166C; <i>flaA</i> ₁ -T174C (positions swapped); Δ <i>flaAB</i> ₂	markerless insertion of cysteine-labeled <i>flaB</i> ₁ gene downstream of the <i>flaA</i> ₁ promoter into S4794	this study
S5705 FlaAAB	<i>flaA</i> ₁ -T174C; <i>flaA</i> ₁ -T174C (<i>E. coli</i> optimized); <i>flaB</i> ₁ -T166C; Δ <i>flagAB</i> ₂	markerless insertion of cysteine-labeled <i>flaA</i> ₁ and an additional <i>E. coli</i> optimized <i>flaA</i> ₁ into S4352	this study
S5706 FlaAA stub	<i>flaA</i> ₁ -T174C; <i>flaA</i> ₁ -T174C (<i>E. coli</i> optimized); Δ <i>flaB</i> ₁ ; Δ <i>flagAB</i> ₂	markerless insertion of cysteine-labeled <i>flaA</i> ₁ and an additional <i>E. coli</i> optimized <i>flaA</i> ₁ and Δ <i>flaB</i> ₁ into S4433	this study
S5707 FlaBBA	<i>flaB</i> ₁ -T166C; <i>flaB</i> ₁ -T166C (<i>E. coli</i> optimized); <i>flaA</i> ₁ -T174C (positions swapped); Δ <i>flagAB</i> ₂	markerless insertion of cysteine-labeled <i>flaB</i> ₁ and an additional <i>E. coli</i> optimized <i>flaB</i> ₁ downstream of the <i>flaA</i> ₁ promoter into S4794	this study
S5708 FlaBB stub	<i>flaB</i> ₁ -T166C; <i>flaB</i> ₁ -T166C (<i>E. coli</i> optimized); Δ <i>flaA</i> ₁ (positions swapped); Δ <i>flagAB</i> ₂	markerless insertion of cysteine-labeled <i>flaB</i> ₁ and an additional <i>E. coli</i> optimized <i>flaB</i> ₁ downstream of the <i>flaA</i> ₁ promoter and Δ <i>flaA</i> ₁ into S4433	this study
S3142	Δ <i>rpoN</i> (Sputcn32_0715)	markerless deletion of the <i>pseG</i> gene (sigma factor 54)	this study
S2673	Δ <i>fliA</i> ₁ (Sputcn32_2559)	markerless deletion of the <i>fliA</i> ₁ gene (sigma factor 28)	this study
S3139	Δ <i>fliR</i> ₁ (Sputcn32_2580)	markerless deletion of the <i>fliR</i> ₁ gene	this study
S3174	Δ <i>fliRBC</i> (Sputcn32_2578-2579)	markerless deletion of the <i>fliR</i> _B and <i>fliR</i> _C genes	this study
S3864	Δ <i>maf1</i> (Sputcn32_2630)	markerless deletion of the <i>maf1</i> gene	this study
S3863	Δ <i>pseG</i> (Sputcn32_2626)	markerless deletion of the <i>pseG</i> gene	this study
S4440	pBTOK-RBS- <i>fliS</i> ₁ -RBS- <i>flaA</i> ₁ -T174C	stable integration of overproduction vector pBTOK producing the full length proteins FliS ₁ and FlaA ₁	this study

S4441	$\Delta flaA_1$; $\Delta flaAB_2$ -- pBTOK-RBS- <i>fliS</i> ₁ -RBS- <i>flaA</i> ₁ -T174C	markerless deletion of polar minor flagellin gene and both lateral flagellin genes and stable integration of overproduction vector pBTOK producing the full length proteins FliS ₁ and FlaA ₁	this study
S4442	$\Delta flaAB_1$; $\Delta flaAB_2$ -- pBTOK-RBS- <i>fliS</i> ₁ -RBS- <i>flaA</i> ₁ -T174C	markerless deletion of both polar flagellin genes and both lateral flagellin genes and stable integration of overproduction vector pBTOK producing the full length proteins FliS ₁ and FlaA ₁	this study
S3127	$\Delta fliS_1$ (Sputcn32_2581)	markerless deletion of the <i>fliS</i> ₁ gene	this study
S4394	<i>fliS</i> ₁ -FLAG	markerless insertion of the <i>fliS</i> ₁ gene with a c-terminal FLAG-tag	this study
S3791	$\Delta flaB_1$; <i>flaA</i> ₁ -S129N- N134T	markerless insertion of amino-acid-swapped <i>flaA</i> ₁ gene into $\Delta flaA_1$ and deletion of polar major flagellin gene	this study
S3792	$\Delta flaA_1$; <i>flaB</i> ₁ -N129T- T134N	markerless insertion of amino-acid-swapped <i>flaB</i> ₁ gene into $\Delta flaB_1$ and deletion of polar major flagellin gene	this study

Shewanella oneidensis

S565	MR-1	wild type	7
S1021	$\Delta flaA$ (SO_3238)	markerless deletion of polar minor flagellin gene	8
S1020	$\Delta flaB$ (SO_3237)	markerless deletion of polar major flagellin gene	8
S4858	<i>flaA</i> -T121C	markerless insertion of cysteine-labeled <i>flaA</i> gene into $\Delta flaA$	this study
S4857	<i>flaB</i> -S174C	markerless insertion of cysteine-labeled <i>flaB</i> gene into $\Delta flaB$	this study

Supplementary Table 2: Plasmids

Name	Insert	Purpose	Reference
pNPTS138-R6KT	<i>mob</i> RP4+ <i>ori</i> -R6K <i>sacB</i> β -galactosidase fragment alpha Km ^r	suicide plasmid for in-frame deletions or integrations	9
pNPTS138-R6KT- flag-clusterI-KO	$\Delta flaAB_1$ (Sputcn32_ 2585-2586)	in-frame deletion fragment	5
pNPTS138-R6KT- flag-clusterII-KO	$\Delta flaAB_2$ (Sputcn32_ 3455-3456)	in-frame deletion fragment	5
pNPTS138-R6KT- <i>flaA</i> ₁ -KO-ext	$\Delta flaA_1$ (Sputcn32_2586)	in-frame deletion fragment	6
pNPTS138-R6KT- <i>flaB</i> ₁ -KO-ext	$\Delta flaB_1$ (Sputcn32_2585)	in-frame deletion fragment	6
pNPTS138-R6KT- <i>flaA</i> ₁ -S169C	<i>flaA</i> ₁ -S169C (Sputcn32_2586)	in-frame insertion fragment; serine 169 substituted with cysteine	this study
pNPTS138-R6KT- <i>flaA</i> ₁ -T174C	<i>flaA</i> ₁ -T174C (Sputcn32_2586)	in-frame insertion fragment; threonine 174 substituted with cysteine	6
pNPTS138-R6KT- <i>flaB</i> ₁ -T166C	<i>flaB</i> ₁ -T166C (Sputcn32_2585)	in-frame insertion fragment, threonine 166 substituted with cysteine	6

pNPTS138-R6KT- <i>flaB₁</i> -S174C	<i>flaB₁</i> -S174C (Sputcn32_2585)	in-frame insertion fragment; serine 174 substituted with cysteine	6
pNPTS138-R6KT- <i>flaB₁</i> -KO - <i>flaA₁</i> - T174C (positions swapped)	Δ <i>flaB₁</i> (Sputcn32_2585) - <i>flaA₁</i> -T174C (Sputcn32_2586)	in-frame insertion fragment; Δ <i>flaB₁</i> replaces <i>flaA₁</i> and <i>flaA₁</i> replaces <i>flaB₁</i> ; threonine 174 of <i>flaA₁</i> substituted with cysteine	this study
pNPTS138-R6KT- <i>flaB₁</i> -T166C - <i>flaA₁</i> -KO (positions swapped)	<i>flaB₁</i> -T166C (Sputcn32_2585) - Δ <i>flaA₁</i> (Sputcn32_2586)	in-frame insertion fragment; <i>flaB₁</i> replaces <i>flaA₁</i> and Δ <i>flaA₁</i> replaces <i>flaB₁</i> ; threonine 166 of <i>flaB₁</i> substituted with cysteine	this study
pNPTS138-R6KT- <i>flaB₁</i> -KO - <i>flaA₁</i> (positions swapped)	Δ <i>flaB₁</i> (Sputcn32_2585) - <i>flaA₁</i> (Sputcn32_2586)	in-frame insertion fragment; Δ <i>flaB₁</i> replaces <i>flaA₁</i> and <i>flaA₁</i> replaces <i>flaB₁</i>	this study
pNPTS138-R6KT- <i>flaB₁</i> (positions swapped)	<i>flaB₁</i> -T166C (Sputcn32_2585)	in-frame insertion fragment; <i>flaB₁</i> replaces deletion fragment of <i>flaA₁</i>	this study
pNPTS138-R6KT- <i>flaB₁</i> -T166C (positions swapped)	<i>flaB₁</i> -T166C (Sputcn32_2585)	in-frame insertion fragment; <i>flaB₁</i> replaces deletion fragment of <i>flaA₁</i> ; threonine 166 of <i>flaB₁</i> substituted with cysteine	this study
puc57-KAN- <i>flaA₁</i> (<i>E. coli</i> optimized)	<i>flaA₁</i> (<i>E. coli</i> optimized)	synthetic <i>flaA₁</i> of <i>Shewanella</i> <i>putrefaciens</i> CN-32 codon optimized for <i>Escherichia coli</i> K-12 to prevent recombination with the native <i>flaA₁</i>	this study
puc57-KAN- <i>flaB₁</i> (<i>E. coli</i> optimized)	<i>flaB₁</i> (<i>E. coli</i> optimized)	synthetic <i>flaB₁</i> of <i>Shewanella</i> <i>putrefaciens</i> CN-32 codon optimized for <i>Escherichia coli</i> K-12 to prevent recombination with the native <i>flaB₁</i>	this study
pNPTS138-R6KT- double- <i>flaA₁</i> - for Δ <i>flaA₁</i>	<i>flaA₁</i> -T174C; <i>flaA₁</i> .T174C (<i>E. coli</i> optimized)	in-frame insertion fragment; <i>flaA₁</i> and an additional <i>E. coli</i> optimized <i>flaA₁</i> replace the deletion fragment of <i>flaA₁</i> ; threonine 174 of both <i>flaA₁</i> genes substituted with cysteine	this study
pNPTS138-R6KT- double- <i>flaA₁</i> - for Δ <i>flaAB₁</i>	<i>flaA₁</i> -T174C; <i>flaA₁</i> -T174C (<i>E. coli</i> optimized); Δ <i>flaB₁</i>	in-frame insertion fragment; <i>flaA₁</i> and an additional <i>E. coli</i> optimized <i>flaA₁</i> and deletion of <i>flaB₁</i> replace the deletion fragment of <i>flaAB₁</i> ; threonine 174 of both <i>flaA₁</i> genes substituted with cysteine	this study
pNPTS138-R6KT- double- <i>flaB₁</i> - for Δ <i>flaB₁</i> <i>flaA₁</i> (position swapped)	<i>flaB₁</i> -T166C; <i>flaB₁</i> -T166C (<i>E. coli</i> optimized) (positions swapped)	in-frame insertion fragment; <i>flaB₁</i> and an additional <i>E. coli</i> optimized <i>flaB₁</i> replace the position swapped deletion fragment of <i>flaB₁</i> ; threonine 166 of both <i>flaB₁</i> genes substituted with cysteine	this study
pNPTS138-R6KT- double- <i>flaA₁</i> - for Δ <i>flaA₁</i>	<i>flaB₁</i> -T166C; <i>flaB₁</i> -T166C (<i>E. coli</i> optimized); Δ <i>flaA₁</i> (positions swapped)	in-frame insertion fragment; <i>flaB₁</i> and an additional <i>E. coli</i> optimized <i>flaB₁</i> and deletion of <i>flaA₁</i> (position swapped) replace the deletion fragment of <i>flaAB₁</i> ; threonine 166 of both <i>flaB₁</i> genes substituted with cysteine	this study

pNPTS138-R6KT- <i>rpoN</i> -KO	$\Delta rpoN$ (Sputcn32_0715)	in-frame deletion fragment	this study
pNPTS138-R6KT- <i>fliA</i> ₁ -KO	$\Delta fliA_1$ (Sputcn32_2559)	in-frame deletion fragment	this study
pNPTS138-R6KT- <i>fliA</i> ₁ -KO	$\Delta fliA_1$ (Sputcn32_2580)	in-frame deletion fragment	this study
pNPTS138-R6KT- <i>fliBC</i> -KO	$\Delta fliBC$ (Sputcn32_2578-79)	in-frame deletion fragment	this study
pNPTS138-R6KT- <i>maf1</i> -KO	$\Delta maf1$ (Sputcn32_2630)	in-frame deletion fragment	this study
pNPTS138-R6KT- <i>pseG</i> -KO	$\Delta pseG$ (Sputcn32_2626)	in-frame deletion fragment	this study
pNPTS138-R6KT- <i>fliS</i> ₁ -KO	$\Delta fliS_1$ (Sputcn32_2581)	in-frame deletion fragment	this study
pNPTS138-R6KT- <i>fliS</i> ₁ -FLAG	<i>fliS</i> ₁ -FLAG (Sputcn32_2581)	in-frame insertion fragment; c-terminal FLAG-tagged version of <i>fliS</i> ₁	this study
pNPTS138-R6KT- <i>flaA</i> ₁ -S129N-N134T	<i>flaA</i> ₁ -S129N-N134T (Sputcn32_2586)	in-frame insertion fragment; amino acid swap with <i>flaB</i> ₁	this study
pNPTS138-R6KT- <i>flaB</i> ₁ -N129T-T134N	<i>flaB</i> ₁ -N129T-T134N (Sputcn32_2581)	in-frame insertion fragment; amino acid swap with <i>flaA</i> ₁	this study
pBTOK	pBBR1-MCS2 backbone (pBBR origin, Km ^r); TetR, Promoter and multiple cloning site of pASK-IBA3plus and <i>E. coli</i> rrnB1 T1 and lambda phage T0 terminator	overproduction plasmid inducible with anhydrotetracycline	10
pBTOK-RBS- <i>fliS</i> ₁ -RBS- <i>flaA</i> ₁ -T174C	RBS- <i>fliS</i> ₁ - (Sputcn32_2581) - RBS- <i>flaA</i> ₁ -T174C (Sputcn32_2586)	overproduction of wild-type <i>fliS</i> ₁ and cysteine-labeled <i>flaA</i> ₁ , both with the ribosome binding site sequence AGGAGG; threonine 174 of <i>flaA</i> ₁ substituted with cysteine	this study

Supplementary Table 3: Oligonucleotides

#	Name	Sequence 5'-3'	Purpose
B 31	BamHI-flagL-fwd	AGG ATC CTG ACA CTG TAT TTA TGG CGC AGG	construction of in-frame deletion vector pNPTS138-R6KT-R6KT-flag-clusterII-KO
B 32	OL-flagL-rev	CAG TAG ACC GTG AAC ACC TAA CAT ATT AAT TCT CCA G	
B 33	OL-flagL-fwd	GGT GTT CAC GGT CTA CTG CGT TAA TCT AGC TC	
B 34	PspOMI-flagL-rev	TGT CGG GCC CGT CGC CGT CGC ATT TTC GC	
B 35	Check-flagL-fwd	GTA TTA GCT TCG ATC GGG ATT GG	check primer for <i>flaAB</i> ₂
B 36	Check-flagL-rev	GTT ACC CTT TGG CGC ATC GG	
B 45	EcoRI-flagP-fwd	A GAA TTC GAA GTT AAA GTG TCT GGG AAA CCC	construction of in-frame deletion vector
B 46	OL-flagP-rev	TCA CCT CTT AAC TGT AAT AGC CAT AGT ATT TTC CTC	

B 47	OL-flagP-fwd	ATT ACA GTT AAG AGG TGA GAC AGT GAT AGG GA	pNPTS138-R6KT- R6KT-flag-cluster1-KO
B 48	PspOMI-flagP- rev	T CTA GGG CCC TAA GCC TCT GTT TTC ATC AAA AGC C	
B 49	Check-flagP-fwd	AAT TTT GAT GCG ACT ACC CCC G	check primer for <i>flaAB</i> ₁
B 50	Check-flagP-rev	TAT CTA GAC CTG ACC CCA TGC C	
MJK 26	OL_ <i>flaA</i> ₁ _KO_ ext_rv	GTG ACA GCG CAA TAG CCA TAG TAT TTT CCT CTT CTA AG	construction of in-frame deletion vector pNPTS138-R6KT- <i>flaA</i> ₁ -KO-ext
MJK 27	OL_ <i>flaA</i> ₁ _KO_ ext_fw	TAT GGC TAT TGC GCT GTC ACT ACT GGG ATA ATT TAC	
FR 299	EcoRV_ <i>flaA</i> ₁ _KO_ fw	GAA TTC GTG GAT CCA GAT GAA GTT AAA GTG TCT GGG AAA CCC	
FR 302	EcoRV_ <i>flaA</i> ₁ _KO_ rv	CAA GCT TCT CTG CAG GAT GCA TCG CAC CTT CAG AAA TTT GG	
MJK 28	OL_ <i>flaB</i> ₁ _KO_ ext_rv	AGG CCA CTT GGG CCA TGA TCG TTT CCT CTG TA	construction of in-frame deletion vector pNPTS138-R6KT- <i>flaB</i> ₁ -KO-ext
MJK 29	OL_ <i>flaB</i> ₁ _KO_ ext_fw	GAT CAT GGC CCA AGT GGC CTT ATC ACT GCT GTA ATA G	
FR 295	EcoRV_ <i>flaB</i> ₁ _KO_ fw	GAA TTC GTG GAT CCA GAT ATA ACC AAC GTG CAG CGT TAG G	
FR 298	EcoRV_ <i>flaB</i> ₁ _KO_ rv	CAA GCT TCT CTG CAG GAT CAG CTA ATG CCA ACG CTT CTT C	
MJK 76	<i>FlaA</i> ₁ -S169C-R	CCA TTA AAC ACC CCG CAT TAT TGG TAC C	construction of in-frame insertion vector pNPTS138-R6KT- <i>flaA</i> ₁ -S169C
MJK 77	<i>FlaA</i> ₁ -S169C-F	ATG CGG GGT GTT TAA TGG TTA GTA CAT TAA CG	
MJK 78	<i>FlaA</i> ₁ -T174C-R	TCG TTA AAC AAC TAA CCA TTA AAC TCC CCG CAT TAT TGG	construction of in-frame insertion vector pNPTS138-R6KT- <i>flaA</i> ₁ -T174C
MJK 79	<i>FlaA</i> ₁ -T174C-F	TGG TTA GTT GTT TAA CGA TTG CAA CTT CAG GTG GTC G	
MJK 82	<i>FlaB</i> ₁ -T166C-R	CTG ATG CAC AGG TTT TTG ACA CAG AAA TCG	construction of in-frame insertion vector pNPTS138-R6KT- <i>flaB</i> ₁ -T166C
MJK 83	<i>FlaB</i> ₁ -T166C-F	CAA AAA CCT GTG CAT CAG CAT TAA AAG TTG G	
MJK 86	<i>FlaB</i> ₁ -S174C-R	ATA TCT AAA CAA CCA ACT TTT AAT GCT GAT GC	construction of in-frame insertion vector pNPTS138-R6KT- <i>flaB</i> ₁ -S174C
MJK 87	<i>FlaB</i> ₁ -S174C-F	AGT TGG TTG TTT AGA TAT TAA AGG CTC TGC	
MJK 186	<i>A</i> ₁ us-oe <i>B</i> ₁ ko-R	GCA GTG ATA AGG CCA CTT GGG CCA TAG TAT TTT CCT CTT CTA AGT ATC TTG C	construction of in-frame insertion vectors pNPTS138-R6KT- <i>flaB</i> -KO - <i>flaA</i> ₁ (positions swapped) and pNPTS138-R6KT- <i>flaB</i> ₁ -KO - <i>flaA</i> ₁ -T174C (positions swapped)
MJK 187	<i>A</i> ₁ ds-oe <i>B</i> ₁ ko-F	CCA AGT GGC CTT ATC ACT GCT GTA ATT TAC TAA GCA GAA CAT ATC AAT ACA GGA CGT TGC	
MJK 188	<i>B</i> ₁ us-oe <i>A</i> ₁ -R	TAA TAG CCA TGA TCG TTT CCT CTG TAT ACC	
MJK 189	<i>A</i> ₁ -oe <i>B</i> ₁ us-F	GGA AAC GAT CAT GGC TAT TAC AGT TAA TAC CAA CGT GAC	
MJK 190	<i>A</i> ₁ -oe <i>B</i> ₁ ds-R	TTG CTT TCT ATT ATC CCA GTA GTG ACA GCG C	
MJK 191	<i>B</i> ₁ ds-oe <i>A</i> ₁ -F	ACT GGG ATA ATA GAA AGC AAG AGG TGA GAC AGT G	

MJK 180	A1us-oeB1_R	TAA TGG CCA TAG TAT TTT CCT CTT CTA AGT ATC TTG C	construction of in-frame insertion vector pNPTS138-R6KT- <i>flaB₁</i> -T166C - <i>flaA₁</i> -KO (positions swapped)
MJK 181	B1-oeA1us_F	GGA AAA TAC TAT GGC CAT TAC AGT AAA CAC TAA CG	
MJK 182	B1-oeA1ds_R	GCT TAG TAA ATT ACA GCA GTG ATA AGG CCA C	
MJK 183	dsA1-oeB1_F	ACT GCT GTA ATT TAC TAA GCA GAA CAT ATC AAT ACA GGA CGT TGC	
MJK 184	usB1-oeA1ko_R	CCA GTA GTG ACA GCG CAA TAG CCA TGA TCG TTT CCT CTG TAT ACC	
MJK 185	B1ds-oeA1ko_F	TAT TGC GCT GTC ACT ACT GGG ATA ATA GAA AGC AAG AGG TGA GAC AGT GAT AGG	
MJK 258	OL_FlaB_PS_R	GTG TTT ACT GTA ATG GCC ATA GTA TTT TCC TCT TCT AAG TAT C	construction of in-frame insertion vectors pNPTS138-R6KT- <i>flaB₁</i> (positions swapped) and pNPTS138-R6KT- <i>flaB₁</i> -T166C (positions swapped)
MJK 259	FlaB_F	ATG GCC ATT ACA GTA AAC ACT AAC G	
MJK 260	FlaB_R	TTA CAG CAG TGA TAA GGC CAC TTG	
MJK 261	OL_FlaB_PS_F	CAA GTG GCC TTA TCA CTG CTG TAA TTT AC	
MJK 262	Eco_FlaB_PS_R	GCC AAG CTT CTC TGC AGG ATT TGC ACC TTC AGC GAT CTG GG	
MJK 270	OL_FlaA-A_R	ATT TGC TTC CTC TTC TAA GAA TCG AAT TAT CCC AGT AGT GAC AGC GC	construction of in-frame insertion vectors pNPTS138-R6KT- double- <i>flaA₁</i> - for Δ <i>flaA₁</i> and pNPTS138-R6KT- double- <i>flaA₁</i> - for Δ <i>flaAB₁</i>
MJK 271	OL_A-FlaA_F	TTC GAT TCT TAG AAG AGG AAG CAA ATA TGG CTA TTA CGG TTA ACA CGA ATG TAA CAT C	
MJK 272	OL_A-HOM_R	GAT ATG TTC TGC TTA GTA AAT TAG CCC AGA AGC GAC AGC G	
MJK 273	OL_HOM-A_F	TTT ACT AAG CAG AAC ATA TCA ATA CAG GAC G	
MJK 274	OL_FlaB-B_R	ATT TGC TTC CTC TTC TAA GAA TCG AAT TAC AGC AGT GAT AAG GCC ACT TGA G	
MJK 275	OL_B-FlaB_F	TTC GAT TCT TAG AAG AGG AAG CAA ATA TGG CAA TTA CCG TGA ATA CAA ACG TTA C	construction of in-frame insertion vectors pNPTS138-R6KT- double- <i>flaB₁</i> - for Δ <i>flaB₁</i> and pNPTS138-R6KT- double- <i>flaB₁</i> - for Δ <i>flaAB₁</i>
MJK 276	OL_B-HOM_R	GAT ATG TTC TGC TTA GTA AAT TAT AAA AGA CTC AAT GCC ACT TGA GGC	
MJK 277	check_inBsth_R	GCG ATC CTA CCT TCA ATG CAG	check primer for double flagellin constructs (<i>flaA₁</i> and/or <i>flaB₁</i>)
MJK 278	check_outBsth_R	AGT AGG CAA AAG CAA CGT CCT G	
MJK 279	check_inAsth_R	CGT TGT TTG TGC CTA CGC TG	
FR 44	NheI_rpoN_KO_fw	GTA GCT AGC GAA GAA CGC GAA GAA GAA CTG G	construction of in-frame deletion vector
FR 45	OL_rpoN_KO_rv	GCT ATA AAC TCG CTT TCA TGT TAC CGC TGA TC	

FR 46	OL_rpoN_KO_fw	CAT GAA AGC GAG TTT ATA GCC TAC TAT GGA TAT CGG	pNPTS138-R6KT- <i>rpoN</i> -KO
FR 47	PspOMI_rpoN_KO_rv	TCC GGG CCC CGT TAC CTA TAC CTG TGC TCC	
FR 76	check_rpoN_fw	CTA TGC ATC TTC GCG CCC G	check primer for <i>rpoN</i>
FR 77	check_rpoN_rv	CGC TTT CAT GTT ACC GCT GAT C	
B 262	EcoRI-fliA1-KO-fwd	CGA ATT CCG TGC TTT CAG TGA GAT GCG	construction of in-frame deletion vector pNPTS138-R6KT- <i>fliA1</i> -KO
B 263	OL-fliA1-KO-rev	GAG CTT AGC GGC TTT ATT CAC TCG TTT TTT CCT C	
B 264	OL-fliA1-KO-fwd	AAT AAA GCC GCT AAG CTC AAG CAC TGG ACA TAA	
B 265	PspOMI-fliA1-KO-rev	TCC GGG CCC CAA CTA AAT GCT GAG CCT GCT C	
B 266	Check-fliA1-KO-fwd	GCA CCC AAG GTA TGG TGG AAC	check primer for <i>fliA1</i>
B 267	Check-fliA1-KO-rev	TGC AAG TTC TCT AAA TAA ATC ATC AGC	
FR 68	NheI_flrA1_KO_new_fw	GTA GCT AGC AGT AAT AGT TTG AAC ATG GAT GAA GG	construction of in-frame deletion vector pNPTS138-R6KT- <i>fliA</i> -KO
FR 69	OL_flrA1_new_rv	AAG ACT ATT CAT CTG TTT GCA TCA TTC AGT AGG C	
FR 70	OL_flrA1_new_fw	GCA AAC AGA TGA ATA GTC TTT TGC ATT TTT AGT TAT ATT ATT G	
FR 71	PspOMI_flrA1_KO_rv	TCC GGG CCC CAG ATA ACC GCT GCA GAT GTG	
FR 34	Check-flrA1-KO-fwd_new	GCT AAC TTG AAT AAT GAT GTG AAA GC	check primer for <i>fliA</i>
FR 35	Check-flrA1-KO-rev_new	CCG GAG TTA AAG GAG TAA TGG C	
FR 134	NheI-flrBC1-KO-fwd	GTA GCT AGC CGC ACT TGT ACC GTC GCT TC	construction of in-frame deletion vector pNPTS138-R6KT- <i>fliBC</i> -KO
FR 135	OL-flrBC1-KO-rev	CAC TAG CAA ACA GCT CGT ATG CGA GAT ATG GGG	
FR 136	OL-flrBC1-KO-fwd	TCG CAT ACG AGC TGT TTG CTA GTG TGC TTA AAT GTC	
FR 137	PspOMI-flrBC1-KO-rev	TCC GGG CCC GGA ACA TGC ATG GTC TGG CAA C	
FR 138	Check-flrBC1-KO-fwd	GCA GAT TGC CAA CGC AAG GAT C	check primer for <i>fliBC</i>
FR 139	Check-flrBC1-KO-rev	CTA CGT GTG TTG CAA GAG CGA G	
MK 98	EcoRV_KO_Maf1_US_fw	GAA TTC GTG GAT CCA GAT GTC GGA GGC CAG TTT AGT TG	construction of in-frame deletion vector pNPTS138-R6KT- <i>maf1</i> -KO
MK 99	OL_KO_Maf1_US_rv	AAA GTG GTG GGG TTT GTA GTT GCA TAT TTT CCT C	
MK 100	OL_KO_Maf1_DS_fw	ACT ACA AAC CCC ACC ACT TTA GCC CTA ATA TTG	
SH 555	Maf1 dwn rev	GCC AAG CTT CTC TGC AGG AT TTG CTA CGA ACA CCG GCA CC	
MK 101	chk_KO_Maf1_fw	CGA CAT TAC CAT AAC GAA CTG C	check primer

SH 557	Maf1 check dwn	TAA AGG TGC TGG CAC ATA GAG G	for <i>maf-1</i>
MK 94	EcoRV_KO_PseG_US_fw	GAA TTC GTG GAT CCA GAT GAT ACT GAC GTT GCC TTT ATA TC	construction of in-frame deletion vector pNPTS138-R6KT- <i>pseG</i> -KO
MK 95	OL_KO_PseG_US_rv	TTT AAC TTT CGG CCA ATT TCA TAA CTT TCC TTG	
MK 96	OL_KO_PseG_DS_fw	GAA ATT GGC CGA AAG TTA AAT CAT GCA GGT AAT C	
MK 102	EcoRV_KO_PseG_DS_rv	CAA GCT TCT CTG CAG GAT GAA AAC TCA CTA TCA ACA CCG C	
MK 97	chk_KO_PseG_fw	CCA ACA CTA AAC CCG AGT TTC	check primer for <i>pseG</i>
SH 548	PseG check fw	TGT ACA TCC ATA ATG CAC TCG TCC	
MJK 145	XbaI-nC_RBS_fliS_F	AAT GAA TAG TTC GAC AAA AAT AGG AGG GCA AAT ATG AGA GGA TCG CTG CAA TCA TAT CG	construction of overproduction vector pBTOK-RBS- <i>fliS₁</i> -RBS- <i>flaA₁</i> -T174C
MJK 146	OL_fliS_to_flA1_R	CAT ATT TGC CCT CCT TCC TAA ATT ACC TTA ACT CGC GTC GG	
MJK 147	OL_flA1_to_fliS_F	GGA AGG AGG GCA AAT ATG GCT ATT ACA GTT AAT ACC AAC GTG ACT TCG	
MJK 148	Bsp-nC_flA1_R	GGA GTC CAA GCT CAG CTA ATG AAA TTA TCC CAG TAG TGA CAG CGC	
FR 116	NheI_fliS1_fw	GTA GCT AGC TGG GTC GCA AGC AAT TTT ATT GC	construction of in-frame deletion vector pNPTS138-R6KT- <i>fliS1</i> -KO
FR 117	OL_fliS1_KO_rv	GAG AGG ATC GGC GAG TTA AGG TAA TTT AGG ACG	
FR 118	OL_fliS1_KO_fw	CTT AAC TCG CCG ATC CTC TCA TAA ATA CCT ACC	
FR 119	PspOMI_fliS1_rv	TCC GGG CCC TTG CTG ACC AAA GGG AAG CC	
FR 140	check_fliS1_fw	GCT TAG TTT GAT TAG CAC TTG TAG G	check primer for <i>fliS₁</i>
FR 141	check_fliS1_rv	CTG AAG ATA TGT CCA GTA TTG AAG C	
MJK 141	EcoRV_fliS_C_F	GAA TTC GTG GAT CCA GAT AGT ATC TTC AAG GAC AGC TTG ACC	construction of in-frame insertion vector pNPTS138-R6KT- <i>fliS₁</i> -FLAG
MJK 142	OL-STP_FLAG_fliS_R	AAT ATC ATG ATC TTT ATA ATC GCC ATC ATG ATC TTT ATA ATC ACT CGC GTC GGA ATG AGA GG	
MJK 143	OL+STP_FLAG_fliS_F	ATT ATA AAG ATC ATG ATA TTG ATT ATA AAG ATG ATG ATG ATA AAT AAG GTA ATT TAG GAC GGG TCA AGG G	
MJK 144	EcoRV_fliS_KI_R	CAA GCT TCT CTG CAG GAT CAA ACA ATA ATA TCG GTT GCC ACG C	
MJK 149	Check_fliS1-Flag-F	GTC AAC TTT TAC TCG ATG TGC TGG	check primer for <i>fliS₁</i>
MJK 150	Check_fliS1-Flag-R	TCT TCA ATT TGT CCA AGC ACA TTG G	
MJK 1	OL_flA1_S129_N_N134T_rv	AGT AGT ACC AAA AGC GGT ATT GTC ACC AAT GG	construction of in-frame insertion vector

MJK 2	OL_flA1_S129 N_N134T_fw	GAC AAT ACC GCT TTT GGT ACT ACT AAA CTG ATG AC	pNPTS138-R6KT- <i>flaA</i> ₁ .S129N-N134T
MJK 3	OL_flA1_N129 S_T134N_rv	AGT ATT ACC AAA GGC CGT ACT TGT ACC GAT TGC	construction of in-frame insertion vector
MJK 4	OL_flA1_N129 S_T134N_fw	ACA AGT ACG GCC TTT GGT AAT ACT AAA TTA CTT GAT GG	pNPTS138-R6KT- <i>flaB</i> ₁ .N129T-T134N
MJK 5	flaA1_qPCR_fw	GTT GGT ACC AAT AAT GCG GGG AG	qRT-PCR amplifying DNA fragments of <i>flaA</i> ₁ (Sputcn32_2586)
MJK 6	flaA1_qPCR_rv	CTA AAC GGT TTT GTT TAG CAC CTA ACG	
Product length: 151 bp; efficiency: 1.98			
MJK 13	flaB1_neu_qPC R_fw	CTG CGA TTG ATG CTG CAA TTA AAA CC	qRT-PCR amplifying DNA fragments of <i>flaB</i> ₁ (Sputcn32_2585)
MJK 14	flaB1_neu_qPC R_rv	GCA ATA CTT GGT TCT TGG TCA TTT GC	
Product length: 189 bp; efficiency: 2.00			
FR 233	gyrA_qPCR_fw	CAG AAT CGC CTG AGC TTG TTG C	qRT-PCR amplifying DNA fragments of <i>gyrA</i> (Sputcn32_2070)
FR 234	gyrA_qPCR_rv	GAG CAA GGT TGG GAA TTA GGC C	
Product length: 144 bp; efficiency: 2.01			

Supplementary Table 4: Summary of screw formation, helix parameter and qPCR data and statistics

Screw formation 0% Ficoll (Fig. 4)				
Measurements				
Sample	Screw count	Regular count	Screw (%)	N
Wild type	12	287	4.01	299
FlaB-only	153	152	50.16	305
FlaAAB	5	292	1.68	297
Statistics*				
Combination	t	df	P-value	Test
Wild type vs. FlaB-only	NA	NA	2.32E-26	Fisher's exact test
Wild type vs. FlaAAB	NA	NA	0.139	Fisher's exact test
FlaB-only vs. FlaAAB	NA	NA	2.93E-32	Fisher's exact test

Screw formation 15% Ficoll (Fig. 4)				
Measurements				
Sample	Screw count	Regular count	Screw (%)	N
Wild type	150	147	50.51	297
FlaB-only	270	40	87.10	310
FlaAAB	78	243	24.30	321
Statistics*				
Combination	t	df	P-value	Test
Wild type vs. FlaB-only	NA	NA	3.09E-05	Fisher's exact test
Wild type vs. FlaAAB	NA	NA	4.43E-06	Fisher's exact test
FlaB-only vs. FlaAAB	NA	NA	9.74E-19	Fisher's exact test

Screw formation 0 vs. 15% Ficoll (Fig. 4)				
Statistics*				
Combination	t	df	P-value	Test
Wild type vs. Wild type	NA	NA	2.53E-26	Fisher's exact test
FlaB-only vs. FlaB-only	NA	NA	1.99E-05	Fisher's exact test
FlaAAB vs. FlaAAB	NA	NA	3.57E-15	Fisher's exact test

Helix parameters: Arc length (Supplementary Fig. 6)				
Measurements				
Sample	Average (μm)	Median (μm)	SD (μm)	N
Wild type	6.67	6.66	0.75	50
FlaAAB	6.71	6.82	0.66	50
FlaB-only	5.75	5.71	0.77	50
FlaA-only	6.45	6.35	1.68	50
FlaBA	5.71	5.52	1.29	50
FlaBBA	6.67	6.54	1.41	50
Statistics*				
Combination	t	df	P-value	Test
Wild type vs. FlaAAB	0.30	98.00	0.763	t-test
Wild type vs. FlaB-only	-5.96	98.00	3.95E-08	t-test
Wild type vs. FlaA-only	-0.82	67.81	0.417	Welch's t-test
Wild type vs. FlaBA	-4.48	78.56	2.49E-05	Welch's t-test
Wild type vs. FlaBBA	0.00	74.53	1.000	Welch's t-test
FlaAAB vs. FlaB-only	6.63	98.00	1.88E-09	t-test
FlaAAB vs. FlaA-only	1.00	63.68	0.321	Welch's t-test
FlaAAB vs. FlaBA	4.83	72.68	7.48E-06	Welch's t-test
FlaAAB vs. FlaBBA	0.19	69.21	0.848	Welch's t-test
FlaB-only vs. FlaA-only	2.66	68.85	0.010	Welch's t-test
FlaB-only vs. FlaBA	0.19	79.95	0.849	Welch's t-test
FlaB-only vs. FlaBBA	3.98	75.83	1.55E-04	Welch's t-test
FlaA-only vs. FlaBA	2.46	98.00	0.016	t-test
FlaA-only vs. FlaBBA	0.68	98.00	0.496	t-test
FlaBA vs. FlaBBA	3.50	98.00	0.001	t-test

Helix parameters: Axis length (Supplementary Fig. 6)				
Measurements				
Sample	Average (μm)	Median (μm)	SD (μm)	N
Wild type	4.71	4.68	0.43	50
FlaAAB	4.82	4.97	0.48	50
FlaB-only	3.96	3.90	0.51	50
FlaA-only	4.72	4.54	1.16	50
FlaBA	4.28	4.22	0.99	50
FlaBBA	4.80	4.72	1.05	50

Statistics*				
Combination	t	df	P-value	Test
Wild type vs. FlaAAB	1.12	98.00	0.265	t-test
Wild type vs. FlaB-only	-7.95	98.00	3.18E-12	t-test
Wild type vs. FlaA-only	0.00	62.32	0.997	Welch's t-test
Wild type vs. FlaBA	-2.82	66.83	0.006	Welch's t-test
Wild type vs. FlaBBA	0.55	64.97	0.584	Welch's t-test
FlaAAB vs. FlaB-only	8.59	98.00	1.35E-13	t-test
FlaAAB vs. FlaA-only	0.57	65.55	0.568	Welch's t-test
FlaAAB vs. FlaBA	3.43	70.97	0.001	Welch's t-test
FlaAAB vs. FlaBBA	0.09	68.75	0.932	Welch's t-test
FlaB-only vs. FlaA-only	4.19	67.07	8.38E-05	Welch's t-test
FlaB-only vs. FlaBA	-2.00	72.87	0.049	Welch's t-test
FlaB-only vs. FlaBBA	5.06	70.51	3.17E-06	Welch's t-test
FlaA-only vs. FlaBA	2.01	98.00	0.047	t-test
FlaA-only vs. FlaBBA	0.40	98.00	0.692	t-test
FlaBA vs. FlaBBA	2.54	98.00	0.013	t-test

Helix parameters: Diameter (Supplementary Fig. 6)				
Measurements				
Sample	Average (μm)	Median (μm)	SD (μm)	N
Wild type	0.57	0.58	0.05	50
FlaAAB	0.51	0.51	0.05	50
FlaB-only	0.60	0.60	0.05	50
FlaA-only	0.35	0.35	0.03	50
FlaBA	0.33	0.33	0.03	50
FlaBBA	0.37	0.37	0.03	50
Statistics*				
Combination	t	df	P-value	Test
Wild type vs. FlaAAB	-6.11	98.00	2.04E-08	t-test
Wild type vs. FlaB-only	2.44	98.00	0.017	t-test
Wild type vs. FlaA-only	-25.42	83.81	3.78E-41	Welch's t-test
Wild type vs. FlaBA	-28.18	76.30	4.45E-42	Welch's t-test
Wild type vs. FlaBBA	-22.60	83.98	1.86E-37	Welch's t-test
FlaAAB vs. FlaB-only	-8.86	98.00	3.55E-14	t-test
FlaAAB vs. FlaA-only	20.57	90.75	6.13E-36	Welch's t-test
FlaAAB vs. FlaBA	23.53	83.29	1.49E-38	Welch's t-test
FlaAAB vs. FlaBBA	17.47	90.90	8.27E-31	Welch's t-test
FlaB-only vs. FlaA-only	-29.05	85.77	3.65E-46	Welch's t-test
FlaB-only vs. FlaBA	32.10	78.15	9.18E-47	Welch's t-test
FlaB-only vs. FlaBBA	-26.16	85.94	1.08E-42	Welch's t-test
FlaA-only vs. FlaBA	2.27	98.00	0.025	t-test
FlaA-only vs. FlaBBA	3.63	98.00	4.52E-04	t-test
FlaBA vs. FlaBBA	6.17	98.00	1.55E-08	t-test

Helix parameters: Pitch (Supplementary Fig. 6)				
Measurements				
Sample	Average (μm)	Median (μm)	SD (μm)	N
Wild type	1.75	1.73	0.10	50
FlaAAB	1.66	1.67	0.09	50
FlaB-only	1.80	1.79	0.07	50
FlaA-only	1.18	1.18	0.04	50
FlaBA	1.18	1.17	0.05	50
FlaBBA	1.21	1.21	0.05	50
Statistics*				
Combination	t	df	P-value	Test
Wild type vs. FlaAAB	-4.31	98.00	3.91E-05	t-test
Wild type vs. FlaB-only	2.87	88.35	0.005	Welch's t-test
Wild type vs. FlaA-only	-37.47	65.98	3.42E-46	Welch's t-test
Wild type vs. FlaBA	-35.66	75.81	3.96E-49	Welch's t-test
Wild type vs. FlaBBA	-33.57	76.65	1.38E-47	Welch's t-test
FlaAAB vs. FlaB-only	-8.08	98.00	1.71E-12	t-test
FlaAAB vs. FlaA-only	34.48	68.92	3.37E-45	Welch's t-test
FlaAAB vs. FlaBA	32.58	79.83	7.16E-48	Welch's t-test
FlaAAB vs. FlaBBA	30.35	80.72	6.59E-46	Welch's t-test
FlaB-only vs. FlaA-only	-53.53	79.93	2.27E-64	Welch's t-test
FlaB-only vs. FlaBA	49.33	98.00	5.25E-71	t-test
FlaB-only vs. FlaBBA	-46.52	98.00	1.29E-68	t-test
FlaA-only vs. FlaBA	-0.08	98.00	0.939	t-test
FlaA-only vs. FlaBBA	3.26	98.00	0.002	t-test
FlaBA vs. FlaBBA	2.85	98.00	0.005	t-test

Helix parameters: flagellar stub length (Supplementary Fig. 5)				
Measurements				
Sample	Average (μm)	Median (μm)	SD (μm)	N
FlaA	0.94	0.91	0.29	50
FlaAA	1.53	1.53	0.43	50
FlaB	0.39	0.39	0.08	50
FlaBB	0.54	0.51	0.13	50
Statistics*				
Combination	t	df	P-value	Test
FlaA vs. FlaAA	7.95	85.57	7.01E-12	Welch's t-test
FlaA vs. FlaB	12.72	56.76	2.92E-18	Welch's t-test
FlaA vs. FlaBB	-8.75	68.38	9.08E-13	Welch's t-test
FlaAA vs. FlaB	18.09	52.50	3.26E-24	Welch's t-test
FlaAA vs. FlaBB	15.30	57.98	5.04E-22	Welch's t-test
FlaB vs. FlaBB	6.75	81.97	1.98E-09	Welch's t-test

qRT-PCR: Relative transcription level (RTL) flagellins (Supplementary Fig. 7)				
Measurements				
Sample	Average (RTL)	Median (RTL)	SD (RTL)	N
<i>flaA</i>	1.07	1.04	0.12	3
<i>flaB</i>	1.87	1.96	0.25	3
Statistics*				
Combination	t	df	P-value	Test
<i>flaA</i> vs. <i>flaB</i>	-4.12	4.00	0.015	t-test

* The color code indicates significant differences: **blue shading** = significant; **yellow shading** = not significant (Bonferroni corrected; *P*-value threshold = 0.05 divided by the number of tests).

Supplementary Table 5: Sequences of the synthetic *flaA* and *flaB* genes

Synthetic gene	<i>flaA</i> _{ECopt}
Native gene	<i>flaA</i> (Sputcn32_2586)
Modifications	The sequence was codon-optimized for <i>Escherichia coli</i> K-12 to prevent recombination with the native flagellin gene(s). Threonine 174 was substituted by cysteine for fluorescent labeling.
Sequence synthetic gene (5'-3')	ATG GCT ATT ACG GTT AAC ACG AAT GTA ACA TCT ATG AAA GCT CAA AAG AAC CTT AAC ACT AGC TCA AGC GGG CTG GCC ACT TCC ATG GAG CGT TTA TCC AGT GGC CTG CGC ATT AAC AGT GCC AAA GAC GAC GCA GCT GGC TTG GCT ATC TCC AAT CGC CTG AAC TCA CAA GTG CGC GGG TTG GAT GTG GGC ATG CGC AAC GCT AAT GAC GCA ATC TCT ATC GCG CAA ATC GCG GAA GGT GCC ATG CAG GAG CAA ACC AAC ATG CTG CAA CGC ATG CGT GAT CTG ACC GTG CAG GCG GAA AAT GGT GCG AAC TCG ACC GAT GAC CTG GAC GCA ATC CAA AAG GAA ATC GAT CAG TTA GCT GAA GAG ATC ACA GCC ATT GGC GAT AGT ACC GCA TTC GGC AAT ACT AAA CTT ATG ACT GGG AAT TTT TCT GCC GGC AAG ACC TTT CAA GTT GGG CAC CAA GAA GGT GAA GAC ATT ACC ATC AGC GTA GGC ACA AAC AAC GCC GGC AGC TTA ATG GTC AGT TGT CTT ACA ATC GCC ACA AGT GGC GGG CGT TCG ACC GCA TTG GCG GCC ATC GAT GCT GCA ATC AAG AAC ATT GAC AAC CAA CGC GCT GCT TTA GGA GCC AAA CAG AAC CGT CTG GCG TAT AAC ATC AGC AAC TCC GCA AAT ACG CAG GCA AAC GTA GCT GAC GCA AAG TCC CGT ATC GTG GAT GTT GAT TTT GCG AAG GAG ACC TCA GTA ATG ACG AAA AAT CAG GTT TTG CAA CAG ACC GGA AGT GCT ATG TTA GCC CAA GCC AAT CAG TTA CCC CAG GTG GCG CTG TCG CTT CTG GGC TAA
Sequence native gene (5'-3')	ATG GCT ATT ACA GTT AAT ACC AAC GTG ACT TCG ATG AAG GCA CAG AAA AAT TTA AAT ACG TCT AGT AGT GGT TTA GCA ACC TCT ATG GAA CGT TTA TCA AGT GGC CTG CGC ATC AAT AGC GCC AAA GAC GAC GCC GCT GGT TTA GCC ATT TCA AAT CGT CTA AAC AGT CAG GTA CGT GGT TTA GAT GTG GGA ATG CGC AAT GCT AAT GAT GCG ATC TCC ATT GCC CAG ATC GCT GAA GGT GCA ATG CAA GAG CAG ACT AAC ATG CTG CAA CGT ATG CGT GAT TTG ACT GTA CAA GCT GAA AAC GGT GCA AAT AGC ACC GAT GAC TTA GAT GCA ATA CAA AAA GAG ATC GAT CAA TTA GCT GAA GAG ATT ACT GCC ATT GGT GAC AGT ACC GCT TTT GGT AAT ACT AAA CTG ATG ACA GGG AAT TTT TCT GCG GGA AAA ACC TTC CAA GTA GGG CAC CAA GAA GGT GAA GAT ATC ACT ATT TCC GTT GGT ACC AAT AAT GCG GGG AGT TTA ATG GTT AGT ACA TTA ACG ATT GCA ACT TCA GGT GGT CGC TCT ACG GCC CTC GCA GCC ATT GAT GCG GCA ATT AAA AAT ATT GAT AAC CAA GCT GCA GCG TTA GGT GCT AAA CAA AAC CGT

	AAT ATT GAT AAC CAA CGT GCA GCG TTA GGT GCT AAA CAA AAC CGT TTA GCC TAT AAC ATC AGT AAC AGT GCT AAC ACT CAA GCA AAC GTT GCC GAT GCT AAG AGC CGT ATT GTC GAT GTC GAT TTT GCT AAA GAA ACA TCA GTA ATG ACG AAA AAC CAA GTA TTA CAA CAA ACG GGT TCT GCA ATG TTA GCG CAG GCT AAC CAA TTG CCT CAA GTT GCG CTG TCA CTA CTG GGA TAA
Synthetic gene	<i>flaB</i> _{Ecopt}
Native gene	<i>flaB</i> (Sputcn32_2585)
Modifications	The sequence was codon-optimized for <i>Escherichia coli</i> K-12 to prevent recombination with the native flagellin gene(s). Threonine 166 was substituted by cysteine for fluorescent labeling.
Sequence synthetic gene (5'-3')	ATG GCA ATT ACC GTG AAT ACA AAC GTT ACC TCC CTT AAG GCC CAA AAG AAC TTG AAC ACT TCG GCC AGC GGG TTG GCC ACA TCA ATG GAA CGC CTG TCT TCT GGC CTT CGT ATT AAC GGC GCT AAG GAT GAC GCC GCA GGG TTA GCA ATC TCC AAC CGC TTG AAT TCG CAA GTG CGC GGA CTG GAC GTC GGC ATG CGT AAC GCG AAC GAC GCG ATT TCA ATT GCA CAA ATT TCA GAA GGC GCA ATG CAA GAG CAA ACA AAT ATG CTG CAA CGC ATG CGT GAC CTG ACG GTA CAG GCC GAG AAT GGG GCG AAT AGT TCA GAC GAT CTT ACC TCC ATT CAA AAA GAA ATT GAC CAA TTA GCG CTG GAG ATC ACG GCC ATC GGG ACA AAC ACC GCA TTT GGG ACA ACT AAG TTG CTT GAT GGC ACC TTT TCG GCG GGC AAA ACT TTT CAG GTC GGA CAT CAA TCG GGT GAG GAC ATC ACG ATC TCT GTA TCG AAG ACG TGT GCG TCT GCA TTG AAG GTA GGA TCG CTG GAC ATC AAG GGT TCG GCT CGC GCC TCA GCC TTG GCA GCA ATC GAC GCT GCT ATC AAA ACG ATT GAT AGT CAA CGC GCT GAC TTG GGG GCT AAG CAA AAC CGC TTG GCG TAC AAC ATT TCC AAC TCA GCT AAC ACA CAG GCA AAC ATC TCT GAC GCC AAA TCC CGT ATC GTA GAT GTA GAT TTT GCT AAG GAA ACT AGC CAG ATG ACA AAG AAT CAG GTT TTG CAG CAA ACG GGT TCC GCC ATG TTG GCA CAG GCG AAT CAG TTG CCT CAA GTG GCA TTG AGT CTT TTA TAA
Sequence native gene (5'-3')	ATG GCC ATT ACA GTA AAC ACT AAC GTA ACA TCT TTA AAA GCA CAG AAA AAC CTA AAT ACT TCA GCG AGC GGT TTG GCC ACT TCC ATG GAA CGT TTA TCC AGT GGT CTG CGT ATT AAC GGT GCA AAG GAC GAT GCG GCA GGT TTA GCA ATT TCT AAC CGC TTA AAT AGC CAA GTC CGT GGC TTA GAT GTG GGT ATG CGT AAC GCT AAC GAT GCT ATC TCT ATC GCC CAA ATT TCT GAA GGT GCG ATG CAA GAA CAA ACT AAC ATG CTG CAA CGT ATG CGT GAC TTA ACC GTC CAA GCA GAA AAC GGT GCT AAT AGT TCA GAT GAC TTA ACG TCA ATA CAA AAA GAG ATC GAT CAG TTA GCA TTA GAA ATC ACA GCA ATC GGT ACA AAT ACG GCC TTT GGT ACT ACT AAA TTA CTT GAT GGC ACT TTC TCT GCT GGT AAG ACT TTC CAA GTA GGG CAC CAA TCA GGT GAA GAT ATT ACG ATT TCT GTG TCA AAA ACC ACT GCA TCA GCA TTA AAA GTT GGT AGT TTA GAT ATT AAA GGC TCT GCT CGA GCC TCT GCA CTG GCT GCG ATT GAT GCT GCA ATT AAA ACC ATT GAT AGT CAG CGT GCG GAT CTA GGT GCT AAG CAA AAC CGC TTA GCC TAT AAC ATC AGT AAT AGT GCT AAC ACT CAG GCC AAC ATT TCT GAT GCT AAG AGT CGT ATT GTG GAT GTG GAT TTT GCG AAA GAA ACA TCG CAA ATG ACC AAG AAC CAA GTA TTG CAA CAA ACG GGT TCT GCT ATG TTA GCC CAA GCT AAC CAA TTA CCT CAA GTG GCC TTA TCA CTG CTG TAA

Supplementary Table 6: Parameters used for the simulations

Flagellin type		FlaB		FlaA
Parameter	Description	Stretched	Coiled	Stretched
R	Helical radius	0.315 μm	0.42 μm	0.175 μm
P	Helical pitch	1.91 μm	1.43 μm	1.18 μm
L_c	Contour length	6.5 μm		
A	Bending rigidity	3.5 pN μm^2		
C	Twisting rigidity	3.5 pN μm^2		
K	Stretching stiffness	10000 pN μm^{-1}		
γ_{\perp}	Friction coefficient, normal to flagellum	2.85 η	2.80 η	3.25 η
γ_{\parallel}	Friction coefficient, parallel to flagellum	1.61 η	1.57 η	1.86 η
γ_r	Rotational friction coefficient	0.0012 η		
η	Viscosity	1 mPa s (water at 20 °C)		
h_0	Segment length	0.125 μm		

Supplementary References

1. Sun, L. *et al.* Two residues predominantly dictate functional difference in motility between *Shewanella oneidensis* flagellins FlaA and FlaB. *J. Biol. Chem.* **289**, 14547-14559 (2014).
2. Miller, V. L. & Mekalanos, J. J. A novel suicide vector and its use in construction of insertion mutations: Osmoregulation of outer membrane proteins and virulence determinants in *Vibrio cholerae* requires toxR. *J. Bacteriol.* **170**, 2575–2583 (1988).
3. W. Metcalf, University of Illinois, Urbana-Champaign
4. Fredrickson, J. K. *et al.* Biogenic iron mineralization accompanying the dissimilatory reduction of hydrous ferric oxide by a groundwater bacterium. *Geochim. Cosmochim. Acta.* **62**, 3239–3257 (1998).
5. Bubendorfer, S., Koltai, M., Rossmann, F., Sourjik, V. & Thormann, K. M. Secondary bacterial flagellar system improves bacterial spreading by increasing the directional persistence of swimming. *Proc. Natl. Acad. Sci. USA* **111**, 11485–11490 (2014).
6. Kühn, M. J., Schmidt, F. K., Eckhardt, B. & Thormann, K. M. Bacteria exploit a polymorphic instability of the flagellar filament to escape from traps. *Proc. Natl. Acad. Sci. USA* **114**, 6340–6345 (2017).
7. Venkateswaran, K. *et al.* Polyphasic taxonomy of the genus *Shewanella* and description of *Shewanella oneidensis* sp. nov. *Int. J. Syst. Evol. Microbiol.* **49**, 705–724 (1999).
8. Bubendorfer, S. *et al.* Analyzing the modification of the *Shewanella oneidensis* MR-1 flagellar filament. *PLoS ONE* **8**, e73444 (2013).
9. Lassak, J., Henche, A. L., Binnenkade, L. & Thormann, K. M. ArcS, the cognate sensor kinase in an atypical arc system of *Shewanella oneidensis* MR-1. *Appl. Environ. Microbiol.* **76**, 3263–3274 (2010).
10. Rossmann, F. *et al.* The role of FlhF and HubP as polar landmark proteins in *Shewanella putrefaciens* CN-32. *Mol. Microbiol.* **98**, 727–742 (2015).

Part III.

Discussion

1. Observing *screw thread* formation

1.1. Visualising flagella and filament behaviour

To describe and understand flagella-mediated swimming behaviour it is necessary to monitor the motion of the cell body and the behaviour of the flagellar filament simultaneously (Turner et al. 2016). The cell body is easy to image with standard light microscopy but imaging the filament can be very challenging. Although it can be several μm long, it is only about 20 nm thick and thus scatters light very weakly. In regular brightfield microscopy the flagellar filament usually is completely invisible. There are several options to visualise the filament: One is dark field microscopy, which makes very weakly scattering objects visible, but as the flagellum is right next to the very bright cell body it is usually hard to image. The same is true for non-specific fluorescent labelling in which a fluorescent dye binds any protein on the exterior of the cell. Still, these two techniques were successfully applied to describe and elucidate the *run-reverse-flick* turning behaviour of polarly flagellated bacteria (Xie et al. 2011; Son et al. 2013). However, to image the details of a complex behaviour, such as wrapping the filament around the cell body, higher spatial and temporal resolution of the flagellar filament are required.

A more defined way to image the flagellar filament is fluorescent labelling using selective chemistry to only label the filament and no other proteins on the cell surface. This can be done by introducing cysteine-encoding codons into the flagellin genes and subsequently attaching a maleimide-ligated fluorophore to the assembled filament. At room temperature, the maleimide group selectively and covalently binds to the SH group of cysteine residues but not to chemically similar groups, like OH. Conveniently, there are usually few cysteine residues in outer-membrane proteins or extracellular flagellar components. As a substitution of amino acids always bears the risk of altering the structure or function of a protein, this has to be ruled out thoroughly by immunoblotting, soft-agar spreading assays and single cell swimming analysis. Suitable amino acids for substitution are chemically related residues, such as serine or threonine, which are not located in the coiled-coil regions of the flagellins essential for polymerisation of the filament core but rather on the filament surface. For *Shewanella putrefaciens*, three serine and threonine sites that were predicted to face the surface of the assembled filament were tested. One had a clear swimming defect but the other two did not show any impairment. There was still a significant difference between these two sites in terms of fluorescent emission intensity, probably due to different accessibility of the SH group or different reactivity due to the chemical surroundings. A big help was that *S. putrefaciens* showed autofluorescence in the same emission spectrum as the dye that we used. This was crucial to image cell body and filament simultaneously. If the labelling only marks the filament it can be very hard to determine the exact behaviour of the filament in relation to the cell body. An elegant way to image both objects at the same time is the use of another fluorophore to label the cell body, usually a constitutively expressed fluorescent protein. Using a beam splitter and two cameras it is then possible to image both objects independently, but this requires a more sophisticated setup.

Why was the *screw thread* mode not observed before?

The reason why the wrapping of the flagellar filament around the cell body wasn't described and elucidated in detail before, is likely related to the limitations and challenges of filament imaging techniques. All previous observations of a flipped filament lacked spatial and temporal resolution and did neither describe nor explain the filament behaviour in sufficient detail (Buder 1915; Metzner 1920; Murat et al. 2015). The only other thorough studies on cell body and filament behaviour of polarly flagellated bacteria were done with dark field microscopy and non-specific fluorescent labelling and suffered from high intensity of the cell body (Xie et al. 2011; Son et al. 2013). A filament wrapping around the cell body would have simply not been visible at all. Behaviours that are somewhat similar to filament wrapping and *screw thread* motility have definitely been observed before (see section 3.1), however, many factors have to come together to get good spatial and temporal resolution to actually visualize what the flagellar filament is doing in relation to the cell body. Unfortunately, not all of these factors can be influenced by the researcher.

1.2. Experimental conditions and natural habitat of *Shewanella putrefaciens*

The experimental conditions are also key to observing filament wrapping. An important factor is a high load on the flagellar helix, which will be discussed in more detail in section 2.2. Under free-swimming conditions, the load and thus the torsional forces exerted on the filament might not be high enough to trigger *screw thread* formation. It is therefore possible that the *screw-like* motility was not observed before, partially because swimming is mostly studied under free-swimming conditions. We observed *screw thread* formation under different experimental conditions using standard microscopy agarose patches that are usually employed to immobilise cells. However, instead of letting the culture droplet dry, the cover slip was added before all the liquid was evaporated. This created an uneven surface on the agarose patch with varying distances to the glass cover slip (cf. Kühn et al. 2017, Fig. S1 A). Hence, in some areas of the slide the cells were able to swim freely and in other areas they were immobilised. This was intended to resemble the natural habitat of *S. putrefaciens*, comprising free-swimming as well as structured conditions. At the intersection of these two areas cells were frequently observed to get stuck and either remain stuck or to free themselves by regular backing up or using the *screw-like* movement. This experimental setup is thus very different to regularly employed, liquid-filled chambers.

The strain that we used was isolated from shale sandstone in a uranium mine (Fredrickson et al. 1998), but other strains were also isolated from putrefied butter (hence *putrefaciens*) and marine waters and sediments (Derby et al. 1931; Brettar et al. 1993; Myers et al. 1990). Many of *Shewanella's* habitats are characterised by unrestricted liquid environments as well as confined spaces. Cells can use regular, flagella-mediated swimming to navigate marine waters and larger hydrated pores of the sediment or shale sandstone, but also have to deal with narrow channels and dead ends. Studying the swimming behaviour of *S. putrefaciens* solely under free-swimming conditions would not have revealed the particular *screw thread* motility mode.

2. Formation of the *screw thread*

2.1. Characteristics of the conditions that trigger *screw thread* formation

2.1.1. Agarose-glass interface

The first condition under which we observed the filament of *Shewanella putrefaciens* wrapping around its cell body was described above (section 1.2). The cell was stuck between agarose and glass and regular backing up was not sufficient to free the cell. Why did this specific circumstance trigger *screw thread* formation? To put it in a simple way, the *screw thread* forms when the load and thus the torsional forces exerted on the filament exceed the stability of the helix. When the cell gets stuck, there are probably two factors that increase the load on the flagellum. First, the motor rotation not only rotates the flagellum but usually also counterrotates the cell body. If the cell body is stuck, it can not rotate anymore and thus the full torque of the motor is applied to the rotation of the filament. Furthermore, it was shown for *Escherichia coli* and *Bacillus subtilis* that when the rotation of the helix is inhibited or hampered, and thus the load on the flagellum increases, more stator units or different types of stators can be added to the basal body (Lele et al. 2013; Tipping et al. 2013; Terahara et al. 2017). This increases the torque that the flagellum can generate and helps move through viscous media and constricted spaces. It would also further increase the torsional forces exerted on the filament and thus facilitate *screw thread* formation.

2.1.2. Bulk liquid supplemented with Ficoll

The agarose patch setup is a great way to image *screw thread* formation of single cells in quasi two dimensions with high signal to noise ratio. This also worked reproducibly, however, finding the right spot on the microscope slide was sometimes difficult and time consuming and it didn't allow quantitative analysis. Another approach was to monitor single cells in free-swimming media that were supplemented with Ficoll 400. This allowed us to quantitatively determine the ratio of *screw thread* motility to regular backward swimming for different flagellar filament compositions in a reliable way and over several hundreds of cells. The only downside of this setup is that cells can quickly swim out of focus and the signal to noise ratio suffers in bulk liquid due to increased background light. Ficoll is a highly-branched polymer that is typically used to increase the viscosity of a medium and we imagined this to increase the load on the flagellum. However, increasing the overall viscosity should increase the forces acting on the filament and cell body by the same extent. In other words, everything should behave the same, just slower. What we actually observed was that increasing the concentration of Ficoll indeed increased the fraction of cells swimming in *screw thread* mode. The answer to this dilemma is simple: The forces acting on the filament and the cell body are actually not affected by the same extent in a solution of Ficoll. Although the viscosity is increasing at a macroscopic scale, the dissolved Ficoll polymers are not a uniform medium at the scale of a bacterium or the flagellar filament, but rather form a network of branched polymers. As such, these conditions are somewhat comparable to the agarose network, although not as dense. Ultimately, the cell body probably gets stuck or slowed down in the Ficoll network but the filament is still rotating more or less freely in the liquid between the polymer strands. The filament “sees” a different viscosity than the cell body (Martinez et al. 2014), and hence the effects are likely comparable to the cell body getting stuck between agarose and glass.

2.2. Mechanism of *screw thread* formation

2.2.1. Fundamental principle

The flagellar *screw thread* exclusively formed when the cells rotated their flagellum clockwise (CW), thus pulling the cell body backwards. This was evident from the image sequences obtained of cells being stuck as well as of cells swimming freely in Ficoll-supplemented media. Although it is not always possible to actually see the direction of rotation, it is clear that a filament that was always found to be left-handed has to rotate CW to pull the cell body. It is thus essential to image cell body and flagellum simultaneously to determine the swimming direction without doubt.

The mechanism or principle of *screw thread* formation ultimately comes down to a balance of filament stability versus the torsional forces acting on the flagellar helix. During forward swimming, with the left-handed flagellum rotating counterclockwise (CCW), the viscous drag exerts torsional forces that push the helix towards a left-handed one, which it already is. Therefore, it is a stable configuration. During backward swimming, with the left-handed flagellum rotating CW, the torsional forces push the helix towards becoming right-handed. Thus, to retain the ability to pull the cell body, the handedness and overall helix shape have to remain the same, or in other words, the filament has to be rigid enough to withstand the opposite-handed torsional forces during backward swimming. However, if the forces exceed the stability of the helix it will convert to a right-handed helix. This is exactly what we observed at the very beginning of *screw thread* formation: The flagellar helix unwinds because of the opposite-handed torsional forces and starts to convert to a right-handed helix, which is not completed because of the filament's rigidity (Kühn et al. 2017, Fig. 4). The images obtained from the fluorescently labelled filaments only resolve the transition from a partially unwound left-handed helix to a partially right-handed one to some extent (cf. Kühn et al. 2017, Fig. S2, panels 5-8), but the simulation, which reproduced the overall behaviour very well, clearly shows a partially right-handed helix at the base of the filament (cf. Kühn et al. 2017, Fig. 4 panel two, bottom row). The simulation further suggests that the forces acting on the filament are now pointing towards the cell body and thus the whole filament moves towards the cell. As the motor continues to rotate CW, the filament gets wrapped around the cell body and now, with the filament flipped over, the configuration is very similar to a left-handed helix rotating CCW but attached to the top of the cell rather than the bottom (cf. Fig. 4 A and 6 A). In this configuration the motor is still rotating CW from behind the cell (from top to bottom; Fig. 6 A), but if one looks from the tip of the filament towards the base of the filament (from bottom to top), the helix is rotating CCW around the cell body. Hence, the torsional forces acting on the filament in *screw thread* configuration once again push it towards a left-handed helix, which it already is. The formation of the flagellar *screw thread* can thus be seen as a way to evade the strain that is put on the filament by the opposite-handed torsional forces during backward rotation under high load. Once the filament is in *screw thread* mode, CW rotation of the left-handed helix (seen from behind the cell) is stable as long as the direction of rotation does not change.

2.2.2. Additional factors that facilitate *screw thread* formation

There are two more factors that likely facilitate flipping over and wrapping of the filament around the cell body. The first one is the characteristic of the flagellar helix to adopt different polymorphic forms when mechanical stress is exerted on the helix. From the geometrical parameters that we determined for the regular helix and the helix in *screw thread* mode, it is reasonable to assume that it regularly adopts the *normal* polymorphic form with

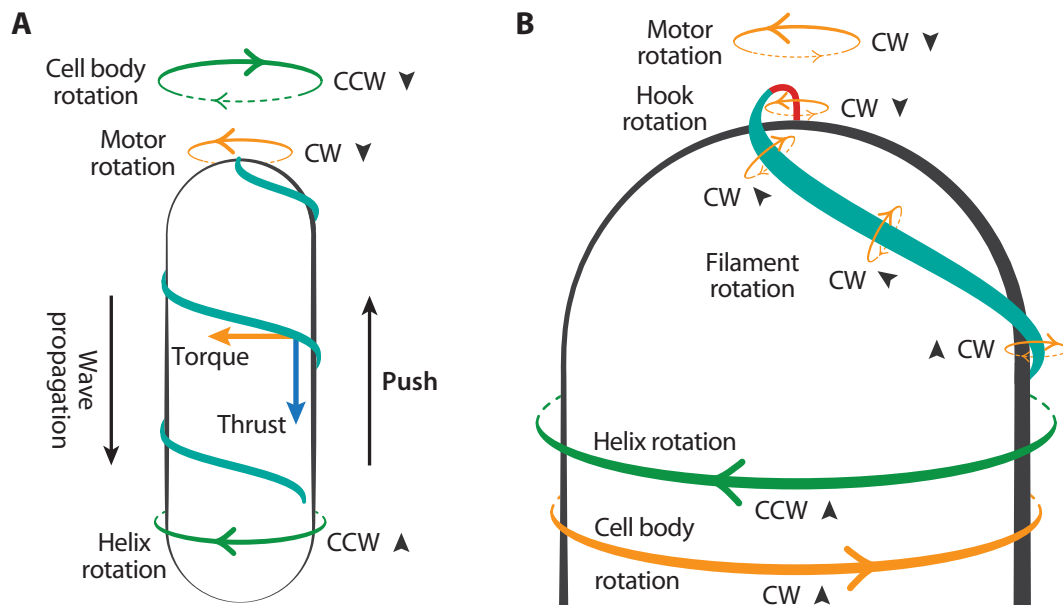


FIGURE 6. Overview of the flagellar filament configuration and rotation in *screw thread* mode. Note that flagellar rotation is generally referred to as counterclockwise (CCW) or clockwise (CW) seen from the tip of the filament towards its base. This is fine as long as the filament points away from the cell body, but it becomes problematic and confusing when the filament flips over, because the direction of rotation inverts when referred to from tip to base. The motor rotation remains the same and it is here always referred to from outside the cell towards the cytoplasmic part of the basal body (cf. Fig. 1). To make this clear, the viewing direction is always indicated by arrow tips. **A** As the cell is swimming backwards (from bottom to top), the motor rotates CW when seen from behind the cell. *Behind*, in this case, is still viewing towards the surface of the flagellated pole (from top to bottom). During regular backward swimming the filament would rotate CW as well, pointing away from the cell body towards the top. Here, the filament is flipped over and the helix rotates CCW around the cell body when viewed in swimming direction or from filament tip to base. The overall mechanism of thrust generation is thus very similar to a cell swimming forwards regularly, just with the filament attached at the top (cf. Fig. 4 A). In this configuration the filament is pushing the cell body backwards and the torsional forces exerted on the filament due to viscous drag are acting in the same handedness that the helix already adopts. Hence, this configuration is stable as long as the motor rotates CW. **B** In *screw thread* motility mode the CW rotation of the motor is transferred to the hook and filament which therefore also rotate CW seen from filament tip to base. However, from the same viewing direction (bottom to top), the flagellar helix rotates CCW around the cell body, which in turn counterrotates CW. This means that the flagellar filament moves CCW around the cell body but internally rotates CW. Thus, the filament can't roll over the cell body and has to move over the cell surface in a certain distance.

a 9:2 ratio of L- and R-type flagellins and the *coiled* form with a ratio of 8:3 in *screw thread* mode (cf. Fig. 3). The geometry doesn't exactly reflect the geometry of polymorphs observed for *Escherichia coli* or *Salmonella enterica*, but the overall shapes and shape transitions are similar. Polymorphic forms are characterised by a local minimum in free energy and hence, adopting a different polymorphic form in *screw thread* mode is energetically favoured over the intermediate state (i.e. the unwound helix that is pushed towards a right-handed helicity). This hypothesis is supported by the numerical simulation, which shows formation of the *screw thread* at lower motor torque when a separate *coiled* polymorph with a local energetic minimum is introduced.

The second factor that might facilitate *screw thread* formation in polarly flagellated bacteria is the dynamic flexibility of the hook, which was suggested to be essential for the *run-reverse-flick* turning mechanism (Son et al. 2013). During CCW forward rotation, the hook is rigid and points the filament away from the cell body. During CW backward rotation however, the hook becomes flexible and buckles as the motor goes back to CCW forward rotation. This allows the filament to flick, which turns the cell body. In case of the *screw thread* formation, the flagellum also rotates CW and thus the hook becomes flexible. It is reasonable to assume that during continued CW rotation the flexible hook allows the filament to flip over and wrap around the cell body.

2.3. Characteristics of the *screw thread* motility at sub-microscopic scales

2.3.1. Relative movement of filament and cell body

The image sequences of the *screw thread* motility show a flipped over and wrapped up filament that is rotating closely around the cell body. This can be clearly seen, but what can not be seen is the rotation of the cell body, the intrinsic rotation of the filament around its own axis (not the helix axis) and the actual distance of the filament to the cell's surface. This is simply due to the spatial resolution being limited by the wavelength of light. However, a reasonable behaviour can be deduced from what is known from regular swimming.

First of all, the flagellar motor rotates around the rod axis, which is perpendicular to the cell envelope. The rotation of the rod is further transferred to the hook and the filament which makes the overall helix rotate around its central axis. In case of polarly flagellated bacteria the axis of the helix is usually aligned with the cellular length axis. If you consider only a short segment of the hook or the filament, it additionally rotates around its own filament axis, although it is unclear to what extent. If you follow the intrinsic rotation of hook and filament it becomes clear that the filament can't roll over the cell body in *screw thread* mode. This is illustrated in Fig. 6 B, in which the visible surface of the cell body moves to the right (CW viewed from the bottom) and the helix moves to the left (CCW viewed from the bottom). The flagellar helix and the cell surface have to move in opposite directions because of the cell body's counterrotation. Furthermore, if there is considerable intrinsic rotation of the filament at all, it is in opposite direction to the cell surface movement as well. Hence, the helix can't roll over the cell body and the distance must be high enough to not stick to the cell surface. As already mentioned, most image sequences were obtained using strains that are deleted for the lateral flagellins to focus only on the polar flagellar filament. Fluorescent microscopy with labelled polar and lateral filaments (in this case an extremely short lateral filament stub) did in fact reveal the counterrotation of the cell body in *screw thread* mode (data not shown).

2.3.2. Universal joint function of the hook

The flagellar hook essentially works as a universal or Cardan joint: It converts the angular rotation of the basal body to the angular rotation of the filament (Samatey et al. 2004). The hook filament must therefore change the protofilament state on the short curve of the hook constantly. The hook can also rotate as a whole around the basal body axis, perpendicular to the cell surface. This might not happen when the basal body is at a lateral position of the cell, like in peritrichous bacteria, but certainly when it is at the cell pole, like in polarly flagellated bacteria. The extent of this overall hook rotation, however, is not known. In other words, it is not clear if the hook works as a perfect Cardan joint or if some of the torque that the motor generates is applied to rotate the hook as a whole. In our simulation, the formation of the *screw thread* was only observed when the torque applied by the motor was split into a component parallel to the filament (representing how well the Cardan joint works) and a component parallel to the motor axis (which makes the hook rotate as a whole). This indicates that in fact the hook might not be a perfect Cardan joint and some of the torque is applied to the overall rotation of the hook. Recently, a similar behaviour of the hook was suggested for *Salmonella enterica* when the cells get stuck: The hook would switch to a "locked" mode in which it rotates as a whole and thus realigns the helical filament to point in the opposite direction and push the cell out of the dead end (Duchesne et al. 2017; Fig. 4 illustrates the two rotation modes of the hook very well).

2.3.3. Screw-like movement during free swimming

During swimming in unrestricted bulk liquids wild-type cells rarely formed *screw threads* unless the medium was supplemented with Ficoll (Kühn et al. 2017, Fig. 3 A). The increased viscosity slowed down the overall swimming speed of the cells to about 16 $\mu\text{m/s}$ on average, both for regular forward and backward swimming (Kühn et al. 2017, Fig. 3 B). Movement in *screw thread* mode under these conditions was significantly slower with the cells moving only at about 5 $\mu\text{m/s}$ on average, which is barely above the background motion due to Brownian motion and general drift. So in bulk liquids, movement in *screw thread* mode is apparently less efficient than regular swimming. The most obvious difference between these swimming modes is the distance of the flagellar helix to the cell body. Furthermore, the geometry of the helix also changes when wrapping around the cell body with the diameter increasing and the pitch decreasing (cf. Kühn et al. 2017, Table S4). Both of these differences might contribute to the reduced propulsion efficiency of the *screw thread* mode in bulk liquid.

A recent study calculated the propulsion efficiency of a microswimmer driven by a helical propeller, depending on the shape of cell body as well as of the flagellar helix. The study doesn't indicate well which absolute helix geometry is more efficient, but obviously any deviation from the optimal helix geometry, i.e. diameter and pitch, reduces the propulsion efficiency (Bet et al. 2017). Although, it is not clear if the regular, wild-type helix geometry is actually the optimal one, increasing the helix diameter and reducing the pitch could very well decrease propulsion efficiency. This was in fact observed for *Thiospirillum jenense* in an early study (Schneider et al. 1974), however, it was not quantified due to limits of the imaging technique.

The proximity of the flagellar helix to the cell body in *screw thread* mode probably affects the propulsion efficiency to a greater extent than the flagellar shape. At low Reynolds numbers viscous drag is the dominant force and it becomes more difficult to move water as one approaches a solid surface, like the cell body (Shapiro 1961; Blake et al. 1974; Sleight 2005). Thus, the flagellar wave is less effective near the cell surface, because water propulsion is restrained by the hydrodynamic interference with the cell body (Higdon 1979; Sleight 2005). This results in the flagellar helix rotating around the cell body without efficient translocation (cf. Kühn et al. 2017, Fig. 2 B). The flagellar wave mostly stirs the liquid in the "no-slip" boundary layer of the cell, but does not produce significant thrust. In regular swimming mode the flagellum points away from the cell body and most of the helix rotates outside the boundary layer, thus providing thrust properly.

2.3.4. Screw-like movement in confined spaces

In a confined space, for example between agarose and glass, the flagellar helix was observed to maintain a fixed overall location relative to the cell's surroundings and to only slide along the filament's internal axis (Kühn et al. 2017, Fig. 2 A). This means that the rotation of the flagellum is most efficient as one full turn moves the cell body by one wavelength. It does, however, not mean that this movement is very fast. The flagellar rotation is much slower than during regular swimming and thus the cell moves very slowly, but without slip of the flagellar helix. If regular reversing is not strong enough to move even a bit, this mode might at least allow for slow translocation at all. Furthermore, it is very unlikely that the flagellar filament moves only in the remaining liquid surrounding the cell body as it would result in a similarly inefficient (i.e. with a lot of slip) movement as in bulk liquids. Hence, the filament probably interacts with asperities of the surface of the agarose patch and thus pushes against a solid object in contrast to only stirring the liquid envelope around the cell body. As the solid agarose does not move under the force of the flagellar wave, the cell translocates very efficiently. Similar to

the filament moving over the cell surface in *screw thread* mode, there must be a certain distance between the filament and the agarose, otherwise the filament would stick to it and immobilise the cell. A thin layer of liquid is probably always covering the filament surface, preventing direct contact to the cell body or any other surface. The thickness of this aqueous film and the surface interaction of the filament in general might be affected by the glycan modifications that are also found on the filament surface of *S. putrefaciens*. Unfortunately, these modifications are essential for a functional flagellum, so the influence of the filament surface properties on surface interaction can't be studied in an easy way.

3. Examples of filament wrapping in other species

3.1. Similar behaviours observed before

Flagellar filaments that flip over and rotate around the cell body have been observed before, since a very long time actually (cf. part I section 4.2). Flagella of the lophotrichous bacterium *Thiospirillum jenense* as well as the leading flagella of bipolarly flagellated *Spirillum volutans* always flip over when the flagella are pulling the cell body (Buder 1915; Metzner 1920). Pulling flagella of lophotrichous *Pseudomonas syncyanea* and amphitrichous *Magnetospirillum magneticum* were found to flip over only sometimes (Reichert 1909; Murat et al. 2015). Although the spatial and temporal resolution of these observations did not allow detailed characterisation of the filament behaviour it is obvious that the filaments are not as close to the cell body as during the *screw thread* formation of *Shewanella*. They rotate around the cell body at a clearly visible distance and the blurry shape of the rotating flagellum was consistently described as a hemisphere ("umbrella" or "parachute"). Furthermore, the flipping of the filament was observed during free-swimming conditions and it is not clear how the filaments would behave in confined spaces, i.e. if they would wrap around the cell body in a similar *screw thread* shape and provide the same benefit as in *Shewanella putrefaciens*.

The mechanism how the flipped-over configuration is formed, on the other hand, is very likely identical to the mechanism of *screw thread* formation, as the filament only flipped over during pulling mode and the same physical principles apply: The viscous drag exerts opposite-handed torsional forces on the backwards rotating filaments, which unwinds the filaments and the torsional strain makes the filament move towards the cell body and flip over. In this flipped-over configuration, not matter if close to the cell body or further away, the backwards rotation is stable as the viscous drag now exerts forces on the filament in the same handedness.

3.2. *Screw thread* formation in other bacteria

In the past two years, filament behaviours that are most comparable to the *screw thread* formation of *S. putrefaciens* were reported for four more bacterial species, all of which are polarly or bipolarly flagellated but with varying numbers of flagella. Filament wrapping in *Burkholderia* sp. RPE64 and *Aliivibrio fischeri*, reported in Kinoshita et al. 2017, was probably discovered at a similar time as our observations on *S. putrefaciens* and the characteristics of the filament behaviour are mostly comparable. In the same year, Hintsche et al. published that *Pseudomonas putida* also wraps its filament bundle around the cell body during backward swimming (we contributed to this observation by constructing the cysteine-modified strain). Finally, in 2018 Constantino et al. reported the filament-wrapping behaviour for bipolarly flagellated *Helicobacter suis*. These

filaments are all wrapping closely around the cell body, resembling a *screw thread*, which distinguishes these observations from the hemisphere shape reported before. All of these filament behaviours are very similar to the *screw thread* formation of *Shewanella*, however, there are some differences. The most striking difference, and that is true for many of the other flipped over or *screw*-like behaviours, is that both stable backward rotation as well as flipping and wrapping of the filament works just as well for multiple flagella as it works for only one flagellum. It is quite difficult to imagine how the filaments manage to not get entangled during backward rotation or wrapping up.

***Burkholderia* and *Aliivibrio fischeri* (Kinosita et al. 2017)**

The image sequences of *Burkholderia* show that its two to three polar flagella rotate as a bundle during CCW rotation but more or less independently during CW rotation when the filaments wrap around the cell body. Once wrapped up, the filaments realign and the bundle reforms, indicating that the bundle is only stable during pushing mode, with the waves propagating from filament base to tip. The sequence of the wrapped-state formation is similar to *S. putrefaciens*: The filaments rotate clockwise and partially convert into a right-handed helix very clearly. During the wrapping process the filaments already adopt the coiled state, which for *S. putrefaciens* was only observed clearly when the filament was already wrapped around the cell body. This indicates the same underlying mechanism, however, the filaments of *Burkholderia* and *A. fischeri* always flipped over when rotating CW, independently of the medium viscosity. Together with the much more clearly observed right-handed conversion, this indicates that the flagellar helix is less stable to *screw thread* formation than in *Shewanella*, which mostly shows stable backwards rotation in regular medium. *Screw*-like movement of *Burkholderia* was also observed on a glass surface, which demonstrated a similar filament-surface interaction with the overall waveform remaining static relative to the surface and the filament only sliding along its internal axis. This provided enough thrust to move the cells over the surface without getting stuck. The overall movement speed in *screw thread* mode was found to be significantly reduced compared to regular forward swimming regardless of the medium composition and viscosity, indicating the same inefficiency of propulsion in bulk liquid with the wrapped up filament.

***Pseudomonas putida* (Hintsche et al. 2017)**

Pseudomonas putida is able to swim forward by rotating its left-handed polar flagellar tuft in a counterclockwise direction and to swim backwards by rotating it clockwise (Harwood et al. 1989). Backward motion was already known to occur in two different speed levels and the image sequences reported in Hintsche et al. 2017 revealed that the fast backward swimming is correlated to a stable puller configuration, with the flagellar tuft being extended from the cell body, and the slow backward swimming is correlated to the filament wrapping around the cell body and moving in *screw thread* mode. Similar to *Burkholderia* and *A. fischeri*, the *screw thread* formed frequently in regular medium without increased viscosity, but not always during backward swimming. The authors hypothesised that rotating several flagella CW already increases the mechanical stress, so that the viscous drag of regular medium is sufficient to induce the filament instability. This implies that bacteria with multiple flagella at one or both poles are generally more likely to flip their filaments over. However, *A. fischeri* with one or two flagella also frequently switches to *screw thread* mode in regular medium and *C. okenii* with several flagella was not found to flip its filament over (Kinosita et al. 2017; Buder 1915). A more systematic and quantitative approach would have to be conducted to study the influence of flagella number on bundle stability.

The flagellar bundle of *P. putida* flipped over during CW rotation, indicating the same torsional-stress-induced mechanism as in *Shewanella*, however, the switch to *screw thread* mode did not occur when switching to backward rotation but rather during backward rotation. This indicates an increase in motor torque prior to *screw thread* formation. Similar to *Burkholderia*, the filaments of *P. putida* were found to unbundle when wrapping around the cell body and reform the bundle when in *screw thread* mode. Because the forces exerted by the flagella during *screw thread* formation are not simply aligned with the cellular axis anymore, the wrapping can turn the cell body in a random direction. We also frequently observed the cell body of *Shewanella* realign during *screw thread* formation or release. Therefore, *screw thread* formation can also be considered another possible turning mechanism for polarly flagellated bacteria, which is induced by a switch in motor rotation or a change in motor torque.

***Helicobacter suis* (Constantino et al. 2018)**

Finally, the four to ten sheathed flagella of *H. suis* were also found to wrap around the cell body, both in regular medium as well as in increased viscosity (Constantino et al. 2018). The flagellar tufts are inserted at both poles and during smooth swimming (forward and backward are indistinguishable) the leading bundle flips over and pushes in the same direction as the lagging flagella, which rotate extended away from the cell body. In contrast to the observations in Murat et al. 2015, the filament bundle was clearly rotating close to the cell body, similar to the *screw thread* mode of *Shewanella*. The wrapping was observed to occur very likely when the sense of motor rotation and swimming direction inverted, indicating the same mechanism as in *Shewanella*. During the wrapping process, the authors didn't see individual filaments unbundle and rebundle after wrapping was complete, like observed for the lophotrichous *screw thread* formers. However, the image sequences were obtained with phase contrast microscopy that can only resolve the flagellar bundle consisting multiple flagella, but not a single filament alone. It is thus possible that unbundled flagella were simply not visible. Unfortunately, the flagellar bundle is easily overshadowed by the cell body and detailed analysis of the filament behaviour is difficult with this technique. Thus, some of the observations reported in Constantino et al. 2018 pose a lot of questions, especially the image sequences (Movie S1, Constantino et al. 2018), which show a flagellar bundle rotating in *screw thread* mode but with the waves propagating from the filament tip to the filament base, like during CW rotation of the extended filament or filament bundle. This was not observed in any of the other *screw thread* formers and should not be a stable configuration. The images do not allow clear determination of the filament's handedness or sense of rotation and it is thus difficult to deduce how this configuration was formed. However, it shows clearly that not every aspect of filament-wrapping is yet understood.

Similar to *Magnetospirillum magneticum* (Murat et al. 2015), the opposite flagella were observed to sometimes adopt the same configuration, either both extended or both wrapped. The double-extended configuration was not observed in increased viscosity, supporting that increased load on the flagella induces filament flipping and wrapping. The cells move erratically in these two configurations, probably because both filament bundles push or pull in opposite directions. This doesn't propel the cell body efficiently in one direction but rather induces cellular realignment and slow movement in a random direction. This confirms the observations of Murat et al. 2015 that *M. magneticum* tumbles when both flagella are in "tuft" or both in "parachute" configuration.

3.3. General distribution of filament wrapping

Taken all these observations together, the filament wrapping is very likely a widespread behaviour that could potentially apply to any polarly flagellated bacterium. Whether the filament rotates in a stable puller configuration or gets unstable and flips over depends only on the forces exerted on the flagellar helix and the filament stability. A very stable helix would not flip over very easily and a very flexible helix would convert to the opposite handedness rather than flipping over. The distinct filament properties, like rigidity or polymorphic shapes, might further influence the shape of the flipped-over configuration, but no matter if “umbrella”, “parachute” or *screw thread*, the scheme and mechanism is very similar.

Interestingly, the examples given above cover a wide range of bacteria from different habitats: *S. putrefaciens* and *A. fischeri* are marine bacteria, which can also colonise animals as a pathogen or symbiont, respectively. *P. putida* is a soil bacterium, *Burkholderia* is an insect gut symbiont and *H. suis* colonises the stomach epithelium similar to *Helicobacter pylori*. What they all have in common is that they navigate structured or viscous environments and the filament wrapping most likely facilitates movement in these habitats.

Behaviours described in the literature that indicate *screw thread* formation

All of the observations of movement in *screw thread* mode clearly show a significantly reduced swimming speed. For *Shewanella* the drop in swimming speed is so pronounced that it almost looks like the cells stop for a moment when reversing and then switch back to forward swimming. This exact behaviour was also mentioned in an early publication about the *run-reverse* swimming of polarly flagellated *Pseudomonas citronellolis* (Taylor et al. 1974). The flagellar filaments were not visualised, but with the new insights into the behaviour of polar flagella it seems reasonable that the filaments of *P. citronellolis* may also flip over and wrap around the cell body.

The same is true for *Pseudomonas fluorescens*, which has one or two flagella inserted at one pole and was found to change swimming speed during reversals (Ping 2012), similar to *P. putida*. Furthermore, a sophisticated “hovering” mode was described with the cell body still rotating but not moving significantly. The image sequences even indicate that the switching occurs during motor reversals. This resembles the switching to the slow *screw thread* mode in bulk liquid very closely.

An earlier publication on *P. putida* using dark-field microscopy described the filament bundle disappearing during reversals (Harwood et al. 1989), which can now clearly be correlated to the filaments wrapping around the cell and thus being outshone by the bright cell body.

4. Benefit of *screw thread* formation

4.1. Navigating structured environments

We observed *screw thread* formation of *Shewanella putrefaciens* frequently when cells got stuck between agarose and glass and the back-up motion resembled a screw being driven into a solid medium without slip of the helical filament or screw thread, respectively (cf. section 2.3.4). On the other hand, the *screw thread* mode did not propel the cells efficiently in bulk liquid because the flagellum rotated with a lot of slip, resembling a

screw inefficiently being driven into a soft medium (cf. section 2.3.3). The same was observed for *Burkholderia* sp. RPE64 in bulk liquid and for motion over a glass surface. Accordingly, the swimming speed of the other *screw thread* formers was found to decrease significantly when wrapping the filament in bulk liquid. Based on these observations, we and others postulated that the *screw*-like movement is mostly advantageous in structured environments when cells are trapped in a dead end or need to get through confined spaces or viscous media. These are conditions that the known *screw thread* formers in fact encounter in their natural habitats. This is a reasonable hypothesis, however, it was only observed for single cells and it is not clear how cells would behave in confined spaces (e.g. how fast they would move) in regular swimming mode under the same conditions. Our experimental setup simply does not allow a detailed characterisation of the cell's surroundings, like the height of the channel or the force by which the cell is trapped. Similarly, it is not clear if cells under *screw-thread*-inducing conditions, other than in viscous bulk liquid, are faster in regular or in *screw thread* mode. Quantitative experiments in chambers with a defined height or a defined decrease in height are also difficult, because every cell has a different diameter and it is simply not clear how the exact conditions for individual cells are. Quantitative measurements on single-cell level in structured environments are thus very difficult. As a consequence, unequivocally proving the benefit of the *screw thread* motility in structured environments requires a population-wide and quantitative assay with cells that can form the *screw thread* and cells that can't, but are otherwise identical. This ideal mutant is basically impossible to obtain, but a mutant with robust, ideally wild-type-like swimming in bulk liquid, would also do.

With the FlaA-only strain we had such a mutant: It produces a flagellar filament exclusively consisting of FlaA flagellin with almost wild-type length but a different helix geometry. Most importantly, cells were never found to switch to *screw thread* mode, regardless of increased viscosity or being stuck between agarose and glass, but they retained robust swimming in bulk liquid. This mutant showed a strongly decreased spreading radius on soft-agar plates compared to strains with a wild-type filament (FlaA and FlaB) or a filament exclusively composed of FlaB flagellin. On the scale of *S. putrefaciens*, the agar appears like a filamentous network of agarose polymers forming large, water-filled pockets, constricted channels and dead ends. There are several factors that influence how well the cells can navigate through this network and spread radially from the point of inoculation. An obvious one is swimming speed, but other properties of navigation, like run times (the time between motor reversals), turning angle and the ability to get through confined spaces and escape from dead ends can strongly affect the spreading capabilities as well. For example, a *che* mutant that is unable to reverse the motor rotation does not spread well in soft agar because cells get stuck irrevocably. In order to verify that the strong defect in spreading of the FlaA-only mutant was only, or at least mostly, due to the defect in *screw thread* formation, we had to determine the other swimming parameters.

As the flagellar filaments of wild-type, FlaA-only and FlaB-only are composed of different flagellins or flagellin proportions it is not surprising that the free-swimming properties differed between the strains (cf. Kühn et al. 2018, Fig. 3). However, the differences that we measured did not correlate at all with the spreading capabilities in soft agar (cf. Kühn et al. 2018, Fig. 1). For example, FlaA-only cells, with a strong defect in spreading, were swimming faster than FlaB-only cells with wild-type-like spreading, regardless of viscosity. Furthermore, the turning angles of FlaA- and FlaB-only showed a very similar distribution under both free-swimming conditions (high and low viscosity), but were significantly different than the wild-type turning distribution, especially under high viscosity. This clearly demonstrates that the impaired spreading of the FlaA-only mutant can not be addressed to the general differences in swimming. The observed *screw thread* formation behaviour, on the

other hand, perfectly correlates with the spreading capabilities. The FlaBA-mutant, with inverted flagellin segments, is also in line with this, however, it shows an even stronger deviation from the wild-type free-swimming behaviour, which likely influences the spreading additionally in a significant but not easily determined way.

4.2. General benefits for swimming motion

Hintsche et al. suggested that the slow-swimming phases when reversing in *screw thread* mode also increase the spreading capabilities in bulk liquid (Hintsche et al. 2017). This is only based on a numerical model, because an experimental population-wide spreading assay in bulk liquid, similar to the soft-agar assay, is technically impracticable, at least for the time being. This might be possible in the future with more advanced tracking microscopes. Still, this simulation suggests that *screw thread* formation is beneficial even during free swimming, which is in contrast to our observations that *S. putrefaciens* does not switch to *screw thread* mode in bulk liquid of normal viscosity very frequently. We argued that the *screw thread* motility does not provide an advantage during free swimming, because it is inefficient. However, these two observations and suggestions are not mutually exclusive, because even if slow phases in *screw thread* mode do increase spreading in bulk liquid, it might not be beneficial in general for all bacteria. This was in fact suggested for *Vibrio alginolyticus* and *Pseudoalteromonas haloplanktis*: Although their diffusivity, i.e. the spreading or exploration capability, is reduced compared to *Escherichia coli*, they accumulate near ephemeral nutrient patches more effectively (Stocker et al. 2008; Stocker 2011; Xie et al. 2011). It is thus possible that some bacteria, such as marine *S. putrefaciens*, suppress *screw thread* formation in bulk liquid not because it is an inefficient mode of swimming, but rather because they don't benefit from increased spreading that comes with introducing slow phases of swimming. In conclusion, the simulation of Hintsche et al. and the different stabilities to *screw thread* formation among the *screw thread* formers indicates that the *screw thread* motility mode does provide benefits in various environments, however, not generally in every environment and in the same way for all bacteria.

5. The two flagellins of *Shewanella putrefaciens*

5.1. Similarities and differences of FlaA and FlaB filaments

5.1.1. Helical shape

The flagellar filament of *Shewanella putrefaciens* is composed of two different flagellin segments, the proximal FlaA segment and the distal FlaB segment. The two flagellin proteins are highly similar at the amino acid level with about 86 % identity. Still, a filament exclusively composed of FlaA shows a very different helical shape, with the diameter reduced to about half and the pitch reduced to about two thirds of the wild-type helix (cf. Kühn et al. 2018, Fig. S6). The helix geometry of a FlaB-only filament is almost identical to the wild type filament. Most differences of the sequence are located in the central, variable region, located in between the two fragments of the D1 domain (cf. Fig. 2 A and Kühn et al. 2018, Fig. S1). This domain is particularly short in *S. putrefaciens* and can hardly be described as a distinct D2 domain as in *Salmonella enterica* or *Pseudomonas aeruginosa*. It is unlikely that the differences in this domain account for the different helix geometries as the residues are likely exposed to the surface and do not participate in the flagellin-flagellin interactions. Much more likely, the geometry-determining residues are located in the D0 or D1 domains as they are forming the central channel

and core of the assembled filament and both lateral and longitudinal flagellin interaction are known to be mediated by these domains (cf. Fig. 2).

Helical shape and polymorphic forms

Different shapes of the flagellar helix can be due to different polymorphic forms, depending on the ratio of L- and R-type protofilaments (cf. Fig. 3). The regular shape of the wild-type and FlaB-only filament is most similar to the *normal* polymorphic form with a ratio of 9:2, although not exactly the same. The shape of the wrapped filament in *screw thread* mode fits well to the *coiled* polymorphic form with a ratio of 8:3. The different shape of the FlaA helix also could be due to the FlaA filament simply adopting a different polymorph as a regular state, because the differences in the D0 and/or D1 domain could change the flagellin-flagellin interactions and could thus make a different polymorphic form more favourable. However, the only other helical, left-handed polymorph is the hyperextended form, which doesn't resemble the FlaA shape at all. The regular shape of the FlaA-only filament most closely resembles the shape of the *curly I* polymorph with a ratio of 6:5, however, this is supposed to be a right-handed helix and the FlaA filament was clearly determined to be left-handed. This challenges the idea of the FlaA filament shape being a different polymorphic form.

Furthermore, I occasionally observed another polymorphic form of the wild-type filament, probably during forward rotation, which was characterised by a very wide diameter, even wider than the helix in *screw thread* mode, and a very small pitch around 0.5 μm (data not shown). Such a coiled state with a very small pitch was sometimes also seen wrapped around the cell body. This raises two possible explanations: First, the fundamental shapes that can be achieved with different ratios of L- and R-type flagellins are very different in *Shewanella*, especially concerning left- and right-handed helicity. The observed shapes of the flagellar helix do not fit well with the current general model of polymorphism, but to be more certain one would have to investigate the flagellar polymorphism of *Shewanella* more thoroughly. Secondly, the differences in FlaA flagellin-flagellin interactions change the basic shape of the known polymorphic forms. The latter option seems more likely as it allows the same fundamental principles to apply for *Shewanella* as for other bacteria. However, not much is known about protofilaments and polymorphism beyond the paradigmatic enteric bacteria *Salmonella* and *E. coli*. Although it is likely that most bacteria follow the paradigm and have eleven protofilaments, this was only determined for a few bacteria and *Campylobacter jejuni* was actually found to have only seven (Galkin et al. 2008). Different helix geometries could be explained by different polymorphs but the more simple explanation would be a modified basic shape of the known polymorphs. For the FlaA-only filament this would mean that it also adopts the *normal* polymorph with a 9:2 protofilament ratio, but with a modified basic geometry.

5.1.2. Posttranslational modification

Role of glycosylation for filament properties

In addition to the different amino acid sequence, the flagellins are differently modified by glycosylation, which results in higher molecular mass of FlaA compared to FlaB. Deleting genes that are essential for glycosylation resulted in non-functional flagella and the two flagellins showed the same molecular mass in immunoblot analyses. Although we didn't study the glycosylation in detail, a previous study on the close relative *Shewanella oneidensis* determined the exact amino acid residues that are modified (Bubendorfer et al. 2013). Five serine residues in FlaA and FlaB were found to be glycosylated, four of those located in a region likely exposed on

the surface of the assembled filament. Deletions that abolished the ability to modify the flagellins lead to a loss of the filament, indicating an essential role for export, polymerisation or structural integrity of the filament. The molecular mass of FlaA and FlaB is the most obvious difference, but the distinct glycosylation might also influence various other parameters of the filament, including shape, rigidity and surface properties. However, as we can not modify or delete the glycosylation machinery this is difficult to study. If the glycosylation in *S. putrefaciens* is similar to *S. oneidensis* and the modified residues are mostly located on the surface of the flagellum, the influence on the helical shape is questionable, because it is mostly determined by the interactions of the residues in the D0 and D1 domains. One of the serine to cysteine substitutions in FlaB, S168C, in fact had a significant defect in spreading in soft-agar. This might have substituted a serine residue that is usually glycosylated. Determining the flagellar helix and swimming parameters of this mutant in detail might shed more light on the role of glycosylation on filament structure and motility in *S. putrefaciens*.

How are the two flagellins modified individually?

The different glycosylation of the flagellins is probably achieved by a sequence-specific glycosylation machinery. As our results suggest that the flagellins are temporally regulated, with FlaA being produced before FlaB, a similar temporal regulation could explain the different extent of modification. However, disturbing the native regulation of the flagellins, i.e. putting *flaA* under the control of the *flaB* promoter, does not change the molecular mass of FlaA and hence the glycosylation is probably not affected by FlaA being produced later. Furthermore, when FlaA is produced from the *flaB* promoter or when it is overproduced from a plasmid, a band of the expected mass of non-glycosylated flagellin appears in the immunoblot analysis, which suggests that the glycosylation machinery is not adapted to handle large quantities of FlaA, but large quantities of FlaB. This further supports the hypothesis that there are, at least partially, specific posttranslational modification machineries for FlaA and FlaB.

5.2. How can the different stability to screw thread formation be explained?

The most prominent phenotypic difference between filaments exclusively composed of FlaA or FlaB is the different stability to *screw thread* formation. This is a very pronounced difference as FlaB filaments already wrapped around the cell body in about half of all observed reversing events in regular medium while FlaA filaments were never observed to do so even at high viscosity. Because FlaA has a higher molecular mass, our first hypothesis was that the FlaA filament is more stable because it is more rigid, possibly caused by the extended glycosylation. A more rigid filament would withstand higher twisting, bending or stretching and compressing forces and thus be able to better resist the torsional forces during backward rotation. Unfortunately, we have no information about the rigidity of FlaA and FlaB filaments. This could be measured by attaching flagellin-antibody-coated beads to the ends of the filaments and pulling on the beads using optical tweezers. Finding the rigidity-determining factor would require a much more thorough study including rigidity measurements of filaments with different flagellin-flagellin interactions, different extent of glycosylation and different helix geometries, and would require much more *Shewanella*-specific information concerning filament structure, flagellin-flagellin interaction and glycosylation mechanism.

The numerical simulation suggested another possible explanation for the different stability to *screw thread* formation. The first version of the simulation in Kühn et al. 2017 modelled the flagellar helix as a string of beads which are connected to each other by elastic bonds with preferred bonding angles. The elastic constants

correspond to the rigidity of the helix but no significant difference in stability to *screw thread* formation could be observed for different values of these elastic constants. The extended simulation in Kühn et al. 2018 included a helix with the parameters measured for the FlaA-only filament. This helix was stable to *screw thread* formation in the tested range of motor torques (cf. Kühn et al. 2018, Fig. 4 b). The elastic constants remained the same as in the simulation of the FlaB-like helix, only the preferred bonding angle changed. This indicates that the geometry alone might affect the stability to *screw thread* formation. The known helix geometries of the other *screw thread* formers (*Burkholderia* sp. RPE64, *Aliivibrio fischeri*, *Pseudomonas putida*), that wrapped the filaments frequently in bulk liquid, are in fact more similar to the FlaB helix. However, there are more factors that affect the *screw thread* formation in these species, such as the motor torque, possibly the number of flagella and potentially more unknown parameters of the flagellar helix. It thus remains an open question, which exact factors are responsible for the different stabilities to *screw thread* formation of different flagellar filaments.

Finally, differences in the polymorphic forms of FlaA and FlaB filaments as well as the energy needed to convert to another polymorph could also affect how easily the filament wraps around the cell body. The wrapped wild-type and FlaB-only filaments probably adopt the *coiled* polymorph which has a lower energy than the *normal* polymorph if it was forced to adopt the same geometry. If the FlaA filament does not have a corresponding polymorph that fits well around the cell body, or the activation energy to convert to that polymorph is much higher, this could also explain the increased stability of FlaA filaments. Again, this would require more thorough investigations of filament polymorphism and rigidity in *Shewanella*.

6. Segmentation of the flagellar filament

6.1. Why is one flagellin not sufficient?

Like many flagellated bacteria, *Shewanella putrefaciens* possesses two distinct flagellins that are both used to assemble the polar flagellar filament. Why do these cells need more than one flagellin at all and why do they not just make a filament that is composed of either FlaA or FlaB? Using only FlaA to assemble the flagellar filament is obviously disadvantageous due to the inability to switch to the *screw thread* motility mode and the resulting weak spreading performance in structured environments. For the FlaB-only mutant it is not so obvious. These cells spread well in soft-agar, even slightly better than wild-type cells, and they can swim generally well in bulk liquid. However, compared to cells with a wild-type filament or a FlaA-only filament, they are in fact significantly slower (cf. Kühn et al. 2018, Fig. 3 c). This might already explain why this flagellin is also not optimal as the only constituent of the filament, but the swimming behaviour of FlaB-only cells is actually more complex. For example, the turning angle distribution shows a tendency towards high turning angles, almost 180°, which corresponds to reversals without efficient realignment (cf. Kühn et al. 2018, Fig. 3 e, f). Although it is not straightforward to test or estimate to which extent the differences in free-swimming behaviour affect spreading in bulk liquid, it is reasonable to assume that *run-reverse* motion without efficient realignment of the cell body is not as effective as *run-reverse-flick* motion with a realignment tendency towards 90°. Furthermore, the slow backward motion in *screw thread* mode, which is much more prevalent with a pure FlaB filament, intuitively is also unfavourable for swimming efficiency. However, Hintsche et al. suggested that introducing slow phases of backward swimming can in fact increase the spreading capabilities in bulk liquid (Hintsche et al. 2017). So are these slow phases of swimming with the wrapped filament beneficial or not? As already

mentioned (section 4.2), high spreading or exploration capabilities might not always be advantageous, and under certain conditions staying near ephemeral nutrient patches and not spreading quickly might be favourable (Stocker 2011; Xie et al. 2011). Ultimately, it is not yet clear to what extent the different aspects of swimming behaviour of the FlaB-only filament (or any filament) affect the overall hunt for nutrients. However, it is clear that FlaB-only cells are swimming significantly slower and the *screw thread* formation might not provide a significant advantage in bulk liquid. Finally, the increased frequency of *screw thread* formation does not result in a pronounced increase in spreading radius in structured environments compared to the wild type (cf. Kühn et al. 2018, Fig. 1 i, j). This indicates that a higher *screw thread* formation frequency than the wild-type level does not even provide a considerable advantage.

So, if neither of the two flagellins of *S. putrefaciens* is sufficient to provide effective motility and navigation in all the different environments that *Shewanella* encounters, why isn't there a flagellin that does both well? This might appear as the easiest solution, however, such a flagellin probably doesn't exist. The demands on the flagellar filament are simply too specific for different conditions. To form the *screw thread*, the filament needs to be flexible enough to become unstable and wrap around the cell body, but in bulk liquid, this is probably not suitable for efficient swimming. Fig. 4 c in Kühn et al. 2018 shows how efficiently the motor torque can be converted into driving force depending on the composition of the filament, based on the numerical simulation. A FlaA-like filament is more efficient than a FlaB-like filament, indicating that FlaA-like filaments are more effective in free swimming. This is in line with our experimental data (Kühn et al. 2018, Fig. 3). In contrast, FlaA-like filaments are disadvantageous in structured environments as they do not form a *screw thread* (Kühn et al. 2018, Fig. 4 a). Hence, the distinct demands on the filament are probably conflicting and the desired filament properties can only be achieved by utilising more than one type of flagellin.

Taken together, using only FlaB as the single constituent of the flagellar filament does not provide the most efficient swimming capabilities in bulk liquid, but using only FlaA does not provide the ability to switch to *screw thread* mode in structured environments. Thus, the wild-type filament is a compromise between the two extremes and the distinct segmentation provides efficient swimming in bulk liquid but allows wrapping of the filament around the cell body under high-load conditions (summarised in Fig. 7). This is balanced in such a way that only very few cells switch to *screw thread* mode in bulk liquid, because it probably isn't beneficial in the oligotrophic marine habitat of *S. putrefaciens*. Furthermore, the basal FlaA segment shows a wide length distribution, which indicates that within a population of *S. putrefaciens* there are subpopulations with filament properties that are advantageous under certain conditions but more disadvantageous under other conditions. However, in such a heterogeneous population some cells will always be well-equipped for efficient motility in a specific environment.

Still, about half of all flagellated bacteria possess only one flagellin gene (Faulds-Pain et al. 2011), including the other known *screw thread* formers (cf. section 3.2). They are nevertheless able to assemble a flagellar filament that confers robust swimming and potentially the ability to switch to *screw thread* mode. However, these filaments might be better-suited for either free swimming or *screw thread* motility. Furthermore, establishing a heterogeneous population of flagellated cells with different filament stabilities isn't possible with only a single flagellin gene, at least not by the mechanism described above. This might be disadvantageous in habitats with rapidly changing environmental conditions.

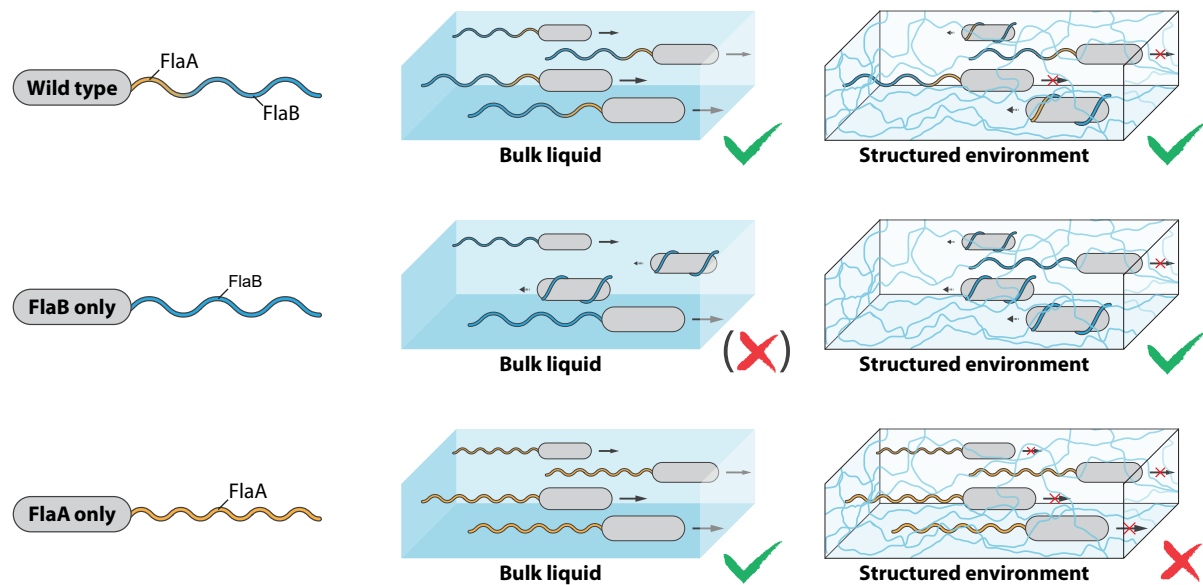


FIGURE 7. **Summary of the performance of different filament types of *Shewanella putrefaciens*.** Wild-type filaments with a short segment of FlaA at the filament base provide efficient propulsion in bulk liquid but retain the ability to switch to *screw thread* swimming mode in structured environments. Filaments exclusively made from FlaB or FlaA show significantly impaired performance in either bulk liquid or structured environments, respectively. FlaB filaments are probably too flexible and possess a less suitable helix geometry to provide an overall efficient propulsion in liquid. FlaA filaments mediate fast swimming in liquid but lack the ability to form the *screw thread* which hampers navigation in structured environments. A similar figure was published online in the "Behind the paper" section of the Nature Research Microbiology Community (<https://naturemicrobiologycommunity.nature.com/users/190538-kai-thormann/posts/42333-how-to-build-a-flagellum-for-all-conditions>).

6.2. How is the segmentation of the filament achieved?

The spatial distribution of the flagellar filament of *S. putrefaciens* with FlaA forming a short segment at the base of the filament and FlaB forming the remaining, major part of the filament is most likely achieved by a temporal transcriptional control. Our working model (cf. Kühn et al. 2018, Fig. 2) is mainly based on the current general model of flagellin transcriptional control and the fact that FlaB production depends on the sigma factor FliA, but FlaA production does not. Basically, we suggest that FlaA is produced before *flaB* transcription can start, because transcription of *flaB* requires active FliA, which in turn requires the hook-basal body complex to be completed and the anti-sigma factor FlgM to be secreted. This is a simple mechanism to ensure that FlaA gets exported first and forms the proximal part of the filament. The model, however, cannot explain everything that it implies and not everything that we see.

First of all, the model implies that FlaA production levels are lower than FlaB production levels. Otherwise the FlaA segment would be longer than the FlaB segment because the filament growth rate decreases with increasing filament length, which is described by the injection-diffusion model (Renault et al. 2017). Thus, the cytoplasmic concentration of FlaB has to be much higher than the concentration of FlaA to explain the short FlaA segment and the long FlaB segment. Our data indicates that the transcription level of *flaB* is in fact higher than that of *flaA* (Kühn et al. 2018, Fig. S7 a). However, there are more possible regulatory stages that we didn't analyse, namely translation, interaction with the chaperone FliS, export efficiency and assembly efficiency. The posttranslational modification, which very likely takes place before the flagellins are exported, might also influence the export and/or assembly efficiency. The amount of available FlaA does in fact influence

the length of the FlaA segment, which was demonstrated by introducing a synthetic version of FlaA directly downstream of the native FlaA. This potentially doubles the production of FlaA and did, in fact, increase the length of the basal FlaA segment (cf. Kühn et al. 2018, Fig. S9 c). Furthermore, overproducing FlaA from a plasmid resulted in very long FlaA-only filaments, however, this also bypasses the native regulation which might have an effect on the FlaA level as well. Specifically, it is likely that transcription of *flaA* is turned off at some point, because FlaA stubs in *flaB* deletion mutants do not grow to longer filaments over time. This should happen eventually even at low expression levels, if FlaA production was not terminated at some point. Also, in some wild-type filaments with fluorescently labelled FlaA, a faint signal of FlaA was visible outwards of the distinct FlaA-only segment (cf. Kühn et al. 2018, Fig. S4 h). This is probably the FlaB segment with some interspersed FlaA. These images indicate that FlaB outperforms FlaA and that FlaA production ceases at some point, because such a faint FlaA signal was never observed in the distal part of the filament.

It would make sense to terminate production of FlaA as soon as FlaB production starts, for example, when the sigma factor *FlaA* gets activated and initiates transcription of *flaB*. In fact, immunoblot analyses indicated that FlaA is more abundant in a *flaA* deletion mutant compared to wild-type levels (cf. Kühn et al. 2018, Fig S2 b). However, the length of the FlaA segment was not affected by the deletion of *flaA* (data not shown).

Another promising candidate was FlaG, which was shown to affect the length of the flagellar filament in several species (McGee et al. 1996; Capdevila et al. 2004) and specifically the length of a FlaA-only filament but not a FlaB-only filament in *Campylobacter jejuni* (note that in *C. jejuni* FlaA and FlaB play different roles than in *S. putrefaciens* and FlaB most likely forms the proximal segment; Inoue et al. 2018). Unfortunately, neither the length of the FlaA nor the length of the FlaB segment was affected by deleting *flaG* in *S. putrefaciens* (data not shown).

Our current model of the regulation of flagellin composition and distribution in the (comparatively simple) case of only two flagellins mostly includes transcriptional control. However, this does not explain the observations made for the FlaBA mutant, with *flaA* and *flaB* coding sequences swapped, or the FlaB stub mutant, with only FlaB being produced from the *flaA* promoter. In both cases, the FlaB segment is much shorter than the corresponding FlaA segment, when only FlaA is expressed from its native promoter (cf. Kühn et al. 2018, Fig. S4 and S5). This strongly indicates that there are more stages of regulation that depend on the different DNA and/or amino acid sequence of FlaA and FlaB.

Other bacteria with similar segmentation of the flagellar filament might also use a similar regulation. A separate control of flagellin genes depending on different sigma factors was in fact reported for *Brachyspira hyodysenteriae* (Li et al. 2010). However, each sigma factor controls two flagellins and one of them isn't even related to known flagellins. Furthermore, there are many bacteria with a more complex segmentation and/or composition of the flagellar filament and the regulation schemes in species with more than two flagellins are likely more complex than in *Shewanella*.

6.3. Why make the filament's base more stable?

A filament exclusively composed of FlaA is more stable to *screw thread* formation than a filament exclusively composed of FlaB. Thus, in order to stabilise the filament, incorporating a segment of FlaA into the FlaB filament is reasonable. But why is FlaA incorporated into the base of the filament and not evenly distributed?

We can not ultimately answer this question, but to stabilise the whole filament it is definitely sufficient to stabilise the basal segment because that's where the torsional forces are highest during rotation. This also leaves the option to adapt the properties of the flagellar filament in a very defined way, depending on environmental conditions, by modifying the length of the FlaA and/or FlaB segment(s). Increasing the length of the FlaA segment did in fact significantly increase the stability to *screw thread* formation without compromising the general spreading capabilities (cf. Kühn et al. 2018, Fig. S9 a and S8 e).

For *Shewanella oneidensis*, FlrB and FlrC were shown to affect the ratio of FlaA and FlaB (Shi et al. 2014), however, deletion of *flrBC* did not affect the ratio in *S. putrefaciens* (cf. Kühn et al. 2018, Fig. S2 b). It is possible that other factors influence the FlaA/B ratio in *S. putrefaciens*, but we did not find a candidate yet. Stabilising the filament can also be achieved by producing both flagellins from the *flaB* promoter. This in fact produces a filament with more or less evenly distributed FlaA and FlaB, and those cells showed a lower tendency to form *screw threads* (data not shown). In principle, one could also imagine destabilising a FlaA filament by incorporating a basal FlaB segment to facilitate *screw thread* formation. A mutant in which the flagellin coding sequences are swapped assembles a filament with only a very short basal FlaB segment (FlaBA), so we can't test this experimentally. However, the corresponding simulation suggests that under the observed conditions at least half of the filament has to be FlaB in order to be able to switch to *screw thread* mode (cf. Kühn et al. 2018, Fig. S9 d).

All in all, the wild-type filament with a basal FlaA segment performed best in all tested environments and a population of wild-type cells showed a wide variation in the length of the basal FlaA segment. Hence, wild-type cells form a heterogeneous population in which some cells are better equipped for free swimming while others are better equipped for *screw thread* motility in structured environments. Yet, in order to ultimately answer which configuration is the best in a specific environment a more in depth study of *screw thread* formation, filament properties and swimming behaviour of all possible configurations is required. This, however, requires a more advanced system to define the composition of the flagellar filament very accurately. Ideally, one would synchronise flagellar assembly and express the flagellins from inducible promoters. When the flagellar assembly comes to a stop after the hook-basal body complex is completed it should be possible to produce one flagellin after the other and create a defined segmentation.

6.4. Can *screw thread* formation explain the maintenance of multiple flagellins in other species?

Many bacteria possess more than a single flagellin gene and some are known to assemble their flagellar filaments using several, distinct flagellins. Filaments of *Caulobacter crescentus*, *Helicobacter pylori* and *Bdellovibrio bacteriovorus* are segmented, like in *S. putrefaciens*, with a distinct flagellin forming each segment. Our results show a great impact of the segmentation on the ability to wrap the flagellar filament around the cell body. Could therefore *screw thread* formation explain why these bacteria (and potentially many others) maintain multiple flagellins? The answer so far is: Maybe, but only *screw thread* formation is probably too specific. All other known bacteria that can switch to the *screw thread* motility mode only have a single flagellin, so it is not even clear if there are other bacteria with a segmented filament that can form the *screw thread*, although it is very likely. More generally though, our results show a clear influence of the filament composition and segmentation on the general swimming behaviour. Wild-type filaments with distinct FlaA and FlaB segments provide fast swimming and efficient turning angles near 90°. The effect of distinct filament properties on turning

are in line with a recent study that suggests a role of the filament properties for the *run-reverse-flick* turning, in addition to the role of the hook (Jabbarzadeh et al. 2018). So even for bacteria that might not be able to form the *screw thread*, incorporating multiple flagellins likely modifies the filament properties in a favourable way that is not possible to achieve with only one type of flagellin.

There are in fact some examples of filament segmentation that influences flagellar properties, like geometry and motility: One example is the flagellar filament of *B. bacteriovorus*, which shows a clear shift in helix morphology from filament base to tip, resulting in a tapered helix shape (Thomashow et al. 1985). This is achieved by the use of distinct flagellin segments along the filament, and deleting individual flagellin genes resulted in decreased swimming speed (Lambert et al. 2006; Iida et al. 2009). However, the exact influence of each flagellin on the filament properties and general motility behaviour was not studied. Furthermore, periplasmic flagella of the spirochete *Brachyspira hyodysenteriae* are known to be constructed from multiple flagellins and deletion of each flagellin does affect helix geometry and motility (Li et al. 2000b; Li et al. 2008). The biggest effect was found for FlaA, however, this protein shows no sequence homology to other flagellins and forms a sheath around the flagellin core that is formed by the FlaB flagellins (Li et al. 2000b). The flagellins are regulated by two different sigma factors, σ^{28} for *flaB*₁ and *flaB*₂ and σ^{70} for *flaA* and *flaB*₃ (Li et al. 2010). There are definitely some interesting similarities to the filament segmentation in *Shewanella*, but differences are to be expected as the flagella of *B. hyodysenteriae* rotate in the periplasm and this probably comes with distinct demands on the filament properties. It would be very interesting to investigate how the swimming behaviour changes in these and other bacteria when the flagellin genes are swapped or the filament composition is changed by other approaches. However, in bacteria with more than two flagellins the regulation is probably more complex than in *Shewanella* and it might be even more challenging to customise the filament properties.

To conclude, balancing the frequency of *screw thread* formation is certainly an obvious reason to maintain multiple flagellins, but its underlying principle, the modulation of filament properties in a defined way, is more likely a general reason to maintain multiple flagellins.

7. Outlook

Bacteria need to move in order to find nutrients, avoid toxic conditions or more generally establish themselves in their favourable environment. Many different strategies have evolved and they reflect the specific demands of the environmental conditions on the motility apparatus. The most prominent bacterial motility apparatus is the bacterial flagellum, which is typically associated with swimming in liquid environments. However, bacteria have adapted the flagellum and associated cellular systems to provide motility in a wide range of environments, which are often characterised by vastly diverse demands on the motility apparatus. The flagellar apparatus of aquatic bacteria is usually adapted for fast swimming, a fast chemotactic response and efficiency to deal with the low availability of nutrients. Nutrient availability in many complex environments such as soil or animal hosts is not a limiting factor and cells can easily grow and maintain multiple flagella, which increases the torque that they can generate. As long as sufficient water is available in these environments, flagellar motility is an important spreading and survival factor and distinct movement schemes have evolved, such as swarming or corkscrew-like motion of spiral-shaped cells.

Although many bacteria with single flagella are better equipped for swimming in aquatic environments, some are known to possess an alternative set of multiple lateral flagella to navigate structured or viscous environments. With the new insights into the *screw thread* motility of *Shewanella putrefaciens*, which is dedicated to movement in structured and confined spaces, we do now understand that also a single polar flagellum can be adapted to provide a more efficient way to navigate structured environments. However, many aspects of this motility mode still pose a lot of questions.

***Screw thread* motility and lateral flagella**

One open question is related to those bacteria with polar and lateral flagella: As lateral flagella are located all over the cell body, they might hamper the wrapping of the polar filament. First image sequences obtained for *S. putrefaciens* with labelled polar and lateral flagella indicate that *screw thread* formation is not generally eliminated when cells have lateral flagella, but the frequency of *screw thread* formation might be reduced on a population-wide level. On the other hand, more flagella sticking out of the cell surface might slow down the counterrotation of the cell body and thus have a similar effect as the Ficoll polymers, i.e. increasing the frequency of *screw thread* formation. Thus, the interplay of *screw thread* motility and lateral flagella is an interesting and promising topic to investigate further, specifically, if these two motility modes can be combined to enhance the movement through structured environments or if the effects are rather completely or partly redundant. This could be tested with our various mutants with and without lateral filaments in soft agar spreading assays.

Molecular determinants of filament properties

There are also many unanswered questions about the polar flagellum alone. This includes what actually determines the filament properties on the molecular level, especially for flagellins with a very high sequence conservation but very distinct filament properties. Furthermore, a more comprehensive understanding is required how bacteria that possess a more complex filament structure and flagellin regulation, such as *Bdellovibrio bacteriovorus*, achieve distinct filament properties.

As already mentioned, the filament surface properties might also influence the interaction with environmental surfaces, other flagella or the cell surface when the filament wraps around the cell body. For *S. putrefaciens*, a more in-depth study of the glycosylation and potential methylation could help understanding the filament surface interactions. Ideally, one would try to generate a functional non-glycosylated filament mutant and analyse its swimming and filament wrapping behaviour.

Ultimately, measuring the physical and biochemical properties of filaments made from only one type of flagellin could help understand the role of each flagellin segment. This also includes the analysis of polymorphs and transitions between polymorphic states upon torsional stress.

Regulation of *screw thread* formation

We were able to show that modifying the length of the basal FlaA segment has a drastic effect on the filament properties, most notably on *screw thread* formation. We further suggested that a population of motile cells might adapt to changing environments by adjusting the length or ratio of the flagellin segments. To investigate this further, a reasonable starting point would be to test if cells actually do this. For example, one could grow cells over a long time in medium that either triggers *screw thread* formation, such as viscous media, or a structured

environment in which the *screw thread* motility actually provides a considerable advantage, like in soft agar. By measuring the length of the FlaA and FlaB segments one could determine if the population adjusts the flagellin ratio over time, for example by reducing the length of the FlaA segment and thereby increasing the frequency of *screw thread* formation. In soft agar, one could generally isolate cells from the outer edge of the spreading colony and analyse the filament segmentation. This fraction contains the fastest spreading cells, which are already known to produce more lateral flagella than cells from the centre of the colony. These cells might have also adjusted the flagellin ratio to facilitate *screw thread* formation.

Another approach would be to take a closer look at potential regulators of flagellin levels. In *Shewanella oneidensis* for example, *flrBC* were shown to affect the ratio of FlaA and FlaB (Shi et al. 2014). Although a *flrBC* deletion in *S. putrefaciens* did not show a clear difference between FlaA and FlaB levels on a Western Blot, the differences might be more pronounced in a direct analysis of the flagellin segmentation or the frequency of *screw thread* formation. A more thorough analysis of both deletion as well as overproduction of *flrBC* in *S. putrefaciens* and *S. oneidensis* could reveal if *flrB* and *flrC* play a role in determining the flagellin ratio.

A completely different way to modify the frequency of *screw thread* formation would be a short-term adaption of the motor rotation speed or motor torque. Higher motor rotation would increase the forces acting on the filament and thus facilitate *screw thread* formation. *Escherichia coli* and *Bacillus subtilis* are known to add more stator units to the motor under high load (Lele et al. 2013; Tipping et al. 2013; Terahara et al. 2017). However, it is not clear if this actually applies to any of the known *screw thread* formers, although Hintsche et al. suggested that the filament wrapping in *Pseudomonas putida* is triggered by increasing the motor rotation rate (Hintsche et al. 2017). A direct effect of the motor rotation rate on *screw thread* formation stands to reason, however, this wasn't tested directly so far. In *S. putrefaciens*, one could monitor the wrapping of the filament over a range of Na⁺ concentrations. As the motor is driven by a sodium-motive force, decreasing the Na⁺ concentration slows down the motor and, if our model is correct, decrease the frequency of *screw thread* formation. A similar approach was used by Son et al. to show the speed and viscous load dependency of the *run-reverse-flick* turning in *Vibrio alginolyticus* (Son et al. 2013).

Distribution of *screw thread* motility among bacteria

The underlying mechanism of *screw* formation mainly relies on the balance of filament stability during backward rotation, when the opposite-handed torsional forces try to invert the filament's helicity. Thus, the mechanism could fundamentally apply to any polarly flagellated bacterium, which is supported by the discovery and characterisation of the *screw thread* motility in other bacteria, both with various flagellation patterns as well as from diverse habitats. Still, the general distribution of the filament wrapping capabilities among bacteria (and maybe archaea) is rather poorly understood. In order to better understand the role of this motility mode, a broad analysis of swimming and filament behaviours is required. The swimming pattern of *S. putrefaciens* cells that frequently switch to *screw thread* mode is very characteristic and it might be possible to determine *screw thread* formation without the need of fluorescent labelling, especially if combined with the use of media with increased viscosity and high-throughput 3D tracking. A very important question is also if human pathogenic bacteria with polar flagellation, such as *Vibrio cholerae*, *Pseudomonas aeruginosa* or *Helicobacter pylori*, are able to use the *screw thread* motility mode. These bacteria encounter viscous or structured environments in the human body and the *screw thread* motility could potentially facilitate host invasion.

Flagella-mediated motility in structured environments

The open questions mentioned so far were all related to the *screw thread* motility mode, but in a more general sense the overall goal is to understand how bacteria use polar flagella, lateral flagella and a combination of both to navigate various structured environments. The next big step would thus be the imaging and tracking of motile bacteria and their movement strategies in structured environments on a single cell level. This is very challenging, especially if the structure is to be well defined. So far, most image sequences were obtained under free-swimming conditions and some in a structured but not well-defined environment (e.g. the agarose-glass interface). Fluorescence microscopy in a homogeneous agarose medium should be possible, however, it is technically challenging because of a lower signal to noise ratio and because finding a suitable cell is much harder in three dimensions than in two. A more promising approach would certainly be the use of custom-made flow chambers in which cells move in quasi two dimensions through custom-made microstructures. Even more challenging would be the construction of host-like environments, for example microvilli-like structures, to study the movement strategies of pathogenic bacteria and better understand the role of different motility modes during host invasion. Furthermore, simultaneous imaging of cellular and filament behaviour should be complemented with high-throughput single cell tracking, for example by holographic microscopy, to monitor the movement patterns of several thousands of cells.

All in all, the bacterial flagellum is an incredible molecular machine that still is far from being fully understood and especially investigating the less extensively studied swimmers can reveal fascinating and widely relevant new insights.

References

- Adler, J. (1965). Chemotaxis in *Escherichia coli*. *Cold Spring Harbor Symposia on Quantitative Biology* 30, pp. 289–92 (cit. on pp. 18, 26, 30).
- Adler, J. (1966). Chemotaxis in bacteria. *Science* 153, pp. 708–716 (cit. on p. 30).
- Adler, J. (1987). How motile bacteria are attracted and repelled by chemicals: An approach to neurobiology. *Biological Chemistry* 368, pp. 163–173 (cit. on p. 30).
- Allen, R. D. and P. Baumann (1971). Structure and arrangement of flagella in species of the genus *Beneckea* and *Photobacterium fischeri*. *Journal of Bacteriology* 107, pp. 295–302 (cit. on p. 12).
- Alley, M. R. K., J. R. Maddock, and L. Shapiro (1992). Polar localization of a bacterial chemoreceptor. *Genes and Development* 6, pp. 825–836 (cit. on p. 31).
- Alm, R. A., P. Guerry, and T. J. Trust (1993). Significance of duplicated flagellin genes in *Campylobacter*. *Journal of Molecular Biology* 230, pp. 359–363 (cit. on p. 13).
- Anand, G. S. and A. M. Stock (2002). Kinetic basis for the stimulatory effect of phosphorylation on the methylesterase activity of CheB. *Biochemistry* 41, pp. 6752–6760 (cit. on p. 31).
- Andrewes, F. W. (1922). Studies in group-agglutination I. The *Salmonella* group and its antigenic structure. *The Journal of Pathology and Bacteriology* 25, pp. 505–521 (cit. on p. 13).
- Armitage, J. P. and R. M. Macnab (1987). Unidirectional, intermittent rotation of the flagellum of *Rhodobacter sphaeroides*. *Journal of Bacteriology* 169, pp. 514–518 (cit. on p. 30).
- Armitage, J. P. and R. Schmitt (1997). Bacterial chemotaxis: *Rhodobacter sphaeroides* and *Sinorhizobium meliloti* - variations on a theme? *Microbiology* 143, pp. 3671–3682 (cit. on pp. 27, 28, 30, 31).
- Armitage, J. P., T. P. Pitta, M. A. S. Vigeant, H. L. Packer, and R. M. Ford (1999). Transformations in flagellar structure of *Rhodobacter sphaeroides* and possible relationship to changes in swimming speed. *Journal of Bacteriology* 181, pp. 4825–4833 (cit. on pp. 27, 30).
- Arora, S. K., A. N. Neely, B. Blair, S. Lory, and R. Ramphal (2005). Role of motility and flagellin glycosylation in the pathogenesis of *Pseudomonas aeruginosa* burn wound infections. *Infection and Immunity* 73, pp. 4395–4398 (cit. on p. 13).
- Asakura, S. (1970). Polymerization of flagellin and polymorphism of flagella. *Advances in Biophysics* 1, pp. 99–155 (cit. on pp. 9, 11).
- Aschtgen, M.-S., J. B. Lynch, E. Koch, J. Schwartzman, M. McFall-Ngai, and E. Ruby (2016). Rotation of *Vibrio fischeri* flagella produces outer membrane vesicles that induce host development. *Journal of Bacteriology* 198, pp. 2156–2165 (cit. on p. 13).
- Atsumi, T., Y. Maekawa, T. Yamada, I. Kawagishi, Y. Imae, and M. Homma (1996). Effect of viscosity on swimming by the lateral and polar flagella of *Vibrio alginolyticus*. *Journal of Bacteriology* 178, pp. 5024–5026 (cit. on pp. 17, 18).
- Auvray, F., J. Thomas, G. M. Fraser, and C. Hughes (2001). Flagellin polymerisation control by a cytosolic export chaperone. *Journal of Molecular Biology* 308, pp. 221–229 (cit. on p. 15).
- Baar, C. et al. (2003). Complete genome sequence and analysis of *Wolinella succinogenes*. *Proceedings of the National Academy of Sciences* 100, pp. 11690–11695 (cit. on p. 21).
- Balaban, M. and D. R. Hendrixson (2011). Polar flagellar biosynthesis and a regulator of flagellar number influence spatial parameters of cell division in *Campylobacter jejuni*. *PLoS Pathogens* 7.e1002420 (cit. on p. 14).
- Ballowitz, E. (1888). Untersuchung über die Struktur der Spermatozoën. *Archiv für mikroskopische Anatomie*. Verlag von Max Cohen und Sohn, Bonn, pp. 401–473 (cit. on p. 6).
- Bange, G., G. Petzold, K. Wild, R. O. Parltitz, and I. Sinning (2007). The crystal structure of the third signal-recognition particle GTPase FlhF reveals a homodimer with bound GTP. *Proceedings of the National Academy of Sciences* 104, pp. 13621–13625 (cit. on p. 14).

References

- Barahona, E., A. Navazo, F. Yousef-Coronado, D. Aguirre de Cárcer, F. Martínez-Granero, M. Espinosa-Urgel, M. Martín, and R. Rivilla (2010). Efficient rhizosphere colonization by *Pseudomonas fluorescens* f113 mutants unable to form biofilms on abiotic surfaces. *Environmental Microbiology* 12, pp. 3185–3195 (cit. on p. 20).
- Barbara, G. M. and J. G. Mitchell (2003). Bacterial tracking of motile algae. *FEMS Microbiology Ecology* 44, pp. 79–87 (cit. on pp. 17, 29).
- Beatson, S. A., T. Minamino, and M. J. Pallen (2006). Variation in bacterial flagellins: from sequence to structure. *Trends in Microbiology* 14, pp. 149–155 (cit. on pp. 9, 11).
- Beeby, M., D. A. Ribardo, C. A. Brennan, E. G. Ruby, G. J. Jensen, and D. R. Hendrixson (2016). Diverse high-torque bacterial flagellar motors assemble wider stator rings using a conserved protein scaffold. *Proceedings of the National Academy of Sciences* 113, E1917–E1926 (cit. on p. 21).
- Berg, H. C. (1971). How to track bacteria. *Review of Scientific Instruments* 42, pp. 868–871 (cit. on p. 16).
- Berg, H. C. (1975). Chemotaxis in bacteria. *Annual Review of Biophysics and Bioengineering* 4, pp. 119–136.
- Berg, H. C. (1991). Bacterial motility: Handedness and symmetry. *Ciba Foundation Symposium* 162, pp. 58–69 (cit. on p. 26).
- Berg, H. C. (2004). *E. coli in motion*. Springer-Verlag, New York (cit. on pp. 23, 25, 26, 28, 31, 32).
- Berg, H. C. and D. A. Brown (1972). Chemotaxis in *E. coli* analysed by 3D tracking. *Nature* 239, pp. 500–504 (cit. on pp. 8, 25).
- Berg, H. C. and R. A. Anderson (1973). Bacteria swim by rotating their flagellar filaments. *Nature* 245, pp. 380–382 (cit. on pp. 8, 23, 26).
- Berg, H. C., D. B. Bromley, and D. B. Charon (1978). Leptospiral motility. *Symposium of the Society for General Microbiology* 28, pp. 285–294 (cit. on p. 22).
- Berg, H. C. and L. Turner (1995). Cells of *Escherichia coli* swim either end forward. *Proceedings of the National Academy of Sciences* 92, pp. 477–479 (cit. on p. 26).
- Bet, B., G. Boosten, M. Dijkstra, and R. van Roij (2017). Efficient shapes for microswimming: From three-body swimmers to helical flagella. *The Journal of Chemical Physics* 146, p. 084904 (cit. on p. 101).
- Blair, D. F. and H. C. Berg (1990). The MotA protein of *E. coli* is a proton-conducting component of the flagellar motor. *Cell* 60, pp. 439–449 (cit. on p. 7).
- Blake, J. R. and M. A. Sleight (1974). Mechanics of ciliary locomotion. *Biological Reviews of the Cambridge Philosophical Society*. Vol. 49, pp. 85–125 (cit. on p. 101).
- Bonifield, H. R. and K. T. Hughes (2003). Flagellar phase variation in *Salmonella enterica* is mediated by a posttranscriptional control mechanism. *Journal of Bacteriology* 185, pp. 3567–3574 (cit. on p. 13).
- Botkin, D. J., A. Abbott, J. K. Howell, M. Mosher, P. E. Stewart, P. A. Rosa, H. Kawabata, H. Watanabe, and S. J. Norris (2006). Transposon mutagenesis of infectious *Borrelia burgdorferi* B31: A pilot study. *Molecular Biology of Spirochetes*. Ed. by F. C. Cabello, D. Hulska, and H. P. Godfrey. IOS Press, Amsterdam, pp. 13–24 (cit. on p. 22).
- Boukhalfa, H., G. a. Icopini, S. D. Reilly, P. Neu, and M. P. Neu (2007). Plutonium (IV) reduction by the metal-reducing bacteria *Geobacter metallireducens* GS-15 and *Shewanella oneidensis* MR-1. *Applied and Environmental Microbiology* 73, pp. 5897–5903 (cit. on p. 32).
- Bradley, D. E. (1980). A function of *Pseudomonas aeruginosa* PAO polar pili: twitching motility. *Canadian Journal of Microbiology* 26, pp. 146–154 (cit. on p. 5).
- Bren, A. and M. Eisenbach (1998). The N terminus of the flagellar switch protein, FliM, is the binding domain for the chemotactic response regulator, CheY. *Journal of Molecular Biology* 278, pp. 507–514 (cit. on p. 31).
- Brennan, C. A., B. C. Krasity, M. J. McFall-Ngai, M. A. Apicella, J. R. Hunt, E. G. Ruby, and N. Kremer (2014). A model symbiosis reveals a role for sheathed-flagellum rotation in the release of immunogenic lipopolysaccharide. *eLife* 3 (cit. on p. 13).
- Brettar, I. and M. G. Hofle (1993). Nitrous oxide producing heterotrophic bacteria from the water column of the central Baltic: Abundance and molecular identification. *Marine Ecology Progress Series* 94, pp. 253–265 (cit. on p. 96).

References

- Bromley, D. B. and N. W. Charon (1979). Axial filament involvement in the motility of *Leptospira interrogans*. *Journal of Bacteriology* 137, pp. 1406–1412 (cit. on p. 21).
- Brown, M. T., B. C. Steel, C. Silvestrin, D. A. Wilkinson, N. J. Delalez, C. N. Lumb, B. Obara, J. P. Armitage, and R. M. Berry (2012). Flagellar hook flexibility is essential for bundle formation in swimming *Escherichia coli* cells. *Journal of Bacteriology* 194, pp. 3495–3501 (cit. on p. 26).
- Bubendorfer, S., S. Held, N. Windel, A. Paulick, A. Klingl, and K. M. Thormann (2012). Specificity of motor components in the dual flagellar system of *Shewanella putrefaciens* CN-32. *Molecular Microbiology* 83, pp. 335–50 (cit. on pp. 19, 32).
- Bubendorfer, S. et al. (2013). Analyzing the modification of the *Shewanella oneidensis* MR-1 flagellar filament. *PLoS ONE* 8.e73444 (cit. on pp. 13, 32, 108).
- Bubendorfer, S., M. Koltai, F. Rossmann, V. Sourjik, and K. M. Thormann (2014). Secondary bacterial flagellar system improves bacterial spreading by increasing the directional persistence of swimming. *Proceedings of the National Academy of Sciences* 111, pp. 11485–90 (cit. on pp. 19, 32).
- Budding, A. E., C. J. Ingham, W. Bitter, C. M. Vandenbroucke-Grauls, and P. M. Schneeberger (2009). The Dienes phenomenon: Competition and territoriality in swarming *Proteus mirabilis*. *Journal of Bacteriology* 191, pp. 3892–3900 (cit. on p. 19).
- Buder, J. (1915). Zur Kenntnis des *Thiospirillum jenense* und seiner Reaktionen auf Lichtreize. *Jahrbücher für wissenschaftliche Botanik*. Vol. 56. Verlag von Gebrüder Borntraeger, Leipzig, pp. 529–584 (cit. on pp. 7, 23–25, 27, 29, 96, 102, 103).
- Bush, M. and R. Dixon (2012). The role of bacterial enhancer binding proteins as specialized activators of σ^{54} -dependent transcription. *Microbiology and Molecular Biology Reviews* 76, pp. 497–529 (cit. on p. 16).
- Bütschli, O. (1884). Protozoa. *Bronns Klassen und Ordnungen des Tierreichs*. Ed. by H. G. Bronn and C. K. Hoffmann. Vol. 1. C. F. Winter'sche Verlagshandlung, Leipzig und Heidelberg, pp. 849–858 (cit. on pp. 7, 23).
- Caccavo, F., R. P. Blakemore, and D. R. Lovley (1992). A hydrogen-oxidizing, Fe(III)-reducing microorganism from the Great Bay estuary, New Hampshire. *Applied and Environmental Microbiology* 58, pp. 3211–3216 (cit. on p. 32).
- Calladine, C. R. (1975). Construction of bacterial flagella. *Nature* 255, pp. 121–124 (cit. on p. 11).
- Calladine, C. R. (1976). Design requirements for the construction of bacterial flagella. *Journal of Theoretical Biology* 57, pp. 469–489 (cit. on p. 11).
- Calladine, C. R. (1978). Change of waveform in bacterial flagella: The role of mechanics at the molecular level. *Journal of Molecular Biology* 118, pp. 457–479 (cit. on pp. 11, 12).
- Campos-García, J., R. Nájera, L. Camarena, and G. Soberón-Chávez (2000). The *Pseudomonas aeruginosa* *motR* gene involved in regulation of bacterial motility. *FEMS Microbiology Letters* 184, pp. 57–62 (cit. on p. 14).
- Capdevila, S., F. M. Martínez-Granero, M. Sánchez-Contreras, R. Rivilla, and M. Martín (2004). Analysis of *Pseudomonas fluorescens* F113 genes implicated in flagellar filament synthesis and their role in competitive root colonization. *Microbiology* 150, pp. 3889–3897 (cit. on p. 113).
- Catlow, H. Y., A. R. Glenn, and M. J. Dilworth (1990). The use of transposon-induced non-motile mutants in assessing the significance of motility of *Rhizobium leguminosarum* biovar Trifolii for movement in soils. *Soil Biology and Biochemistry* 22, pp. 331–336 (cit. on p. 20).
- Celli, J. P. et al. (2009). *Helicobacter pylori* moves through mucus by reducing mucin viscoelasticity. *Proceedings of the National Academy of Sciences* 106, pp. 14321–14326 (cit. on p. 21).
- Chaban, B., I. Coleman, and M. Beeby (2018). Evolution of higher torque in *Campylobacter*-type bacterial flagellar motors. *Scientific Reports* 8.97 (cit. on p. 21).
- Chadsey, M. S., J. E. Karlinsey, and K. T. Hughes (1998). The flagellar anti- σ factor FlgM actively dissociates *Salmonella typhimurium* σ^{28} RNA polymerase holoenzyme. *Genes and Development* 12, pp. 3123–3136 (cit. on p. 15).
- Chang, W. S. and L. J. Halverson (2003). Reduced water availability influences the dynamics, development, and ultrastructural properties of *Pseudomonas putida* biofilms. *Journal of Bacteriology* 185, pp. 6199–6204 (cit. on p. 20).
- Charon, N. W., S. F. Goldstein, S. M. Block, K. Curci, J. D. Ruby, J. A. Kreiling, and R. J. Limberger (1992). Morphology and dynamics of protruding spirochete periplasmic flagella. *Journal of Bacteriology* 174, pp. 832–840 (cit. on p. 21).

References

- Chen, S. et al. (2011). Structural diversity of bacterial flagellar motors. *EMBO Journal* 30, pp. 2972–2981 (cit. on p. 21).
- Chen, X. and H. C. Berg (2000). Torque-speed relationship of the flagellar rotary motor. *Biophysical Journal* 78, pp. 1036–1041 (cit. on p. 17).
- Chevance, F. F. V. and K. T. Hughes (2008). Coordinating assembly of a bacterial macromolecular machine. *Nature Reviews Microbiology* 6, pp. 455–465 (cit. on p. 14).
- Cisneros, L., C. Dombrowski, R. E. Goldstein, and J. O. Kessler (2006). Reversal of bacterial locomotion at an obstacle. *Physical Review E* 73 (cit. on p. 26).
- Cohen, E. J. and K. T. Hughes (2014). Rod-to-hook transition for extracellular flagellum assembly is catalyzed by the L-ring-dependent rod scaffold removal. *Journal of Bacteriology* 196, pp. 2387–2395 (cit. on p. 15).
- Constantino, M. A., M. Jabbarzadeh, H. C. Fu, and R. Bansil (2016). Helical and rod-shaped bacteria swim in helical trajectories with little additional propulsion from helical shape. *Science Advances* 2 (cit. on p. 21).
- Constantino, M. A., M. Jabbarzadeh, H. C. Fu, Z. Shen, J. G. Fox, F. Haesebrouck, S. K. Linden, and R. Bansil (2018). Bipolar lophotrichous *Helicobacter suis* combine extended and wrapped flagella bundles to exhibit multiple modes of motility. *Scientific Reports* 8.14415 (cit. on pp. 35, 104).
- Copeland, M. F. and D. B. Weibel (2009). Bacterial swarming: A model system for studying dynamic self-assembly. *Soft Matter* 5, pp. 1174–1187 (cit. on p. 19).
- Czaban, J., A. Gajda, and B. Wróblewska (2007). The motility of bacteria from rhizosphere and different zones of winter wheat roots. *Polish Journal of Environmental Studies* 16, pp. 301–308 (cit. on p. 20).
- Darnton, N. C., L. Turner, S. Rojevsky, and H. C. Berg (2007a). On torque and tumbling in twimming *Escherichia coli*. *Journal of Bacteriology* 189, pp. 1756–1764 (cit. on pp. 17, 18, 20, 22, 26).
- Darnton, N. C. and H. C. Berg (2007b). Force-extension measurements on bacterial flagella: Triggering polymorphic transformations. *Biophysical Journal* 92, pp. 2230–2236 (cit. on pp. 11, 12).
- Dasgupta, N., S. K. Arora, and R. Ramphal (2000). *flaH*, a gene that regulates flagellar number in *Pseudomonas aeruginosa*. *Journal of Bacteriology* 182, pp. 357–364 (cit. on p. 14).
- Dasgupta, N., M. C. Wolfgang, A. L. Goodman, S. K. Arora, J. Jyot, S. Lory, and R. Ramphal (2003). A four-tiered transcriptional regulatory circuit controls flagellar biogenesis in *Pseudomonas aeruginosa*. *Molecular Microbiology* 50, pp. 809–824 (cit. on pp. 15, 16).
- De Maayer, P. and D. A. Cowan (2016). Flashy flagella: Flagellin modification is relatively common and highly versatile among the *Enterobacteriaceae*. *BMC Genomics* 17 (cit. on p. 13).
- Dechesne, A., G. Wang, G. Gulez, D. Or, and B. F. Smets (2010). Hydration-controlled bacterial motility and dispersal on surfaces. *Proceedings of the National Academy of Sciences* 107, pp. 14369–14372 (cit. on p. 20).
- DePamphilis, M. L. and J. Adler (1971). Fine structure and isolation of the hook-basal body complex of flagella from *Escherichia coli* and *Bacillus subtilis*. *Journal of Bacteriology* 105, pp. 384–395 (cit. on p. 7).
- Derby, H. A. and B. W. Hammer (1931). Bacteriology of butter. IV. Bacteriological studies on surface taint butter. *Iowa Agricultural Research Bulletins* 145, pp. 387–416 (cit. on p. 96).
- Diniz, M. C., A. C. L. Pacheco, K. M. Farias, and D. M. de Oliveira (2012). The eukaryotic flagellum makes the day: Novel and unforeseen roles uncovered after post-genomics and proteomics data. *Current Protein & Peptide Science* 13, pp. 524–546 (cit. on p. 6).
- DiPierro, J. M. and R. N. Doetsch (1968). Enzymatic reversibility of flagellar immobilization. *Canadian Journal of Microbiology* 14, pp. 487–489 (cit. on p. 23).
- Downie, H., N. Holden, W. Otten, A. J. Spiers, T. A. Valentine, and L. X. Dupuy (2012). Transparent soil for imaging the rhizosphere. *PLoS ONE* 7.e44276 (cit. on p. 20).
- Driks, A., R. Bryan, L. Shapiro, and D. J. DeRosier (1989). The organization of the *Caulobacter crescentus* flagellar filament. *Journal of Molecular Biology* 206, pp. 627–636 (cit. on p. 14).
- Duchesne, I., T. Galstian, and S. Rainville (2017). Transient locking of the hook procures enhanced motility to flagellated bacteria. *Scientific Reports* 7.16354 (cit. on p. 100).

References

- Duke, T. A., N. Le Novère, and D. Bray (2001). Conformational spread in a ring of proteins: A stochastic approach to allostery. *Journal of Molecular Biology* 308, pp. 541–553 (cit. on p. 31).
- Eaves-Pyles, T. D., H. R. Wong, K. Odoms, and R. B. Pyles (2001). *Salmonella* flagellin-dependent proinflammatory responses are localized to the conserved amino and carboxyl regions of the protein. *The Journal of Immunology* 167, pp. 7009–7016 (cit. on p. 11).
- Ehlers, K. and G. Oster (2012). On the mysterious propulsion of *Synechococcus*. *PLoS ONE* 7.e36081 (cit. on p. 6).
- Eichler, J. (2012). Response to Jarrell and Albers: The name says it all. *Trends in Microbiology* 20, pp. 512–513 (cit. on p. 6).
- Ely, B., T. W. Ely, J. Crymes, and S. A. Minnich (2000). A family of six flagellin genes contributes to the *Caulobacter crescentus* flagellar filament. *Journal of Bacteriology* 182, pp. 5001–5004 (cit. on p. 14).
- Engelmann, T. W. (1881a). Neue Methode zur Untersuchung der Sauerstoffausscheidung pflanzlicher und thierischer Organismen. *Pflügers Archiv für die gesamte Physiologie des Menschen und der Tiere* 25, pp. 285–292 (cit. on p. 30).
- Engelmann, T. W. (1881b). Zur Biologie der Schizomyceten. *Pflügers Archiv für die gesamte Physiologie des Menschen und der Tiere* 26, pp. 537–545 (cit. on p. 30).
- Erhardt, M., H. M. Singer, D. H. Wee, J. P. Keener, and K. T. Hughes (2011). An infrequent molecular ruler controls flagellar hook length in *Salmonella enterica*. *EMBO Journal* 30, pp. 2948–2961 (cit. on p. 15).
- Evans, K. J., C. Lambert, and R. E. Sockett (2007). Predation by *Bdellovibrio bacteriovorus* HD100 requires type IV pili. *Journal of Bacteriology* 189, pp. 4850–4859 (cit. on p. 5).
- Ewing, C. P., E. Andreishcheva, and P. Guerry (2009). Functional characterization of flagellin glycosylation in *Campylobacter jejuni* 81-176. *Journal of Bacteriology* 191, pp. 7086–7093 (cit. on p. 13).
- Faguy, D. M., K. F. Jarrell, J. Kuzio, and M. L. Kalmokoff (1994). Molecular analysis of archael flagellins: similarity to the type IV pilin-transport superfamily widespread in bacteria. *Canadian Journal of Microbiology* 40, pp. 67–71 (cit. on p. 6).
- Faguy, D. M. and K. F. Farrell (1999). A twisted tale: the origin and evolution of motility and chemotaxis in prokaryotes. *Microbiology* 145, pp. 279–281 (cit. on p. 6).
- Falke, J. J. and G. L. Hazelbauer (2001). Transmembrane signaling in bacterial chemoreceptors. *Trends in Biochemical Sciences* 26, pp. 257–265 (cit. on p. 31).
- Farinha, M. A., B. D. Conway, L. M. G. Glasier, N. W. Ellert, R. T. Irvin, R. Sherburne, and W. Paranchych (1994). Alteration of the pilin adhesin of *Pseudomonas aeruginosa* PAO results in normal pilus biogenesis but a loss of adherence to human pneumocyte cells and decreased virulence in mice. *Infection and Immunity* 62, pp. 4118–4123 (cit. on p. 5).
- Faulds-Pain, A. et al. (2011). Flagellin redundancy in *Caulobacter crescentus* and its implications for flagellar filament assembly. *Journal of Bacteriology* 193, pp. 2695–2707 (cit. on pp. 13, 14, 111).
- Faulds-Pain, A., S. M. Twine, E. Vinogradov, P. C. R. Strong, A. Dell, A. M. Buckley, G. R. Douce, E. Valiente, S. M. Logan, and B. W. Wren (2014). The post-translational modification of the *Clostridium difficile* flagellin affects motility, cell surface properties and virulence. *Molecular Microbiology* 94, pp. 272–289 (cit. on p. 13).
- Faure, L. M. et al. (2016). The mechanism of force transmission at bacterial focal adhesion complexes. *Nature* 539, pp. 530–535 (cit. on p. 6).
- Fedorov, O. V., A. S. Kostyukova, and M. G. Pyatibratov (1988). Architectonics of a bacterial flagellin filament subunit. *FEBS Letters* 241, pp. 145–148 (cit. on p. 11).
- Fenchel, T. (1994). Motility and chemosensory behaviour of the sulphur bacterium *Thiovulum majus*. *Microbiology* 140, pp. 3109–3116 (cit. on p. 21).
- Fenchel, T. and R. Thar (2004). "*Candidatus* Ovobacter propellens": A large conspicuous prokaryote with an unusual motility behaviour. *FEMS Microbiology Ecology* 48, pp. 231–238 (cit. on pp. 22, 29).
- Fera, M. T., T. L. Maugeri, C. Gugliandolo, C. Beninati, M. Giannone, E. La Camera, and M. Carbone (2004). Detection of *Arcobacter* spp. in the coastal environment of the mediterranean sea. *Applied and Environmental Microbiology* 70, pp. 1271–1276 (cit. on p. 21).
- Ferrero, R. L. and A. Lee (1988). Motility of *Campylobacter jejuni* in a viscous environment: comparison with conventional rod-shaped bacteria. *Microbiology* 134, pp. 53–59 (cit. on p. 21).

References

- Ferris, H. U. and T. Minamino (2006). Flipping the switch: bringing order to flagellar assembly. *Trends in Microbiology* 14, pp. 519–526 (cit. on pp. 7, 15).
- Fitzgerald, D. M., R. P. Bonocora, and J. T. Wade (2014). Comprehensive mapping of the *Escherichia coli* flagellar regulatory network. *PLoS Genetics* 10.e1004649 (cit. on p. 15).
- Follet, E. A. C. and J. Gordon (1963). An electron microscope study of *Vibrio* flagella. *Microbiology* 32, pp. 235–239 (cit. on p. 12).
- Fox, J. G. (2002). The non-*H. pylori* helicobacters: Their expanding role in gastrointestinal and systemic diseases. *Gut* 50, pp. 273–283 (cit. on p. 13).
- Francis, N. R., G. E. Sosinsky, D. Thomas, and D. J. DeRosier (1994). Isolation, characterization and structure of bacterial flagellar motors containing the switch complex. *Journal of Molecular Biology* 235, pp. 1261–1270 (cit. on p. 7).
- Frankel, R. B., D. A. Bazylnski, M. S. Johnson, and B. L. Taylor (1997). Magneto-aerotaxis in marine coccoid bacteria. *Biophysical Journal* 73, pp. 994–1000 (cit. on p. 29).
- Fredrickson, J. K., J. M. Zachara, D. W. Kennedy, H. Dong, T. C. Onstott, N. W. Hinman, and S. M. Li (1998). Biogenic iron mineralization accompanying the dissimilatory reduction of hydrous ferric oxide by a groundwater bacterium. *Geochimica et Cosmochimica Acta* 62, pp. 3239–3257 (cit. on p. 96).
- Fuerst, J. A. and J. W. Perry (1988). Demonstration of lipopolysaccharide on sheathed flagella of *Vibrio cholerae* O:1 by protein A-gold immunoelectron microscopy. *Journal of Bacteriology* 170, pp. 1488–1494 (cit. on p. 12).
- Fujii, M., S. Shibata, and S. I. Aizawa (2008). Polar, peritrichous, and lateral flagella belong to three distinguishable flagellar families. *Journal of Molecular Biology* 379, pp. 273–283 (cit. on p. 9).
- Fujita, H., S. Yamaguchi, and T. Iino (1973). Studies on H-O variants in *Salmonella* in relation to phase variation. *Microbiology* 76, pp. 127–134 (cit. on p. 13).
- Furuno, S., K. Pätzolt, K. Rabe, T. R. Neu, H. Harms, and L. Y. Wick (2010). Fungal mycelia allow chemotactic dispersal of polycyclic aromatic hydrocarbon-degrading bacteria in water-unsaturated systems. *Environmental Microbiology* 12, pp. 1391–1398 (cit. on p. 20).
- Galkin, V. E., X. Yu, J. Bielnicki, J. Heuser, C. P. Ewing, P. Guerry, and E. H. Egelman (2008). Divergence of quaternary structures among bacterial flagellar filaments. *Science* 320, pp. 382–385 (cit. on pp. 9, 108).
- Garcia-Sucerquia, J., W. Xu, S. K. Jericho, P. Klages, M. H. Jericho, and H. J. Kreuzer (2006). Digital in-line holographic microscopy. *Applied Optics* 45, pp. 836–850 (cit. on p. 16).
- Garren, M., K. Son, J.-B. Raina, R. Rusconi, F. Menolascina, O. H. Shapiro, J. Tout, D. G. Bourne, J. R. Seymour, and R. Stocker (2014). A bacterial pathogen uses dimethylsulfoniopropionate as a cue to target heat-stressed corals. *The ISME Journal* 8, pp. 999–1007 (cit. on p. 29).
- Gestwicki, J. E., A. C. Lamanna, R. M. Harshey, L. L. McCarter, L. L. Kiessling, and J. Adler (2000). Evolutionary conservation of methyl-accepting chemotaxis protein location in bacteria and archaea. *Journal of Bacteriology* 182, pp. 6499–6502 (cit. on p. 31).
- Gibiansky, M. L., J. C. Conrad, F. Jin, V. D. Gordon, D. A. Motto, M. A. Mathewson, W. G. Stopka, D. C. Zelasko, J. D. Shrout, and G. C. L. Wong (2010). Bacteria Use Type IV Pili to Walk Upright and Detach from Surfaces. *Science* 330, pp. 197–197 (cit. on p. 5).
- Gillen, K. L. and K. T. Hughes (1991). Molecular characterization of *flgM*, a gene encoding a negative regulator of flagellin synthesis in *Salmonella typhimurium*. *Journal of Bacteriology* 173, pp. 6453–6459 (cit. on p. 15).
- Goldstein, S. F. and N. W. Charon (1990). Multiple-exposure photographic analysis of a motile spirochete. *Proceedings of the National Academy of Sciences* 87, pp. 4895–9 (cit. on p. 22).
- Goldstein, S. F., N. W. Charon, and J. A. Kreiling (1994). *Borrelia burgdorferi* swims with a planar waveform similar to that of eukaryotic flagella. *Proceedings of the National Academy of Sciences* 91, pp. 3433–3437 (cit. on p. 21).
- Goldstein, S. F., K. F. Buttle, and N. W. Charon (1996). Structural analysis of the *Leptospiraceae* and *Borrelia burgdorferi* by high-voltage electron microscopy. *Journal of Bacteriology* 178, pp. 6539–6545 (cit. on p. 21).
- Goon, S., J. F. Kelly, S. M. Logan, C. P. Ewing, and P. Guerry (2003). Pseudaminic acid, the major modification on *Campylobacter flagellin*, is synthesized via the Cj1293 gene. *Molecular Microbiology* 50, pp. 659–671 (cit. on p. 13).

References

- Goto, T., K. Nakata, K. Baba, M. Nishimura, and Y. Magariyama (2005). A fluid-dynamic interpretation of the asymmetric motion of singly flagellated bacteria swimming close to a boundary. *Biophysical Journal* 89, pp. 3771–3779 (cit. on p. 25).
- Götz, R., N. Limmer, K. Ober, and R. Schmitt (1982). Motility and chemotaxis in two strains of *Rhizobium* with complex flagella. *Journal of General Microbiology* 128, pp. 789–798 (cit. on pp. 12, 18, 28).
- Götz, R. and R. Schmitt (1987). *Rhizobium meliloti* swims by unidirectional, intermittent rotation of right-handed flagellar helices. *Journal of Bacteriology* 169, pp. 3146–3150 (cit. on pp. 12, 27, 28).
- Gray, J. (1955). The movement of sea-urchin spermatozoa. *Journal of Experimental Biology* 32, pp. 775–801 (cit. on p. 6).
- Green, J. C., C. Kahramanoglou, A. Rahman, A. M. Pender, N. Charbonnel, and G. M. Fraser (2009). Recruitment of the earliest component of the bacterial flagellum to the old cell division pole by a membrane-associated signal recognition particle family GTP-binding protein. *Journal of Molecular Biology* 391, pp. 679–690 (cit. on p. 14).
- Greenbury, C. L. and D. H. Moore (1966). The mechanism of bacterial immobilization by anti-flagellar IgG antibody. *Immunology* 11, pp. 617–625 (cit. on p. 23).
- Griffin, D. M. and G. Quail (1968). Movement of bacteria in moist, particulate systems. *Australian Journal of Biological Sciences* 21, pp. 579–582 (cit. on p. 20).
- Guerry, P., R. A. Alm, M. E. Power, S. M. Logan, and T. J. Trust (1991). Role of two flagellin genes in *Campylobacter motility*. *Journal of Bacteriology* 173, pp. 4757–4764 (cit. on p. 14).
- Guerry, P., P. Doig, R. A. Alm, D. H. Burr, N. Kinsella, and T. J. Trust (1996). Identification and characterization of genes required for post-translational modification of *Campylobacter coli* VC167 flagellin. *Molecular Microbiology* 19, pp. 369–378 (cit. on p. 13).
- Guerry, P., C. P. Ewing, M. Schirm, M. Lorenzo, J. Kelly, D. Pattarini, G. Majam, P. Thibault, and S. Logan (2006). Changes in flagellin glycosylation affect *Campylobacter* autoagglutination and virulence. *Molecular Microbiology* 60, pp. 299–311 (cit. on p. 13).
- Guttenplan, S. B., S. Shaw, and D. B. Kearns (2013). The cell biology of peritrichous flagella in *Bacillus subtilis*. *Molecular Microbiology* 87, pp. 211–229 (cit. on p. 14).
- Haiko, J. and B. Westerlund-Wikström (2013). The role of the bacterial flagellum in adhesion and virulence. *Biology* 2, pp. 1242–1267 (cit. on pp. 9, 11).
- Hajam, I. A., P. A. Dar, I. Shahnawaz, J. C. Jaume, and J. H. Lee (2017). Bacterial flagellin-a potent immunomodulatory agent. *Experimental and Molecular Medicine* 49 (cit. on p. 9).
- Harris, R. F. (1981). Effect of water potential on microbial growth and activity in soils. *Water potential relations in soil microbiology*. Ed. by J. F. Parr, W. R. Gardner, and L. F. Elliott. Soil Science Society of America, pp. 23–96.
- Harshey, R. M. and T. Matsuyama (1994). Dimorphic transition in *Escherichia coli* and *Salmonella typhimurium*: Surface-induced differentiation into hyperflagellate swarmer cells. *Proceedings of the National Academy of Sciences* 91, pp. 8631–8635 (cit. on p. 19).
- Harshey, R. M. (2003). Bacterial motility on a surface: many ways to a common goal. *Annual Review of Microbiology* 57, pp. 249–73 (cit. on p. 20).
- Harwood, C. S., K. Fosnaugh, and M. Dispensa (1989). Flagellation of *Pseudomonas putida* and analysis of its motile behavior. *Journal of Bacteriology* 171, pp. 4063–4066 (cit. on pp. 18, 103, 105).
- Hasegawa, E., R. Kamiya, and S. Asakura (1982). Thermal transition in helical forms of *Salmonella* flagella. *Journal of Molecular Biology* 160.4, pp. 609–621 (cit. on p. 11).
- Hasegawa, K., I. Yamashita, and K. Namba (1998). Quasi- and nonequivalence in the structure of bacterial flagellar filament. *Biophysical Journal* 74, pp. 569–575 (cit. on p. 11).
- Hau, H. H. and J. A. Gralnick (2007). Ecology and biotechnology of the genus *Shewanella*. *Annual Review of Microbiology* 61, pp. 237–58 (cit. on p. 32).
- Hayakawa, J. and M. Ishizuka (2012). Flagellar glycosylation: Current advances. *Glycosylation*. Ed. by S. Petrescu. IntechOpen, pp. 127–152 (cit. on p. 13).

References

- Hayashi, F., K. D. Smith, A. Ozinsky, T. R. Hawn, E. C. Yi, D. R. Goodlett, J. K. Eng, S. Akira, D. M. Underhill, and A. Aderem (2001). The innate immune response to bacterial flagellin is mediated by Toll-like receptor 5. *Nature* 410, pp. 1099–1103 (cit. on p. 11).
- Hazell, S. L., A. Lee, L. Brady, and W. Hennessey (1986). *Campylobacter pyloridis* and gastritis: Association with intercellular spaces and adaptation to an environment of mucus as important factors in colonization of the gastric epithelium. *Journal of Infectious Diseases* 153, pp. 658–663 (cit. on p. 21).
- Henderson, G. P. and G. J. Jensen (2006). Three-dimensional structure of *Mycoplasma pneumoniae*'s attachment organelle and a model for its role in gliding motility. *Molecular Microbiology* 60, pp. 376–385 (cit. on p. 6).
- Hennes, M., J. Tailleur, G. Charron, and A. Daerr (2017). Active depinning of bacterial droplets: The collective surfing of *Bacillus subtilis*. *Proceedings of the National Academy of Sciences* 114, pp. 5958–5963 (cit. on pp. 6, 20).
- Henrichsen, J. (1972). Bacterial surface translocation: A survey and a classification. *Bacteriological Reviews* 36, pp. 478–503 (cit. on p. 19).
- Hess, J. F., K. Oosawa, N. Kaplan, and M. I. Simon (1988). Phosphorylation of three proteins in the signaling pathway of bacterial chemotaxis. *Cell* 53, pp. 79–87 (cit. on p. 31).
- Hickman, J. W. and C. S. Harwood (2008). Identification of FleQ from *Pseudomonas aeruginosa* as a c-di-GMP-responsive transcription factor. *Molecular Microbiology* 69, pp. 376–389 (cit. on p. 15).
- Higdon, J. J. L. (1979). The hydrodynamics of flagellar propulsion: Helical waves. *Journal of Fluid Mechanics* 94, pp. 331–351 (cit. on p. 101).
- Hintsche, M., V. Waljor, R. Großmann, M. J. Kühn, K. M. Thormann, F. Peruani, and C. Beta (2017). A polar bundle of flagella can drive bacterial swimming by pushing, pulling, or coiling around the cell body. *Scientific Reports* 7.16771 (cit. on pp. 27, 30, 35, 103, 107, 110, 117).
- Hirano, T., S. Yamaguchi, K. Oosawa, and S. I. Aizawa (1994). Roles of FlhK and FlhB in determination of flagellar hook length in *Salmonella typhimurium*. *Journal of Bacteriology* 176, pp. 5439–5449 (cit. on p. 15).
- Hirota, N. and Y. Imae (1983). Na⁺-driven flagellar motors of an alkalophilic *Bacillus* strain YN-1. *Journal of Biological Chemistry* 258, pp. 10577–10581 (cit. on p. 22).
- Hizukuri, Y., S. Kojima, and M. Homma (2010). Disulphide cross-linking between the stator and the bearing components in the bacterial flagellar motor. *Journal of Biochemistry* 148, pp. 309–318 (cit. on p. 21).
- Hoeninger, J. F. M. (1965). Development of flagella by *Proteus mirabilis*. *Journal of General Microbiology* 40, pp. 29–42 (cit. on p. 19).
- Homma, M., D. J. DeRosier, and R. M. Macnab (1990). Flagellar hook and hook-associated proteins of *Salmonella typhimurium* and their relationship to other axial components of the flagellum. *Journal of Molecular Biology* 213, pp. 819–832 (cit. on p. 8).
- Horstmann, J. A. et al. (2017). Flagellin phase-dependent swimming on epithelial cell surfaces contributes to productive *Salmonella* gut colonisation. *Cellular Microbiology* 19 (cit. on p. 11).
- Hotani, H. (1980). Micro-video study of moving bacterial flagellar filaments II. Polymorphic transition in alcohol. *BioSystems* 12.3-4, pp. 325–330 (cit. on p. 11).
- Hotani, H. (1982). Micro-video study of moving flagellar filaments III. Cyclic transformation induced by mechanical force. *Journal of Molecular Biology* 156, pp. 791–806 (cit. on p. 11).
- Hughes, K. T. (2017). Flagellum length control: How long is long enough? *Current Biology* 27, R413–R415 (cit. on p. 15).
- Hughes, K. T., K. L. Gillen, M. J. Semon, and J. E. Karlinsey (1993). Sensing structural intermediates in bacterial flagellar assembly by export of a negative regulator. *Science* 262, pp. 1277–1280 (cit. on p. 15).
- Ichinose, Y. et al. (2013). Flagellin glycosylation is ubiquitous in a broad range of phytopathogenic bacteria. *Journal of General Plant Pathology* 79, pp. 359–365 (cit. on p. 13).
- Icopini, G. A., J. G. Lack, L. E. Hersman, M. P. Neu, and H. Boukhalfa (2009). Plutonium(V/VI) reduction by the metal-reducing bacteria *Geobacter metallireducens* GS-15 and *Shewanella oneidensis* MR-1. *Applied and Environmental Microbiology* 75, pp. 3641–3647 (cit. on p. 32).

References

- Iida, Y., L. Hobley, C. Lambert, A. K. Fenton, R. E. Sockett, and S. I. Aizawa (2009). Roles of multiple flagellins in flagellar formation and flagellar growth post bdelloplast lysis in *Bdellovibrio bacteriovorus*. *Journal of Molecular Biology* 394, pp. 1011–1021 (cit. on p. 115).
- Iino, T. (1969). Polarity of flagellar growth in *Salmonella*. *Journal of General Microbiology* 56, pp. 227–239 (cit. on p. 15).
- Iino, T. (1974). Assembly of *Salmonella* flagellin *in vitro* and *in vivo*. *Journal of Supramolecular Structure* 2, pp. 372–384 (cit. on p. 15).
- Iino, T. (1977). Genetics of structure and function of bacterial flagella. *Annual Review of Genetics* 11, pp. 161–182 (cit. on p. 11).
- Ikeda, J. S. et al. (2001). Flagellar phase variation of *Salmonella enterica* serovar typhimurium contributes to virulence in the murine typhoid infection model but does not influence *Salmonella*-induced enteropathogenesis. *Infection and Immunity* 69, pp. 3021–3030 (cit. on p. 13).
- Imada, K. (2018). Bacterial flagellar axial structure and its construction. *Biophysical Reviews* 10, pp. 559–570 (cit. on p. 10).
- Inoue, T., C. S. Barker, H. Matsunami, S.-I. Aizawa, and F. A. Samatey (2018). The FlaG regulator is involved in length control of the polar flagella of *Campylobacter jejuni*. *Microbiology* 164, pp. 740–750 (cit. on p. 113).
- Irikura, V. M., M. Kihara, S. Yamaguchi, H. Sockett, and R. M. Macnab (1993). *Salmonella typhimurium* *fliG* and *fliN* mutations causing defects in assembly, rotation, and switching of the flagellar motor. *Journal of Bacteriology* 175, pp. 802–810 (cit. on p. 7).
- Jabbarzadeh, M. and H. C. Fu (2018). Dynamic instability in the hook-flagellum system that triggers bacterial flicks. *Physical Review E* 97 (cit. on p. 115).
- Jarrell, K. F. and S. V. Albers (2012). The archaellum: An old motility structure with a new name. *Trends in Microbiology* 20, pp. 307–312 (cit. on p. 6).
- Jin, F., J. C. Conrad, M. L. Gibiansky, and G. C. L. Wong (2011). Bacteria use type-IV pili to slingshot on surfaces. *Proceedings of the National Academy of Sciences* 108, pp. 12617–12622 (cit. on p. 5).
- Jones, B. V., R. Young, E. Mahenthiralingam, and D. J. Stickler (2004). Ultrastructure of *Proteus mirabilis* swarmer cell rafts and role of swarming in catheter-associated urinary tract infection. *Infection and Immunity* 72, pp. 3941–3950 (cit. on p. 19).
- Joys, T. M. (1985). The covalent structure of the phase-1 flagellar filament protein of *Salmonella typhimurium* and its comparison with other flagellins. *Journal of Biological Chemistry* 260, pp. 15758–15761 (cit. on p. 11).
- Kagawa, H., S. I. Aizawa, and S. Asakura (1979). Transformations in isolated polyhooks. *Journal of Molecular Biology* 129, pp. 333–336 (cit. on p. 9).
- Kamiya, R. and S. Asakura (1976a). Flagellar transformations at alkaline pH. *Journal of Molecular Biology* 108, pp. 513–518 (cit. on p. 11).
- Kamiya, R. and S. Asakura (1976b). Helical transformations of *Salmonella* flagella *in vitro*. *Journal of Molecular Biology* 106, pp. 167–186 (cit. on p. 11).
- Kanehisa, M. et al. (2008). KEGG for linking genomes to life and the environment. *Nucleic Acids Research* 36, pp. D480–D484 (cit. on p. 14).
- Kanto, S., H. Okino, S. I. Aizawa, and S. Yamaguchi (1991). Amino acids responsible for flagellar shape are distributed in terminal regions of flagellin. *Journal of Molecular Biology* 219, pp. 471–480 (cit. on p. 11).
- Kato, S., M. Okamoto, and S. Asakura (1984). Polymorphic transition of the flagellar polyhook from *Escherichia coli* and *Salmonella typhimurium*. *Journal of Molecular Biology* 173, pp. 463–476 (cit. on p. 9).
- Kearns, D. B. (2010). A field guide to bacterial swarming motility. *Nature Reviews Microbiology* 8, pp. 634–44 (cit. on p. 19).
- Kearns, D. B. and R. Losick (2003). Swarming motility in undomesticated *Bacillus subtilis*. *Molecular Microbiology* 49, pp. 581–590 (cit. on p. 19).
- Kehry, M. R., T. G. Doak, and F. W. Dahlquist (1985). Sensory adaptation in bacterial chemotaxis: Regulation of demethylation. *Journal of Bacteriology* 163, pp. 983–990 (cit. on p. 31).

References

- Khan, S., R. M. Macnab, A. L. DeFranco, and D. E. Koshland (1978). Inversion of a behavioral response in bacterial chemotaxis: Explanation at the molecular level. *Proceedings of the National Academy of Sciences* 75, pp. 4150–4154 (cit. on p. 26).
- Kiehlbauch, J. A., D. J. Brenner, M. A. Nicholson, C. N. Baker, C. M. Patton, A. G. Steigerwalt, and I. K. Wachsmuth (1991). *Campylobacter butzleri* sp. nov. isolated from humans and animals with diarrheal illness. *Journal of Clinical Microbiology* 29, pp. 376–385 (cit. on p. 21).
- Kim, S. Y., X. T. T. Thanh, K. Jeong, S. B. Kim, S. O. Pan, C. H. Jung, S. H. Hong, S. E. Lee, and J. H. Rhee (2014). Contribution of six flagellin genes to the flagellum biogenesis of *Vibrio vulnificus* and *in vivo* invasion. *Infection and Immunity* 82, pp. 29–42 (cit. on p. 14).
- Kinosita, Y., Y. Kikuchi, N. Mikami, D. Nakane, and T. Nishizaka (2017). Unforeseen swimming and gliding mode of an insect gut symbiont, *Burkholderia* sp. RPE64, with wrapping of the flagella around its cell body. *The ISME Journal* 12, pp. 838–848 (cit. on pp. 35, 102, 103).
- Kirov, S. M., B. C. Tassell, A. B. Semmler, L. A. O'Donovan, A. A. Rabaan, and J. G. Shaw (2002). Lateral flagella and swarming motility in *Aeromonas* species. *Journal of Bacteriology* 184, pp. 547–555 (cit. on p. 19).
- Kodama, Y. and K. Watanabe (2004). *Sulfuricurvum kujiense* gen. nov., sp. nov., a facultatively anaerobic, chemolithoautotrophic, sulfur-oxidizing bacterium isolated from an underground crude-oil storage cavity. *International Journal of Systematic and Evolutionary Microbiology* 54, pp. 2297–2300 (cit. on p. 21).
- Kogure, K., U. Simidu, and N. Taga (1981). Bacterial attachment to phytoplankton in sea water. *Journal of Experimental Marine Biology and Ecology* 56, pp. 197–204 (cit. on p. 16).
- Kohlmeier, S., T. H. M. Smits, R. M. Ford, C. Keel, H. Harms, and L. Y. Wick (2005). Taking the fungal highway: Mobilization of pollutant-degrading bacteria by fungi. *Environmental Science and Technology* 39, pp. 4640–4646 (cit. on p. 20).
- Kojima, S. and D. F. Blair (2001). Conformational change in the stator of the bacterial flagellar motor. *Biochemistry* 40, pp. 13041–13050 (cit. on p. 7).
- Kojima, S., K. Yamamoto, I. Kawagishi, and M. Homma (1999). The polar flagellar motor of *Vibrio cholerae* is driven by an Na⁺ motive force. *Journal of Bacteriology* 181, pp. 1927–1930 (cit. on pp. 7, 22).
- Kostrzynska, M., J. D. Betts, J. W. Austin, and T. J. Trust (1991). Identification, characterization, and spatial localization of two flagellin species in *Helicobacter pylori* flagella. *Journal of Bacteriology* 173, pp. 937–946 (cit. on p. 14).
- Koyasu, S. and Y. Shirahihara (1984). *Caulobacter crescentus* flagellar filament has a right-handed helical form. *Journal of Molecular Biology* 173, pp. 125–130 (cit. on p. 28).
- Krikos, A., N. Mutoh, A. Boyd, and M. I. Simon (1983). Sensory transducers of *E. coli* are composed of discrete structural and functional domains. *Cell* 33, pp. 615–622 (cit. on p. 31).
- Kubori, T., M. Okumura, N. Kobayashi, D. Nakamura, M. Iwakura, and S. I. Aizawa (1997). Purification and characterization of the flagellar hook-basal body complex of *Bacillus subtilis*. *Molecular Microbiology* 24, pp. 399–410 (cit. on p. 7).
- Kudo, S., Y. Magariyama, and S. I. Aizawa (1990). Abrupt changes in flagellar rotation observed by laser dark-field microscopy. *Nature* 346, pp. 677–680 (cit. on p. 22).
- Kühn, M. J., F. K. Schmidt, B. Eckhardt, and K. M. Thormann (2017). Bacteria exploit a polymorphic instability of the flagellar filament to escape from traps. *Proceedings of the National Academy of Sciences* 114, pp. 6340–6345 (cit. on pp. 34, 35, 54, 55, 96, 98, 101, 109).
- Kühn, M. J., F. K. Schmidt, N. E. Farthing, F. M. Rossmann, B. Helm, L. G. Wilson, B. Eckhardt, and K. M. Thormann (2018). Spatial arrangement of several flagellins within bacterial flagella improves motility in different environments. *Nature Communications* 9.5369 (cit. on pp. 54, 55, 106, 107, 110–114).
- Kusumoto, A., K. Kamisaka, T. Yakushi, H. Terashima, A. Shinohara, and M. Homma (2006). Regulation of polar flagellar number by the *flhF* and *flhG* genes in *Vibrio alginolyticus*. *Journal of Biochemistry* 139, pp. 113–121 (cit. on p. 14).
- Kusumoto, A., A. Shinohara, H. Terashima, S. Kojima, T. Yakushi, and M. Homma (2008). Collaboration of FlhF and FlhG to regulate polar flagella number and localization in *Vibrio alginolyticus*. *Microbiology* 154, pp. 1390–1399 (cit. on p. 14).
- Kutsukake, K., Y. Ohya, and T. Iino (1990). Transcriptional analysis of the flagellar regulon of *Salmonella typhimurium*. *Journal of Bacteriology* 172, pp. 741–747 (cit. on p. 15).

References

- Kutsukake, K. and T. Iino (1980). Inversions of specific DNA segments in flagellar phase variation of *Salmonella* and inversion systems of bacteriophages P1 and Mu. *Proceedings of the National Academy of Sciences* 77, pp. 7338–7341 (cit. on p. 13).
- Lambert, C., K. J. Evans, R. Till, L. Hobley, M. Capeness, S. Rendulic, S. C. Schuster, S. I. Aizawa, and R. E. Sockett (2006). Characterizing the flagellar filament and the role of motility in bacterial prey-penetration by *Bdellovibrio bacteriovorus*. *Molecular Microbiology* (cit. on pp. 14, 115).
- Larsen, S. H., R. W. Reader, E. N. Kort, W. W. Tso, and J. Adler (1974). Change in direction of flagellar rotation is the basis of the chemotactic response in *Escherichia coli*. *Nature* 249, pp. 74–77 (cit. on pp. 23, 26).
- Leake, M. C., J. H. Chandler, G. H. Wadhams, F. Bai, R. M. Berry, and J. P. Armitage (2006). Stoichiometry and turnover in single, functioning membrane protein complexes. *Nature* 443, pp. 355–358 (cit. on p. 7).
- Lederberg, J. and T. Iino (1956). Phase variation in *Salmonella*. *Genetics* 41, pp. 743–57 (cit. on p. 13).
- Lee, A., S. L. Hazell, J. O'Rourke, and S. Kouprach (1988). Isolation of a spiral-shaped bacterium from the cat stomach. *Infection and Immunity* 56, pp. 2843–2850 (cit. on p. 21).
- Leifson, E. (1960). *Atlas of bacterial flagellation*. Academic Press, New York and London (cit. on p. 18).
- Leifson, E., B. J. Cosenza, R. Murchelano, and R. C. Cleverdon (1964). Motile marine bacteria I. techniques, ecology, and general. *Journal of Bacteriology* 87, pp. 652–666 (cit. on pp. 16, 28).
- Lele, P. P., B. G. Hosu, and H. C. Berg (2013). Dynamics of mechanosensing in the bacterial flagellar motor. *Proceedings of the National Academy of Sciences* 110, pp. 11839–11844 (cit. on pp. 97, 117).
- Lertsethtakarn, P., K. M. Ottemann, and D. R. Hendrixson (2011). Motility and Chemotaxis in *Campylobacter* and *Helicobacter*. *Annual Review of Microbiology* 65, pp. 389–410 (cit. on p. 21).
- Li, C., A. Motaleb, M. Sal, S. F. Goldstein, and N. W. Charon (2000a). Spirochete periplasmic flagella and motility. *Journal of Molecular Microbiology and Biotechnology* 2, pp. 345–354 (cit. on p. 21).
- Li, C., L. Corum, D. Morgan, E. L. Rosey, T. B. Stanton, and N. W. Charon (2000b). The spirochete FlaA periplasmic flagellar sheath protein impacts flagellar helicity. *Journal of Bacteriology* 182, pp. 6698–6706 (cit. on p. 115).
- Li, C., C. W. Wolgemuth, M. Marko, D. G. Morgan, and N. W. Charon (2008). Genetic analysis of spirochete flagellin proteins and their involvement in motility, filament assembly, and flagellar morphology. *Journal of Bacteriology* 190, pp. 5607–5615 (cit. on p. 115).
- Li, C., M. Sal, M. Marko, and N. W. Charon (2010). Differential regulation of the multiple flagellins in spirochetes. *Journal of Bacteriology* 192, pp. 2596–2603 (cit. on pp. 113, 115).
- Li, G. and J. X. Tang (2006). Low flagellar motor torque and high swimming efficiency of *Caulobacter crescentus* swarmer cells. *Biophysical Journal* 91, pp. 2726–2734 (cit. on p. 17).
- Li, H. and V. Sourjik (2011). Assembly and stability of flagellar motor in *Escherichia coli*. *Molecular Microbiology* 80, pp. 886–899 (cit. on p. 14).
- Lim, S. and C. S. Peskin (2012). Fluid-mechanical interaction of flexible bacterial flagella by the immersed boundary method. *Physical Review E* 85 (cit. on p. 26).
- Lin, T., E. B. Troy, L. T. Hu, L. Gao, and S. J. Norris (2014). Transposon mutagenesis as an approach to improved understanding of *Borrelia pathogenesis* and biology. *Frontiers in Cellular and Infection Microbiology* 4 (cit. on p. 22).
- Liu, B., M. Gulino, M. Morse, T. R. Powers, J. X. Tang, and K. S. Breuer (2014). Helical motion of the cell body enhances *Caulobacter crescentus* motility. *Proceedings of the National Academy of Sciences* 111, pp. 11252–11256 (cit. on p. 29).
- Liu, R. and H. Ochman (2007). Origins of flagellar gene operons and secondary flagellar systems. *Journal of Bacteriology* 189, pp. 7098–7104 (cit. on p. 19).
- Lloyd, S. A., H. Tang, X. Wang, S. Billings, and D. F. Blair (1996). Torque generation in the flagellar motor of *Escherichia coli*: Evidence of a direct role for FliG but not for FliM or FliN. *Journal of Bacteriology* 178, pp. 223–231 (cit. on p. 7).
- Locsei, J. T. and T. J. Pedley (2009). Bacterial tracking of motile algae assisted by algal cell's vorticity field. *Microbial Ecology* 58, pp. 63–74 (cit. on p. 17).
- Loewy, Z. G., R. A. Bryan, S. H. Reuter, and L. Shapiro (1987). Control of synthesis and positioning of a *Caulobacter crescentus* flagellar protein. *Genes and Development* 1, pp. 626–635.

References

- Logan, S. M., T. J. Trust, and P. Guerry (1989). Evidence for posttranslational modification and gene duplication of *Campylobacter* flagellin. *Journal of Bacteriology* 171, pp. 3031–3038 (cit. on p. 13).
- Logan, S. M. (2006). Flagellar glycosylation - A new component of the motility repertoire? *Microbiology* 152, pp. 1249–1262 (cit. on p. 13).
- Logan, S. M., J. F. Kelly, P. Thibault, C. P. Ewing, and P. Guerry (2002). Structural heterogeneity of carbohydrate modifications affects serospecificity of *Campylobacter* flagellins. *Molecular Microbiology* 46, pp. 587–597 (cit. on p. 13).
- Lovgren, A., M.-Y. Zhang, A. Engstrom, and R. Landen (2009). Identification of two expressed flagellin genes in the insect pathogen *Bacillus thuringiensis* subsp. *alesti*. *Journal of General Microbiology* 139, pp. 21–30 (cit. on p. 14).
- Lovley, D. R., E. J. Phillips, Y. A. Gorby, and E. R. Landa (1991). Microbial reduction of uranium. *Nature* 350, pp. 413–416 (cit. on p. 32).
- Lowe, G., M. Meister, and H. C. Berg (1987). Rapid rotation of flagellar bundles in swimming bacteria. *Nature* 325.6105, pp. 637–640 (cit. on p. 22).
- Luke, C. J. and C. W. Penn (1995). Identification of a 29 kDa flagellar sheath protein in *Helicobacter pylori* using a murine monoclonal antibody. *Microbiology* 141, pp. 597–604 (cit. on p. 12).
- Machin, K. E. (1963). The control and synchronization of flagellar movement. *Proceedings of the Royal Society of London* 158, pp. 88–104 (cit. on p. 26).
- Macnab, R. M. (1977). Bacterial flagella rotating in bundles: A study in helical geometry. *Proceedings of the National Academy of Sciences* 74, pp. 221–225 (cit. on p. 26).
- Macnab, R. M. and M. K. Ornston (1977). Normal-to-curly flagellar transitions and their role in bacterial tumbling. Stabilization of an alternative quaternary structure by mechanical force. *Journal of Molecular Biology* 112, pp. 1–30 (cit. on pp. 11, 26, 27).
- Maddock, J. R. and L. Shapiro (1993). Polar location of the chemoreceptor complex in the *Escherichia coli* cell. *Science* 259, pp. 1717–1723 (cit. on p. 31).
- Magariyama, Y., S. Sugiyama, K. Muramoto, Y. Maekawa, I. Kawagishi, Y. Imae, and S. Kudo (1994). *Very fast flagellar rotation* (cit. on pp. 17, 18, 22).
- Maki-Yonekura, S., K. Yonekura, and K. Namba (2010). Conformational change of flagellin for polymorphic supercoiling of the flagellar filament. *Nature structural & molecular biology* 17, pp. 417–422 (cit. on pp. 9–11).
- Maniyeri, R. and S. Kang (2014). Numerical study on bacterial flagellar bundling and tumbling in a viscous fluid using an immersed boundary method. *Applied Mathematical Modelling* 38, pp. 3567–3590 (cit. on p. 26).
- Manson, M. D., P. Tedesco, H. C. Berg, F. M. Harold, and C. Van der Drift (1977). A protonmotive force drives bacterial flagella. *Proceedings of the National Academy of Sciences* 74, pp. 3060–3064 (cit. on p. 22).
- Martínez, A., S. Torello, and R. Kolter (1999). Sliding motility in *Mycobacteria*. *Journal of Bacteriology* 181, pp. 7331–7338 (cit. on p. 6).
- Martinez, V. A., J. Schwarz-Linek, M. Reufer, L. G. Wilson, A. N. Morozov, and W. C. K. Poon (2014). Flagellated bacterial motility in polymer solutions. *Proceedings of the National Academy of Sciences* 111, pp. 17771–17776 (cit. on p. 97).
- Matz, C. and K. Jürgens (2005). High motility reduces grazing mortality of planktonic bacteria. *Applied and Environmental Microbiology* 71, pp. 921–929 (cit. on p. 13).
- McCarter, L. L. (2001). Polar flagellar motility of the *Vibrionaceae*. *Microbiology and Molecular Biology Reviews* 65, 445–462, table of contents (cit. on pp. 15, 16).
- McCarter, L. L. (2004). Dual flagellar systems enable motility under different circumstances. *Journal of Molecular Microbiology and Biotechnology* 7, pp. 18–29 (cit. on p. 19).
- McCarter, L. L. (2006). Regulation of flagella. *Current Opinion in Microbiology* 9, pp. 180–186 (cit. on pp. 15, 16).
- McCarter, L. L., M. Hilmen, and M. Silverman (1988). Flagellar dynamometer controls swarmer cell differentiation of *V. parahaemolyticus*. *Cell* 54, pp. 345–351 (cit. on pp. 17, 18).
- McCarter, L. L. and M. Silverman (1990). Surface-induced swarmer cell differentiation of *Vibrio parahaemolyticus*. *Molecular Microbiology* 4, pp. 1057–1062 (cit. on pp. 12, 17, 18).

References

- McClung, C., D. Patriquin, and R. Davis (1983). *Campylobacter nitrofigilis* sp. nov., a nitrogen-fixing bacterium associated with roots of *Spartina alterniflora* Loisel. *International Journal of Systematic Bacteriology* 33, pp. 605–612 (cit. on p. 21).
- McGee, K., P. Hörstedt, and D. L. Milton (1996). Identification and characterization of additional flagellin genes from *Vibrio anguillarum*. *Journal of Bacteriology* 178, pp. 5188–5198 (cit. on p. 113).
- McQuiston, J. R., P. I. Fields, R. V. Tauxe, and J. M. Logsdon (2008). Do *Salmonella* carry spare tyres? *Trends in Microbiology* 16, pp. 142–148 (cit. on p. 13).
- Merino, S. and J. M. Tomás (2014). Gram-negative flagella glycosylation. *International Journal of Molecular Sciences* 15, pp. 2840–2857 (cit. on p. 13).
- Merz, A. J., M. So, and M. P. Sheetz (2000). Pilus retraction powers bacterial twitching motility. *Nature* 407, pp. 98–102 (cit. on p. 5).
- Metzner, P. (1920). Die Bewegung und Reizbeantwortung der bipolar begeißelten Spirillen. *Jahrbücher für wissenschaftliche Botanik*. Vol. 59. Verlag von Gebrüder Borntraeger, Leipzig, pp. 957–958 (cit. on pp. 30, 96, 102).
- Mignot, T., J. W. Shaevitz, P. L. Hartzell, and D. R. Zusman (2007). Evidence that focal adhesion complexes power bacterial gliding motility. *Science* 315, pp. 853–856 (cit. on p. 6).
- Milburn, M. V., G. G. Privé, D. L. Milligan, W. G. Scott, J. Yeh, J. Jancarik, D. E. Koshland, and S. H. Kim (1991). Three-dimensional structures of the ligand-binding domain of the bacterial aspartate receptor with and without a ligand. *Science* 254, pp. 1342–1347 (cit. on p. 31).
- Miller, W. L., M. J. Matewish, D. J. McNally, N. Ishiyama, E. M. Anderson, D. Brewer, J. R. Brisson, A. M. Berghuis, and J. S. Lam (2008). Flagellin glycosylation in *Pseudomonas aeruginosa* PAK requires the O-antigen biosynthesis enzyme WbpO. *Journal of Biological Chemistry* 283, pp. 3507–3518 (cit. on p. 13).
- Millikan, D. S. and E. G. Ruby (2004). *Vibrio fischeri* flagellin A is essential for normal motility and for symbiotic competence during initial squid light organ colonization. *Journal of Bacteriology* 186, pp. 4315–4325 (cit. on p. 14).
- Minamino, T. and K. Namba (2004). Self-assembly and type III protein export of the bacterial flagellum. *Journal of Molecular Microbiology and Biotechnology* 7, pp. 5–17 (cit. on p. 7).
- Minamino, T., H. U. Ferris, N. Moriya, M. Kihara, and K. Namba (2006). Two parts of the T3S4 domain of the hook-length control protein fliK are essential for the substrate specificity switching of the flagellar type III export apparatus. *Journal of Molecular Biology* 362, pp. 1148–1158 (cit. on p. 15).
- Minamino, T., K. Imada, and K. Namba (2008). Mechanisms of type III protein export for bacterial flagellar assembly. *Molecular BioSystems* 4, pp. 1105–1115 (cit. on p. 7).
- Mitchell, J. G. (1991). The influence of cell size on marine bacterial motility and energetics. *Microbial Ecology* 22, pp. 227–238 (cit. on pp. 16, 17).
- Mitchell, J. G. (2002). The energetics and scaling of search strategies in bacteria. *The American Naturalist* 160, pp. 727–740 (cit. on pp. 16, 17).
- Miyata, M. (2008). Centipede and inchworm models to explain *Mycoplasma* gliding. *Trends in Microbiology* 16, pp. 6–12 (cit. on p. 6).
- Mohari, B., M. A. Thompson, J. C. Trinidad, S. Setayeshgar, and C. Fuqua (2018). Multiple flagellin proteins have distinct and synergistic roles in *Agrobacterium tumefaciens* motility. *Journal of Bacteriology*, pp. 812–856 (cit. on p. 14).
- Molaei, M. and J. Sheng (2014). Imaging bacterial 3D motion using digital in-line holographic microscopy and correlation-based de-noising algorithm. *Optics Express* 22, pp. 32119–32137 (cit. on p. 16).
- Morett, E. and L. Segovia (1993). The σ^{54} bacterial enhancer-binding protein family: Mechanism of action and phylogenetic relationship of their functional domains. *Journal of Bacteriology* 175, pp. 6067–6074 (cit. on p. 16).
- Morgan, D. G., J. W. Baumgartner, and G. L. Hazelbauer (1993a). Proteins antigenically related to methyl-accepting chemotaxis proteins of *Escherichia coli* detected in a wide range of bacterial species. *Journal of Bacteriology* 175, pp. 133–140 (cit. on p. 31).
- Morgan, D. G., R. M. Macnab, N. R. Francis, and D. J. DeRosier (1993b). Domain organization of the subunit of the *Salmonella typhimurium* flagellar hook. *Journal of Molecular Biology* 229, pp. 79–84 (cit. on p. 9).

References

- Murat, D., M. Hérissé, L. Espinosa, A. Bossa, F. Alberto, and L.-F. Wu (2015). Opposite and coordinated rotation of amphitrichous flagella governs oriented swimming and reversals in a magnetotactic spirillum. *Journal of Bacteriology* 197, pp. 3275–3282 (cit. on pp. 27, 30, 96, 102, 104).
- Murthy, K. G. K., A. Deb, S. Goonesekera, C. Szabó, and A. L. Salzman (2004). Identification of conserved domains in *Salmonella muenchen* flagellin that are essential for its ability to activate TLR5 and to induce an inflammatory response *in vitro*. *Journal of Biological Chemistry* 279, pp. 5667–5675 (cit. on p. 11).
- Muskotál, A., R. Király, A. Sebestyén, Z. Gugolya, B. M. Végh, and F. Vonderviszt (2006). Interaction of FliS flagellar chaperone with flagellin. *FEBS Letters* 580, pp. 3916–3920 (cit. on p. 15).
- Myers, C. R. and K. H. Nealson (1988). Bacterial manganese reduction and growth with manganese oxide as the sole electron acceptor. *Science* 240, pp. 1319–1321 (cit. on p. 32).
- Myers, C. R. and K. H. Nealson (1990). Respiration-linked proton translocation couples to anaerobic reduction of manganese(IV) and iron(III) in *Shewanella putrefaciens* MR-1. *Journal of Bacteriology* 172, pp. 6232–6238 (cit. on pp. 32, 96).
- Nakane, D., K. Sato, H. Wada, M. J. McBride, and K. Nakayama (2013). Helical flow of surface protein required for bacterial gliding motility. *Proceedings of the National Academy of Sciences* 110, pp. 11145–11150 (cit. on p. 5).
- Namba, K., I. Yamashita, and F. Vonderviszt (1989). Structure of the core and central channel of bacterial flagella. *Nature* 342, pp. 648–654 (cit. on p. 9).
- Nelson, S. S., S. Bollampalli, and M. J. McBride (2008). SprB is a cell surface component of the *Flavobacterium johnsoniae* gliding motility machinery. *Journal of Bacteriology* 190, pp. 2851–2857 (cit. on p. 5).
- Newton, S. M., R. D. Wasley, A. Wilson, L. T. Rosenberg, J. F. Miller, and B. A. Stocker (1991). Segment IV of a *Salmonella* flagellin gene specifies flagellar antigen epitopes. *Molecular Microbiology* 5, pp. 419–425 (cit. on p. 11).
- Noguchi, H. (1918). Morphological characteristics and nomenclature of *Leptospira (Spirochaeta) icterohaemorrhagiae* (Inada and Ido). *Journal of Experimental Medicine* 27, pp. 575–592 (cit. on p. 22).
- Nothhaft, H. and C. M. Szymanski (2010). Protein glycosylation in bacteria: Sweeter than ever. *Nature Reviews Microbiology* 8, pp. 765–778 (cit. on p. 13).
- Nuijten, P. J. M., F. J. A. M. van Asten, W. Gaastra, and van der Zeijst Bernard A. M. (1990). Structural and functional analysis of two *Campylobacter jejuni* flagellin genes. *The Journal of Biological Chemistry* 265, pp. 798–17804 (cit. on p. 14).
- O'Brien, E. J. and P. M. Bennett (1972). Structure of Straight flagella from a mutant *Salmonella*. *Journal of Molecular Biology* 70, pp. 133–144 (cit. on p. 9).
- Ohnishi, K., K. Kutsukake, H. Suzuki, and T. Iino (1990). Gene *fliA* encodes an alternative sigma factor specific for flagellar operons in *Salmonella typhimurium*. *MGG Molecular & General Genetics* 221, pp. 139–147 (cit. on p. 15).
- On, S. (2001). Taxonomy of *Campylobacter*, *Arcobacter*, *Helicobacter* and related bacteria: current status, future prospects and immediate concerns. *Journal of Applied Microbiology* 90, 1S–15S (cit. on p. 21).
- Or, D., B. F. Smets, J. M. Wraith, A. Dechesne, and S. P. Friedman (2007). Physical constraints affecting bacterial habitats and activity in unsaturated porous media - a review. *Advances in Water Resources* 30, pp. 1505–1527 (cit. on pp. 19, 20).
- O'Toole, G. A. and R. Kolter (1998). Flagellar and twitching motility are necessary for *Pseudomonas aeruginosa* biofilm development. *Molecular Microbiology* 30, pp. 295–304 (cit. on p. 5).
- Ozin, A. J., L. Claret, F. Auvray, and C. Hughes (2003). The FliS chaperone selectively binds the disordered flagellin C-terminal D0 domain central to polymerisation. *FEMS Microbiology Letters* 219, pp. 219–224 (cit. on p. 15).
- Paul, K. and D. F. Blair (2006). Organization of FliN subunits in the flagellar motor of *Escherichia coli*. *Journal of Bacteriology* 188, pp. 2502–2511 (cit. on p. 31).
- Paulick, A., A. Koerdt, J. Lassak, S. Huntley, I. Wilms, F. Narberhaus, and K. M. Thormann (2009). Two different stator systems drive a single polar flagellum in *Shewanella oneidensis* MR-1. *Molecular Microbiology* 71, pp. 836–850 (cit. on p. 32).

References

- Paulick, A., N. J. Delalez, S. Brenzinger, B. C. Steel, R. M. Berry, J. P. Armitage, and K. M. Thormann (2015). Dual stator dynamics in the *Shewanella oneidensis* MR-1 flagellar motor. *Molecular Microbiology* 96, pp. 993–1001 (cit. on pp. 7, 32).
- Pearce, U. B. and B. A. D. Stocker (1967). Phase variation of flagellar antigens in *Salmonella*: Abortive transduction studies. *Microbiology* 49, pp. 335–349 (cit. on p. 13).
- Picardeau, M., A. Brenot, and I. Saint Girons (2001). First evidence for gene replacement in *Leptospira* spp. Inactivation of *L. biflexa* flaB results in non-motile mutants deficient in endoflagella. *Molecular Microbiology* 40, pp. 189–199 (cit. on p. 21).
- Pilizota, T., M. T. Brown, M. C. Leake, R. W. Branch, R. M. Berry, and J. P. Armitage (2009). A molecular brake, not a clutch, stops the *Rhodobacter sphaeroides* flagellar motor. *Proceedings of the National Academy of Sciences* 106, pp. 11582–11587 (cit. on p. 30).
- Ping, L. (2012). Cell orientation of swimming bacteria: From theoretical simulation to experimental evaluation. *Science China Life Sciences* 55, pp. 202–209 (cit. on pp. 8, 17, 18, 20, 28, 105).
- Ping, L., J. Birkenbeil, and S. Monajembashi (2013). Swimming behavior of the monotrichous bacterium *Pseudomonas fluorescens* SBW25. *FEMS Microbiology Ecology* 86, pp. 36–44 (cit. on pp. 18, 20, 27–29).
- Pion, M., R. Bshary, S. Bindschedler, S. Filippidou, L. Y. Wick, D. Job, and P. Junier (2013). Gains of bacterial flagellar motility in a fungal world. *Applied and Environmental Microbiology* 79, pp. 6862–6867 (cit. on p. 20).
- Platzer, J., W. Sterr, M. Hausmann, and R. Schmitt (1997). Three genes of a motility operon and their role in flagellar rotary speed variation in *Rhizobium meliloti*. *Journal of Bacteriology* 179, pp. 6391–6399 (cit. on p. 28).
- Poggio, S., C. Abreu-Goodger, S. Fabela, A. Osorio, G. Dreyfus, P. Vinuesa, and L. Camarena (2007). A complete set of flagellar genes acquired by horizontal transfer coexists with the endogenous flagellar system in *Rhodobacter sphaeroides*. *Journal of Bacteriology* 189, pp. 3208–3216 (cit. on p. 19).
- Prouty, M. G., N. E. Correa, and K. E. Klose (2001). The novel σ^{54} - and σ^{28} -dependent flagellar gene transcription hierarchy of *Vibrio cholerae*. *Molecular Microbiology* 39, pp. 1595–1609 (cit. on p. 15).
- Purcell, E. M. (1977). Life at low Reynolds number. *American Journal of Physics* 45, p. 3 (cit. on pp. 16, 22, 23).
- Purcell, E. M. (1997). The efficiency of propulsion by a rotating flagellum. *Proceedings of the National Academy of Sciences* 94, pp. 11307–11311 (cit. on p. 16).
- Raatz, M., M. Hintsche, M. Bahrs, M. Theves, and C. Beta (2015). Swimming patterns of a polarly flagellated bacterium in environments of increasing complexity. *European Physical Journal: Special Topics* 224, pp. 1185–1198 (cit. on p. 16).
- Ramanan, R., B. H. Kim, D. H. Cho, H. M. Oh, and H. S. Kim (2016). *Algae-bacteria interactions: Evolution, ecology and emerging applications* (cit. on p. 16).
- Reboul, C. F., D. A. Andrews, M. F. Nahar, A. M. Buckle, and A. Roujeinikova (2011). Crystallographic and molecular dynamics analysis of loop motions unmasking the peptidoglycan-binding site in stator protein MotB of flagellar motor. *PLoS ONE* 6:e18981 (cit. on p. 21).
- Reichert, K. (1909). Über die Sichtbarmachung der Geisseln und die Geisselbewegung der Bakterien. *Zentralblatt für Bakteriologie, Parasitenkunde und Infektionskrankheiten* 51, pp. 14–94 (cit. on pp. 27, 29, 102).
- Reid, S. W., M. C. Leake, J. H. Chandler, C.-J. Lo, J. P. Armitage, and R. M. Berry (2006). The maximum number of torque-generating units in the flagellar motor of *Escherichia coli* is at least 11. *Proceedings of the National Academy of Sciences* 103, pp. 8066–8071 (cit. on pp. 7, 21).
- Reid, S. D., R. K. Selander, and T. S. Whittam (1999). Sequence diversity of flagellin (fliC) alleles in pathogenic *Escherichia coli*. *Journal of Bacteriology* 181, pp. 153–160 (cit. on p. 11).
- Renault, T. T. et al. (2017). Bacterial flagella grow through an injection-diffusion mechanism. *eLife* 6 (cit. on pp. 15, 112).
- Ringo, D. L. (1967). Flagellar motion and fine structure of the flagellar apparatus in *Chlamydomonas*. *The Journal of cell biology* 33.3, pp. 543–571 (cit. on p. 23).
- Rohwer, F., V. Seguritan, F. Azam, and N. Knowlton (2002). Diversity and distribution of coral-associated bacteria. *Marine Ecology Progress Series* 243, pp. 1–10 (cit. on p. 16).

References

- Rossez, Y., E. B. Wolfson, A. Holmes, D. L. Gally, and N. J. Holden (2015). Bacterial flagella: Twist and stick, or dodge across the kingdoms. *PLoS Pathogens* 11.e1004483 (cit. on p. 9).
- Ruby, J. D., H. Li, H. Kuramitsu, S. J. Norris, S. F. Goldstein, K. F. Buttler, and N. W. Charon (1997). Relationship of *Treponema denticola* periplasmic flagella to irregular cell morphology. *Journal of Bacteriology* 179.5, pp. 1628–1635 (cit. on p. 21).
- Ruby, J. D. and N. W. Charon (1998). Effect of temperature and viscosity on the motility of the spirochete *Treponema denticola*. *FEMS Microbiology Letters* 169, pp. 251–254 (cit. on p. 21).
- Russo, A. F. and D. E. Koshland (1983). Separation of signal transduction and adaptation functions of the aspartate receptor in bacterial sensing. *Science* 220, pp. 1016–1020 (cit. on p. 31).
- Sagi, Y., S. Khan, and M. Eisenbach (2003). Binding of the chemotaxis response regulator CheY to the isolated, intact switch complex of the bacterial flagellar motor. *Journal of Biological Chemistry* 278, pp. 25867–25871 (cit. on p. 31).
- Samatey, F. A., H. Matsunami, K. Imada, S. Nagashima, T. R. Shaikh, D. R. Thomas, J. Z. Chen, D. J. Derosier, A. Kitao, and K. Namba (2004). Structure of the bacterial flagellar hook and implication for the molecular universal joint mechanism. *Nature* 431, pp. 1062–1068 (cit. on pp. 9, 100).
- Sang, S. Y. and J. J. Mekalanos (2008). Decreased potency of the *Vibrio cholerae* sheathed flagellum to trigger host innate immunity. *Infection and Immunity* 76, pp. 1282–1288 (cit. on p. 13).
- Scharf, B., H. Schuster-Wolff-Bühring, R. Rachel, and R. Schmitt (2001). Mutational analysis of the *Rhizobium lupini* H13-3 and *Sinorhizobium meliloti* flagellin genes: Importance of flagellin A for flagellar filament structure and transcriptional regulation. *Journal of Bacteriology* 183, pp. 5334–5342 (cit. on pp. 12, 14).
- Scharf, B. (2002). Real-time imaging of fluorescent flagellar filaments of *Rhizobium lupini* H13-3: Flagellar rotation and pH-induced polymorphic transitions. *Journal of Bacteriology* 182, pp. 2793–2801 (cit. on pp. 12, 27, 28, 31).
- Scher, F. M., J. W. Kloepper, and C. A. Singleton (1985). Chemotaxis of fluorescent *Pseudomonas* spp. to soybean seed exudates *in vitro* and in soil. *Canadian Journal of Microbiology* 31, pp. 570–574 (cit. on p. 20).
- Schneider, W. R. and R. N. Doetsch (1974). Effect of viscosity on bacterial motility. *Journal of Bacteriology* 117, pp. 696–701 (cit. on pp. 18, 101).
- Schniederberend, M., K. Abdurachim, T. S. Murray, and B. I. Kazmierczaka (2013). The GTPase activity of FlhF is dispensable for flagellar localization, but not motility, in *Pseudomonas aeruginosa*. *Journal of Bacteriology* 195, pp. 1051–1060 (cit. on p. 14).
- Schoenhofen, I. C., E. Vinogradov, D. M. Whitfield, J. R. Brisson, and S. M. Logan (2009). The CMP-legionaminic acid pathway in *Campylobacter*: Biosynthesis involving novel GDP-linked precursors. *Glycobiology* 19, pp. 715–725 (cit. on p. 13).
- Schuhmacher, J. S. et al. (2015). MinD-like ATPase FlhG effects location and number of bacterial flagella during C-ring assembly. *Proceedings of the National Academy of Sciences* 112, pp. 3092–3097 (cit. on p. 14).
- Schuster, S. C. and E. Baeuerlein (1992). Location of the basal disk and a ringlike cytoplasmic structure, two additional structures of the flagellar apparatus of *Wolinella succinogenes*. *Journal of Bacteriology* 174, pp. 263–268 (cit. on p. 21).
- Senior, B. W. (1977). The Dienes phenomenon: Identification of the determinants of compatibility. *Journal of General Microbiology* 102, pp. 235–44 (cit. on p. 19).
- Seville, M., T. Ikeda, and H. Hotani (1993). The effect of sugars on the morphology of the bacterial flagellum. *FEBS Letters* 332, pp. 260–262 (cit. on p. 11).
- Shapiro, A. H. (1961). *Shape and flow: The fluid dynamics of drag*. Doubleday Anchor Books, New York (cit. on pp. 23, 101).
- Shi, M., T. Gao, L. Ju, Y. Yao, and H. Gao (2014). Effects of FlrBC on flagellar biosynthesis of *Shewanella oneidensis*. *Molecular Microbiology* 93, pp. 1269–1283 (cit. on pp. 114, 117).
- Shibata, S., M. Alam, and S. I. Aizawa (2005). Flagellar filaments of the deep-sea bacteria *Idiomarina loihiensis* belong to a family different from those of *Salmonella typhimurium*. *Journal of Molecular Biology* 352, pp. 510–516 (cit. on p. 9).
- Shigematsu, M., Y. Meno, H. Misumi, and K. Amako (1995). The measurement of swimming velocity of *Vibrio cholerae* and *Pseudomonas aeruginosa* using the video tracking method. *Microbiology and Immunology* 39, pp. 741–744 (cit. on p. 22).

References

- Shimada, K., R. Kamiya, and S. Asakura (1975). Left-handed to right-handed helix conversion in *Salmonella* flagella. *Nature* 254, pp. 332–334 (cit. on p. 11).
- Shrivastava, A., R. G. Rhodes, S. Pochiraju, D. Nakane, and M. J. McBride (2012). *Flavobacterium johnsoniae* RemA is a mobile cell surface lectin involved in gliding. *Journal of Bacteriology* 194, pp. 3678–3688 (cit. on p. 5).
- Sikorski, J. et al. (2010). Complete genome sequence of *Sulfurospirillum deleyianum* type strain (5175 T). *Standards in Genomic Sciences* 2, pp. 149–157 (cit. on p. 21).
- Silverman, M., J. Zieg, and M. Simon (1979). Flagellar-phase variation: Isolation of the *rh1* gene. *Journal of Bacteriology* 137, pp. 517–523 (cit. on p. 13).
- Silverman, M. R. and M. I. Simon (1972). Flagellar assembly mutants in *Escherichia coli*. *Journal of Bacteriology* 112, pp. 986–993 (cit. on p. 23).
- Silverman, M. R. and M. I. Simon (1974). Flagellar rotation and the mechanism of bacterial motility. *Nature* 249, pp. 73–74 (cit. on pp. 23, 26).
- Skerker, J. M. and H. C. Berg (2001). Direct observation of extension and retraction of type IV pili. *Proceedings of the National Academy of Sciences* 98, pp. 6901–6904.
- Sleigh, M. A. (2005). Mechanisms of flagellar propulsion. *Protoplasma* 164, pp. 45–53 (cit. on p. 101).
- Soby, S. and K. Bergman (1983). Motility and chemotaxis of *Rhizobium meliloti* in soil. *Applied and Environmental Microbiology* 46, pp. 995–998 (cit. on p. 20).
- Sockett, H., S. Yamaguchi, M. Kihara, V. M. Irikura, and R. M. Macnab (1992). Molecular analysis of the flagellar switch protein FliM of *Salmonella typhimurium*. *Journal of Bacteriology* 174, pp. 793–806 (cit. on p. 7).
- Son, K., J. S. Guasto, and R. Stocker (2013). Bacteria can exploit a flagellar buckling instability to change direction. *Nature Physics* 9, pp. 494–498 (cit. on pp. 8, 18, 20, 27–29, 95, 96, 99, 117).
- Son, K., D. R. Brumley, and R. Stocker (2015). Live from under the lens: Exploring microbial motility with dynamic imaging and microfluidics. *Nature Reviews Microbiology* 13, pp. 761–775 (cit. on p. 29).
- Son, K., F. Menolascina, and R. Stocker (2016). Speed-dependent chemotactic precision in marine bacteria. *Proceedings of the National Academy of Sciences* 113, pp. 8624–8629 (cit. on pp. 18, 29).
- Song, W. S. and S. I. Yoon (2014). Crystal structure of FliC flagellin from *Pseudomonas aeruginosa* and its implication in TLR5 binding and formation of the flagellar filament. *Biochemical and Biophysical Research Communications* 444, pp. 109–115 (cit. on p. 10).
- Sourjik, V. (2004). Receptor clustering and signal processing in *E. coli* chemotaxis. *Trends in Microbiology* 12, pp. 569–576 (cit. on p. 31).
- Sourjik, V. and R. Schmitt (1996). Different roles of CheY1 and CheY2 in the chemotaxis of *Rhizobium meliloti*. *Molecular Microbiology* 22, pp. 427–436 (cit. on p. 28).
- Springer, W. R. and D. E. Koshland (1977). Identification of a protein methyltransferase as the *cheR* gene product in the bacterial sensing system. *Proceedings of the National Academy of Sciences* 74, pp. 533–537 (cit. on p. 31).
- Sterzenbach, T. et al. (2008). Role of the *Helicobacter hepaticus* flagellar sigma factor FliA in gene regulation and murine colonization. *Journal of Bacteriology* 190, pp. 6398–6408 (cit. on p. 21).
- Stevens, J. M., E. E. Galyov, and M. P. Stevens (2006). Actin-dependent movement of bacterial pathogens. *Nature Reviews Microbiology* 4, pp. 91–101 (cit. on p. 6).
- Stocker, R. (2011). Reverse and flick: Hybrid locomotion in bacteria. *Proceedings of the National Academy of Sciences* 108, pp. 2635–2636 (cit. on pp. 17, 18, 107, 111).
- Stocker, R., J. R. Seymour, A. Samadani, D. E. Hunt, and M. F. Polz (2008). Rapid chemotactic response enables marine bacteria to exploit ephemeral microscale nutrient patches. *Proceedings of the National Academy of Sciences* 105, pp. 4209–4214 (cit. on pp. 16, 17, 107).
- Sun, H., D. R. Zusman, and W. Shi (2000). Type IV pilus of *Myxococcus xanthus* is a motility apparatus controlled by the *frz* chemosensory system. *Current Biology* 10, pp. 1143–1146 (cit. on p. 5).
- Sun, M., M. Wartel, E. Cascales, J. W. Shaevitz, and T. Mignot (2011). Motor-driven intracellular transport powers bacterial gliding motility. *Proceedings of the National Academy of Sciences* 108, pp. 7559–7564 (cit. on p. 6).

References

- Suzuki, H. and T. Iino (1973). *In vitro* synthesis of phase-specific flagellin of *Salmonella*. *Journal of Molecular Biology* 81, pp. 57–70 (cit. on p. 13).
- Suzuki, H., K. Yonekura, and K. Namba (2004). Structure of the rotor of the bacterial flagellar motor revealed by electron cryomicroscopy and single-particle image analysis. *Journal of Molecular Biology* 337, pp. 105–113 (cit. on p. 7).
- Sycuro, L. K., Z. Pincus, K. D. Gutierrez, J. Biboy, C. A. Stern, W. Vollmer, and N. R. Salama (2010). Peptidoglycan crosslinking relaxation promotes *Helicobacter pylori*'s helical shape and stomach colonization. *Cell* 141, pp. 822–833 (cit. on p. 21).
- Szymanski, C. M., D. H. Burr, and P. Guerry (2002). *Campylobacter* protein glycosylation affects host cell interactions. *Infection and Immunity* 70, pp. 2242–2244 (cit. on p. 13).
- Taguchi, F. et al. (2006). Identification of glycosylation genes and glycosylated amino acids of flagellin in *Pseudomonas syringae* pv. *tabaci*. *Cellular Microbiology* 8, pp. 923–938 (cit. on p. 13).
- Taguchi, F., S. Shibata, T. Suzuki, Y. Ogawa, S. I. Aizawa, K. Takeuchi, and Y. Ichinose (2008). Effects of glycosylation on swimming ability and flagellar polymorphic transformation in *Pseudomonas syringae* pv. *tabaci* 6605. *Journal of Bacteriology* 190, pp. 764–768 (cit. on p. 13).
- Taguchi, F., T. Suzuki, K. Takeuchi, Y. Inagaki, K. Toyoda, T. Shiraishi, and Y. Ichinose (2009). Glycosylation of flagellin from *Pseudomonas syringae* pv. *tabaci* 6605 contributes to evasion of host tobacco plant surveillance system. *Physiological and Molecular Plant Pathology* 74, pp. 11–17 (cit. on p. 13).
- Takai, K., M. Suzuki, S. Nakagawa, M. Miyazaki, Y. Suzuki, F. Inagaki, and K. Horikoshi (2006). *Sulfurimonas parvalvinellae* sp. nov., a novel mesophilic, hydrogen- and sulfur-oxidizing chemolithoautotroph within the epsilonproteobacteria isolated from a deep-sea hydrothermal vent polychaete nest, reclassification of *Thiomicrospira denitrificans* as *Sulfurimonas denitrificans* comb. nov. and emended description of the genus *Sulfurimonas*. *International Journal of Systematic and Evolutionary Microbiology* 56, pp. 1725–1733 (cit. on p. 21).
- Taute, K. M., S. Gude, S. J. Tans, and T. S. Shimizu (2015). High-throughput 3D tracking of bacteria on a standard phase contrast microscope. *Nature Communications* 6.8776 (cit. on p. 16).
- Taylor, B. L. and D. E. Koshland (1974). Reversal of flagellar rotation in monotrichous and peritrichous bacteria: Generation of changes in direction. *Journal of Bacteriology* 119, pp. 640–642 (cit. on pp. 27–29, 105).
- Tecon, R. and D. Or (2016). Bacterial flagellar motility on hydrated rough surfaces controlled by aqueous film thickness and connectedness. *Scientific Reports* 6.19409 (cit. on p. 20).
- Terahara, N., Y. Noguchi, S. Nakamura, N. Kami-ike, M. Ito, K. Namba, and T. Minamino (2017). Load- and polysaccharide-dependent activation of the Na⁺-type MotPS stator in the *Bacillus subtilis* flagellar motor. *Scientific Reports* 7.46081 (cit. on pp. 97, 117).
- Thomashow, L. S. and S. C. Rittenberg (1985). Waveform analysis and structure of flagella and basal complexes from *Bdellovibrio bacteriovorus* 109J. *Journal of Bacteriology* 163, pp. 1038–1046 (cit. on p. 115).
- Tipping, M. J., N. J. Delalez, R. Lim, R. M. Berry, and J. P. Armitage (2013). Load-dependent assembly of the bacterial flagellar motor. *mBio* 4 (cit. on pp. 97, 117).
- Togashi, F., S. Yamaguchi, M. Kihara, S. I. Aizawa, and R. M. Macnab (1997). An extreme clockwise switch bias mutation in *fliG* of *Salmonella typhimurium* and its suppression by slow-motile mutations in *motA* and *motB*. *Journal of Bacteriology* 179, pp. 2994–3003 (cit. on p. 26).
- Toker, A. S., M. Kihara, and R. M. Macnab (1996). Deletion analysis of the FliM flagellar switch protein of *Salmonella typhimurium*. *Journal of Bacteriology* 178, pp. 7069–7079 (cit. on p. 31).
- Toker, A. S. and R. M. Macnab (1997). Distinct regions of bacterial flagellar switch protein FliM interact with FliG, FliN and CheY. *Journal of Molecular Biology* 273, pp. 623–634 (cit. on p. 7).
- Torsvik, V., L. Øvreås, and T. F. Thingstad (2002). Prokaryotic diversity - Magnitude, dynamics, and controlling factors. *Science* 296, pp. 1064–1066 (cit. on p. 19).
- Toutain, C. M., M. E. Zegans, and G. A. O'Toole (2005). Evidence for two flagellar stators and their role in the motility of *Pseudomonas aeruginosa*. *Journal of Bacteriology* 187, pp. 771–777 (cit. on p. 19).

References

- Trachtenberg, S., D. J. DeRosier, S. I. Aizawa, and R. M. Macnab (1986). Pairwise perturbation of flagellin subunits. The structural basis for the differences between plain and complex bacterial flagellar filaments. *Journal of Molecular Biology* 190, pp. 569–576 (cit. on pp. 12, 14).
- Tronick, S. R. and R. J. Martinez (1971). Methylation of the flagellin of *Salmonella typhimurium*. *Journal of Bacteriology* 105, pp. 211–219 (cit. on p. 13).
- Turnbull, G. A., J. A. W. Morgan, J. M. Whipps, and J. R. Saunders (2001). The role of motility in the in vitro attachment of *Pseudomonas putida* PaW8 to wheat roots. *FEMS Microbiology Ecology* 35, pp. 57–65 (cit. on p. 20).
- Turner, L., W. S. Ryu, and H. C. Berg (2000). Real-time imaging of fluorescent flagellar filaments. *Journal of Bacteriology* 182, pp. 2793–2801 (cit. on pp. 11, 26, 27, 33).
- Turner, L., R. Zhang, N. C. Darnton, and H. C. Berg (2010). Visualization of flagella during bacterial swarming. *Journal of Bacteriology* 192, pp. 3259–3267 (cit. on pp. 19, 26).
- Turner, L., L. Ping, M. Neubauer, and H. Berg (2016). Visualizing flagella while tracking bacteria. *Biophysical Journal* 111, pp. 630–639 (cit. on pp. 26, 95).
- Ueno, T., K. Oosawa, and S. I. Aizawa (1992). M ring, S ring and proximal rod of the flagellar basal body of *Salmonella typhimurium* are composed of subunits of a single protein, FliF. *Journal of Molecular Biology* 227, pp. 672–677 (cit. on p. 7).
- Van Amsterdam, K. and A. Van Der Ende (2004). *Helicobacter pylori* HP1034 (*ylxH*) is required for motility. *Helicobacter* 9.5, pp. 387–395 (cit. on p. 14).
- Van Leeuwenhoek, A. (1683). *Arcana naturae detecta* (cit. on pp. 7, 16).
- Vig, D. K. and C. W. Wolgemuth (2012). Swimming dynamics of the lyme disease spirochete. *Physical Review Letters* 109 (cit. on p. 21).
- Vladimirov, N., D. Lebiedz, and V. Sourjik (2010). Predicted auxiliary navigation mechanism of peritrichously flagellated chemotactic bacteria. *PLoS Computational Biology* 6.e1000717 (cit. on p. 26).
- Wadhams, G. H. and J. P. Armitage (2004). Making sense of it all: Bacterial chemotaxis. *Nature Reviews Molecular Cell Biology* 5, pp. 1024–1037 (cit. on p. 31).
- Wagenknecht, T., D. J. DeRosier, S. I. Aizawa, and R. M. Macnab (1982). Flagellar hook structures of *Caulobacter* and *Salmonella* and their relationship to filament structure. *Journal of Molecular Biology* 162, pp. 69–87 (cit. on p. 8).
- Walsby, A. E. (1975). Gas Vesicles. *Annual Review of Plant Physiology* 26, pp. 427–439 (cit. on p. 6).
- Wang, F., A. M. Burrage, S. Postel, R. E. Clark, A. Orlova, E. J. Sundberg, D. B. Kearns, and E. H. Egelman (2017). A structural model of flagellar filament switching across multiple bacterial species. *Nature Communications* 8.960 (cit. on pp. 9–11).
- Wang, F. et al. (2008). Environmental adaptation: Genomic analysis of the piezotolerant and psychrotolerant deep-sea iron reducing bacterium *Shewanella piezotolerans* WP3. *PLoS ONE* 3.e1937 (cit. on p. 19).
- Wang, G. and D. Or (2010). Aqueous films limit bacterial cell motility and colony expansion on partially saturated rough surfaces. *Environmental Microbiology* 12, pp. 1363–1373 (cit. on p. 20).
- Wang, G. and D. Or (2012). A hydration-based biophysical index for the onset of soil microbial coexistence. *Scientific Reports* 2.881 (cit. on p. 20).
- Warmink, J. A. and J. D. Van Elsas (2009). Migratory response of soil bacteria to *Lyophyllum* sp. strain Karsten In soil microcosms. *Applied and Environmental Microbiology* 75, pp. 2820–2830.
- Warmink, J. A., R. Nazir, B. Corten, and J. D. van Elsas . (2011). Hitchhikers on the fungal highway: The helper effect for bacterial migration via fungal hyphae. *Soil Biology and Biochemistry* 43, pp. 760–765 (cit. on p. 20).
- Warren, R. J. and B. Marshall (1983). Unidentified curved bacilli on gastric epithelium in active chronic gastritis. *The Lancet* 321, pp. 1273–1275 (cit. on p. 18).
- Weger, L. A. de, C. I. van Der Vlugt, A. H. Wijfjes, P. A. Bakker, B. Schippers, and B. Lugtenberg (1987). Flagella of a plant-growth-stimulating *Pseudomonas fluorescens* strain are required for colonization of potato roots. *Journal of Bacteriology* 169, pp. 2769–2773 (cit. on p. 20).

References

- Wei, L. N. and T. M. Joys (1985). Covalent structure of three phase-1 flagellar filament proteins of *Salmonella*. *Journal of Molecular Biology* 186, pp. 791–803 (cit. on p. 11).
- Welch, M., K. Oosawa, S. Aizawa, and M. Eisenbach (1993). Phosphorylation-dependent binding of a signal molecule to the flagellar switch of bacteria. *Proceedings of the National Academy of Sciences* 90, pp. 8787–8791 (cit. on p. 7).
- Whitman, W. B., D. C. Coleman, and W. J. Wiebe (1998). Prokaryotes: The unseen majority. *Proceedings of the National Academy of Sciences* 95, pp. 6578–6583 (cit. on p. 20).
- Wick, L. Y., R. Remer, B. Würz, J. Reichenbach, S. Braun, F. Schäfer, and H. Harms (2007). Effect of fungal hyphae on the access of bacteria to phenanthrene in soil. *Environmental Science and Technology* 41, pp. 500–505 (cit. on p. 20).
- Wigneshweraraj, S. et al. (2008). Modus operandi of the bacterial RNA polymerase containing the σ^{54} promoter-specificity factor. *Molecular Microbiology* 68.3, pp. 538–546 (cit. on p. 16).
- Wildschutte, H., D. M. Wolfe, A. Tamewitz, and J. G. Lawrence (2004). Protozoan predation, diversifying selection, and the evolution of antigenic diversity in *Salmonella*. *Proceedings of the National Academy of Sciences* 101, pp. 10644–10649 (cit. on p. 13).
- Wilhelms, M., R. Molero, J. G. Shaw, J. M. Tomás, and S. Merino (2011). Transcriptional hierarchy of *Aeromonas hydrophila* polar-flagellum genes. *Journal of Bacteriology* 193, pp. 5179–5190 (cit. on p. 16).
- Wilson, D. R. and T. J. Beveridge (1993). Bacterial flagellar filaments and their component flagellins. *Canadian Journal of Microbiology* 39, pp. 451–472 (cit. on pp. 13, 18).
- Wilson, L. G., V. A. Martinez, J. Schwarz-Linek, J. Talleur, G. Bryant, P. N. Pusey, and W. C. K. Poon (2011). Differential dynamic microscopy of bacterial motility. *Physical Review Letters* 106 (cit. on p. 16).
- Wirth, R. (2012). Response to Jarrell and Albers: Seven letters less does not say more. *Trends in Microbiology* 20, pp. 511–512 (cit. on p. 6).
- Wolgemuth, C. W. (2015). Flagellar motility of the pathogenic spirochetes. *Seminars in Cell and Developmental Biology* 46, pp. 104–112 (cit. on pp. 21, 22).
- Wylie, D., A. Stock, C. Y. Wong, and J. Stock (1988). Sensory transduction in bacterial chemotaxis involves phosphotransfer between CHE proteins. *Biochemical and Biophysical Research Communications* 151, pp. 891–896 (cit. on p. 31).
- Xie, L., T. Altindal, S. Chattopadhyay, and X.-L. Wu (2011). Bacterial flagellum as a propeller and as a rudder for efficient chemotaxis. *Proceedings of the National Academy of Sciences* 108, pp. 2246–2251 (cit. on pp. 8, 17, 20, 27, 28, 95, 96, 107, 111).
- Xie, L. and X. L. Wu (2014). Bacterial motility patterns reveal importance of exploitation over exploration in marine microhabitats. Part I: Theory. *Biophysical Journal* 107, pp. 1712–1720 (cit. on p. 17).
- Yamaguchi, S., S. I. Aizawa, M. Kihara, M. Isomura, C. J. Jones, and R. M. Macnab (1986). Genetic evidence for a switching and energy-transducing complex in the flagellar motor of *Salmonella typhimurium*. *Journal of Bacteriology* 168, pp. 1172–1179 (cit. on p. 7).
- Yamamoto, M., M. Ohnishi-Kameyama, C. L. Nguyen, F. Taguchi, K. Chiku, T. Ishii, H. Ono, M. Yoshida, and Y. Ichinose (2011). Identification of genes involved in the glycosylation of modified viosamine of flagellins in *Pseudomonas syringae* by mass spectrometry. *Genes* 2, pp. 788–803 (cit. on p. 13).
- Yamashita, L., K. Hasegawa, H. Suzuki, F. Vonderviszt, Y. Mimori-Kiyosue, and K. Namba (1998). Structure and switching of bacterial flagellar filaments studied by X-ray fiber diffraction. *Nature Structural Biology* 5, pp. 125–132 (cit. on p. 11).
- Yanagihara, S., S. Iyoda, K. Ohnishi, T. Iino, and K. Kutsukake (1999). Structure and transcriptional control of the flagellar master operon of *Salmonella typhimurium*. *Genes & Genetic Systems* 74, pp. 105–111 (cit. on p. 15).
- Yokoseki, T., K. Kutsukake, K. Ohnishi, and T. Iino (1995). Functional analysis of the flagellar genes in the fliD operon of *Salmonella typhimurium*. *Microbiology* 141, pp. 1715–1722 (cit. on p. 15).
- Yonekura, K., S. Maki, D. G. Morgan, D. J. DeRosier, F. Vonderviszt, K. Imada, and K. Namba (2000). The bacterial flagellar cap as the rotary promoter of flagellin self-assembly. *Science* 290, pp. 2148–2152 (cit. on p. 15).
- Yonekura, K., S. Maki-Yonekura, and K. Namba (2003). Complete atomic model of the bacterial flagellar filament by electron cryomicroscopy. *Nature* 424, pp. 643–650 (cit. on pp. 9, 10).

References

- Yoshioka, K., S. I. Aizawa, and S. Yamaguchi (1995). Flagellar filament structure and cell motility of *Salmonella typhimurium* mutants lacking part of the outer domain of flagellin. *Journal of Bacteriology* 177, pp. 1090–1093 (cit. on p. 11).
- Young, I. M. and J. W. Crawford (2004). Interactions and self-organization in the soil-microbe complex. *Science* 304, pp. 1634–1637 (cit. on pp. 19, 20).
- Zhou, J., S. A. Lloyd, and D. F. Blair (2002). Electrostatic interactions between rotor and stator in the bacterial flagellar motor. *Proceedings of the National Academy of Sciences* 95, pp. 6436–6441 (cit. on p. 7).
- Zhu, S., T. Nishikino, B. Hu, S. Kojima, M. Homma, and J. Liu (2017). Molecular architecture of the sheathed polar flagellum in *Vibrio alginolyticus*. *Proceedings of the National Academy of Sciences* 114, pp. 10966–10971 (cit. on pp. 8, 12).

Acknowledgements

An erster Stelle möchte ich mich bei meinem Doktorvater Prof. Dr. Kai Thormann bedanken. Dafür, dass er mir die Gelegenheit gegeben hat, unter seiner Anleitung an diesem sehr spannenden Thema zu forschen, dass er immer eine offene Tür und ein offenes Ohr für alle Fragen und Diskussionen hatte und für all die guten Ratschläge, Anregungen und Ideen und für die Freiheit, mit der ich meiner Forschung nachgehen durfte.

Für die Übernahme des Zweitgutachtens möchte ich mich bei Apl. Prof. Dr. Peter Friedhoff bedanken, sowie bei Prof. Dr. Sylvia Schnell und Prof. Dr. Reinhard Dammann für die Teilnahme an meiner Prüfungskommission.

Ein besonderer Dank gilt unseren Kooperationspartnern von der Philipps-Universität Marburg, Prof. Dr. Bruno Eckhardt und Felix Schmidt, sowie von der University of York, Dr. Laurence Wilson und Nicola Farthing, für die ausgezeichnete Zusammenarbeit, die hilfreichen Diskussionen und Fragen und die Mitwirkung an den beiden großartigen Publikationen. Bei Prof. Dr. Bruno Eckhardt möchte ich mich außerdem für die weitere finanzielle Unterstützung zum Abschließen dieser Doktorarbeit bedanken.

Ein großer Dank gilt auch allen aktuellen und ehemaligen Mitgliedern der AG Thormann, dafür, dass ihr so eine tolle und besondere Arbeitsatmosphäre geschaffen habt und mir jederzeit theoretisch und praktisch weitergeholfen habt. Danke Flo, Suse, Max, Anna, Meike, John, Tim, Anja, Ulrike und nicht zu vergessen Kerstin, Lasse, Lukas, Bina, Isi, Tabea, Vanessa und Dirk, die über eine lange Zeit als Bachelor- und Masterstudenten oder als Hiwi Teil der AG Thormann waren und sind. Nicht zuletzt wegen euch allen haben mir die Jahre in Gießen sehr viel Spaß gemacht und ich habe sehr gerne mit euch zusammen gearbeitet.

Besonders meine Bürokollegen Anna, Meike und Max haben mir durch ihre kritischen Bemerkungen über meine Abbildungen und meine Farbwahl sehr geholfen. Danke Suse und Flo, dass ihr mir viele neue Methoden gezeigt und mir mit eurer Erfahrung geholfen habt. Danke Max für alles was mit Digitalem zu tun hat, vor allem Illustrator, Photoshop, Benchling und, ja, Google. Danke Ulrike für die große Hilfe beim Erstellen unzähliger Flagellinmutanten und dein magisches Geschick bei Kolonie-PCRs.

Ich danke auch allen Mitgliedern der AG Klug und AG Hackenberg für die gute Nachbarschaft und Zusammenarbeit, sowie eure Hilfsbereitschaft bei allem was mit RNA zu tun hat, danke insbesondere Carina und Hendrik.

Zu guter Letzt ein großes Dankeschön an meine Familie, meine Eltern Doris und Olaf und meinen Bruder Jan, sowie meine Partnerin Franzl. Danke für eure Liebe, euer Vertrauen und eure bedingungslose Unterstützung bei allem, was ich mir in den Kopf gesetzt habe.

Curriculum vitae

Aus Datenschutzgründen aus der elektronischen Fassung entfernt.